Synthetic and Mechanistic Investigations of Ruthenium Olefin Metathesis Catalysts

Thesis by

Melanie Sarah Sanford

In Partial Fulfillment of the Requirements
for the Degree of
Doctor of Philosophy

California Institute of Technology
Pasadena, California

2001
(Submitted May 21, 2001)

For my Family

Acknowledgments

I want to begin by acknowledging my advisor, Professor Bob Grubbs, for providing a truly unique environment for doing chemistry. I was totally overwhelmed when I first joined his group, but I really appreciate (in retrospect, at least) the fact that he let me make my own mistakes and learn how to approach scientific problems independently. Bob has been incredibly patient and supportive of my many crazy ideas, and it has been inspiring to see his continued enthusiasm for science. Professor Jackie Barton has also been very supportive of all of my scientific/teaching pursuits, and I am grateful to her, as well as to Professors John Bercaw and Dave MacMillan, for taking the time to serve on my committee.

I would like to thank Larry Henling and Mike Day for carrying out all of the X-ray crystallographic studies described in this thesis. Dian Buchness should be acknowledged for her tireless efforts at keeping the department running smoothly, and Linda Syme does an incredible job of keeping Bob and all of his papers, schedules, and trips under control. Tom Dunn should also be thanked for keeping the electronics in the department working. Jeff Yoder and Ola Wendt have both helped me a lot with the 500 MHz NMR and with the CIFIT program. Many of the results described in Chapter 2 could not have been obtained without their assistance. Michelle Valdez was a SURF in the group and did some of the work described in Chapter 6. I also need to thank all of the people who have proofread my props and various chapters of this thesis, including Justin Gallivan, Jon Seiders, Jen Love, Tina Trnka, Steve Goldberg, JP Morgan, Bill Ward, Arnab Chatterjee, Antek Wong-Foy, and Jeff Yoder.

Adam Matzger joined the Grubbs group as a post-doc within a few months of me, and I cannot thank him enough for all of his support, advice, and friendship. Adam has always challenged me to think about science in new ways, and we have had insightful scientific discussions about virtually all of the chemistry discussed in this thesis. Adam has also been my biggest cheerleader in the group, and I have really appreciated his encouragement, particularly during the (many) times when my chemistry was going nowhere. He is a phenomenal chemist and a great friend, and 201 Church is definitely not the same without him. Fortunately, however, Adam's desk in 201 was taken over by

Justin Gallivan, another terrific chemist, fountain of knowledge about all things biological, foos-ball champion, and all-around great guy.

Mike Ulman and Tom Wilhelm both taught me a tremendous amount about ruthenium olefin metathesis catalysts and organometallic techniques, as well as about how to get along in the Grubbs group. Mike was my mentor on the tempermental "wet" dry box, and we spent many an evening together doing surgery on the box (and often barely avoiding electrocution). I'm happy to say that the wdb has fallen into the able hands of Bill Ward and Jen Love, who I trust will treat it well. (Bill – be sure to take care of #2 #1). Mike was also the person who first started thinking about the mechanism of olefin metathesis in the *N*-heterocyclic carbene catalyst systems, and he contributed significantly to the mechanistic work described in Chapter 2.

Other group members who departed before me include Tom Kirkland, Dave Lynn, Delwin Elder, Marcus Weck, Eric Connor, and Helen Blackwell, and I really appreciate all of their help and support during my first few years in the group. I particularly want to thank Helen, Eric, and Dave for many enjoyable Fridays at the Ath after Organometallics and numerous drinks at sleazy bars around Pasadena. I also need to thank the "chicks" – Helen, Heather Maynard, Amy Giardello, Mary Gin, Jen Love, and Tina Trnka – for enjoyable lunches at Goldsteins on Wednesdays.

It has been a real pleasure to work with Jen Love on a variety of different projects over the past year and a half, and Jen's synthetic and mechanistic work has contributed greatly to Chapters 2 and 3 of this thesis. She has also lent an empathetic ear to my many gripes about chemistry, politics (both local and national), and general injustice around the world. Both Jen and Helen have been much-needed female friends and mentors to me here at Caltech, and I look forward to the day that they will both be fantastic chemistry professors.

Todd Younkin is my only remaining classmate in the group, and I think that it is fair to say that we have both gone through some life changing experiences in the time we have been here. Through all of this, Todd has been a source of humor, perspective, and insightful scientific advice, and I appreciate his friendship and support. JP Morgan has also been a great friend, and I really admire his seemingly endless patience, his passion for teaching, and his general philosophy on life. Bill Ward's diverse interests in fly-

fishing, opera, ranting, cooking, foos-ball, piano, large hats, and jumpers make him a true original, and it has been great to get to know him both in lab and at our frequent concert engagements. I also need to thank Bill and JP along with Jen Love, Justin, Dan Sanders, and Oren Scherman, for *many* hours spent chatting (and/or arguing) about current events and politics. The official international gesture for chad-punching (one of Sherm's finest inventions) was borne of one of those discussions.

Arnab Chatterjee introduced me to the wonder that is Las Vegas, and has generally served as the group liaison to various forms of debauchery. Tina Trnka has been a sounding board for ideas about catalyst design, and will continue to carry the organometallic torch in the group. It has also been good to get to know the first and second year grad students, including Oren, Dan, Diego Benitez, Tae Lim Choi (TLC), Drew Waltman, Christie Morrill, and Isaac Rutenberg, and I wish you all luck in the *long* journey ahead of you. Recently, the group has been filled with a fantastic bunch of organic post-docs who have all helped and inspired me a great deal. They include Jon Seiders, Steve Goldberg, Dean Toste, Hyunjin Kim, Choon Woo Lee (a.k.a. Chuck Lewis), Andreas Kilbinger, Justin Gallivan, Jen Love, and Stu Cantrill. I particularly need to thank Jon Seiders for his advice about chemistry (especially dynamic NMR), as well as for hosting great TI parties.

I want to thank the 130 Church/foos crowd for many, many enjoyable evenings at the Rathskeller – I never knew grad school could be this fun! Justin "sexithiophene" Gallivan generally lead the charge to the Ath and never quit once he got there. Steve Goldberg is as good at foos as he is at chemistry, and he (usually) was patient with my inconsistent goaltending and my propensity for talking while playing. I think that the Goldberg/Stanford team still holds the record for the most victories in one evening. Drew "chops" Waltman and Dean "of defense or Canada" Toste could always be counted on to bring a great game and a dose of humorous commentary to the table. Other players included Jason "Rinaldo" Belitsky, Andreas Kilbinger, Oren Scherman, Jon Seiders, Bill "brick house" Ward, JP Morgan, Dan Sanders, Todd Younkin, Stu Cantrill, Arnab Chatterjee, Antek Wong-Foy, Jen Love and Martha Gallivan (go chicks!). If this whole chemistry thing doesn't work out, I'm hoping to join the foos pro-tour.

Outside of the Grubbs group, I have enjoyed spending time with Jeff, Shelley, and Jordan Yoder, and I hope that we will have a chance to play some cards/dice in the near future. I've also has a great time with Ola Wendt, John Scollard, and Chris and Jennifer Levy, and the Levy's have fed me more delicious meals than I can count. Chris Treadway has also been a good friend and a constant source of investing advice and 1980's trivia. I am incredibly lucky to have a number of friends outside of Caltech, and I want to thank Enza, Megan, Steph, Morgan, Anna Davis, Anna Mitescu, Meghan, and Es for their friendship and for *many* hours spent on the phone! Their visits over the past five years have played a large role in maintaining my sanity.

I want thank Mom, Dad, Andrew, and Gram (*i.e.,* all of the "Sons") for all of your love and support. I'm not sure how I ended up in chemistry as the daughter of a political scientist and a historian, but I really appreciate your enthusiasm and encouragement through all of this science stuff. You guys are the greatest!

Last, but definitely not least, I have to thank Foy. It has been almost five years since we first met at the central Catalina dumpster, and I can't imagine what grad school would have been like without you. You have been incredibly patient with my impatient ways, and you are the main reason that I have not had a heart attack during this whole endeavor. You are a truly amazing person, and I cannot thank you enough for your love, friendship, and support.

Abstract

The ruthenium-based catalysts $(PCy_3)_2(Cl)_2Ru{=}CHPh$ (**1**) and $(IMesH_2)(PCy_3)(Cl)_2Ru{=}CHPh$ (**2**) [$IMesH_2$ = 1,3-dimesityl-4,5-dihydroimidazol-2-ylidene] show high olefin metathesis activity in the presence of most common functional groups and have been widely used in synthetic chemistry. This thesis describes mechanistic, structural, and synthetic studies aimed at understanding the reactivity of these complexes, and at developing new olefin metathesis catalysts with superior properties.

Chapter 2 details the effects of ligand variation on the mechanism and activity of ruthenium-based olefin metathesis catalysts. A series of ruthenium complexes of the general formula $(L)(PR_3)(X)_2Ru{=}CHR^1$ were prepared, and the influence of the ancillary ligands L, X, R, and R^1 on the rates of phosphine dissociation and initiation as well as on the overall catalytic activity was examined.

Chapter 3 describes the synthesis of a series of ruthenium benzylidenes containing *N*-heterocyclic carbene ligands. The new complexes, of the general formula $(IMesH_2)(X)_m(L)_nRu{=}CHPh$, were prepared using a variety of synthetic methods, and the bis-pyridine adduct $(IMesH_2)(Cl)_2(C_5H_5N)_2Ru{=}CHPh$ served as a particularly valuable synthon in these systems. Several of these compounds were characterized by X-ray crystallography, and the barriers to benzylidene and *N*-heterocyclic carbene rotation were determined using ^1H NMR spectroscopy.

Chapter 4 describes the preparation of a series of four-coordinate ruthenium benzylidenes that serve as analogues of the 14-electron olefin metathesis intermediate $(L)(Cl)_2Ru{=}CHPh$. These coordinatively unsaturated species have the general formula $(L)(OR)_2Ru{=}CHPh$, and are stabilized by sterically bulky and π-donating alkoxide ligands, such as *tert*-butoxide, hexafluoro-*tert*-butoxide, and perfluoro-*tert*-butoxide. The new compounds were characterized by X-ray crystallography, and their reactivity with incoming ligands, including substituted alcohols, phenols, carboxylates, and pyridine, was investigated. In addition, their olefin metathesis activities were examined in the presence and absence of HCl co-catalyst.

Chapters 5 and 6 describe the synthesis and characterization of neutral and cationic tris(pyrazolyl)borate ruthenium complexes. The new complexes were characterized by NMR spectroscopy and X-ray crystallography, and their olefin metathesis activities were explored.

Table of Contents

List of Figures

List of Tables

List of Schemes

Chapter 1: Introduction

Introduction

Ruthenium-catalyzed olefin metathesis has become an important carbon-carbon bond forming reaction over the past decade. The exponential increase in the use of olefin metathesis by organic and polymer chemists is largely due to the advent of the well-defined and synthetically accessible ruthenium catalysts **1.1**[1] and **1.2**[2] (Figure 1). Extensive mechanistic investigations of these benzylidenes have been undertaken in order to understand how they work and how they can be improved.[3,4,5,6] The ultimate goal of these studies is to generate new catalysts with improved activity, thermal stability, functional group tolerance, and stereoselectivity. This introduction is meant to provide a concise review of our current understanding of the mechanism of ruthenium-catalyzed olefin metathesis reactions, with an emphasis on the chemistry of **1.1**, **1.2**, and their derivatives.

Figure 1. Widely Used Ruthenium Olefin Metathesis Catalysts.

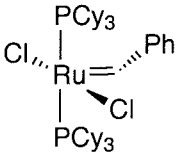

(1.1)

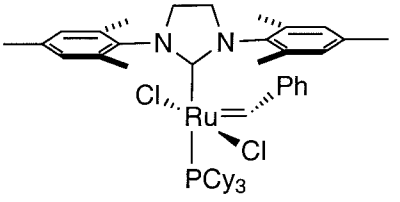

(1.2)

Past I. General Mechanism

Initial mechanistic studies of catalyst **1.1** and its analogues established that olefin metathesis reactions in these systems are inhibited by the addition of free phosphine.[3] This result suggests that phosphine loss is required for catalytic activity, and implicates a "dissociative" mechanism, involving metallacyclobutane formation from the 16-electron olefin adduct **1.3a** (Scheme 1, Path A).[3] In contrast, an "associative" reaction pathway, involving metallacycle formation from the 18-electron olefin complex **1.3b** (Scheme 1, Path B), does not contribute significantly to olefin metathesis reactions in these systems.[7]

Scheme 1

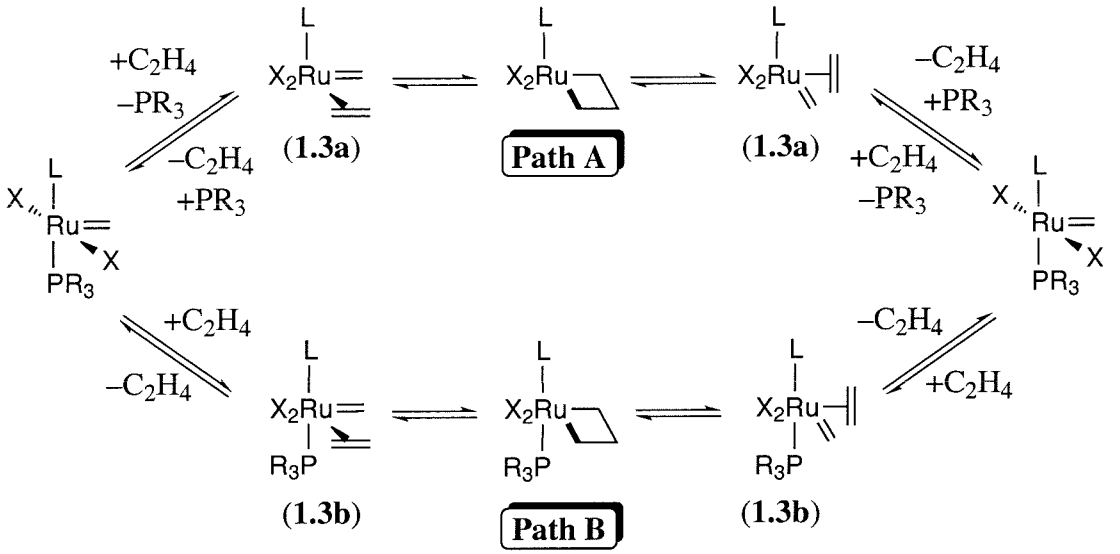

More recently, we have investigated the mechanism of the initial ligand substitution of phosphine with olefinic substrate (Scheme 2). In the two limiting cases, this reaction could proceed by an associative pathway, involving the 18-electron olefin intermediate (or transition state) **1.3b** (Scheme 2, Path B), or by a dissociative pathway,

Scheme 2

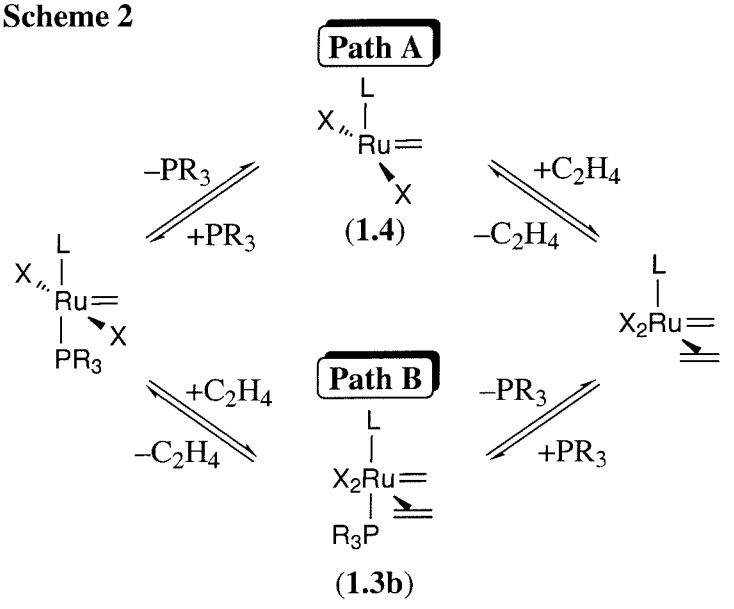

involving the 14-electron intermediate **1.4** (Scheme 2, Path A). As described in Chapter 2, kinetic studies clearly reveal that the phosphine/olefin substitution proceeds in a dissociative fashion, *via* the four-coordinate complex **1.4**.

The most "up to date" proposed catalytic cycle for olefin metathesis reactions mediated by the complexes $(L)(X)_2(PR_3)Ru{=}CHR'$ is outlined in Figure 2.[8] In a first step, these five-coordinate ruthenium adducts undergo phosphine dissociation to produce the 14-electron intermediate $(L)(X)_2Ru{=}CHR'$ (**1.4**).[4] Complex **1.4** reacts with an olefinic substrate to afford the ruthenium-olefin complex **1.3a**. Complex **1.3a** then undergoes carbon-carbon bond formation to generate a ruthenium(IV) metallacyclobutane (**1.5**), which may be a discrete intermediate[3] or a transition state[5a] along the reaction coordinate. Based on the mechanism outlined in Figure 2, the overall "metathesis activity" of a ruthenium alkylidene is dictated by the relative magnitudes of k_1 and k_{-1}/k_2 (Figure 2), which can both be determined experimentally.[9] In general, high olefin metathesis activity is observed when k_1 is relatively large and k_{-1}/k_2 is relatively small.

Figure 2. Mechanism of Metathesis Reactions Catalyzed by $(L)(PR_3)(X)_2Ru{=}CHR'$.

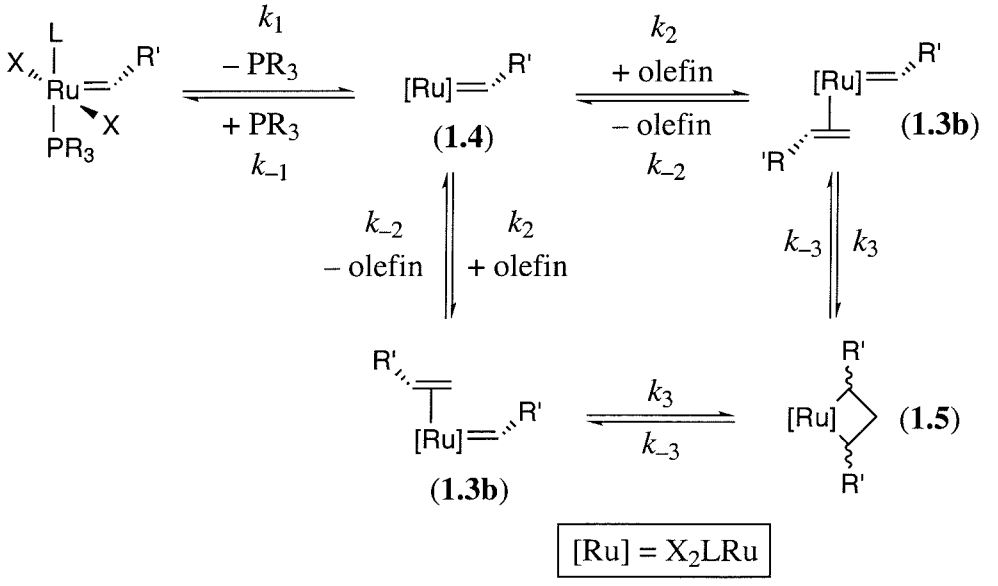

At this point, a brief comparison of the rate constants k_1 and k_{-1}/k_2 in catalysts **1.1** and **1.2** is instructive, because it highlights the important, and often competing, processes that determine catalyst activity in these systems. The values of k_1 (the initiation rate constant) in these complexes differ by two orders of magnitude at 80 °C, and the less "active" metathesis catalyst (**1.1**) initiates faster.[4] In contrast, the k_{-1} to k_2 ratio in catalyst **1.2** is greater than that in **1.1** by a factor of 10^4.[4,10] These results suggest that the four coordinate, *N*-heterocyclic carbene complex $(IMesH_2)(Cl)_2Ru{=}CHPh$ [$IMesH_2$ = 1,3-dimesityl-4,5-dihydroimidazol-2-ylidene] has dramatically improved selectivity for binding olefins over PCy_3 as compared to the analogous phosphine adduct, $(PCy_3)(Cl)_2Ru{=}CHPh$. The relative magnitudes of k_1 and k_{-1}/k_2 translate into approximately 10^2-10^3 higher catalytic activity of **1.2**, as measured by the rate of the ring opening metathesis polymerization of cyclooctadiene[11] and/or the ring closing metathesis of diethyl diallylmalonate.[2]

Part II. Ancillary Ligand and Substrate Effects

Introduction

In the complexes $(L)(X)_2(PR_3)Ru{=}CHR'$, modification of the ancillary ligands has a tremendous impact on the values of k_1, k_{-1}/k_2 and on the overall catalytic activity. High initiation rates (k_1) are desirable, because rapid initiation translates into controlled polymerization reactions, lower catalyst loadings, and lower reaction temperatures. Increased catalytic activity is also important, because it results in faster reaction rates and a larger pool of accessible substrates and products. This section focuses on the relationship between catalyst structure and initiation/activity in ruthenium-based olefin metathesis catalysts.

Catalyst Initiation

Introduction. In a catalytic reaction, "initiation" is defined as the step that provides entry for a dormant pre-catalyst into the catalytic cycle. According to the mechanism outlined in Figure 2, the initiation event in olefin metathesis reactions catalyzed by $(L)(X)_2(PR_3)Ru{=}CHR'$ involves dissociation of phosphine to produce

complex **1.4** (with a rate constant of k_1). Notably, early mechanistic investigations of **1.1** and its analogues relied on a slightly different definition of the initiation event.[1,12] These studies defined the "initiation" rate as the rate of a stoichiometric reaction between an olefin and a ruthenium alkylidene (with a rate constant of k_{obs}). Importantly, when the steady state approximation is applied to intermediate **1.4**, the two rate constants – k_1 and k_{obs} – are closely related. Under these conditions, k_{obs} becomes equal to k_1 at high concentrations of olefin, where k_2[olefin] >> k_{-1}[PR_3].[4] The first half of this section on initiation will describe direct measurements of k_1, while the second part will present data concerning k_{obs}.

k_1. The initiation rate constant (k_1) has been probed as a function of catalyst structure using ^{31}P magnetization transfer experiments, and the results are summarized in Figure 3.[4] In the complexes $(L)(X)_2(PR_3)Ru{=}CHR'$, k_1 increases by two orders of magnitude when X is changed from chloride to iodide.[4a] The magnitude of this increase is the same for both the bis-phosphine (L = PCy_3) and the *N*-heterocyclic carbene (L = $IMesH_2$) complexes, suggesting that the acceleration in phosphine dissociation occurs by a similar mechanism in both catalyst systems. Iodide ligands are significantly larger and more electron donating than chlorides, and it is unclear at this time whether the observed increase in initiation rate is a steric or an electronic effect.

Figure 3. Ancillary Ligand Effects on Catalyst Initiation.

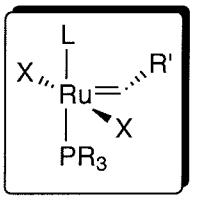

L = $IMesH_2$ < PCy_3

X = Cl < Br < I

R' = H << Ph < Alkyl < CO_2R

R = Bu < Cy < Bn < Ph

Increasing k_1 ⟶

The initiation rate increases over approximately four orders of magnitude as R' is varied from H to CO_2R (k_1 for CO_2R > alkyl > Ph >> H).[4,13] For the ester-substituted carbenes [R' = CO_2Cy, $CO_2{}^tBu$, CO_2Me], the values of k_1 have only been measured qualitatively, but are at least 10^2 times larger than those of their benzylidene analogues.[13] In contrast, the methylidenes $(PCy_3)_2(Cl)_2Ru{=}CH_2$ (**1.6**) and $(IMesH_2)(Cl)_2(PCy_3)Ru{=}CH_2$ (**1.7**) initiate 10^2-10^3 times slower than **1.1** and **1.2**, respectively.[4a] The extremely low initiation rate of methylidene **1.7** means that the formation of this species can effectively shut down catalysis.[4a,14] As a result, the substitution of olefinic substrates with alkyl or phenyl groups should be used to prevent the generation of methylidene intermediates in reactions catalyzed by **1.2**.[15]

In the *N*-heterocyclic carbene complexes $(IMesH_2)(Cl)_2(PR_3)Ru{=}CHPh$, k_1 decreases by more than two orders of magnitude as PR_3 is changed from PPh_3 to PBu_3 (k_1 for PPh_3 > PBn_3 > PCy_3 > PBu_3),[4,16] indicating that larger and less electron-donating phosphine ligands dissociate faster. The electronic contribution of the phosphine ligand to k_1 has been examined directly in a series of isosteric *para*-substituted triphenylphosphine derivatives.[16] In the complexes $(IMesH_2)(Cl)_2[P(p\text{-}C_6H_4X)_3]Ru{=}CHPh$ [X = CF_3, Cl, F, H, OMe], a Hammett ρ value of +1.8 is obtained, indicating that electron withdrawing *para* substituents labilize the triarylphosphine ligands.[16] These results are in agreement with a thermochemical investigation of Ru–P bond enthalpies (ΔH_{Ru-P}) in related ruthenium alkylidenes.[17] In a study of the complexes $(PR_3)_2(Cl)_2Ru{=}CHCH{=}C(Ph)_2$ [R = Cy, ^{i}Pr, ^{i}Bu, Bn, Ph], Nolan and coworkers have shown that ΔH_{Ru-P} increases linearly with the pK_a of the coordinated phosphine ligand.[17,18]

***k*$_{obs}$.** Olefin substitution has a dramatic effect on the magnitude of k_{obs} in the reactions of olefinic substrates with catalyst **1.1**.[12] For example, under otherwise identical conditions, *cis*-olefins, such as *cis*-3-hexene, react almost twice as fast as their *trans* analogues.[12] In addition, the values of k_{obs} for electron-rich olefinic substrates (*e.g.*, ethyl vinyl ether) are qualitatively larger than those for electron poor olefins (*e.g.*, methyl acrylate). The contribution of olefin electronics to k_{obs} has been measured directly in the reactions of *para*-substituted styrene derivatives with **1.1**.[12] A Hammett ρ value of –0.84 is obtained in these systems, indicating an increase in k_{obs} for electron rich olefins.[19] Schwab *et al.* have examined k_{obs} as a function of benzylidene *para*-substitution in the

reactions of $(PCy_3)_2(Cl)_2Ru{=}CH\text{-}p\text{-}C_6H_4X$ [X = Me, NMe_2, OMe, F, Cl, NO_2] with 1-hexene. Interestingly, this study shows *no* linear correlation between the σ^+ electronic parameters and k_{obs}, and all of the *para* substituents lead to a decrease in k_{obs} relative to hydrogen.[1]

General. Although catalyst initiation is an important aspect of olefin metathesis reactions, it is not always practical to carry out a detailed mechanistic study of initiation in each new catalyst. As a result, we have developed several reactions that serve as qualitative probes of initiation rates in these systems. The ring opening metathesis polymerization of cyclooctadiene serves as a first assay of initiation kinetics, and "slow" initiators generally show less than 5% of the "propagating species" ([Ru]=CHP where P = polymer chain) by ^{1}H NMR spectroscopy. The reaction of ruthenium alkylidenes with ethyl vinyl ether can be used as a second initiation "litmus test," and "fast" initiators react quantitatively with the substrate within 15 minutes at room temperature.[4] Using these criteria, catalyst initiation has been evaluated in a wide variety of ruthenium alkylidenes. Representative catalysts that exhibit "fast" initiation rates are summarized in Figure 4, and include benzylidene **1.1**,[4] the bimetallic Ru-Rh complex **1.8**,[20] and the bis-pyridine adduct **1.9**.[21] In general, "fast" initiators contain one or more labile ligands, such as the chloride bridges in **1.8** or the pyridines of **1.9**. In contrast, complexes showing "slow" initiation rates include **1.2**,[4] the Schiff base adduct **1.10**,[22] the intramolecular ether chelates **1.11** and **1.12**,[23] the bis-NHC complex **1.13**,[24] and the *cis*-phosphine catalyst **1.14**

Figure 4. Catalysts Exhibiting "Fast" Initiation Rates.

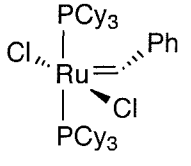

(1.1)

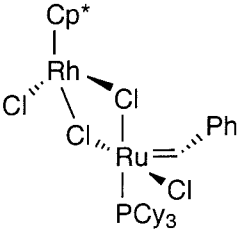

(1.8)

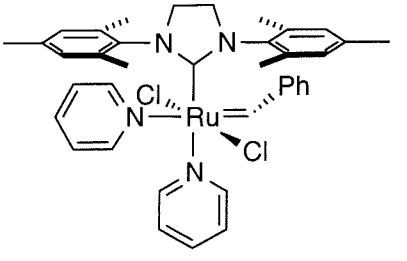

(1.9)

(Figure 5).[25] These "slow" initiators generally contain chelating or other strongly coordinating ligands, which are believed to limit the formation of open coordination sites at the ruthenium center.

Figure 5. Catalysts Exhibiting "Slow" Initiation Rates.

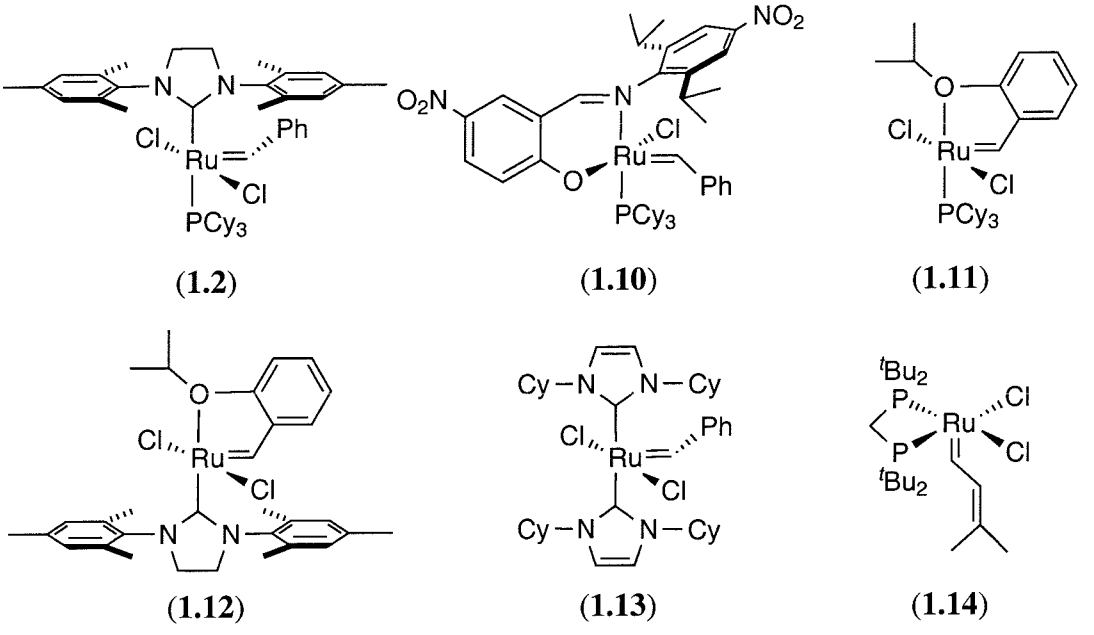

Mass Spectrometric Studies

In solution, it is difficult to obtain absolute rate constants for the steps that follow phosphine dissociation, because none of the intermediates – **1.4**, **1.3a**, or **1.5** – can be isolated or even observed spectroscopically. However, Chen and coworkers have developed a mass spectrometric technique for directly measuring the reactivity of intermediate **1.4** in the gas phase.[5] Complex **1.4** is generated *in situ* by tuning the tube lens potential such that it induces loss of a single PCy_2R ligand from the electrosprayed complex $(PCy_2R)_2(Cl)_2Ru{=}CHPh$ [R = $CH_2CH_2NMe_3^+$]. In general, the reaction rates of **1.4** in the gas phase are accelerated by a factor of 10^4 relative to those in solution, predominantly due to ion-dipole interactions.[5b]

Interestingly, the mass spectrometric studies reveal many similarities between the reactivity of intermediate **1.4** in the gas phase and that of catalyst **1.1** in CD_2Cl_2 solution. These results suggest that the reactivity and selectivity of **1.1** in solution is dominated by the k_2 and k_3 terms, rather than by initiation (k_1). The gas phase studies show complex **1.4** reacts with norbornene almost 150 times faster than with cyclopentene, and the authors attribute this result to the reversibility of metallacycle formation in the latter reaction.[5b] The kinetic product of the reaction between **1.4** and 1-butene is the propylidene, and the kinetic selectivity for propylidene formation in the gas phase is comparable to that observed for **1.1** in solution.[5b] Finally, Chen and coworkers note that the mixed halide species $(PCy_2R)(Cl)(I)Ru{=}CHPh$ reacts slowly with olefinic substrates as compared to the analogous di-chloride adduct.[5b] This result is consistent with our solution phase studies which suggest that k_2 for iodide-substituted ruthenium benzylidenes is significantly lower than that for the analogous di-chloride complexes.[3,4a]

Chen and coworkers have investigated the reactivity of a series of *para*-substituted benzylidenes $(PCy_2R)(Cl)_2Ru{=}CH(p\text{-}C_6H_4X)$ [X = H, F, CO_2Me, Me, ^tBu, OMe] with 1-butene using their mass spectrometric technique. A Hammett ρ value of $+0.69 \pm 0.01$ is observed, indicating that the reaction rates are faster for benzylidenes containing electron withdrawing substituents.[5a] Interestingly, *no* linear correlation between the σ^+ electronic parameter and reaction rate is observed for the same series of substituted benzylidenes in CD_2Cl_2 solution.[1] These conflicting results are presumably due to competing effects of benzylidene substitution on k_1 and k_2 in these systems.[26] Chen and coworkers also report an inverse secondary kinetic isotope effect ($k_H/k_D = 0.80 \pm 0.03$) for the reaction of $(PCy_2R)(Cl)_2Ru{=}CHEt$ with styrene and styrene-d_8. Based on these results, they conclude that the metallacyclobutane (**1.5**) is a transition state rather than a discrete intermediate along the olefin metathesis reaction coordinate in these systems.[5a]

Catalyst Activity

The metathesis activity of a ruthenium alkylidene can be defined as the rate of catalytic turnover (as measured by the disappearance of an alkene starting material or the appearance of an olefinic product) in a catalytic olefin metathesis reaction. The most

common reaction used to evaluate catalyst activity is the ring opening metathesis polymerization of cyclooctadiene, and the kinetics of this polymerization have been measured for a variety of neutral and cationic ruthenium alkylidenes.[4b,11,20,24,25a] Unfortunately, a direct comparison of these studies is impossible, because the polymerizations have all been carried out under different reaction conditions. However, in general, the fastest reaction rates are observed for complex **1.2**,[11] the di-cationic *cis*-phosphine adduct **1.15**,[25a] and the bimetallic *N*-heterocyclic carbene complex **1.16** (Figure 6).[24]

The rates of catalytic reactions are critical for some applications, but the utility of a metathesis catalyst is also dependent on the scope of substrates with which it reacts. As a result, the reactions of ruthenium alkylidenes with "difficult" olefinic substrates (*i.e.*, substrates of traditionally low reactivity) can also be used to evaluate metathesis activity. The intermolecular cross metathesis of methyl acrylate with an unfunctionalized olefin serves as an excellent "litmus test" for catalytic activity. Complex **1.1** is a poor catalyst for this reaction, and high ruthenium loadings (> 20 mol%) are required to achieve low (< 45%) yields of cross-products.[27] In contrast, the highly "active" catalysts **1.2** and **1.17**[28] produce high (> 90%) yields of product in the presence of only 5 mol% of ruthenium.[29]

Figure 6. Catalysts Exhibiting High Catalytic Activity.

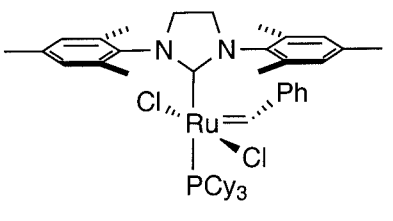

(1.2)

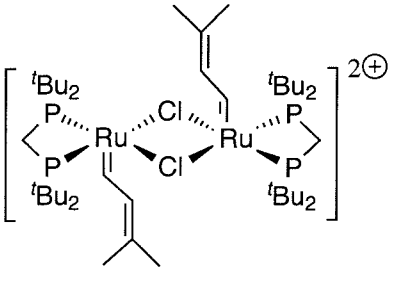

(1.15)

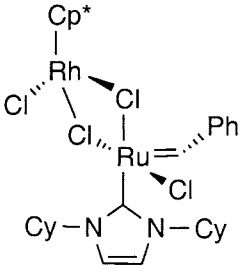

(1.16)

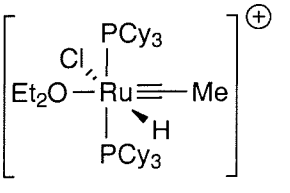

(1.17)

Part III. Mechanism of Decomposition

Introduction. Olefin metathesis activity is not only dependent on the rates of initiation and propagation of catalytic metathesis reactions, but also on the stability of the catalysts under the reaction conditions. As a result, understanding the decomposition mechanisms available to ruthenium alkylidenes is critical to the development of new catalysts with improved properties. This section highlights some important aspects of the decomposition pathways of **1.1**, **1.2**, and their derivatives.

Decomposition in Air. The complexes **1.1** and **1.2** are stable for weeks in the presence of water, and are air-stable for months in the solid state. However, in solution, alkylidene **1.1** and its analogues react with O_2 to produce tricyclohexylphosphine oxide, benzaldehyde, and a mixture of unknown ruthenium products.[30,31] The phosphine oxide is generated by the oxidation of dissociated PCy_3, but the mechanism of aldehyde formation in these systems is poorly understood. Importantly, the higher air stability of **1.2** relative to that of **1.1**[32] is likely due to the lower rates of phosphine dissociation in the former complex.[4]

Decomposition in the Presence of Functional Groups. Ruthenium catalysts are generally described as "functional group tolerant" because they maintain catalytic activity in the presence of carboxylic acids, aldehydes, alcohols, ketones, and amides. However, catalysts **1.1** and **1.2** are deactivated by some functional groups, particularly those that readily coordinate to the ruthenium center. For example, both **1.1** and **1.2** decompose rapidly in the presence of nitriles, 1° amines, and carbon monoxide, and **1.1** undergoes reaction with H_2 to afford the ruthenium hydride complexes $(PCy_3)_2(Cl)Ru(H_2)(H)$ and $(PCy_3)_2(Cl)_2Ru(H)_2$.[33] Complexes **1.1** and **1.2** also react with 1° alcoholic solvents to produce carbonyl hydrides,[34] and with acidic chlorinated solvents (*e.g.*, $C_2H_4Cl_2$ and $C_2H_2Cl_4$) to afford the phosphonium salt, $HPCy_3Cl$ and a mixture of ruthenium decomposition products. Other solvents, including DMSO, DMF and CH_3CN, also promote the decomposition of **1.1** and **1.2**, but the products of these reactions have not been fully characterized.

Thermal Decomposition of Alkylidenes. Ulman and Grubbs have carried an investigation of the thermal decomposition of $(L)(Cl)_2(PR_3)Ru{=}CHR'$, and have shown that the ancillary ligands dramatically affect the decomposition rates in these systems.[35]

In general, the thermal stability of complexes containing *N*-heterocyclic carbene ligands is 1-2 orders of magnitude higher than that of the analogous bis-phosphine adducts. In addition, the thermolytic half-life ($t_{1/2}$) increases from minutes to days at 55 °C when the R' substituent is varied from CO_2R to Ph ($t_{1/2}$ for R' = Ph > alkyl > H > CO_2R).[14,35]

The decomposition of the propylidene complex $(PCy_3)_2(Cl)_2Ru{=}CHEt$ (**1.18**) proceeds by second order kinetics and is inhibited by the addition of free PCy_3. The major products observed in solution after thermolysis of **1.18** are PCy_3, *trans*-3-hexene, and a mixture of ruthenium hydrides. Based on this data, Ulman and Grubbs propose that alkylidene decomposition proceeds by phosphine dissociation followed by the bimolecular coupling of two equivalents of complex **1.4** (Figure 5). Notably, this mechanism implies a direct correlation between the rate of thermal decomposition and that of phosphine dissociation in **1.18**.[36]

Figure 7. Mechanism of Decomposition of Complex **1.18**.

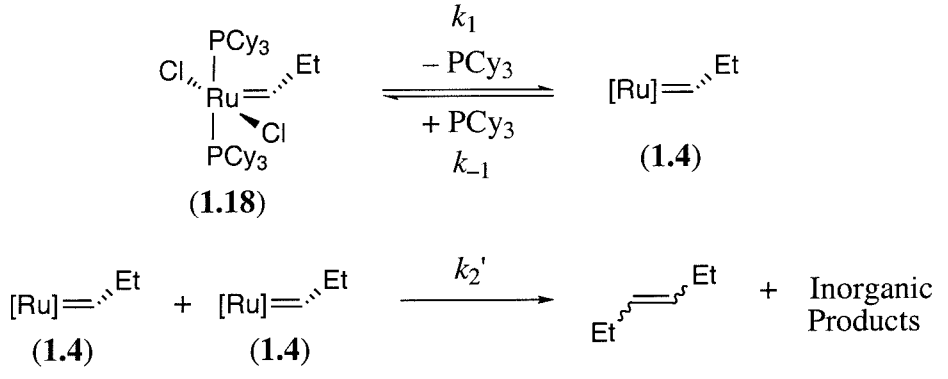

Thermal Decomposition of Methylidenes. In contrast to complex **1.18**, the methylidene $(PCy_3)_2(Cl)_2Ru{=}CH_2$ (**1.6**) decomposes according to first order kinetics, and its decomposition is not inhibited by the addition of free phosphine.[35] The thermolytic decomposition products include free PCy_3 and a mixture of ruthenium products, and ethylene is *not* observed in the reaction mixture.[37] Deuteration of the methylidene ligand leads to the incorporation of deuterium into the PCy_3, suggesting that the decomposition of **1.6** may proceed by phosphine activation.[35] The authors note that the first order

kinetics associated with the decomposition of **1.6** suggest that methylidene decomposition cannot be curtailed by dilution.

Part IV. Olefin Metathesis Intermediates[38]

Intermediate 1.4. The four-coordinate 14-electron intermediate **1.4** is generated upon dissociation of phosphine from the square pyramidal species $(L)(PR_3)(X)_2Ru{=}CHR'$. The reactivity of complex **1.4** with free phosphine, olefinic substrates and/or another equivalent of **1.4** is critical to determining the activity and longevity of these metathesis catalysts. Complex **1.4** has not been observed by ^1H NMR spectroscopy in solutions of **1.1** or **1.2**, indicating that the k_{-1}/k_1 ratio (K_{eq}) is at least 10^2.[39] As described above, Chen and coworkers have directly accessed intermediate **1.4** in the gas phase by selective removal of a phosphine ligand from the complexes $(PCy_2R)_2(Cl)_2Ru{=}CHPh$.[5] These mass spectrometric measurements provide the first direct (non-kinetic) evidence for the existence of complex **1.4**, but they provide no information concerning its structure.

Figure 8. Synthetic Analogues of Intermediate **1.4**.

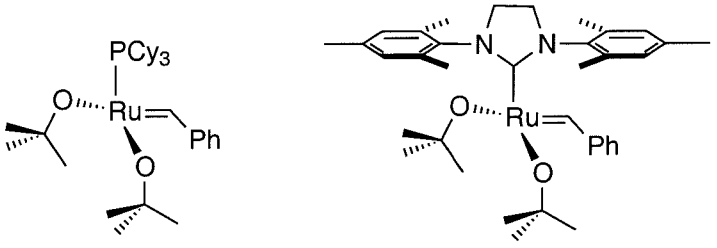

(1.19) **(1.20)**

The complexes $(L)(O^tBu)_2Ru{=}CHPh$ [L = PCy_3 (**1.19**) or $IMesH_2$ (**1.20**)] (Figure 8) have been prepared as models for intermediate **1.4** and are described in detail in Chapter 4.[40] X-ray crystallography reveals that complex **1.19** assumes a trigonal pyramidal geometry, with the phenyl group of the benzylidene occupying the open

coordination site below the trigonal plane.[40] This structure suggests that olefinic substrates may bind in the coordination site below the X–Ru–X plane (X = alkoxide or halide), and that benzylidene rotation may serve as a barrier to olefin coordination in **1.19**, **1.20** and **1.4**. Interestingly, the ^{1}H NMR spectra of **1.19** and **1.20** indicate that rotation about the [Ru]=C_α bond (benzylidene rotation) and about the C_α–C_β bond (phenyl group rotation) are both fast down to –120 °C.[41] Furthermore, *N*-heterocyclic carbene rotation in complex **1.20** is fast at room temperature.[41] These low rotational barriers suggest that complex **1.4** possesses relatively little structural rigidity, which may have important implications for the design of stereoselective olefin metathesis catalysts.

Intermediate 1.3a. The olefin adduct **1.3a** is a second proposed intermediate along the metathesis reaction coordinate. Three potential structures of this complex have been suggested in the literature and are summarized in Figure 9. The first possibility, complex **A**, involves olefin binding below the Cl–Ru–Cl plane, in the coordination site vacated by the departed phosphine ligand. This structure was discounted in early mechanistic studies of the ruthenium catalysts $(PR_3)_2(X)_2Ru{=}CHCH{=}C(Ph)_2$ because of perceived difficulties in achieving microscopic reversibility.[3] However, more recent calculations in the Chen group[5a] as well as in our group[42] have implicated **A** as a low energy intermediate in metathesis reactions catalyzed by **1.1**, **1.2**, and their derivatives. As summarized in Figure 10, both of these computational studies show that microscopic reversibility is readily accommodated by a mechanism that involves "swinging" of the metallacyclobutane moiety through the Cl–Ru–Cl plane.[5a,42]

Figure 9. Possible Geometries of Intermediate **1.3a**.

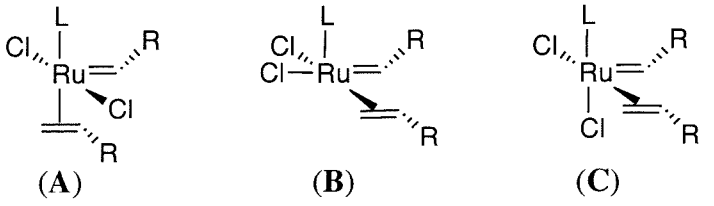

Figure 10. Mechanism Involving Olefin Complex **A** and "Swinging" Metallacycle.

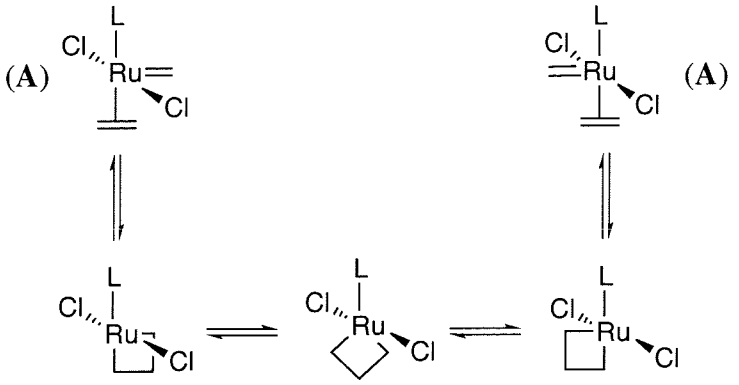

Snapper and coworkers have isolated the only reported example of a ruthenium alkylidene/olefin adduct by the reaction of **1.1** with a functionalized cyclobutene (Figure 11).[43] This olefin complex (**1.21**) has been fully characterized by X-ray crystallography, and assumes geometry **A**, with the olefin coordinated in the site vacated by the phosphine ligand. This intramolecular chelate serves as a viable catalyst for olefin metathesis reactions although it initiates significantly slower than complex **1.1**. As described above,

Figure 11. Ruthenium Olefin Adducts.

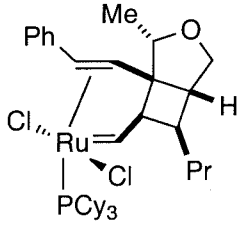

(**1.21**)

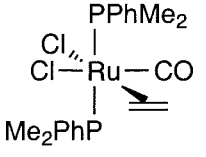

(**1.22**)

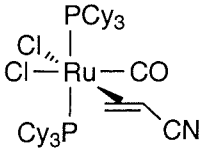

(**1.23**)

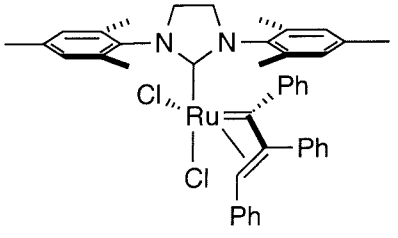

(**1.24**)

geometry **A** is also supported by the solid state structure of complex **1.19**, which shows an open coordination site below the Cl–Ru–Cl plane.[40]

A second possible geometry of the ruthenium-olefin adduct **1.3b** involves a *trans* to *cis* isomerization of the chloride ligands within Cl–Ru–Cl plane to produce complex **B** (Figure 9). Geometry **B** was favored in the early mechanistic investigations by Dias *et al.* because it readily accommodates microscopic reversibility (Figure 12). Structure **B** is also supported by a quantum molecular dynamics study of olefin metathesis reactions catalyzed by analogues of **1.1**.[6] Importantly, the *trans/cis* isomerization of halide ligands is well-precedented in ruthenium alkylidenes that are closely related to **1.1** and **1.2**.[44]

Figure 12. Mechanism Involving Olefin Adduct **B**.

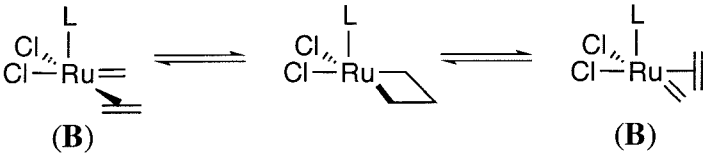

The complexes $(PR_3)_2(Cl)_2(CO)Ru(CH_2{=}CHR')$ [PR_3 = PMe_2Ph , R' = H (**1.22**) and PR_3 = PCy_3, R' = CN (**1.23**)] (Figure 11) have been proposed as relevant models for the olefin adduct **B**.[3] These compounds contain a CO in place of =CHR ligand; however, the π-acidity of carbon monoxide can render it a good substitute for an alkylidene at electron rich metal centers.[3] The geometries of **1.22** and **1.23** have been unambiguously assigned by NMR spectroscopy and/or X-ray crystallography, and both compounds assume structures that are analogous to that of **B**, except that they contain an additional phosphine ligand.[45,46] The solid state structure of $(PCy_3)(O^tBu)_2Ru{=}CHPh$ (**1.19**) also may have some relevance to olefin complex **B**. The crystal structure of **1.19** shows the beginning of a *trans/cis* isomerization of the alkoxide ligands, and the O–Ru–O angle is only 133.19°.[40] (In contrast, the Cl–Ru–Cl angle in **1.1** is 168.2°).[34]

A final possible structure of intermediate **1.3a** involves another *cis/trans* isomerization of the halide ligands to produce the olefin adduct **C** (Figure 9). DFT calculations show complex **C** as the lowest-lying intermediate along the ruthenium olefin

metathesis reaction coordinate.[5a] Additionally, modeling studies suggest that an intermediate of geometry **C** would account for the observed stereoselectivities in asymmetric ring closing metathesis reactions catalyzed by chiral derivatives of **1.2**.[47] Once again, the *trans/cis* isomerization of halide ligands is well-precedented,[44] and isomerization to produce **C** might be favored (relative to that producing **B**) due to the relatively large trans influence of the alkylidene ligand.[48] However, the any mechanism involving intermediate **C** requires significant motion of the chloride ligands about the metal center in order to accommodate microscopic reversibility (Figure 13).

Figure 13. Mechanism Involving Olefin Adduct **C**.

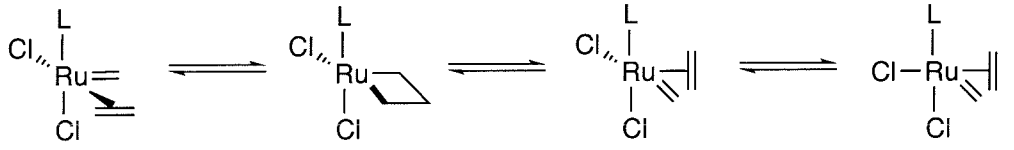

The viability of structure **C** is supported by the recently reported η^3-vinylcarbene complex **1.24** (Figure 9).[49] Complex **1.24** is prepared by the reaction of **1.2** with diphenylacetylene, and this phosphine-free species shows a *trans/cis* isomerization of the chloride ligands relative to the starting material. X-ray crystallographic analysis of **1.21** indicates that one chloride ligand is *trans* to the *N*-heterocyclic carbene and while the other is *trans* to the coordinated olefin. Interestingly, **1.24** is a poor catalyst for olefin metathesis reactions.[49]

Intermediate 1.5. The metallacyclobutane **1.5** is a final proposed intermediate in ruthenium-catalyzed olefin metathesis, and the formation and breakdown of **1.5** is generally believed to be the stereoselectivity-determining step in these reactions. Metallacyclobutane complexes of early transition metals are well-known, and, for example, metathesis-active metallacyclobutanes of titanium,[50] molybenum[51] and tungsten[51] have been reported. X-ray crystallographic analysis shows that titanacyclobutanes generally assume a planar structure,[50] while Mo and W metallacycles can be either planar or puckered, depending on the nature of the ring substituents and the

ancillary ligands.[51] DFT calculations of the reaction between $(PH_3)_2(Cl)_2Ru{=}CH_2$ and ethylene show the metallacyclobutane as a discrete intermediate along the reaction coordinate, and suggest that **1.5** adopts an approximately planar geometry.[5a,42] However, ruthenium(IV) metallacyclobutanes have never been isolated or observed during olefin metathesis reactions of $(L)(X)_2(PR_3)Ru{=}CHR'$.

A number of ruthenium(II) metallacyclobutanes have been described in the literature.[52] Most recently, Bergman and coworkers have prepared a 2,2-dimethyl-ruthenacycle (**1.25**) (Figure 14) by the reaction of $(SiP_3)(PMe_3)Ru(Cl)_2$ with 2 equivalents of Me_3CCH_2MgCl.[53] The crystal structure of complex **1.25** shows that the four-membered ring assumes a planar geometry with no close contacts between the methyl groups and the ruthenium center. This ruthenium(II) complex does not catalyze olefin metathesis reactions or undergo cleavage to produce a ruthenium alkylidene. Instead, the metallacycle undergoes reversible β-methyl transfer to produce free PMe_3 and a ruthenium methyl allyl complex, $(SiP_3)(Me)Ru(\eta^3\text{-}CH_2C(Me)CH_2)$. The ligand environment, metal oxidation state, and reactivity of **1.25** suggest that it does not serve as a good model for the metathesis intermediate **1.5**.

Figure 14. Bergman's Ruthenium(II) Metallacyclobutane.

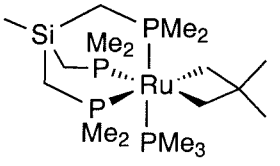

(1.25)

Part V. Thesis Research

This thesis describes recent contributions to our understanding of the mechanism and activity of ruthenium olefin metathesis catalysts. Chapter 2 details mechanistic studies of the catalysts $(L)(X)_2(PCy_3)Ru{=}CHR^1$ that were carried out in collaboration with Dr. Jennifer Love and Dr. Michael Ulman. These investigations probe the rate constants k_1, k_2 and k_{-1} as a function of the ligand environment, solvent, and incoming

olefinic substrate. Chapter 3 describes new synthetic methods, developed in collaboration with Dr. Jennifer Love, for the preparation of *N*-heterocyclic carbene-containing ruthenium benzylidenes. In addition, the barriers to benzylidene, phenyl, and *N*-heterocyclic carbene rotation in ruthenium olefin metathesis catalysts are discussed. Chapter 4 describes the synthesis, structure, and reactivity of a series of four-coordinate ruthenium benzylidenes which serve as models for the 14-electron olefin metathesis intermediate **1.4**. Finally, Chapters 5 and 6 describe the synthesis and reactivity of tris(pyrazolyl)borate ruthenium complexes.

References and Notes

(1) Schwab, P.; Grubbs, R. H.; Ziller, J. W. *J. Am. Chem. Soc.* **1996**, *118*, 100.

(2) Scholl, M.; Ding, S.; Lee, C. W.; Grubbs, R. H. *Org. Lett.* **1999**, *1*, 953.

(3) Dias, E. L.; Nguyen, S. T.; Grubbs, R. H. *J. Am. Chem. Soc.* **1997**, *119*, 3887.

(4) These results are detailed in Chapter 2, and several accounts of this work have appeared. (a) Sanford, M. S.; Love, J. A.; Grubbs, R. H. *J. Am. Chem. Soc.* **2001**, in press. (b) Sanford, M. S.; Ulman, M.; Grubbs, R. H. *J. Am. Chem. Soc.* **2001**, *123*, 749.

(5) (a) Adlhart, C.; Hinderling, C.; Baumann, H.; Chen, P. *J. Am. Chem. Soc.* **2000**, *122*, 8204. (b) Hinderling, C.; Adlhart, C.; Chen, P. *Angew. Chem., Int. Ed.* **1998**, *37*, 2685.

(6) Aagaard, O. M.; Meier, R. J.; Buda, F. *J. Am. Chem. Soc.* **1998**, *120*, 7174.

(7) Early mechanistic studies of the catalysts $(PR_3)_2(X)_2Ru{=}CHCH{=}C(Ph)_2$ suggested a small contribution (< 5%) from an "associative" mechanism (Scheme 1, Path B) [ref. 3], but we feel that this can be discounted based on more recent studies [ref. 4]. The "associative" mechanism was originally proposed on the basis of two observations: (i) a double exponential fit of the kinetic data and (ii) a non-zero intercept in a plot of k_{obs} versus $1/[PCy_3]$ for the catalytic ring closing metathesis of diethyl diallylmalonate. The double exponential behavior can be explained by competing *dissociative* reactions of the ruthenium catalyst with either the diene substrate or ethylene (generated throughout the RCM reaction). The second argument is not particularly compelling because the observed intercept of 2.42×10^{-4} was extremely close to zero.

(8) It is important to emphasize that the mechanism described in Figure 2 applies only to the complexes $(L)(X)_2(PR_3)Ru{=}CHR'$ and cannot be generalized to other ruthenium metathesis catalysts. It is possible, and even likely, that related catalysts operate in the same reaction manifold, but such conclusions should only be drawn after careful mechanistic study of the individual systems.

(9) The rate constants associated with metallacycle formation (k_3) and metallacycle break down (k_{-3}) also contribute to metathesis activity, however, these are not easily accessed by simple kinetic measurements.

(10) As outlined in detail in ref. 4, k_{-1}/k_2 (unlike k_1) is an olefin dependent term. Electron rich olefins, such as ethyl vinyl ether, provide close to a lower limit for this ratio.

(11) Bielawski, C. W.; Grubbs, R. H. *Angew. Chem., Int. Ed.* **2000**, *39*, 2903.

(12) Ulman, M.; Grubbs, R. H. *Organometallics* **1998**, *17*, 2484.

(13) Ulman, M.; Belderrain, T. R.; Grubbs, R. H. *Tetrahedron Lett.* **2000**, *41*, 4689.

(14) Ulman, M., Ph.D. Thesis, California Institute of Technology, Pasadena, CA, 2000.

(15) Kirkland, T. A.; Lynn, D. M.; Grubbs, R. H. *J. Org. Chem.* **1998**, *63*, 9904.

(16) The PBu_3 complexes as well as the *para*-substituted PPh_3 derivatives have been investigated by Jennifer A. Love. Love, J. A.; Grubbs, R. H. **2001**, unpublished results.

(17) Cucullu, M. E.; Li, C.; Nolan, S. P.; Nguyen, S. T.; Grubbs, R. H. *Organometallics* **1998**, *17*, 5565.

(18) Thermochemical studies have shown that Ru–NHC bond dissociation energies (BDE's) are 8-10 kcal/mol larger than the analogous $Ru–PR_3$ BDE's. This data is consistent with the observation that the NHC ligands do not dissociate appreciably in **1.2** and related compounds. Huang, J.; Schanz, H.-J.; Stevens, E. D.; Nolan, S. P. *Organometalllics* **1999**, *18*, 2370.

(19) Ulman and Grubbs have also probed the effects of olefin substitution on the *selectivity* of the reactions between benzylidene **1.1** and olefinic substrates [ref. 12]. Unhindered terminal olefins, such as styrene, 1-hexene, and 4-methyl-1-pentene, react rapidly with **1.1** to produce a substituted benzylidene or alkylidene as the kinetic product. In contrast, β-branched olefins, such as 3-methyl-1-pentene and *tert*-butyl ethylene, react much more slowly with **1.1**, and produce only the methylidene $(PCy_3)_2(Cl)_2Ru{=}CH_2$.

(20) Dias, E. L.; Grubbs, R. H. *Organometallics* **1998**, *17*, 2758.

(21) Sanford, M. S.; Love, J. A.; Henling, L. M.; Day, M. W.; Grubbs, R. H. **2001**, manuscript in preparation.

(22) Chang, S.; Jones, L.; Wang, C.; Henling, L. M.; Grubbs, R. H. *Organometallics* **1998**, *17*, 3460.

(23) (a) Kingsbury, J. S.; Harrity, J. P. A.; Bonitatebus, P. J.; Hoveyda, A. H. *J. Am. Chem. Soc.* **1999**, *121*, 791. (b) Garber, S. B.; Kingsbury, J. S.; Gray, B. L.; Hoveyda, A. H. *J. Am. Chem. Soc.* **2000**, *122*, 8168.

(24) Weskamp, T.; Schattenmann, W. C.; Spiegler, M.; Herrmann, W. A. *Angew. Chem., Int. Ed.* **1998**, *37*, 2490.

(25) (a) Hansen, S. M.; Volland, M. A. O.; Rominger, F.; Eisentrager, F.; Hofmann, P. *Angew. Chem., Int. Ed.* **1999**, *38*, 1273. (b) Hansen, S. M.; Rominger, F.; Metz, M.; Hofmann, P. *Chem. Eur. J.* **1999**, *2*, 557.

(26) Investigations on the effects of benzylidene substitution on k_1 are currently underway. Love, J. A.; Grubbs, R. H. **2001**, unpublished results.

(27) Seshadri, H.; Lovely, C. J. *Org. Lett.* **2000**, *2*, 327.

(28) Stuer, W.; Wolf, J.; Werner, H.; Schwab, P.; Schulz, M. *Angew. Chem., Int. Ed.* **1998**, *37*, 3421.

(29) Chatterjee, A. K.; Morgan, J. P.; Scholl, M.; Grubbs, R. H. *J. Am. Chem. Soc.* **2000**, *122*, 3783.

(30) Dias, E. L., Ph.D. Thesis, California Institute of Technology, Pasadena, CA, 1997.

(31) Dias, E. L.; Grubbs, R. H. *Organometallics* **1998**, *17*, 2758.

(32) Scholl, M., Ph.D. Thesis, California Institute of Technology, Pasadena, CA, 2000.

(33) (a) Drouin, S. D.; Yap, G. P. A.; Fogg, D. E. *Inorg. Chem.* **2000**, *23*, 5412. (b) Olivan, M.; Caulton, K. G. *Inorg. Chem.* **1999**, *38*, 566.

(34) Trnka, T. M.; Henling, L. M.; Day, M. W.; Grubbs, R. H. **2000**, unpublished results.

(35) Ulman, M.; Grubbs, R. H. *J. Org. Chem.* **1999**, *64*, 7202.

(36) There is a qualitative relationship between k_1 and the rate of decomposition in these complexes, and current work is aimed at quantitating this effect. Love, J. A.; Sanford, M. S.; Grubbs, R. H. **2000**, unpublished results.

(37) Preliminary results indicate that the decomposition of $(IMesH_2)(PCy_3)(Cl)_2Ru{=}CH_2$ proceeds in an analogous manner to that of **1.6**. Love, J. A.; Sanford, M. S.; Grubbs, R. H. **2000**, unpublished results.

(38) The relevance of any of the intermediates described herein to the metathesis catalytic cycle must be considered in the context of the Halpern postulate: "compounds that are readily isolable are probably not true intermediates." Halpern, J. *Science* **1982**, *217*, 401.

(39) We observe peaks in the ^1H NMR spectrum of $(IMesH_2)(PCy_3)(I)_2Ru{=}CHPh$ that are preliminarily assigned as $(IMesH_2)(I)_2Ru{=}CHPh$ (Chapter 3). However, further studies are required in order to definitively assign these resonances. Love, J. A.; Sanford, M. S.; Grubbs, R. H. **2001**, unpublished results.

(40) These complexes are described in detail in Chapter 4, and a preliminary account of this work has been reported. Sanford, M. S.; Henling, L. M.; Day, M. W.; Grubbs, R. H. *Angew. Chem., Int. Ed.* **2000**, *39*, 3451.

(41) In contrast, benzylidene/phenyl rotation in **1.1** becomes slow (on the NMR time scale) at –78 °C, and benzylidene/phenyl rotation in **1.2** becomes slow at –10 °C. Furthermore, *N*-heterocyclic carbene rotation in **1.2** is slow even at 100 °C by ^1H NMR spectroscopy. These rotational barriers are discussed in detail in Chapter 3.

(42) Benitez, D.; Goddard, W. A.; Grubbs, R. H. **2000**, unpublished results.

(43) Tallarico, J. A.; Bonitatebus, P. J.; Snapper, M. L. *J. Am. Chem. Soc.* **1997**, *119*, 7157.

(44) For example, see: Bianchini, C.; Lee, H. M. *Organometallics* **2000**, *19*, 1833.

(45) Moers, F. G.; Langhout, J. P. *J. Inorg. Nucl. Chem.* **1977**, *39*, 591.

(46) Brown, L. D.; Barnard, C. F. J.; Daniels, J. A.; Mawby, R. J.; Ibers, J. A. *Inorg. Chem.* **1978**, *17*, 2932.

(47) Seiders, T. J.; Ward, D. W.; Grubbs, R. H. **2001**, unpublished results.

(48) Sanford, M. S.; Henling, L. M.; Grubbs, R. H. *Organometallics* **1998**, *17*, 5384.

(49) Trnka, T. M.; Henling, L. M.; Day, M. W.; Grubbs, R. H. **2001**, submitted to *Organometallics*.

(50) Lee, J. B.; Gajda, G. J.; Schaefer, W. P.; Howard, T. R.; Ikariya, T.; Straus, D. A.; Grubbs, R. H. *J. Am. Chem. Soc.* **1981**, *103*, 7358.

(51) Feldman, J.; Schrock, R. R. *Prog. Inorg. Chem.* **1991**, *39*, 1.

(52) Anderson, R. A.; Jones, R. A.; Wilkinson, G. *J. Chem. Soc., Dalton Trans.* **1978**, 446.

(53) (a) McNeill, K.; Anderson, R. A.; Bergman, R. G. *J. Am. Chem. Soc.* **1997**, *119*, 11244. (b) McNeill, K.; Anderson, R. A.; Bergman, R. G. *J. Am. Chem. Soc.* **1995**, *117*, 3625.

Chapter 2: Mechanism and Activity of Ruthenium Olefin Metathesis Catalysts[1]

Abstract

This chapter details the effects of ligand variation on the mechanism and activity of ruthenium-based olefin metathesis catalysts. A series of ruthenium complexes of the general formula $(L)(PR_3)(X)_2Ru{=}CHR^1$ have been prepared, and the influence of the substituents L, X, R, and R^1 on the rates of phosphine dissociation and initiation as well as overall activity for olefin metathesis reactions was examined. In all cases, initiation proceeds by dissociative substitution of a phosphine ligand (PR_3) with an olefinic substrate. All of the ligands L, X, R, and R^1 have a significant impact on initiation rates and on catalyst activity. The origins of the observed substituent effects as well as the implications of these studies for the design of new olefin metathesis catalysts and substrates are discussed in detail.

Introduction

Over the past decade, olefin metathesis has emerged as a powerful method for the formation of carbon-carbon double bonds.[2] In particular, the ruthenium-based catalyst $(PCy_3)_2(Cl)_2Ru{=}CHPh$ (**2.1**) (Figure 1)[3] has been used extensively in organic and polymer chemistry due to its high reactivity with olefinic substrates in the presence of most common functional groups.[4] The mechanism of olefin metathesis reactions catalyzed by **2.1** and its analogues has been the subject of intense experimental[1,5,6] and theoretical[7] investigation, with the ultimate goal of facilitating the rational design of new catalysts displaying superior activity, stability, and selectivity. Early mechanistic studies of the catalysts $(PR_3)_2(X)_2Ru{=}CHR$[1] established that phosphine dissociation is a critical step along the olefin metathesis reaction coordinate, and demonstrated that catalysts containing bulky and electron-donating phosphine ligands display the highest catalytic activity.[5a] This trend was explained by the increased *trans* effect of larger and more basic phosphines, which was believed to accelerate dissociation of the second PR_3 ligand and to stabilize the Ru(IV) metallacyclobutane intermediate.[5a]

On the basis of these important studies, we[8] and others[9,10] have developed a new class of ruthenium alkylidenes containing *N*-heterocyclic carbene (NHC) ligands, which are significantly larger and more electron donating than trialkyl phosphines.[11] The new complexes were prepared by substitution of a single PCy_3 ligand of **2.1** with an *N*-heterocyclic carbene to produce products of the general formula $(NHC)(PCy_3)(Cl)_2Ru{=}CHPh$. These "second generation" ruthenium olefin metathesis catalysts exhibit dramatically increased reactivity with olefinic substrates relative to the parent catalyst **2.1**. For example, in ring closing metathesis (RCM) and cross metathesis (CM) reactions, NHC-ruthenium complexes catalyze the formation of tri- and tetra-substituted olefins[8,12,13] as well as functionalized alkenes[14] in good to excellent yields. The NHC-complexes, particularly **2.8** and **2.14** (Figure 1), are also highly active catalysts for the ring opening metathesis polymerization of cyclooctadiene (COD).[15] In fact, the rate of COD polymerization catalyzed by **2.8** even surpasses that of electrophilic early transition metal-based catalyst systems.[16] The high activity of the NHC-catalysts was originally attributed to increased labilization of the phosphine due to the large *trans*-effect of the NHC ligands.[8–10] However, in a preliminary communication, we reported the

surprising result that phosphine dissociation in **2.8** is extremely slow relative to that in **2.1**.[1b]

We describe herein an extensive and systematic evaluation of the effects of ligand variation on the kinetics and mechanism of ruthenium catalyzed olefin metathesis reactions. A series of ruthenium complexes with the general formula $(L)(PR_3)(X)_2Ru{=}CHR^1$ have been examined, and the influence of the substituents L, X, R, and R^1 on the rate of phosphine exchange and on the kinetics of initiation and propagation in olefin metathesis reactions is described in detail. Based on this data, a detailed mechanism for ruthenium based olefin metathesis catalysis is presented. Finally, the implications of these studies for the design of new catalysts and substrates are discussed.

Figure 1. Ruthenium Catalysts **2.1** – **2.14**.

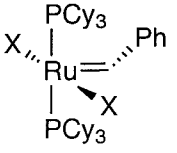

X = Cl (**2.1**)
X = Br (**2.2**)
X = I (**2.3**)

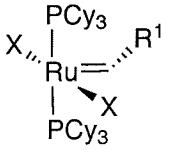

R^1 = H (**2.4**)
R^1 = CH_2CH_3 (**2.5**)

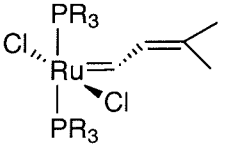

R = Cy (**2.6**)
R = Cp (**2.7**)

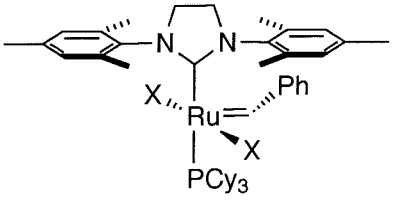

X = Cl (**2.8**)
X = Br (**2.9**)
X = I (**2.10**)

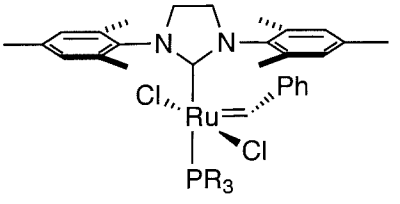

R = Ph (**2.11**)
R = Bn (**2.12**)

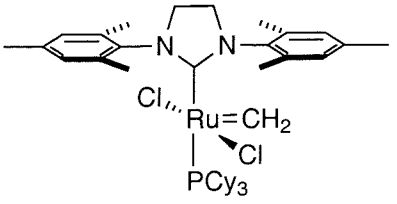

(**2.13**)

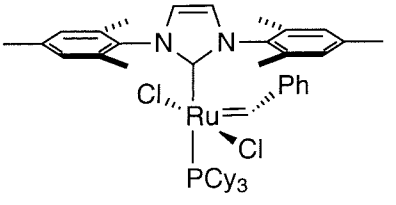

(**2.14**)

Results

Phosphine Exchange. A series of ruthenium catalysts of the general formula $(L)(PR_3)(X)_2Ru{=}CHR^1$ (Figure 1) were prepared in order to probe the effect of each substituent (X, L, R, and R^1) on catalyst reactivity. The bis-phosphine complexes (**2.1–2.7**) and the NHC-coordinated complexes (**2.8–2.14**) represent the two major classes of ruthenium metathesis catalysts developed in our group over the past several years. Initial investigations of catalysts **2.1–2.14** were focused on the ligand exchange of phosphine with olefinic substrate (Scheme 1). An understanding of this initial ligand substitution is critical because this reaction allows entry of **2.1–2.14** into the olefin metathesis catalytic cycle. In the two limiting cases, this substitution could occur according to an associative (Scheme 1a) or a dissociative (Scheme 1b) pathway. In the former pathway, olefin coordination to form an 18-electron intermediate (or transition state) (**A**) is followed by dissociation of phosphine, while in the latter, phosphine dissociation to generate a 14-electron intermediate (**B**) is followed by trapping with the olefinic substrate. Early mechanistic studies, involving analogues of catalysts **2.1–2.3**,[17] could not distinguish between these two pathways, but an associative exchange was proposed on the basis of a preference for the 18-electron over the 14-electron intermediate.[5a] It has proven difficult to investigate this ligand displacement directly in

Scheme 1

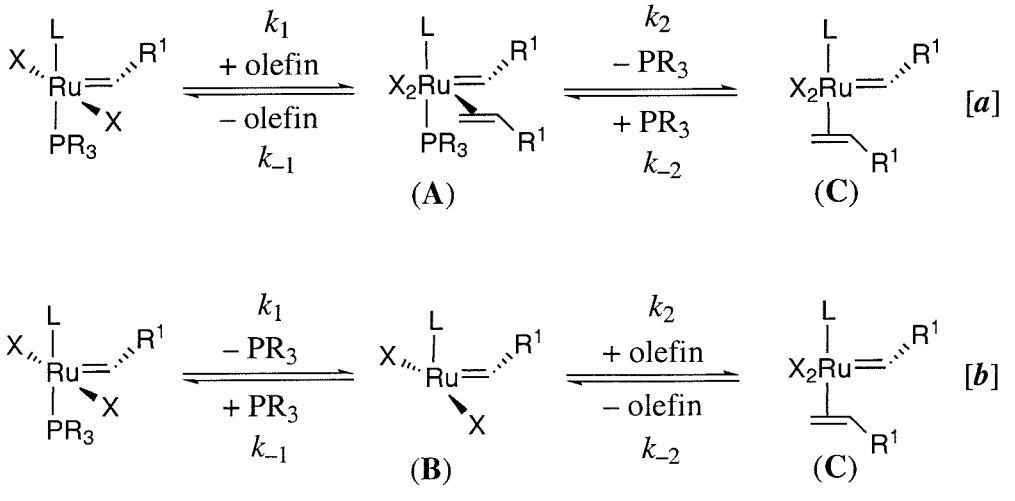

solution because the putative ruthenium-olefin adduct (**C**) has not been observed by spectroscopic methods.[18] As a result, we undertook studies using the degenerate exchange of free and bound PR_3 (Scheme 2) as a simple, but potentially relevant, model system for the phosphine/olefin substitution.

Scheme 2

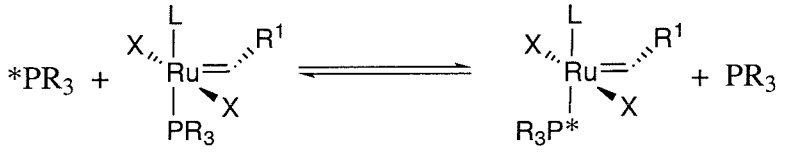

^{31}P NMR spectroscopy showed that phosphine exchange in catalysts **2.1–2.14** is relatively slow on the NMR time scale, and coalescence of the free and bound phosphine signals was not observed up to 80 °C in toluene-d_8.[19] Therefore, ^{31}P NMR magnetization transfer (MT) experiments were utilized to determine phosphine exchange rates in **2.1–2.14**. In these MT experiments, the free phosphine resonance was selectively inverted using a DANTE pulse sequence,[20] and ^{31}P NMR spectra were recorded after variable mixing times (ranging between 0.00003 and 50 seconds). The time dependent magnetization data was analyzed using the computer program CIFIT,[21] and rate constants (k_B) for the exchange between bound and free phosphine were obtained for all of the catalysts. This analysis also provided T_1 values for both free and bound phosphine, and independent T_1 analysis showed good agreement with the calculated values.

The rate constants and activation parameters for phosphine exchange in ruthenium complexes **2.1–2.14** are summarized in Table 1, and the same data are presented in descending order of rate constants in Table 2. The values of k_B at 80 °C for **2.1–2.14** range over *six orders of magnitude*! In fact, the rate constants at the high and low ends of the scale could not be measured by magnetization transfer at 80 °C, and were obtained by extrapolation from Eyring plots. For the olefin metathesis catalysts $(L)(PR_3)(X)_2Ru{=}CHR^1$, all of the ligands X, L, R, and R^1 were found to have a significant influence on the rate of phosphine exchange. The most striking ligand effect in this series involves the two most widely used ruthenium-based olefin metathesis catalysts: $(PCy_3)_2(Cl)_2Ru{=}CHPh$ (**2.1**) and $(IMesH_2)(PCy_3)(Cl)_2Ru{=}CHPh$ (**2.8**) ($IMesH_2$ = 1,3-

dimesityl-4,5-dihydroimidazol-2-ylidene). The simple substitution of one PCy_3 ligand of **2.1** with an *N*-heterocyclic carbene ($IMesH_2$) results in a *decrease* in phosphine exchange rate of over two orders of magnitude.[22] The large difference in k_B is particularly notable because **2.8** exhibits much higher olefin metathesis activity than **2.1**,[15] and the bulky and highly basic $IMesH_2$ ligand was originally designed to accelerate the phosphine dissociation event.

Table 1. Rate Constants and Activation Parameters for Phosphine Exchange.[a]

Catalyst	k_B (s^{-1}) 80 °C[b]	$\Delta H^{\ddagger}$ (kcal/mol^{-1})	$\Delta S^{\ddagger}$ (eu)	$\Delta G^{\ddagger}$ (298 K) (kcal/mol^{-1})
2.1	9.6 ± 0.2	23.6 ± 0.5	12 ± 2	19.88 ± 0.06
2.2	30 ± 2	23.1 ± 0.3	13 ± 1	19.11 ± 0.03
2.3	1660 ± 220[c]	19.0 ± 0.5	10 ± 2	16.12 ± 0.01
2.4[d]	——	——	——	——
2.5	19.4 ± 0.8	24.3 ± 0.6	16 ± 2	19.6 ± 0.1
2.6	0.33 ± 0.02	24 ± 1	8 ± 3	22.0 ± 0.2
2.7	1.42 ± 0.06	24 ± 1	11 ± 3	21.1 ± 0.1
2.8	0.13 ± 0.01	27 ± 2	13 ± 6	23.0 ± 0.4
2.9	0.52 ± 0.02	27 ± 2	15 ± 6	22.0 ± 0.4
2.10	29 ± 3	23 ± 4	12 ± 11	19.0 ± 0.5
2.11	7.5 ± 0.5[c]	21 ± 3	5 ± 9	19.6 ± 0.3
2.12	0.165 ± 0.006	27 ± 1	13 ± 4	22.7 ± 0.3
2.13[d]	——	——	——	——
2.14	0.03 ± 0.01[c]	25 ± 4	6 ± 11	24 ± 1

[a] Reactions were carried out in toluene-d_8 with 1 eq of Ru ([Ru] = 0.04 M) and 1.5 eq of free PR_3 (relative to bound PR_3). [b] Values for k_B are reported per coordinated PR_3 ligand. [c] Values for k_B at 80 °C were extrapolated from Eyring plots. [d] Values for k_B in complexes **2.4** and **2.13** could not be determined due to catalyst decomposition at the elevated temperatures required for these experiments.

Table 2. Rate Constants for Phosphine Exchange in Descending Order.[a]

Catalyst	k_B (s^{-1}) 80 °C[b]	$\Delta G^{\ddagger}$ (298 K) (kcal/mol^{-1})
2.3	1660 ± 220[c]	16.12 ± 0.01
2.2	30 ± 2	19.11 ± 0.03
2.10	29 ± 3	19.0 ± 0.5
2.5	19.4 ± 0.8	19.6 ± 0.1
2.11	7.5 ± 0.5[c]	19.6 ± 0.3
2.1	9.6 ± 0.2	19.88 ± 0.06
2.7	1.42 ± 0.06	21.1 ± 0.1
2.6	0.33 ± 0.02	22.0 ± 0.2
2.9	0.52 ± 0.02	22.0 ± 0.4
2.12	0.165 ± 0.006	22.7 ± 0.3
2.8	0.13 ± 0.01	23.0 ± 0.4
2.14	0.03 ± 0.01[c]	24 ± 1

[a] Reactions were carried out in toluene-d_8 with 1 eq of Ru ([Ru] = 0.04 M) and 1.5 eq of free PR_3 (relative to bound PR_3). [b] Values for k_B are reported per coordinated PR_3 ligand. [c] Values for k_B at 80 °C were extrapolated from Eyring plots.

More subtle changes of the phosphine and/or the *N*-heterocyclic carbene L-type ligands also have a significant impact on the rate of phosphine dissociation. For example, in the bis-phosphine complexes, substitution of tricyclohexyl with tricyclopentyl phosphine (catalysts **2.6** and **2.7**, respectively) leads to a four-fold increase in k_B. The result is intriguing because PCy_3 and PCp_3 are believed to have very similar steric and electronic parameters.[23]

In the *N*-heterocyclic carbene containing catalysts, replacing the $IMesH_2$ ligand (containing a saturated imidazolyl ring) with the IMes (IMes = 1,3-dimesitylimidazol-2-ylidene) ligand (containing an unsaturated imidazolyl ring) curtails k_B by close to an order of magnitude (complexes **2.8** and **2.14**, respectively). In addition, substitution of the PCy_3 ligand of **2.8** with PPh_3 (**2.11**) leads to a fifty-fold increase in the rate of phosphine exchange. However, when the PCy_3 of **2.8** is replaced with PBn_3 (**2.12**) (a

phosphine with steric and electronic properties that are intermediate between PPh_3 and PCy_3),[24] only a very small increase in k_B is observed.

Substitution of the X-type ligands also has a large influence on k_B. As X is changed from chloride to bromide to iodide (catalysts **2.1**, **2.2**, and **2.3**, respectively), the phosphine exchange rate increases by two orders of magnitude. The increase in k_B between **2.1** and **2.2** (a factor of about 3) is much less than that between **2.2** and **2.3** (a factor of approximately 55). The phosphine exchange rate in the di-iodide catalyst, $(PCy_3)_2(I)_2Ru$=CHPh (**2.3**) (1660 s^{-1} at 80 °C) is the largest observed for any ruthenium complex in this study. Halide substitution in the $IMesH_2$ ligated complexes (catalysts **2.8**, **2.9**, and **2.10**) shows almost identical trends in k_B as in the bis-phosphine series, and the di-iodide catalyst $(IMesH_2)(PCy_3)(I)_2Ru$=CHPh (**2.10**) exchanges phosphine almost 225 times faster than the di-chloride complex **2.8**. Notably, olefin metathesis activity in catalysts **2.1**–**2.3** is *inversely proportional* to k_B. For example, the relative rates (k_{rel}) for the RCM of diethyl diallylmalonate have been reported as approximately 20 (catalyst **2.1**), 15 (catalyst **2.2**), and 1 (catalyst **2.3**).[5a,17]

Finally, the nature of the substituent (R^1) on the carbene α-carbon also affects the dynamics of phosphine exchange. The magnitude of k_B for $R^1 = CH_3CH_2$ (**2.5**) > Ph (**2.1**) > $CHCH=C(CH_3)_2$ (**2.6**) >> H (**2.4**). In fact, the value of k_B for the methylidene complexes $(PCy_3)_2(Cl)_2Ru=CH_2$ (**2.4**) and $(IMesH_2)(PCy_3)(Cl)_2Ru=CH_2$ (**2.13**) could not even be measured using this technique because of catalyst instability at the temperatures required for magnetization transfer experiments.

Examination of the rate constant (k_B) as a function of phosphine concentration established a dissociative mechanism for this degenerate exchange reaction. For all of the catalysts **2.1**–**2.14**, k_B was independent (within error) of [PR_3] over a wide range of phosphine concentrations (0.04 M to 0.77 M). Activation parameters for phosphine dissociation in each complex were obtained from Eyring plots, and the results are summarized in Table 1. In addition, a representative Eyring plot (for complex **2.6**) is shown in Figure 2. The activation entropies ($\Delta S^{\ddagger}$) in these systems are all positive in sign and range between 5 and 16 eu. Typically, values of $\Delta S^{\ddagger}$ above 10 eu indicate a dissociative reaction mechanism.[25] The values of $\Delta H^{\ddagger}$ in catalysts **2.1**–**2.14** are all relatively large (> 19 kcal/mol) and positive in sign. Although less diagnostic, these

enthalpies of activation are also consistent with dissociative ligand exchange.[25] Interestingly, our experimental values for $\Delta H^{\ddagger}$ in catalysts **2.1** (23.6 ± 0.5 kcal/mol) and **2.14** (25 ± 4 kcal/mol) are in excellent agreement with ligand dissociation energies (ΔE) calculated by Herrmann for related model compounds (ΔE in $(PMe_3)_2(Cl)_2Ru{=}CH_2$ and $(NHC)(PMe_3)(Cl)_2Ru{=}CH_2$ (NHC = 1,3-dihydroimidazol-2-ylidene) were calculated to be 25.8 and 24.9 kcal/mol respectively).[10]

Figure 2. Eyring Plot for Phosphine Exchange in Complex **2.6**.

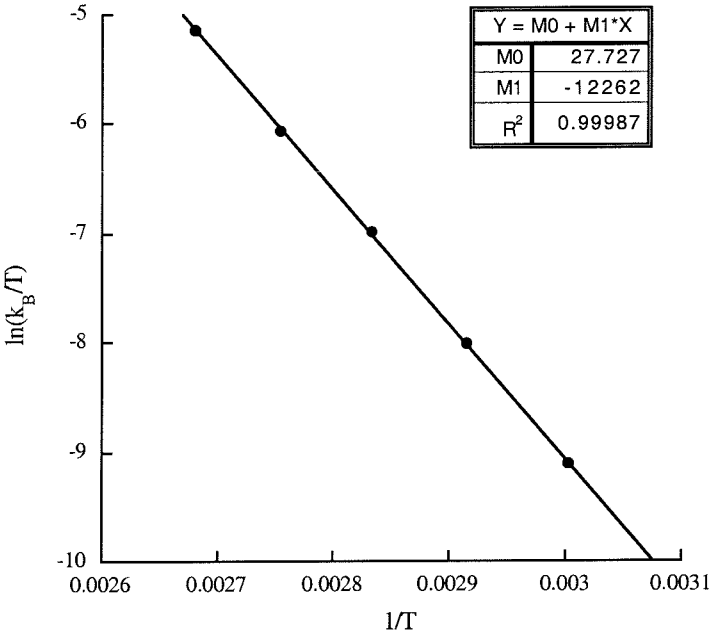

The magnetization transfer data described above suggests that phosphine substitution in complexes **2.1–2.14** proceeds by a dissociative mechanism. As summarized in Scheme 3, this mechanism involves initial phosphine dissociation to produce a four-coordinate, 14-electron intermediate $(L)(X)_2Ru{=}CHR^1$ (**B**). This intermediate has not been observed by ^{31}P or ^{1}H NMR spectroscopy, indicating that the equilibrium for phosphine dissociation lies very far towards the 16-electron starting material in these systems. In the degenerate exchange, this 14-electron intermediate

undergoes rapid trapping by free PR_3 to regenerate the starting complex. Importantly, recent results have shown that four-coordinate ruthenium carbenes similar to the proposed intermediate **B** can be stable under certain conditions.[18,26]

Scheme 3

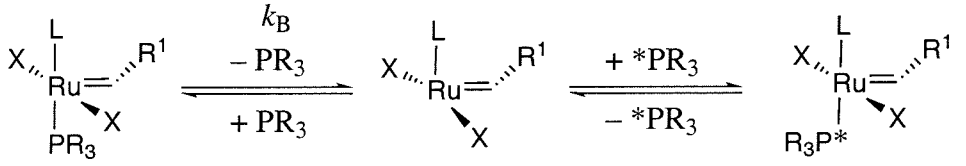

Initiation Kinetics. The phosphine exchange rates observed for complexes **2.1–2.14** are clearly not directly proportional to their olefin metathesis activities. In fact, an approximately inverse relationship between olefin metathesis activity and k_B is observed. As such, we considered that k_B might, instead, be related to the initiation rates of these catalysts. The initiation event involves the initial substitution of phosphine with olefinic substrate, which allows entry of the "dormant" species **2.1–2.14** into the olefin metathesis catalytic cycle. The kinetics of initiation can be measured by monitoring the stoichiometric reaction of a ruthenium complex with a judiciously chosen olefin, ethyl vinyl ether. The reaction of ruthenium carbenes with ethyl vinyl ether has been utilized as a method for quenching ring opening metathesis polymerizations.[27] This reaction is highly regioselective and results in the quantitative formation of a Fischer carbene complex (**D**) and an olefin capped polymer chain (Scheme 4). Ethyl vinyl ether offers the advantages that it reacts rapidly, quantitatively, and irreversibly with all of the catalysts

Scheme 4

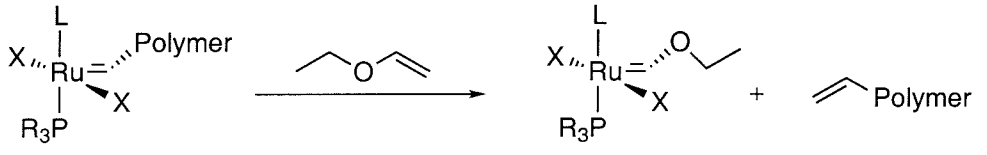

(D)

under investigation.[28] As a result, these reactions generally proceed with clean kinetics, and provide close to an upper limit for the initiation rates of catalysts **2.1–2.14**.[29]

Under saturation conditions, the initiation kinetics of catalysts **2.1–2.14** may be related to the rates of phosphine exchange in these systems. As shown in Scheme 1b, dissociative substitution of phosphine with olefinic substrate proceeds through the four-coordinate intermediate **B**. Application of the steady state approximation to **B** affords the rate expression shown in Eq 1. Under conditions where $k_{-1}[PR_3] << k_2[\text{olefin}]$ (saturation), this expression is reduced to Eq 2, and phosphine dissociation becomes the rate-determining step of the reaction. As described above, the rate constant for phosphine dissociation ($k_1 = k_B$) has already been determined for catalysts **2.1–2.14**.

$$\text{Rate} = k_1k_2[\text{Ru}][\text{olefin}]/\{k_{-1}[PR_3] + k_2[\text{olefin}]\} \quad \text{(Eq 1)}$$

$$\text{Rate} = k_1[\text{Ru}] \text{ when } k_{-1}[PR_3] << k_2[\text{olefin}] \quad \text{(Eq 2)}$$

Initiation Kinetics by NMR Spectroscopy. The reactions of catalysts **2.1–2.14** with ethyl vinyl ether were studied by ^{1}H NMR spectroscopy using a large excess of olefin (15 eq to 60 eq relative to [Ru]). The disappearance of the starting catalyst (0.017 M in toluene-d_8) was monitored as a function of time, and, unless otherwise noted, the reactions showed clean first order kinetics over at least three half lives. Initial investigations focused on the reactivity of the NHC-coordinated complexes **2.8–2.12** and **2.14**. For all of these catalysts, the initiation rate constant (k_{Init}) was *completely independent* of olefin concentration over a concentration range of 0.173 M to 1.02 M. Additionally, k_{Init} was insensitive to the structure of the vinyl ether substrate. For example, the values of k_{Init} for the reaction of **2.8** with ethyl vinyl ether, ethyl 1-propenyl ether, 2,3-dihydrofuran, and 3,4-dihydropyran[30] were identical within the error of the measurements (in each case, $k_{\text{Init}} = (4.6 \pm 0.4) \times 10^{-4}$ s^{-1} at 35 °C). These results demonstrate that saturation conditions (Eq 2) are achieved even at relatively low concentrations of olefinic substrate, and suggest that phosphine dissociation is the rate-determining step of these reactions. This can be confirmed by comparison of the k_{Init} values with the phosphine dissociation rates (k_B) of these catalysts. (Values of k_B were extrapolated to the appropriate temperature from the Eyring plots of the magnetization

transfer data). As shown in Table 3, k_{Init} and k_B are identical (within error) for each of the catalysts **2.8**–**2.12** and **2.14**.

The methylidene complex **2.13** was a notable anomaly in the NHC-coordinated catalyst systems. Extremely high temperatures (> 80 °C) were required in order to observe appreciable reaction of **2.13** with ethyl vinyl ether, implying that phosphine dissociation from this complex is extremely slow. In fact, under these forcing reaction conditions, the decomposition of **2.13** occurred on the same time scale as the initiation event, and, as such, only an upper limit for k_{Init} could be established for this complex ($k_{Init} \leq 1 \times 10^{-3}$ s^{-1} at 85 °C).

Table 3. ^{1}H NMR Initiation Kinetics.[a]

Catalyst	T (°C)	k_{Init} (s^{-1})	k_B (predicted) (s^{-1})[b]
2.1	10	$(1.0 \pm 0.1) \times 10^{-3}$	$(3.8 \pm 0.6) \times 10^{-3}$
2.2	0	$(1.1 \pm 0.1) \times 10^{-3}$	$(3.1 \pm 0.4) \times 10^{-3}$
2.3[c]	5	$(2.4 \pm 0.4) \times 10^{-3}$	1.7 ± 0.1
2.4	40	$(8.5 \pm 0.3) \times 10^{-3}$	——
2.5	0	$(5.4 \pm 0.5) \times 10^{-4}$	$(1.1 \pm 0.2) \times 10^{-3}$
2.6	25	$(1.0 \pm 0.1) \times 10^{-3}$	$(9 \pm 3) \times 10^{-4}$
2.7	25	$(1.5 \pm 0.3) \times 10^{-3}$	$(4.0 \pm 0.8) \times 10^{-3}$
2.8	35	$(4.6 \pm 0.4) \times 10^{-4}$	$(4 \pm 3) \times 10^{-4}$
2.9	35	$(2.0 \pm 0.1) \times 10^{-3}$	$(1.8 \pm 0.8) \times 10^{-3}$
2.10	0	$(2.8 \pm 0.2) \times 10^{-3}$	$(2 \pm 1) \times 10^{-3}$
2.11	10	$(3.3 \pm 0.2) \times 10^{-3}$	$(4 \pm 2) \times 10^{-3}$
2.12	50	$(5.4 \pm 0.5) \times 10^{-3}$	$(4 \pm 1) \times 10^{-3}$
2.13[c]	85	$\leq 1 \times 10^{-3}$	——
2.14	50	$(5 \pm 2) \times 10^{-4}$	$(1.0 \pm 0.6) \times 10^{-3}$

[a] Reactions were carried out in toluene-d_8, [Ru] = 0.017 M and [olefin] = 0.50 M (30 eq) [b] k_B (predicted) was determined by extrapolation of Eyring plots from the magnetization transfer data to the temperature of the initiation experiment for each catalyst. [c] Complexes **2.3** and **2.13** did not show clean first order kinetics.

Several of the bis-phosphine catalysts showed saturation kinetics by ^{1}H NMR spectroscopy. The initiation rate constants (k_{Init}) for the reactions of complexes **2.4** and **2.6** with ethyl vinyl ether were found to be independent of olefin concentration ([olefin] = 0.173 M to 1.02 M). Furthermore, k_{Init} in these systems showed excellent agreement with the predicted values of k_B (Table 3).[31] This data indicates that, in **2.4** and **2.6**, phosphine dissociation is the slow step of the reaction sequence. Notably, the bis-phosphine methylidene **2.4** initiated quite slowly relative to the other bis-phosphine catalysts (Table 2). However, initiation in catalyst **2.4** (k_{Init} = 8.5 x 10^{-4} s^{-1} at 40 °C) was still significantly more efficient than in the NHC methylidene **2.13**, and methylidene decomposition was not competitive with initiation at 40 °C in this system.

NMR initiation kinetics of the bis-phosphine catalysts **2.1**, **2.2**, **2.3**, **2.5**, and **2.7** showed an approximately linear dependence on olefin concentration. In these complexes, k_B is large (for **2.1**, **2.2**, **2.3**, **2.5**, and **2.7**, $k_B > 1$ s^{-1} at 80 °C), and phosphine dissociation is not rate determining at low concentrations of olefin. In fact, even up to the highest concentrations accessible by NMR spectroscopy (approximately 120 eq of ethyl vinyl ether relative to [Ru]), k_{Init} remained strongly dependent on [olefin]. Importantly, these NMR experiments are still consistent with a dissociative mechanism, since the values obtained for k_{Init} are well below those predicted by magnetization transfer for saturation conditions (Table 3).

Initiation Kinetics by UV-vis Spectroscopy. Because saturation could not be achieved by ^{1}H NMR spectroscopy, we studied initiation kinetics in catalysts **2.1**, **2.2**, **2.3**, **2.5**, and **2.7** by UV-vis spectroscopy. The reaction of these ruthenium complexes with ethyl vinyl ether was accompanied by a color change from purple/red to orange and a corresponding blue shift of the visible absorbance. This relatively weak band (extinction coefficients typically range from 700 to 1500 $dm^3 mol^{-1} cm^{-1}$) is likely due to metal to ligand charge transfer (MLCT) into the π^* orbital of the Ru=CHR^1 bond.[32] The MLCT band provides an excellent handle for following both the disappearance of starting material and the appearance of product. The reactions of catalysts **2.1**, **2.2**, **2.4**, and **2.7** (0.77 mM in toluene) with ethyl vinyl ether were each monitored at an appropriate wavelength (of the product), and the kinetics data showed clean first order fits over 5 half lives.[33] For each complex, the initiation rate constant was determined as a function of

Figure 3. Plot of k_{Init} versus [olefin] for Catalyst **2.1**.

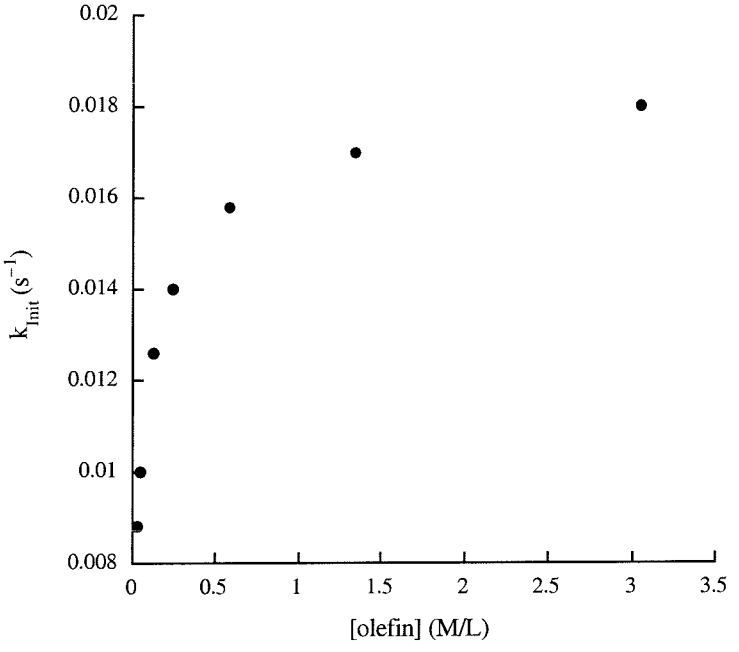

Table 4. UV-Vis Initiation Kinetics.[a]

Complex	T (°C)	Wavelength (nm)	k_{Init} (s^{-1})	k_B (predicted) (s^{-1})
2.1	20	484	0.016 ± 0.001	0.016 ± 0.002
2.2	20	486	0.057 ± 0.002	0.060 ± 0.005
2.5	20	354	0.028 ± 0.002	0.026 ± 0.003
2.7	30	468	0.074 ± 0.002	0.079 ± 0.003

[a] Reactions carried out in toluene; [Ru] = 0.77 mM and [olefin] = 0.58 M.

ethyl vinyl ether concentration ([olefin] = 0.024 M to 1–3 M), and a representative plot of k_{Init} versus [olefin] (for complex **2.1**) is shown in Figure 3. As expected for a dissociative substitution, k_{Init} becomes independent of [ethyl vinyl ether] at high concentrations where k_2[olefin] becomes much greater than $k_{-1}[PR_3]$. Most importantly, the values obtained for k_{Init} at saturation were identical to the predicted k_B's, within the error of the two measurements (Table 4).[34] The UV-vis data as well as the ^{1}H NMR studies described above confirm that dissociative substitution of phosphine for olefinic substrate (Scheme 1b) is the operative initiation pathway in all of the catalysts **2.1–2.14**.

Solvent Effects on Initiation. Changes of solvent were found to have a significant impact on the initiation rates of catalysts **2.1–2.14**. A systematic examination of catalyst initiation as a function of solvent was carried out using complexes **2.1** (by UV-vis spectroscopy) and **2.8** (by ^{1}H NMR spectroscopy). As summarized in Table 5, k_{Init} was found to be roughly proportional to the dielectric constant of the reaction medium. For both catalysts, the initiation rate increased by approximately 40% upon moving from toluene (ε = 2.38) to dichloromethane (ε = 8.9).[35] Both the magnitude and direction of this solvent effect are typical of dissociative ligand substitution reactions. For example, recent studies of dissociative exchange at neutral Pt(II) centers showed a three-fold increase in rate constant upon moving from toluene to CH_2Cl_2.[36] The rate acceleration is these systems is likely the result of increased stabilization of the four-coordinate intermediate **B** and/or of free PCy_3, since both are expected to be more polar than the ruthenium starting material. The stabilization of **B** may involve coordination of solvent to the electron deficient Ru(II) center (particularly in the case of THF and diethyl ether); however, no evidence of solvento-adducts has been detected by ^{1}H or ^{31}P NMR spectroscopy.[37] These solvent effects are particularly significant in light of recent gas phase mass spectrometric investigations of ruthenium olefin metathesis reactions.[6] While these studies provide extremely valuable information that cannot be obtained through solution studies, they do not take into account solvent interactions which may be critical, particularly when highly polar and/or charged intermediates are involved.

Table 5. Solvent Effects on Initiation.

Catalyst	Solvent	Dielectric Constant (ε)	k_{Init} (s^{-1})
2.1[a]	Pentane	1.84	0.013 ± 0.001
2.1[a]	Toluene	2.38	0.016 ± 0.001
2.1[a]	Diethyl Ether	4.34	0.022 ± 0.004
2.1[a]	CH_2Cl_2	8.9	0.021 ± 0.001
2.1[a]	THF	7.32	0.032 ± 0.004
2.8[b]	Toluene-d_8	2.38	$(4.6 \pm 0.4) \times 10^{-4}$
2.8[b]	CD_2Cl_2	8.9	$(6.1 \pm 0.2) \times 10^{-4}$
2.8[b]	THF-d_8	7.32	$(1.0 \pm 0.1) \times 10^{-3}$

[a] Reactions kinetics measured by UV-Vis spectroscopy (484 nm) at 20 °C with [Ru] = 0.77 mM and [olefin] = 0.58 M. [b] Reaction kinetics measured by ^{1}H NMR spectroscopy at 35 °C with [Ru] = 0.017 M and [olefin] = 0.50 M.

Estimation of k_{-1}/k_2. As summarized in Scheme 1b, the dissociative reactions of ruthenium complexes **2.1–2.14** with olefinic substrates are governed by two important factors. The first factor is the rate of phosphine dissociation [$k_1 = k_B = k_{Init}$ (saturation)] to produce the 14-electron intermediate **B**, and a second consideration is the reactivity of this intermediate. Complex **B** can be trapped by free PR_3 to regenerate the 16-electron starting material (at a rate proportional to k_{-1}), or it can bind olefinic substrate and undergo productive olefin metathesis reactions (at a rate proportional to k_2). An estimate of the ratio of these two rate constants (k_{-1}/k_2) can be obtained by manipulation of Eq 1. In the presence of a large excess of olefin and of free PR_3, a linear relationship between $1/k_{obs}$ and $[PR_3]/[olefin]$ (Eq 3) is obtained.

$$1/k_{obs} = k_{-1}[PR_3]/k_1k_2[olefin] + 1/k_1 \qquad \text{(Eq 3)}$$

Notably, two important assumptions were made in the derivation of Eq 3. First, this equation requires that olefin coordination is essentially irreversible ($k_2 >> k_{-2}$). This is obviously somewhat unrealistic since the reversibility of this step is crucial to

achieving catalytic turnover in olefin metathesis reactions. However, the use of ethyl vinyl ether (which undergoes a single, irreversible olefin metathesis event with **2.1**–**2.14**)[28] should improve the validity of the assumption in these systems. A second approximation inherent to this derivation is that all of the steps subsequent to olefin coordination (particularly metallacylobutane formation) are fast. This is likely a better assumption for the NHC-containing complexes (**2.8**–**2.14**) than for the bis-phosphine adducts (**2.1**–**2.7**). The former contain highly electron donating *N*-heterocyclic carbene ligands which are expected to better stabilize high oxidation state ruthenium intermediates. In systems where this approximation is not good, k_{-1}/k_2 is likely to be overestimated since additional k_3 and k_{-2} terms are not included. However, despite these caveats, we feel that Eq 3 provides a very simple and useful starting point for understanding the olefin metathesis reactivity of catalysts **2.1**–**2.14**.

^{1}H NMR kinetics of the reactions of the ruthenium complexes (0.017 mM in toluene-d_8) with ethyl vinyl ether were utilized to determine $1/k_{obs}$ as a function of [PR_3]/[olefin]. Both the concentration of PR_3 and the concentration of ethyl vinyl ether were varied, and the data showed the expected linear correlations for all of the catalysts investigated. The values obtained for k_1 [1/(intercept) of the linear curve fit] were generally close to k_B (predicted from the magnetization experiments). These values provide a third *independent* verification of k_1, and further confirm that a dissociative mechanism is operating in these systems.

The bis-phosphine complexes **2.1**, **2.2**, **2.3**, and **2.6** as well as the $IMesH_2$ catalysts **2.8**, **2.10**, **2.11**, and **2.12** were investigated in this study, and k_{-1}/k_2 for each complex is listed in Table 6. A comparison of compounds **2.1** and **2.8** is indicative of the dramatic differences between the two series of catalysts, and an overlaid plot of $1/k_{obs}$ versus [PCy_3]/[olefin] for **2.1** and **2.8** is shown in Figure 4. At 50 °C, k_{-1}/k_2 is 1.3 x 10^4 for complex **2.1** and 1.25 for complex **2.8**. The decrease of *four orders of magnitude* in k_{-1}/k_2 between **2.1** and **2.8** reflects a large (and general) increased selectivity for **2.8** to bind olefinic substrates in preference to PR_3. In both catalyst series, substitution of chloride with iodide results in a 100-fold increase in the k_{-1} to k_2 ratio. However, the relative difference in k_{-1}/k_2 for catalysts **2.3** and **2.10** remains four orders of magnitude. Also notable are the differences in k_{-1}/k_2 between **2.2** (8.2 x 10^4) and **2.10** (3.3 x 10^2).

Figure 4. $1/k_{obs}$ versus $[PCy_3]/[olefin]$ for Catalysts **2.1** and **2.8**.

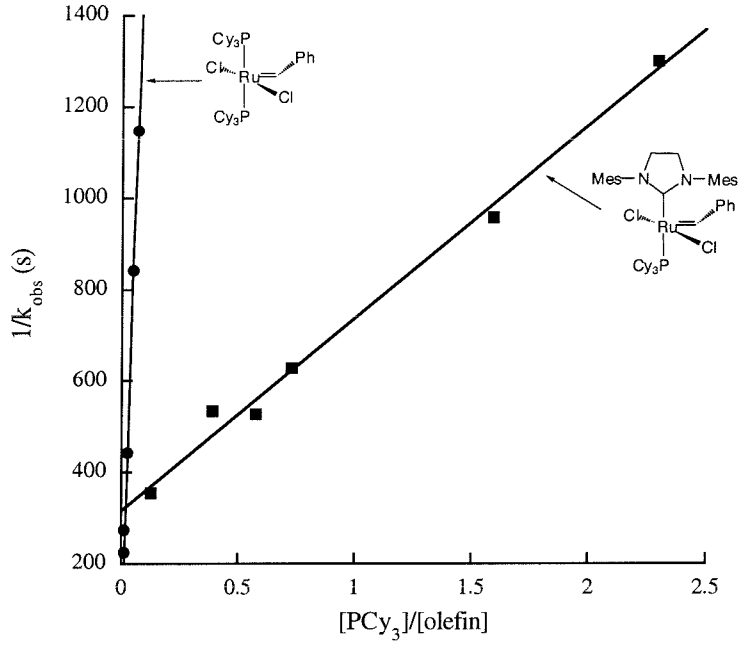

Table 6. Values of k_{-1}/k_2 for Selected Catalysts and Olefinic Substrates.[a]

Catalyst	Substrate[b]	T (°C)	k_{-1}/k_2
2.1	A	50	1.3×10^4
2.2	A	50	8.2×10^4
2.3	A	50	2.6×10^6
2.6	A	50	8.1×10^2
2.8	A	50	1.25
2.8	B	50	0.67
2.8	C	50	7.2
2.10	A	50	3.3×10^2
2.11	A	*25*	2.3
2.12	A	50	2.2

[a] Reaction kinetics measured by ^{1}H NMR spectroscopy with [Ru] = 0.017 M in toluene-d_8. [b] A = ethyl vinyl ether; B = 2,3-dihydrofuran; C = *tert*-butyl vinyl ether.

These catalysts dissociate phosphine at similar rates, and yet their k_{-1} to k_2 ratios differ by two orders of magnitude.

A final comparison can be made between the $IMesH_2$ benzylidenes **2.8** and **2.11**, which contain PCy_3 and PPh_3, respectively. The magnitude of k_2 is identical in these two catalysts, since they both produce the same intermediate – $(IMesH_2)(Cl)_2Ru{=}CHPh$ – upon dissociation of phosphine. As such, the values of k_{-1}/k_2 for **2.8** and **2.11** reflect the relative affinity of this intermediate for binding PCy_3 versus PPh_3. However, as shown in Table 5, these reactions were carried out at substantially different temperatures (due to the extremely high reactivity of **2.11**), so these values can only be compared qualitatively.[38] It is important to point out that ethyl vinyl ether is an electron rich olefin and reacts extremely rapidly with all of the catalysts **2.1–2.14**. Therefore, the data in Table 5 represent close to the lower limit of k_{-1}/k_2 for these systems. Nevertheless, we anticipate that the *relative* differences between these values for the catalysts should remain constant across a range of olefinic substrates.

In order to investigate k_{-1}/k_2 as a function of the incoming olefin, the reactions of catalyst **2.8** with the substituted vinyl ethers 2,3-dihydrofuran and *tert*-butyl vinyl ether were carried out. As expected, the sterically encumbered *tert*-butyl vinyl ether afforded a significantly larger k_{-1}/k_2 value (7.2) than the two smaller substrates.[39] However, attempts to carry out the analogous experiments with catalyst **2.1** were unsuccessful, due to extremely poor kinetic data. As a result, these experiments did not allow comparison of the relative magnitudes of k_{-1}/k_2 for the two catalysts between olefinic substrates.

Relative Catalyst Activities.[40] The ring opening metathesis polymerization of cyclooctadiene has been studied using the new NHC-catalysts **2.8**, **2.9**, **2.10**, **2.11**, and **2.13**. This reaction is frequently utilized as a standard for comparing the "activities" of single component olefin metathesis catalysts.[10,15,41] In these systems, the rate of polymerization reflects the efficiency of both the initiation and the propagation steps of the metathesis reaction. As a result, the relative contributions of initiation and propagation to the overall activity of the catalysts can be difficult to deconvolute. Furthermore, the presence of multiple catalytically active species throughout a given polymerization[42] often precludes a simple kinetic analysis of the data. However, this reaction still serves as a useful benchmark for comparing the *relative activities* of our

new ruthenium complexes. The ROMP of cyclooctadiene catalyzed by **2.8**, **2.9**, **2.10**, **2.11**, and **2.13** was carried out at 20 °C in CD_2Cl_2, and the reactions were monitored by ^1H NMR spectroscopy. In all cases, the disappearance of product was monitored over at least three half lives, and the data were fitted to a first order exponential. Although the first order fits were not excellent for all of the catalysts, this treatment of the data has been shown to provide a good approximation of the lower limit of metathesis activity in related systems.[10,43]

The di-iodide catalyst **2.10** shows a slightly higher rate of polymerization than the di-chloride complex **2.8** (k_{rel} = 1 for **2.8** and 1.4 for **2.10**). The small increase in rate does not directly correlate with the amount of catalytically active species formed, since **2.10** initiates almost quantitatively (as determined by the nearly complete conversion of starting benzylidene to a new alkylidene), while initiation of **2.8** is highly inefficient. This indicates that the propagating species formed upon phosphine dissociation from **2.10** is significantly less active for metathesis than the propagating species from **2.8**. This result is consistent with earlier studies of metathesis activity in the di-chloride and di-iodide bis-phosphine catalysts **2.1** and **2.3**.[5a,17] Catalyst **2.9** has an initiation rate intermediate between those of **2.8** and **2.10**, and is also expected to have an intermediate propagation rate. It is therefore noteworthy that **2.9** shows the same activity as **2.10** for COD polymerization (k_{rel} = 1.4), presumably due to the competing effects of initiation and propagation.

Of further interest is a comparison of the relative activities of **2.8** and **2.11**. Complexes **2.8** and **2.11** dissociate PR_3 to generate the same propagating species, so the rates of propagation in these two catalysts should be identical. However, catalyst **2.11** initiates more than 50 times faster than **2.8**, and is therefore expected to be an exceptionally fast olefin metathesis catalyst. Under the same conditions used to measure the reaction rate of **2.8**, the polymerization of COD catalyzed by **2.11** is complete within seconds of adding monomer. In fact, the loading of catalyst **2.11** must be reduced 50-fold (relative to that of **2.8**) in order to achieve similar rates of polymerization. These results demonstrate that, with the appropriate choice of catalyst, highly efficient polymerizations can be achieved at significantly lower catalyst concentrations.[44] In contrast, methylidene **2.13** reacts exceptionally slowly with cyclooctadiene, and the relative rate of

polymerization with this catalyst is over *four orders of magnitude lower* than that of catalyst **2.8**. This is a particularly significant observation because this complex is a crucial intermediate during ring closing and cross-metathesis reactions of terminal olefins. The initiation studies described above suggest that this result is due, in large part, to the slow rate of phosphine dissociation in catalyst **2.13**.

Table 7. Values of k_{rel} for the ROMP of COD with Selected Catalysts.[a]

Catalyst	[Ru] (mM)	COD : Ru	k_{rel}
2.8	5	300	1.0
2.9	5	300	1.4
2.10	5	300	1.4
2.11	0.05	30000	0.5
2.13	5	300	6×10^{-4}

[a] Reaction kinetics measured by ^{1}H NMR spectroscopy in CD_2Cl_2

Discussion

Mechanism of Ruthenium Catalyzed Olefin Metathesis Reactions. Based on all of the above data, we propose a general mechanism for olefin metathesis reactions catalyzed by **2.1–2.14**. As summarized in Scheme 5,[45] substitution of phosphine with olefinic substrate occurs in a dissociative fashion, to generate the four-coordinate intermediate **B**. Importantly, our results provide *no* evidence that an associative reaction pathway (involving the 18-electron olefin adduct **A**) contributes significantly to the metathesis reactions of any of these catalysts.[5a] Additionally, the data presented herein argue against a mechanism involving attack by phosphine on the carbene carbon to generate ylidic intermediates, as proposed by Hofmann and coworkers.[32] In the bis-phosphine systems (complexes **2.1–2.7**), the 14-electron intermediate **B** is formed frequently (k_1 is large). However, under our reaction conditions, the recoordination of free PR_3 is competitive with substrate binding ($k_{-1}/k_2 >> 1$). As a result, the active species

Scheme 5

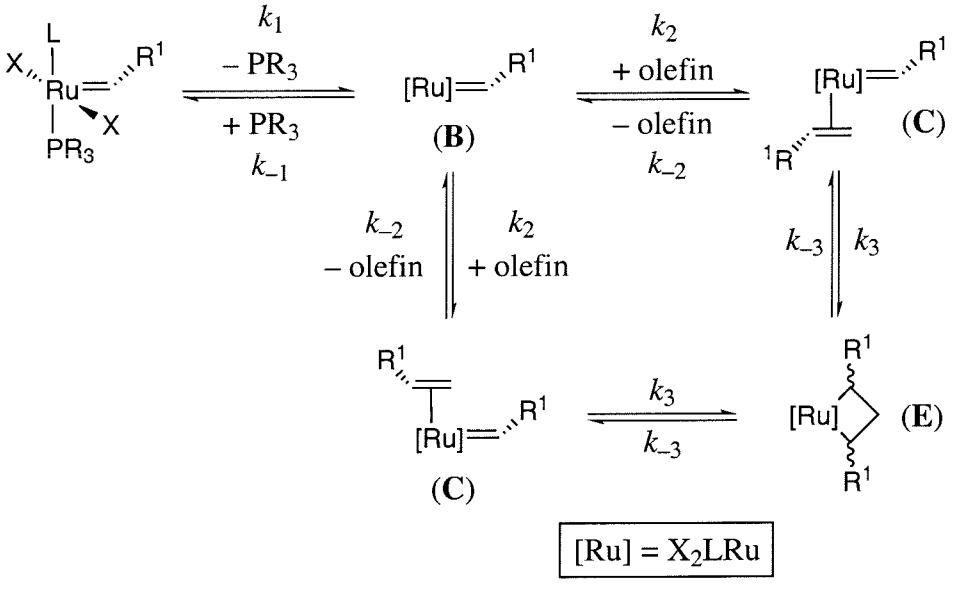

carries out few catalytic turnovers before being "quenched" with free PR_3. In contrast, the NHC complexes (**2.8–2.14**) dissociate phosphine relatively inefficiently (k_1 is small). However, once the phosphine dissociates, coordination of olefin is facile compared to re-binding of PR_3 ($k_{-1}/k_2 \sim 1$ and [olefin] is high). As such, the NHC complexes can perform multiple olefin metathesis events before they recoordinate phosphine and return to their resting state.

Notably, the catalytic cycle shown in Scheme 5 does not indicate stereochemistry about the ruthenium center for the important catalytic intermediates **C** and **E**. Several possibilities for the geometries of **C** and **E** have been proposed by our group[5] and by Chen and coworkers.[6] However, the current work provides no evidence to support or refute either of these possibilities.[46] Another mechanistic question which remains concerns the possibility that metallacyclobutane (**E**) is a transition state rather than an intermediate along the olefin metathesis reaction coordinate.[6] Once again, this question cannot be answered definitively based on the investigations described herein.

Ligand Effects on Olefin Metathesis Reactions. Although olefin metathesis reactions catalyzed by the complexes $(L)(PR_3)(X)_2Ru{=}CHR^1$ proceed according to the

same general mechanistic pathway, the ancillary ligands play a significant role in determining the relative rates of the individual steps along the reaction coordinate.

L–Type Ligand. The most important ligand effect in these systems involves the huge increase in olefin metathesis activity upon changing the L ligand from a phosphine to an *N*-heterocyclic carbene (*e.g.*, catalysts **2.1** and **2.8**, respectively). The high activity of **2.8** relative to **2.1** can be understood based on the k_{-1} to k_2 ratios of these two catalysts, which show that the $IMesH_2$ ligand increases selectivity for binding olefinic substrates over free phosphine by *four orders of magnitude.* This improved selectivity may be explained by the electronic properties of the NHC's, which are known to be excellent donor ligands relative to trialkyl phosphines.[11,47,48] Cavell and coworkers have compared a series of Pd(0)-olefin complexes containing either *N*-heterocyclic carbenes or phosphines as ancillary ligands.[49] ^1H and ^{13}C NMR as well as IR spectroscopic studies indicate that the electron donating NHC's promote and stabilize metal-to-olefin backbonding to a much greater extent than the phosphine ligands in these systems.[49] Cavell's study is consistent with our observations that the NHC-coordinated complexes **2.8–2.14** show increased affinities for π-acidic olefinic substrates relative to σ-donating PR_3. Additionally, the $IMesH_2$ catalyst, **2.8**, is much more active for the polymerization of COD than the IMes complex, **2.14**,[15] and the $IMesH_2$ ligand is a better electron donor than IMes.[11] Importantly, in addition to stabilizing the olefin complex **C**, electron donation from NHC's is expected to accelerate the oxidative addition required for metallacyclobutane formation.

The dramatic decrease in initiation upon substitution of phosphine ligands with *N*-heterocyclic carbenes is much more difficult to rationalize. X-ray crystallographic studies of these complexes suggest that this is not a ground state effect. A comparison of crystal structures reveals that the Ru-PCy_3 distance barely changes upon substituting the *trans* ligand from PCy_3 to IMes (the Ru–PCy_3 distances in **2.1** are 2.4097(6) and 2.4221(6) Å[50] and the Ru–PCy_3 distance in **2.14** = 2.419(3) Å).[9] The 640-fold difference in k_1 between these two catalysts may reflect different reorganizational energies associated with the transition states for phosphine dissociation. Alternatively, the variation in initiation rates may simply be the result of a steric effect. Although both PCy_3 and IMes (and $IMesH_2$) are large ligands, the distribution of steric bulk about the

ruthenium center is dramatically different in each case.[11] These differential steric distributions may lead to a destabilizing interaction in complexes **2.1–2.7** or a stabilizing interaction in **2.8–2.14** which changes the activation energy required for phosphine loss. We anticipate that future studies of k_1 as a function of NHC ligand (where the steric and electronic parameters of this ligand are varied substantially) will provide further insights into the origin of this important effect.

Phosphine Ligand (PR_3). Changing the phosphine ligand (PR_3) in the $IMesH_2$ coordinated catalysts has a dramatic effect on both catalyst initiation and on catalyst activity. For example, replacing the PCy_3 of catalyst **2.8** with PPh_3 (**2.11**) leads to an increase in k_1 of over two orders of magnitude. This effect may be related to the lower basicity of the PPh_3 ligand relative to PCy_3 (the pK_a's of the conjugate acids are 2.73 and 9.7, respectively),[51] since a less electron donating phosphine is generally expected to be more labile.[52] Interestingly, however, the PBn_3 complex **2.12** initiates at almost the same rate as complex **2.8**, despite the fact that PBn_3 (pK_a = 6.0) is significantly less basic than PCy_3.[51] This result clearly indicates there is not a linear correlation between phosphine pK_a and k_1, and the complexities of the steric and electronic changes resulting from phosphine variation in these systems are still under investigation. Importantly, the PPh_3 catalyst **2.11** polymerizes COD more than 50 times faster than the PCy_3 complex **2.8**.[44] A comparison of the k_{-1}/k_2 ratios for these two catalysts (k_{-1}/k_2 = 1.25 and 2.2 for **2.8** and **2.11**, respectively) indicates that this result is almost completely due to the improved initiation efficiency of **2.11**.

Halide Ligand (X). The halide ligands also have a significant impact on the initiation rates of the catalysts $(L)(PR_3)(X)_2Ru{=}CHR^1$. In both the bis-phosphine complexes (**2.1** and **2.3**) and the $IMesH_2$ complexes (**2.8** and **2.10**), changing the X-type ligands from chloride to iodide leads to an approximately 250-fold increase in initiation. (Changing from chloride to bromide results in a much smaller, three-fold increase in k_1). We believe that the increase in initiation is predominantly due to the increase in steric bulk upon moving from chloride to iodide. The ionic radii of Cl^- and I^- are 167 pm and 206 pm, and the covalent radii of Cl and I are 99 pm and 133 pm, respectively.[53] The larger size of the latter is expected to increase steric crowding at the ruthenium center, thus promoting PR_3 dissociation. Electronics may also play a role in these systems;

however, *cis* electronic effects on dissociative ligand substitution reactions are generally relatively small.[53] Notably, alkoxide X-type ligands are even larger and more electron donating than iodide ligands; in fact, alkoxides are often formally counted as XL ligands, donating *three* electrons to a metal center.[54] We have shown previously that replacing the chlorides of **2.1** with *tert*-butoxides results in the generation of $(PCy_3)(O^tBu)_2Ru{=}CHPh$ (which can be considered an analogue of **B**) and free PCy_3.[26] The stability of this four coordinate *tert*-butoxide adduct clearly demonstrates that the appropriate choice of X-type ligand can effectively promote complete phosphine dissociation.

While the di-iodo catalysts **2.3** and **2.30** initiate efficiently, their olefin metathesis activities are comparable to, or even lower than,[5] those of the parent di-chloride complexes. The moderate olefin metathesis activities of **2.3** and **2.10** are related to the k_{-1} to k_2 ratios in these systems. In both the bis-phosphine and the $IMesH_2$ catalyst series, moving from the di-chloride to the di-iodide complex leads to an approximately 100-fold increase in k_{-1}/k_2. The reasons behind this large shift in k_{-1}/k_2 are poorly understood at this time, since it is impossible to separate the effects of the two rate constants. One possible explanation involves the suggestion that olefin coordination requires a *trans* to *cis* isomerization of the X-type ligands.[5] This might be less favorable when the X-ligands are sterically large, and could lead to a decrease in k_2 for the di-iodo catalysts.

Carbene Ligand (R^1). The R^1 ligand also has a large influence on the initiation rates of these catalysts, and k_1 increases substantially as R^1 is changed from H (**2.4**) to $CHCH{=}C(Me)_2$ (**2.6**) to Ph (**2.1**) to CH_2CH_3 (**2.5**). Earlier studies of initiation in ruthenium olefin metathesis catalysts (using different methodology) showed similar trends in the initiation rate as a function of R^1.[3,5b] These results can be rationalized based on the steric and electronic features of the R^1 substituent. Bulky and electron donating R^1 groups (*e.g.,* alkyl) lead to higher initiation rates because they more effectively promote phosphine dissociation. In contrast, small and electronically neutral groups (*e.g.,* H) are less effective at labilizing the phosphine ligand.[5b] The effect of R^1 is significant because, unlike the other ligands, this substituent can change throughout an olefin metathesis reaction. An alkylidene moiety is generated after one turnover of a typical ring opening metathesis polymerization and becomes the propagating species. Similarly, a ruthenium

methylidene is generated upon initiation of ring closing and cross metathesis reactions as well as during the acyclic diene metathesis (ADMET) polymerization of terminal olefins.

It is particularly important to point out that the methylidene complexes **2.4** and especially **2.13** are *extremely poor initiators* for olefin metathesis reactions at ambient temperatures. Catalyst **2.13** is an active olefin metathesis catalyst in its phosphine free form, and multiple catalytic turnovers can be achieved when it is generated *in situ* from **2.8**. However, when $(IMesH_2)(Cl)_2Ru{=}CH_2$ is trapped with free PCy_3, it is essentially incapable of re-entering the olefin metathesis catalytic cycle. This is manifest in the extremely low activity of **2.13** in the polymerization of cyclooctadiene. Because of the slow initiation rates of **2.4** and **2.13**, the formation of these complexes should be avoided if at all possible. In many instances, substrate design can be utilized to limit the generation of methylidene intermediates.[55] Substitution of the X and/or PR_3 ligands of **2.4** or **2.13** should provide an additional means of improving the initiation efficiencies of these catalysts.

Implications for Olefin Metathesis Reactions. The results described herein have significant implications for the selection and implementation of current olefin metathesis catalysts, as well as for the design of new catalysts and substrates for olefin metathesis reactions.

Catalyst Loadings. A first consideration involves the catalyst loading required for a metathesis polymerization and/or an organic reaction. Lower catalyst loadings facilitate the development of more cost efficient and atom economical processes,[56] and make metathesis catalysts more attractive for processes in which residual metal contamination is undesirable. When catalyst initiation is inefficient (as for complex **2.8** and particularly **2.13**), the majority of catalyst added to a given reaction remains unused.[57] Faster initiation rates permit a decrease in catalyst loading while maintaining high catalytic olefin metathesis activity. For this reason, the new complexes **2.10** and **2.11** are excellent alternatives to **2.8** for wide variety of catalytic applications. These complexes maintain the superior activity and functional group tolerance of the parent catalyst **2.8** (in fact, the active species, $(IMesH_2)(Cl)_2Ru{=}CHPh$, for **2.11** is identical to that in **2.8**) but initiate almost 2 orders of magnitude faster. As shown in Table 6, the catalyst loading of **2.11**

can be lowered at least 50-fold relative to that of **2.8** to achieve similar levels of activity for the ROMP of cyclooctadiene.[44]

Kinetic Selectivity. Faster initiation rates also allow for catalysis at lower temperatures than were previously viable. Lowering the temperature is particularly advantageous for the development of selective olefin metathesis reactions. There is intense current interest in the selective formation of either *cis* or *trans* olefinic products, as well as in the development of chiral catalysts for the kinetic resolution of racemic olefins.[58,59] However, secondary metathesis events are known to occur readily in these systems and may erode the kinetic selectivity of the catalysts.[60] The development of catalysts that initiate and propagate olefin metathesis at lower temperatures should provide a versatile tool for the optimization of selectivity in metathesis reactions.

Catalyst Decomposition Rates. We believe that the initiation kinetics of catalysts **2.1–2.14** may also be related to the decomposition rates of these complexes. The thermal decomposition of complexes **2.1** and **2.5** has been studied in detail, and has been proposed to occur via phosphine dissociation followed by bimolecular coupling of two four-coordinate ruthenium fragments.[61] These results suggest that catalyst initiation and decomposition in these systems proceed through a common intermediate, **B**. In general, it has been observed that NHC-coordinated complexes exhibit dramatically improved thermal stabilities relative to their bis-phosphine analogues. For example, Nolan and coworkers have demonstrated that complex **2.14** shows no signs of decomposition after 1 hour at 100 °C in toluene-d_8.[62] (Under the same conditions, complex **2.1** is 75% decomposed.) This remarkable stability was originally attributed to steric and electronic stabilization of the 14-electron intermediate, (IMes)$(Cl)_2$Ru=CHPh, by the IMes ligand.[62] While such stabilization may take place, we suggest that the thermal longevity of **2.14** (and related NHC complexes) is predominantly due to reduced rates of phosphine dissociation in **2.14** relative to **2.1**. Since decomposition is second order in **B**, the rate of decomposition is extremely sensitive to the concentration of **B** in solution, particularly in the absence of olefinic substrates.[61]

Notably, the methylidene complexes **2.4** and **2.13** decompose relatively rapidly despite exhibiting very slow rates of initiation. However, both of these complexes appear to decompose by a different pathway than ruthenium alkylidenes and benzylidenes. The

decomposition of **2.4** and **2.13** is not inhibited by the addition of free PCy_3.[63] Furthermore, the decomposition of **2.4** has been shown to exhibit *first order* kinetics.[61] Based on these results, methylidene decomposition has been proposed to occur via intramolecular C-H activation of an L-type ligand, rather than involving the intermediate **B**. In any case, a quantitative investigation of the correlation between k_B and decomposition rate in all of the catalysts **2.1**–**2.14** is currently underway.

Polymerization Reactions. A final important implication of these mechanistic studies involves the control of molecular weight distributions in ring opening metathesis polymerizations. It has been observed that the polymerization of highly strained monomers with catalyst **2.1**, and particularly **2.8**, results in products with broad molecular weight distributions.[3,15,64] These distributions are the result of a large disparity between the rate of initiation (k_1) and the rate of propagation (k_P) of a polymerization reaction. (Using both catalysts **2.1** and **2.8**, $k_1 << k_P$ for many monomers). New procedures for decreasing k_P and/or for increasing k_1 should result in dramatically narrowed polydispersities (PDI's). The mechanism outlined in Scheme 5 suggests a facile method for achieving the former. The addition of free PR_3 to a polymerization will not affect k_1, since k_1 is independent of $[PR_3]$. However, free phosphine will decrease the rate of propagation by lowering the number of catalytic turnovers that occur before the active species is trapped with free PR_3 (effectively increasing $k_{-1}[PR_3]$ relative to k_2[olefin]). Alternatively, our studies suggest methods for increasing k_1 by modifying either the X-type ligands or the phosphine ligands of catalysts **2.1** and **2.8**. Implementation of both of these strategies has proven successful for lowering PDI's in ruthenium catalyzed ROMP reactions.[65]

In summary, the reactivity of a series of ruthenium metathesis catalysts has been studied in detail. The multi-step nature of the olefin metathesis reaction renders mapping the entire reaction coordinate an extremely challenging endeavor. However, this investigation has brought us a few steps closer to understanding the subtle effects of ligand variation on ligand substitution kinetics as well as on catalyst initiation and activity in these ruthenium-based systems. Our studies also provide some insights into methods for tuning both reaction conditions and ligands in order to achieve specific catalytic properties. Many of the subtle and surprising factors governing ligand effects

(particularly those involving *N*-heterocyclic carbenes) in these systems have yet to be unraveled.

Experimental Section

General Procedures: Manipulation of organometallic compounds was performed using standard Schlenk techniques under an atmosphere of dry argon or in a nitrogen-filled Vacuum Atmospheres drybox ($O_2 < 2$ ppm). NMR spectra were recorded on a Varian Inova (499.85 MHz for ^1H; 202.34 MHz for ^{31}P; 125.69 MHz for ^{13}C) or on a Varian Mercury 300 (299.817 for ^1H; 121.39 MHz for ^{31}P; 74.45 MHz for ^{13}C). ^{31}P NMR spectra were referenced using H_3PO_4 (δ = 0 ppm) as an external standard. UV-vis spectra were recorded on an HP 8452A Diode Array Spectrophotometer.

Materials and Methods. Benzene-d_6 were dried by passage through solvent purification columns.[66] Toluene-d_8 and THF-d_8 were dried by vacuum transfer from Na/benzophenone. CD_2Cl_2, and ethyl vinyl ether were dried by vacuum transfer from CaH_2. All phosphines were obtained from commercial sources and used as received. Ruthenium complexes **2.1**,[3] **2.2**,[5a] **2.3**,[5a] **2.4**,[3] **2.5**,[3] **2.6**,[67] **2.7**,[68] **2.8**,[1a] and **2.14**[69] were prepared according to literature procedures. Complexes **2.9–2.12** were prepared as described in Chapter 3 of this thesis.

(IMesH$_2$)(PCy$_3$)(Cl)$_2$Ru=CH$_2$ (2.13). Complex **2.1** (300 mg, 0.35 mmol) was dissolved in benzene (10 mL) and pressurized with ~1.5 atm of ethylene. The reaction mixture was stirred at 50 °C for 90 minutes during which time a color change from pink to dark brown was observed. The brown solution was cooled to room temperature, and the product was purified by column chromatography (gradient elution: 100% pentane to 8:1 pentane/diethyl ether) according to the procedure of Hoveyda[70] to afford an orange-yellow solid (97 mg, 36% yield). $^{31}P\{^1H\}$ NMR (C_6D_6): δ 38.6 (s). ^1H NMR (C_6D_6): δ 18.41 (s, 2H, Ru=C*H*$_2$), 6.92 (s, 2H, Mes C*H*), 6.70 (s, 2H, Mes C*H*), 3.22 (m, 4H, C*H*$_2$C*H*$_2$), 2.78 (s, 6H, ortho C*H*$_3$), 2.53 (s, 6H, ortho C*H*$_3$), 2.37 (m, 3H, PC*y*$_3$), 2.18 (s, 3H, para C*H*$_3$), 2.10 (s, 3H, para C*H*$_3$), 1.61 (m, 12H, PC*y*$_3$), 1.10 (m, 18H, PC*y*$_3$). $^{13}C\{^1H\}$ (C_6D_6): δ 294.75 (d, Ru=*C*H$_2$, J_{CP} = 10 Hz), 222.52 (d, Ru-*C*(N)$_2$, J_{CP} = 75 Hz),

139.59, 138.95, 138.41, 138.11, 137.76, 135.33, 130.49, 130.00, 128.91, 128.67, 128.03, 127.84, 51.97 (d, J_{CP} = 3 Hz), 50.33 (d, J_{CP} = 1 Hz), 31.03, 30.89, 29.51, 28.37, 28.29, 28.29, 27.03, 21.53 (d, J_{CP} = 3 Hz), 20.42, 19.42. Anal. Calcd for $C_{40}H_{61}N_2Cl_2PRu$: C, 62.16; H, 7.96; N, 3.62. Found: C, 61.12; H, 7.75; N, 3.64.

Magnetization Transfer Experiments. The ruthenium alkylidene (0.024 mmol) and PCy_3 (in equivalents relative to [Ru]) were combined in toluene-d_8 (600 μL) in an NMR tube, and the resulting solution was allowed to thermally equilibrate in the NMR probe. The free phosphine resonance was selectively inverted using a DANTE pulse sequence[20] and after variable mixing times (between 0.00003 and 50 s), a non-selective 90° pulse was applied and an FID recorded. ^{1}H decoupling was applied during the 90° pulse. Spectra were collected as 4-8 transients with relaxation delays between 30 and 50 seconds. The peak heights of the free and bound phosphine at variable mixing times were analyzed using the computer program CIFIT[21] in order to obtain the exchange rate of bound phosphine with free phosphine (k_B).

NMR Initiation Kinetics. The ruthenium alkylidene (0.0106 mmol) was dissolved in toluene-d_8 (600 μL) in an NMR tube fitted with a screw cap containing a rubber septum. The resulting solution was allowed to equilibrate in the NMR probe at the appropriate temperature, and ethyl vinyl ether (in equivalents relative to [Ru]) was injected into the NMR tube neat. Reactions were monitored by measuring the peak heights of the starting alkylidene as a function of time over at least three half lives. The data was fitted to a first order exponential using Varian kinetics software.[71]

UV-Vis Initiation Kinetics. In a cuvette fitted with a rubber septum, a solution of ethyl vinyl ether (in equivalents relative to the [Ru]) in toluene (1.6 mL) was prepared. The solution was allowed to thermally equilibrate in the UV-vis spectrometer at the appropriate temperature. To the temperature equilibrated solution was added 100 μL of a 0.0139 M stock solution of the ruthenium catalyst in toluene. The kinetics of the reaction were followed by monitoring the appearance of the product as a function of time. The data was collected over 5 half lives and kinetics traces were fitted to a first order exponential.

$1/k_{obs}$ versus [PCy_3]/[olefin] for Catalysts 2.1, 2.2, and 2.3. Ruthenium catalyst (0.0106 mmol) and PCy_3 (in equivalents relative to [Ru] from a 0.061 M stock solution in toluene-d_8) were combined in an NMR tube fitted with a screw cap containing a rubber septum. The resulting solutions were diluted to a total volume of 600 μL with toluene-d_8. The tubes were allowed to thermally equilibrate in the NMR probe, and the ethyl vinyl ether (in equivalents relative to [Ru]) was injected neat into the NMR tube. Reactions were monitored by measuring the peak heights of the starting alkylidene as a function of time over at least three half lives as described above.

$1/k_{obs}$ versus [PR_3]/[olefin] for Catalysts 2.6, 2.8, 2.10, 2.11, and 2.12. Ruthenium catalyst (0.0106 mmol) and PR_3 (in equivalents relative to [Ru]) were combined in an NMR tube fitted with a screw cap containing a rubber septum. The solids were dissolved in 600 μL of toluene-d_8. Each solution was allowed to thermally equilibrate at in the NMR probe, and ethyl vinyl ether (in equivalents relative to [Ru]) was injected neat into the NMR tube. Reactions were monitored by measuring the peak heights of the starting alkylidene as a function of time over at least three half lives.

ROMP of Cyclooctadiene. The ruthenium alkylidene (0.003 mmol) was dissolved in CD_2Cl_2 (600 μL) in an NMR tube fitted with a screw cap containing a rubber septum. The resulting solution was allowed to equilibrate in the NMR probe at 20 °C, and COD (0.90 mmol) was injected into the NMR tube neat. Reactions were monitored by measuring the peak heights of the COD olefinic signal as a function of time over at least three half lives. The data was fitted to a first order exponential using Varian kinetics software.[71] For catalyst **2.11**, the same procedure was followed with the exception that 0.006 μmol ruthenium alkylidene was used.

References and Notes

(1) Portions of this chapter were previously described in two separate publications: (a) Sanford, M. S.; Love, J. A.; Grubbs, R. H. *J. Am. Chem. Soc.* **2001**, in press. (b) Sanford, M. S.; Ulman, M.; Grubbs, R. H. *J. Am. Chem. Soc.* **2001**, *123*, 749.

(2) Ivin, K. J.; Mol, J. C. *Olefin Metathesis and Metathesis Polymerization*, Academic Press: San Diego, CA, 1997.

(3) Schwab, P.; Grubbs, R. H.; Ziller, J. W. *J. Am. Chem. Soc.* **1996**, *118*, 100.

(4) For recent reviews in this area see: (a) Trnka, T. M.; Grubbs, R. H. *Acc. Chem. Res.* **2001**, *34*, 18. (b) Furstner, A. *Angew. Chem., Int. Ed.* **2000**, *39*, 3012. (c) Grubbs, R. H.; Chang, S. *Tetrahedron* **1998**, *54*, 4413.

(5) (a) Dias, E. L.; Nguyen, S. T.; Grubbs, R. H. *J. Am. Chem. Soc.* **1997**, *119*, 3887. (b) Ulman, M.; Grubbs, R. H. *Organometallics* **1998**, *17*, 2484.

(6) (a) Adlhart, C.; Volland, M. A. O.; Hofmann, P.; Chen, P. *Helv. Chim. Acta* **2000**, *83*, 3306. (b) Adlhart, C.; Chen, P. *Helv. Chim. Acta* **2000**, *83*, 2192. (c) Adlhart, C.; Hinderling, C.; Baumann, H.; Chen, P. *J. Am. Chem. Soc.* **2000**, *122*, 8204. (d) Hinderling, C.; Adlhart, C.; Chen, P. *Angew. Chem., Int. Ed.* **1998**, *37*, 2685.

(7) (a) Meier, R. J.; Aagaard, O. M.; Buda, F. *J. Mol. Cat. A* **2000**, *160*, 189. (b) Aagaard, O. M.; Meier, R. J.; Buda, F. *J. Am. Chem. Soc.* **1998**, *120*, 7174.

(8) (a) Morgan, J. P.; Grubbs, R. H. *Org. Lett.* **2000**, *2*, 3153. (b) Scholl, M.; Ding, S.; Lee, C. W.; Grubbs, R. H. *Org. Lett.* **1999**, *1*, 953. (c) Scholl, M.; Trnka, T. M.; Morgan, J. P.; Grubbs, R. H. *Tetrahedron Lett.* **1999**, *40*, 2247.

(9) Huang, J.; Stevens, E. D.; Nolan, S. P.; Peterson, J. L. *J. Am. Chem. Soc.* **1999**, *121*, 2674.

(10) Weskamp, T.; Kohl, F. J.; Hieringer, W.; Gliech, D.; Herrmann, W. A. *Angew. Chem., Int. Ed.* **1999**, *38*, 2416.

(11) (a) Herrmann, W. A.; Kocher, C. *Angew. Chem., Int. Ed. Engl.* **1997**, *36*, 2162. (b) Huang, J.; Schanz-H. J.; Stevens, E. D.; Nolan, S. P. *Organometallics* **1999**, *18*, 2370.

(12) Ackermann, L.; Furstner, A.; Weskamp, T.; Kohl, F. J.; Herrmann, W. A. *Tetrahedron Lett.* **1999**, *40*, 4787.

(13) Chatterjee, A. K.; Grubbs, R. H. *Org. Lett.* **1999**, *1*, 1751.

(14) (a) Choi, T.-L.; Chatterjee, A. K.; Grubbs, R. H. *Angew. Chem., Int. Ed.* **2001**, *40*, 1277. (b) Chatterjee, A. K.; Morgan, J. P.; Scholl, M.; Grubbs, R. H. *J. Am. Chem. Soc.* **2000**, *122*, 3783.

(15) Bielawski, C. W.; Grubbs, R. H. *Angew. Chem. Int. Ed.* **2000**, *39*, 2903.

(16) (a) Schrock, R. R. *Polyhedron* **1995**, *14*, 3177. (b) Schrock, R. R. *Tetrahedron* **1999**, *55*, 8141.

(17) The mechanistic studies detailed in ref. 5a involved the diphenylvinyl carbene analogues of benzylidenes **2.1–2.3**.

(18) Chen and coworkers have provided mass spectrometric evidence that *dissociative* substitution of phosphine with olefinic substrates occurs in ruthenium catalyzed olefin metathesis reactions in the gas phase [ref. 6].

(19) Even at 100 °C, only catalyst **2.3** shows significant line broadening. Higher temperatures were not accessible in these systems because catalyst decomposition was observed.

(20) Morris, G. A.; Freeman, R. *J. Magn. Res.* **1978**, *29*, 433.

(21) Bain, A. D.; Kramer, J. A. *J. Magn. Res.* **1996**, *118A*, 21.

(22) The values of k_B are reported per coordinated phosphine ligand. As such, the phosphine exchange rate in solution for the bis-phosphine complexes **2.1–2.7** is actually double the values reported in Table 1.

(23) Cole, M. L.; Hibbs, D. E.; Jones, C.; Smithies, N. A. *J. Chem. Soc., Dalton Trans.* **2000**, 545.

(24) Tolman, C. A. *Chem. Rev.* **1977**, *77*, 313.

(25) Atwood, J. D. *Inorganic and Organometallic Reaction Mechanisms*, VCH: New York, 1997, p. 13-14.

(26) (a) Sanford, M. S.; Henling, L. M.; Day, M. W.; Grubbs, R. H. *Angew. Chem., Int. Ed.* **2000**, *39*, 3451. (b) Coalter, J. N.; Bollinger, J. C.; Eisenstein, O.; Caulton, K. G. *New J. Chem.* **2000**, *24*, 925.

(27) For a recent example see: Maynard, H. D.; Okada, S. Y.; Grubbs, R. H. *Macromolecules* **2000**, *33*, 6239.

(28) Fischer carbene complexes can be active catalysts for olefin metathesis reactions under some conditions (see references below). However, throughout the kinetics experiments described herein, Fischer carbene formation is quantitative and irreversible by ^{1}H NMR spectroscopy. (a) Katayama, H.; Urushima, H.; Nishioka, T.; Wada, C.; Nagao, M.; Ozawa, F. *Angew. Chem., Int. Ed.* **2000**, *39*, 4513. (b) van der Schaaf, P. A.; Kolly, R.; Kirner, H. J.; Rime, F.; Muhlebach, A.; Hafner, A. *J. Organomet. Chem.* **2000**, *606*, 65. (c) Katayama, H.; Urushima, H.; Ozawa, F. *J. Organomet. Chem.* **2000**, *611*, 332.

(29) Previously, initiation studies in catalysts **2.1–2.14** utilized terminal olefinic substrates such as 1-hexene [ref. 2 and 4b] or 1-butene [ref. 5c]. However, unlike the reaction with ethyl vinyl ether, these reactions are readily reversible and lead to the formation of both kinetic (alkylidene) and thermodynamic (methylidene) products. Particularly in the case of the NHC-containing catalysts **2.8–2.14**, the simultaneous formation of alkylidene and methylidene products leads to complications in the kinetic analysis.

(30) The reaction of 3,4–dihydropyran is particularly significant because it involves the ring opening a relatively low strained six-membered ring. This is typically a challenge for olefin metathesis catalysts (the ring opening of cyclohexene, for example, is only effected by extremely thermodynamically unstable carbenes) and speaks to the favorable thermodynamics associated with the generation of Fischer carbene moieties. Ulman, M.; Belderrain, T. R.; Grubbs, R. H. *Tetrahedron Lett.* **2000**, *41*, 4689.

(31) The values of k_B (predicted) [Tables 3 and 4] for the bis-phosphine complexes **2.1–2.7** are actually $2 \bullet k_B$, because k_B is the dissociation rate per coordinated phosphine ligand.

(32) This assignment is consistent with Hofmann's calculations which suggest that the LUMO of catalyst **2.1** (and its analogues) is localized primarily on C_α. Hansen, S. M.; Rominger, F.; Metz, M.; Hofmann, P. *Chem. Eur. J.* **1999**, *2*, 557.

(33) The reaction of **2.3** with ethyl vinyl ether showed anomalous UV-vis and NMR kinetics data, and quantitative measurement of the initiation rate of this complex was not

possible. However, the value of k_{Init} for **2.3** was qualitatively much faster than that of the other four catalysts.

(34) When the UV-vis initiation experiments were carried out in neat ethyl vinyl ether, the values obtained for k_{Init} were significantly (~20-40%) higher than k_B (predicted). We have good evidence that this is a solvent effect resulting from changing the reaction medium from toluene to the more polar ethyl vinyl ether.

(35) Gordon, A. J.; Ford, R. A. *The Chemists Companion*, John Wiley and Sons: New York, 1972, p. 2.

(36) Plutino, M. R.; Scolaro, L. M.; Romeo, R.; Grassi, A. *Inorg. Chem.* **2000**, *39*, 2712.

(37) Interestingly, ruthenium alkylidenes that are stabilized by *intramolecular* ethereal ligands have been prepared. (a) Kingsbury, J. S.; Harrity, J. P. A.; Bonitatebus, P. J.; Hoveyda, A. H. *J. Am. Chem. Soc.* **1999**, *121*, 791. (b) Garber, S. B.; Kingsbury, J. S.; Gray, B. L.; Hoveyda, A. H. *J. Am. Chem. Soc.* **2000**, *122*, 8168.

(38) We feel that a reasonable comparison can be made in these systems because k_{-1}/k_2 is a ratio of second order rate constants. As such, the temperature dependence of k_{-1} and k_2 should be roughly equivalent.

(39) The k_{-1}/k_2 values for the reaction of **2.8** with ethyl vinyl ether and 2,3-dihydrofuran are 1.25 and 0.67, which are essentially equivalent within the error of the measurement.

(40) The catalyst activity studies were carried out by Dr. Jennifer Love.

(41) Weskamp, T.; Schattenmann, W. C.; Spiegler, M.; Herrmann, W. A. *Angew. Chem., Int. Ed.* **1998**, *37*, 2490.

(42) The catalytically active species in these reaction mixtures include the un-initiated pre-catalyst and multiple ruthenium alkylidenes with appended polymer chains. Each of these complexes can initiate and propagate at different rates.

(43) Dias, E. L.; Grubbs, R. H. *Organometallics* **1998**, *17*, 2758.

(44) Notably, catalyst **2.11** carries out the RCM of terminal olefinic substrates with less than a two-fold increase in rate relative to **2.8**. This appears to be due to competitive inhibition of the RCM reaction by ethylene generated as a consequence of the ring closing reaction.

(45) Scheme 5 outlines a generic *degenerate* olefin metathesis reaction (*i.e.,* the ruthenium starting material and product are the same).

(46) Investigations on this topic are currently in progress. Benitez, D.; Goddard, W. A.; Grubbs, R. H. **2000**, unpublished results.

(47) The pK_a of 1,3-diisopropyl-4,5-dimethylimidazol-2-ylidene (an NHC closely related to the IMes ligand) is 26. Alder, R. W.; Allen, P. R.; Williams, S. J. *J. Chem. Soc., Chem. Commun.* **1995**, 1267.

(48) Lappert, M. F. *J. Organomet. Chem.* **1975**, *100*, 139.

(49) McGuinness, D. S.; Cavell, K. J.; Skeleton, B. W.; White, A. H. *Organometallics* **1999**, *18*, 1596.

(50) Trnka, T. M.; Henling, L. M.; Grubbs, R. H. **2000**, unpublished results.

(51) Streuli, C. A. *Anal. Chem.* **1960**, *32*, 985.

(52) Notably, k_B for the PPh_3 complex $(PPh_3)_2(Cl)_2Ru{=}CHCH{=}C(Me)_2$ at 80 °C is $2.4 \pm 0.3\ s^{-1}$ [relative to $0.33 \pm 0.2\ s^{-1}$ in $(PCy_3)_2(Cl)_2Ru{=}CHCH{=}C(Me)_2$ (**6**)]. This result indicates that PPh_3 dissociation (and therefore initiation) is efficient in the bis-triphenylphosphine systems as well as in the mixed NHC-PPh_3 complex, **2.11**.

(53) Huheey, J. E.; Keiter, E. A.; Keiter, R.L. *Inorganic Chemistry: Principles of Structure and Reactivity*, Harper Collins: New York, 1993, Ch. 13.

(54) Crabtree, R. H. *The Organometallic Chemistry of the Transition Metals*, John Wiley and Sons: New York, 1994.

(55) Kirkland, T. A.; Lynn, D. M.; Grubbs, R. H. *J. Org. Chem.* **1998**, *63*, 9904.

(56) Trost, B. M. *Science* **1991**, *254*, 1471.

(57) The low initiation efficiency of **2.8**, **2.13**, and **2.14** suggests that attempts to recycle these catalysts using "boomerang" polymer supports will only result in the recovery of un-initiated **2.8**. (a) Ahmed, M.; Arnauld, T.; Barrett, A. G. M.; Braddock, D. C.; Procopiou, P. A. *Synlett*, **2000**, *7*, 1007. (b) Jafarpour, L.; Nolan, S. P. *Org. Lett.* **2000**, *2*, 4075.

(58) Fujimura, O.; Grubbs, R. H. *J. Am. Chem. Soc.* **1996**, *118*, 2499.

(59) Alexander, J. B.; La, D. S.; Cefalo, D. R.; Hoveyda, A. H.; Schrock, R. R. *J. Am. Chem. Soc.* **1998**, *120*, 4041.

(60) Lee, C. W.; Grubbs, R. H. *Org. Lett.* **2000**, *2*, 2145.

(61) Ulman, M.; Grubbs, R. H. *J. Org. Chem.* **1999**, *64*, 7202.

(62) Huang, J.; Schanz, H. J.; Stevens, E. D.; Nolan, S. P. *Organometallics* **1999**, *18*, 5375.

(63) Ulman, M., Ph.D. Thesis, California Institute of Technology, 2000.

(64) Robson, D. A.; Gibson, V. C.; Davies, R. G.; North, M. *Macromolecules* **1999**, *32*, 6371.

(65) Bielawski, C. W.; Grubbs, R.H. **2001**, manuscript in preparation.

(66) Pangborn, A. B.; Giardello, M. A.; Grubbs, R. H.; Rosen, R. K.; Timmers, F. J. *Organometallics* **1996**, *15*, 1518.

(67) Wilhelm, T. E.; Belderrain, T. R.; Brown, S. N.; Grubbs, R. H. *Organometallics*, **1997**, *16*, 3867.

(68) Complex **2.7** was prepared by methodology analogous to that used to prepare **2.6**. Wilhelm, T. E., Ph.D. Thesis, California Institute of Technology, 1998.

(69) Jafarpour, L.; Nolan, S. P.; *Organometallics* **2000**, *19*, 2055.

(70) Garber, S. B.; Kingsbury, J. S.; Gray, B. L.; Hoveyda, A. H. *J. Am. Chem. Soc.* **2000**, *117*, 8168.

(71) VNMR 6.1B Software, Varian Associates, Inc.

Chapter 3: Synthesis and Characterization of *N*-Heterocyclic Carbene Coordinated Ruthenium Benzylidenes[1]

Abstract

The synthesis and reactivity of ruthenium benzylidenes containing the $IMesH_2$[a] ligand are described. $(IMesH_2)(PCy_3)(Cl)_2Ru{=}CHPh$ (**3.2**) reacts with an excess of NaI to afford the di-iodide complex $(IMesH_2)(PCy_3)(I)_2Ru{=}CHPh$ (**3.4**). The analogous di-bromide species, $(IMesH_2)(PCy_3)(Br)_2Ru{=}CHPh$ (**3.5**), is available by the reaction of $KO^tBu/IMesH_2[BF_4]$ with $(PCy_3)_2(Br)_2Ru{=}CHPh$. The addition of an excess of pyridine to **3.2** produces $(IMesH_2)(Cl)_2(C_5H_5N)_2Ru{=}CHPh$ (**3.7**). Complex **3.7** reacts with phosphines, including PPh_3 and PBn_3, to generate the new products $(IMesH_2)(PPh_3)(Cl)_2Ru{=}CHPh$ (**3.8**) and $(IMesH_2)(PBn_3)(Cl)_2Ru{=}CHPh$ (**3.9**), respectively. The bis-pyridine adduct, **3.7**, also reacts readily with KTp[b] to form $Tp(IMesH_2)(Cl)Ru{=}CHPh$ (**3.10**) and with KO^tBu to produce the four coordinate species $(IMesH_2)(O^tBu)_2Ru{=}CHPh$ (**3.11**). The crystal structures of **3.2** and **3.7** are reported. In addition, the rates of benzylidene and *N*-heterocyclic carbene rotation in complexes **3.2–3.9** are discussed.

[a] $IMesH_2$ = 1,3-dimesityl-4,5-dihydroimidazol-2-ylidene
[b] Tp = tris(pyrazolyl)borate

Introduction

Olefin metathesis is a carbon-carbon bond forming reaction that is widely used in both organic and polymer chemistry.[2] In particular, the ruthenium-based metathesis catalyst $(PCy_3)_2(Cl)_2Ru{=}CHPh$ (**3.1**) (Figure 1)[3] has been employed for the construction of small molecules, macromolecular architectures, and natural products in the presence of most common functional groups.[4] Recently, *N*-heterocyclic carbene (NHC) coordinated ruthenium complexes,[5,6,7] particularly $(IMesH_2)(PCy_3)(Cl)_2Ru{=}CHPh$ (**3.2**) [$IMesH_2$ = 1,3-dimesityl-4,5-dihydroimidazol-2-ylidene],[8] have been introduced and shown to exhibit dramatically increased olefin metathesis activity relative to **3.1**.[8,9] Mechanistic studies of **3.2** and the related complexes $(IMesH_2)(PR_3)(X)_2Ru{=}CHR^1$ have revealed that all of the ancillary ligands – PR_3, X, and R^1 – affect the rates of both initiation and propagation in olefin metathesis reactions.[1a] As a result, significant current effort has focused on modification of the ligand environment of **3.2** in order to prepare new metathesis catalysts with improved activity, selectivity, and functional group tolerance. This chapter describes our recent work involving the synthesis of ruthenium benzylidenes of the general formula $(IMesH_2)(X)_m(L)_nRu{=}CHPh$, and the spectroscopic and structural characterization of these new complexes.

Figure 1. Ruthenium Based Olefin Metathesis Catalysts.

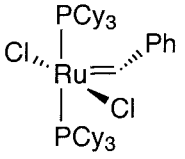

(**3.1**)

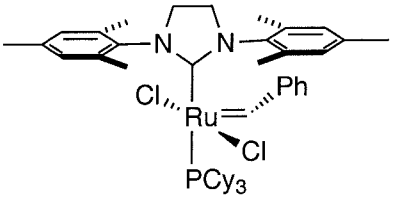

(**3.2**)

Results and Discussion

Synthesis of $(IMesH_2)(PCy_3)(Cl)_2Ru{=}CHPh$ (3.2). A recent report from our group described the preparation of catalyst **3.2** by the reaction of **3.1** with 1.4 equivalents of $IMesH_2[BF_4]$ and 1.4 equivalents of KO^{t}Bu (Scheme 1).[8] ^{1}H NMR spectroscopic

studies indicated that this reaction produced **3.2** in 90-95% yield after 30 minutes at 80 °C,[10] and isolated catalyst yields of 75-80% were obtained upon recrystallization of the crude reaction mixture from methanol.[8] However, this recrystallization produced the product in only 85-90% purity,[8] and samples were typically contaminated with reaction by-products including salts ($IMesH_2[BF_4]$ and KBF_4) and free PCy_3, which both dramatically decrease the activity of **3.2** for olefin metathesis reactions.[1,11] In addition, traces of ruthenium-containing impurities such as complex **3.1**, the *tert*-butoxide ruthenium adduct $(PCy_3)(O^tBu)_2Ru{=}CHPh$[12] and several ruthenium hydrides, were detected in samples of **3.2**. The hydride impurities are particularly undesirable, because they promote the isomerization of olefins during metathesis reactions.[13]

Scheme 1

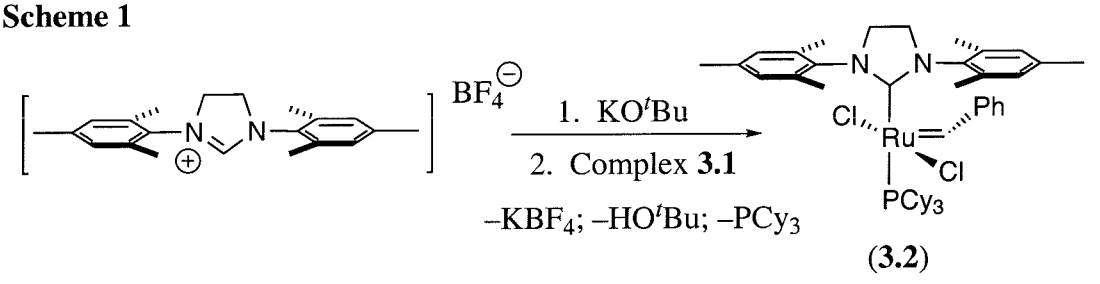

(3.2)

In order to obtain clean and reproducible samples of catalyst **3.2**, an optimized procedure for the purification of this complex has been developed. After the reaction between **3.1** and $IMesH_2[BF_4]/KO^tBu$ is complete, the solvents are removed under vacuum. The solids are then redissolved in benzene, and the resulting suspension is filtered through Celite in order to remove residual salts. The product is recrystallized from benzene/methanol and washed with methanol and pentane to remove free phosphine as well as ruthenium-containing impurities. This new procedure affords complex **3.2** in 50-60% yield as a cranberry red solid.

More recently, efficient and high-yielding "one-pot" procedures have been developed for the preparation of **3.2**[14] and the related complex $(IMes)(PCy_3)(Cl)_2Ru{=}CHPh$ [IMes = 1,3-dimesityl-imidazol-2-ylidene] (**3.3**).[15] Hoveyda and coworkers have also demonstrated that catalyst **3.2** and its derivatives can purified by column chromatography on silica gel.[16] Both of these procedures provide **3.2** in high purity and excellent yields (70-90%).[14-16] Additionally, an "in-situ" preparation of

catalyst **3.2** has been described and optimized for a variety of ring closing metathesis (RCM) and cross metathesis (CM) reactions.[17]

The red complex **3.2** is soluble in benzene and THF and is slightly soluble in pentane and methanol. Benzylidene **3.2** undergoes slow decomposition in methanol solution to generate a ruthenium hydrido carbonyl complex.[18] This catalyst also decomposes in chlorinated solvents such as $C_2H_4Cl_2$, and $C_2H_2Cl_4$ at elevated temperatures to produce the phosphonium salt, $HPCy_3Cl$, and an intractable mixture of ruthenium products. However, **3.2** is soluble and indefinitely stable in methylene chloride at ambient temperatures. In addition, catalyst initiation is more efficient in CH_2Cl_2 than in aromatic solvents, such as benzene or toluene,[1] making CH_2Cl_2 an ideal medium for olefin metathesis reactions catalyzed by **3.2** and its derivatives.

Figure 2. Exchanging Protons due to Alkylidene Rotation.

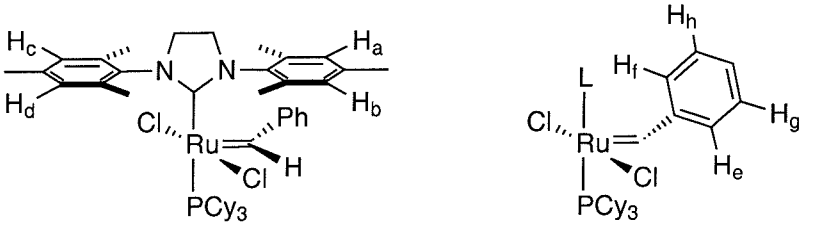

The benzylidene proton of **3.2** appears as a singlet at 19.06 ppm in CD_2Cl_2. This downfield chemical shift is typical of ruthenium benzylidenes, including **3.1** (in which H_α appears at 20.02 ppm)[3] and **3.3** (in which H_α appears at 19.16 ppm).[5,6e] The lack of phosphorus coupling to H_α suggests that the solid state P–Ru–C_α–H_α dihedral angle is approximately 90°.[19,20] The ^1H NMR spectrum of complex **3.2** at room temperature shows several broad signals in the aromatic region due to hindered rotation about the Ru=C_α and the C_α–C_β bonds. However, this dynamic behavior can be frozen out on the NMR time scale, and at –80 °C, sharp resonances are observed for each of the four $IMesH_2$ aromatic protons H_a, H_b, H_c, and H_d, as well as for the benzylidene protons H_e, H_f, H_g, and H_h (Figure 2). The activation barriers to benzylidene rotation in **3.2** and related NHC-ruthenium complexes are discussed in detail later in this chapter. Notably, in the low temperature (–80 °C) ^1H NMR spectrum of this complex, one of the aromatic protons of the $IMesH_2$ ligand appears as a singlet at 5.34 ppm. The solid state structure

of **3.2** indicates that this unusual upfield chemical shift is caused by the orientation of the mesityl ring, which positions this proton directly above the aromatic system of the benzylidene ligand.

X-ray Crystal Structure of Complex 3.2. Crystals suitable for X-ray diffraction studies were grown by slow diffusion of pentane into a benzene solution of **3.2** at room temperature. A labeled view of the complex is shown in Figure 3, and selected bond distances and bond angles are reported in Table 1.[21] The Ru–C(22) (benzylidene carbon) bond length of 1.835(2) Å is similar to that of related five-coordinate ruthenium benzylidenes; for example, the Ru=C_α distance is 1.838(2) Å in complex **3.1**[18] and is 1.841(11) Å in complex **3.3**.[6e] The Ru–C(1) ($IMesH_2$ carbon) distance is almost 0.2 Å longer than that of Ru–C(22), highlighting the differences in metal-carbon bonding between the two carbene ligands. The longer Ru–C(1) bond involves a dative-type interaction with relatively little contribution of backbonding from the metal center, while the shorter Ru–C(22) bond clearly has significant double bond character. The Ru–C(1) distance of 2.085(2) Å is virtually identical to that in complex **3.3** [d(Ru–C) = 2.069(11) Å],[6e] indicating that the substantial electronic differences between the IMes and $IMesH_2$ ligands[22] are not reflected in the ground state structures of these ruthenium adducts.

A comparison of the Ru–P bond lengths of **3.1**, **3.2** and **3.3** reveals that they are essentially identical; d(Ru–P) is 2.4159(6) Å,[18,23] 2.4245(5) Å, and 2.419(3) Å, respectively.[6e] In contrast, the phosphine dissociation rate (k_B) for these catalysts has been shown to vary by over three orders of magnitude; k_B for **3.1**, **3.2**, and **3.3** is 9.6 s^{-1}, 0.13 s^{-1} and 0.03 s^{-1}, respectively.[1] The negligible differences in Ru–P distances between these complexes suggest that the enhanced lability of the phosphine ligand in **3.1** (relative that in **3.2** and **3.3**) is not a ground state effect.

As anticipated from the ^{1}H NMR spectral data, the mesityl hydrogen bound to C(17) is positioned directly above the aromatic ring of the benzylidene ligand. This accounts for the shielding of the H(17) resonance due to the ring current of the aromatic ring. The P–Ru–C(22)–H(22) torsion angle of 100.0° is close to 90°, which is consistent with the lack of H_α–P coupling in the ^{1}H NMR spectrum of complex **3.2**.[20]

Figure 3. Labeled View of Complex **3.2** with 50% Probability Ellipsoids.

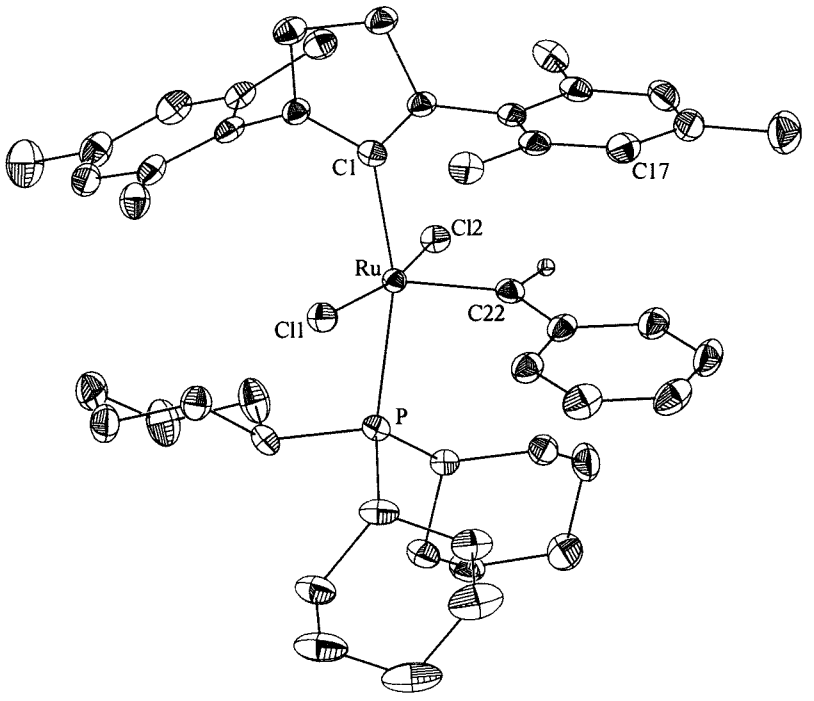

Table 2. Selected Bond Lengths [Å] and Angles [deg] for Complex **3.2**.

	Bond Lengths (Å)		
Ru–C(1)	2.0847(19)	Ru–C(22)	1.835(2)
Ru–Cl(1)	2.3912(5)	Ru–Cl(2)	2.3988(5)
Ru–P	2.4245(5)	C(22)–C(23)	1.470(3)
	Bond Angles (deg)		
C(22)–Ru–C(1)	100.24(8)	C(1)–Ru–Cl(1)	83.26(5)
C(22)–Ru–Cl(1)	103.15(7)	C(1)–Ru–Cl(2)	94.55(5)
C(22)–Ru–Cl(2)	89.14(7)	C(1)–Ru–P	163.73(6)
C(22)–Ru–P	95.89(6)	Cl(1)–Ru–Cl(2)	167.707(18)

Synthesis of $(IMesH_2)(PCy_3)(X)_2Ru=CHPh$. The reaction of **3.2** with an excess of NaI at room temperature results in a color change from red to dark green and the formation of $(IMesH_2)(PCy_3)(I)_2Ru=CHPh$ (**3.4**) (Scheme 2).[24] Filtration of the reaction mixture to remove NaI/NaCl provides the di-iodide complex in 80% yield as an olive green solid. Notably, this reaction takes almost 8 hours to reach completion at 25 °C, while, in comparison, halide exchange between **3.1** and NaI proceeds quantitatively within 1 hour at room temperature.[25] This result demonstrates that substitution of a phosphine ligand of **3.1** with an *N*-heterocyclic carbene has a dramatic effect on the lability of the X-type ligands in these systems.

Scheme 2

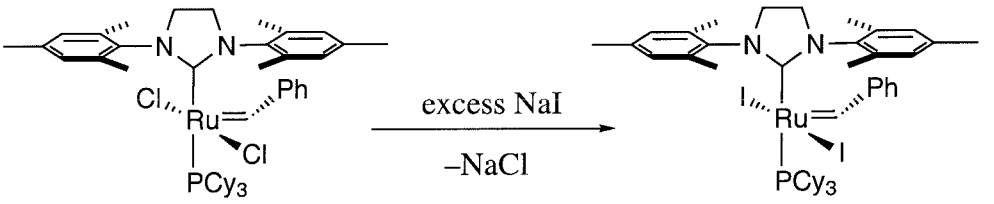

(**3.2**) (**3.4**)

Attempts to substitute the chloride ligands of **3.2** with bromides using LiBr or NaBr in THF were unsuccessful. These reactions resulted in only partial conversion to the desired product even after long reaction times (> 24 hours), elevated temperatures (50 °C), and in the presence of a large excess (> 50 equivalents) of the bromide salt.[24] However, by analogy to the synthesis of compound **3.2**,[8] $(IMesH_2)(PCy_3)(Br)_2Ru=CHPh$ (**3.5**) could be prepared by the reaction of $(PCy_3)_2(Br)_2Ru=CHPh$ with $IMesH_2[BF_4]$ and

Scheme 3

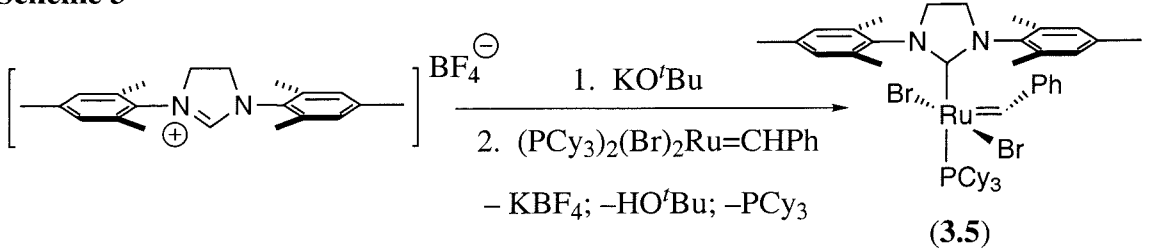

(**3.5**)

KO^{t}Bu (Scheme 3). This transformation provides **3.5** as a pink solid after purification by recrystallization or column chromatography.

The ^{1}H NMR features of **3.4** and **3.5** are similar to those of **3.2**, and broad resonances are observed in the aromatic region of these spectra at room temperature due to restricted benzylidene/phenyl rotation. The ^{1}H NMR of **3.4** shows traces of two minor carbene resonances at 18.14 and 17.17 ppm (< 5% of the total) in addition to the major peak at 19.09 ppm. These signals are observed even in analytically pure samples of **3.4**, but disappear completely upon the addition of 1 equivalent of free PCy_3. Based on this data, we speculate that these two upfield signals may correspond to the four-coordinate, phosphine-dissociated adduct $(IMesH_2)(I)_2Ru{=}CHPh$ (**3.6**) (Figure 4). Fourteen-electron complexes of this type have been proposed as intermediates in olefin metathesis reactions catalyzed by ruthenium benzylidenes.[1] Additionally, analogues of **3.6** containing large and electron donating alkoxide ligands have been prepared and isolated.[12] The observation of **3.6**, but not its chloride or bromide analogues, may be due to the lower barrier to phosphine dissociation in **3.4** relative to that in **3.2** or **3.5**.[1] Complex **3.4** has been shown to dissociate phosphine almost two orders of magnitude more efficiently than the dichloride catalyst **3.2**.[1]

Figure 4. Possible Structural Isomers of Complex **3.6**.

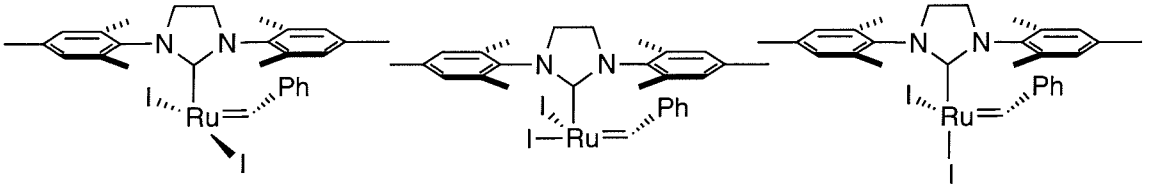

(3.6a) **(3.6b)** **(3.6c)**

Three isomeric structures of complex **3.6** are represented in Figure 4. Isomer **3.6a** is the product of direct phosphine dissociation from the square pyramidal starting material **3.5**, while structures **3.6b** and **3.6c** result from PCy_3 loss followed by a *trans* to *cis* isomerization of the iodide ligands. Notably, isomerization of the halide ligands has been proposed as a key mechanistic feature in ruthenium catalyzed olefin metathesis reactions.[25] Additionally, facile *cis/trans* isomerization of halide ligands has been observed in related ruthenium benzylidene species.[26] Calculations indicate that

complexes similar to **3.6a**,[27,28] **3.6b**,[29] and **3.6c**[27] can all be low energy intermediates along the olefin metathesis reaction coordinate. The four-coordinate alkoxide adducts $(PCy_3)(OR)_2Ru{=}CHPh$ assume a "trigonal pyramidal" geometry which is intermediate between that of **3.6a** and **3.6b**. In contrast, a series of η^3-vinylcarbene complexes with geometries similar to that of **3.6c** have recently been described.[30] The two upfield benzylidene signals observed in the ^1H NMR spectrum of **3.5** are believed to correspond to two of the three isomers of **3.6** (Figure 4). However, the low concentration of these species in solution and the difficulties associated with their isolation has rendered definitive assignment impossible at this time.

Scheme 4

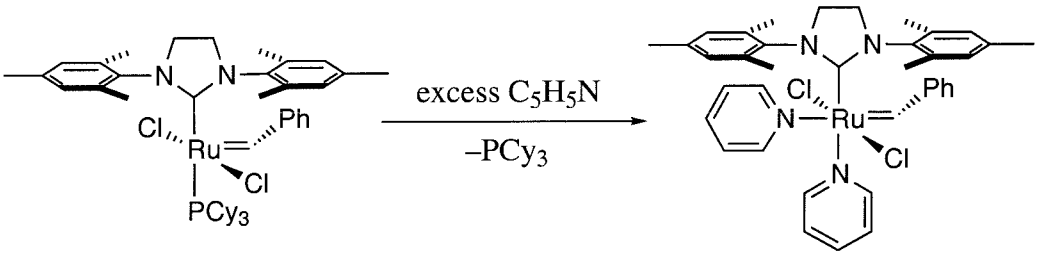

(**3.2**) (**3.7**)

Synthesis of $(IMesH_2)(Cl)_2(C_5H_5N)_2Ru{=}CHPh$. The reaction of complex **3.2** with a large excess (~100 equivalents) of pyridine results in a rapid color change from red to bright green, and transfer of the resulting solution to cold (–10 °C) pentane leads to the precipitation of the bis-pyridine adduct $(IMesH_2)(Cl)_2(C_5H_5N)_2Ru{=}CHPh$ (**3.7**) (Scheme 4).[31,32] Complex **3.7** can be purified by several washes with pentane, and is isolated as an air-stable green solid that is soluble in CH_2Cl_2, benzene, and THF. This procedure provides **3.7** in 80-85% yield and is easily carried out on a multi-gram scale. The formulation of **3.7** as the bis-pyridine adduct can be confirmed by ^1H NMR integration and X-ray crystallography. However, **3.7** loses solvent under prolonged exposure to vacuum, and elemental analyses consistently corresponded to the mono-pyridine complex, $(IMesH_2)(Cl)_2(C_5H_5N)Ru{=}CHPh$.[31] Both ^{13}C and ^1H NMR spectroscopy of **3.7** show broad resonances in the aromatic and aliphatic regions at room temperature, indicating the participation of one (or multiple) fluxional processes.

However, the complexity of this dynamic behavior, which appears to involve pyridine rotation and exchange, benzylidene rotation and *N*-heterocyclic carbene rotation, has precluded definitive interpretation of the NMR spectral data at this time.

X-ray Structure of Complex 3.7. There are a number of potential structural isomers of $(IMesH_2)(Cl)_2(C_5H_5N)_2Ru{=}CHPh$, and three of these are depicted in Figure 5. A first possibility, complex **3.7a**, is formed by coordination of the pyridines *trans* to the two carbene ligands. Alternatively, isomers **3.7b** and **3.7c** are generated by binding of one pyridine *trans* to a chloride and the second pyridine *trans* to either the benzylidene (**3.7b**) or the *N*-heterocyclic carbene (**3.7c**). It has been suggested that the related complex $(PCy_3)(C_5H_5N)_2(Cl)_2Ru{=}CHPh$ adopts a structure analogous to **3.7b**, but no structural or spectroscopic evidence has been presented to support (or refute) this claim.[31]

Figure 5. Possible Structural Isomers of Complex **3.7**.

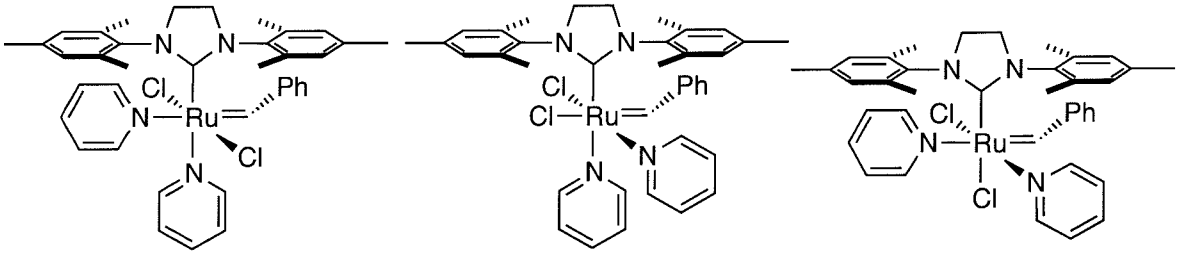

To distinguish these three structural possibilities, crystals of complex **3.7** were grown by vapor diffusion of pentane into a saturated benzene solution at room temperature. Two independent (but very similar) molecules of **3.7** appear in each unit cell, and the bond lengths and angles for molecule B are reported in Table 2.[33] In addition, a labeled view of the complex is shown in Figure 6.[21] In the solid state, this six-coordinate ruthenium complex adopts an octahedral geometry that clearly corresponds to isomer **3.7a**. The Ru–C(1) (benzylidene carbon) bond length of 1.873(4) Å is slightly longer than that of related five-coordinate ruthenium benzylidenes, including **3.1** (1.838(2) Å),[18] **3.2** (1.835(2) Å), and **3.3** (1.841(11) Å).[6e] The elongated $Ru{=}C_\alpha$ bond is likely due to the presence of a *trans* pyridine ligand.[34] The Ru–C(38) (NHC) bond length

Figure 6. Labeled View of **3.7** with 50% Probability Ellipsoids.

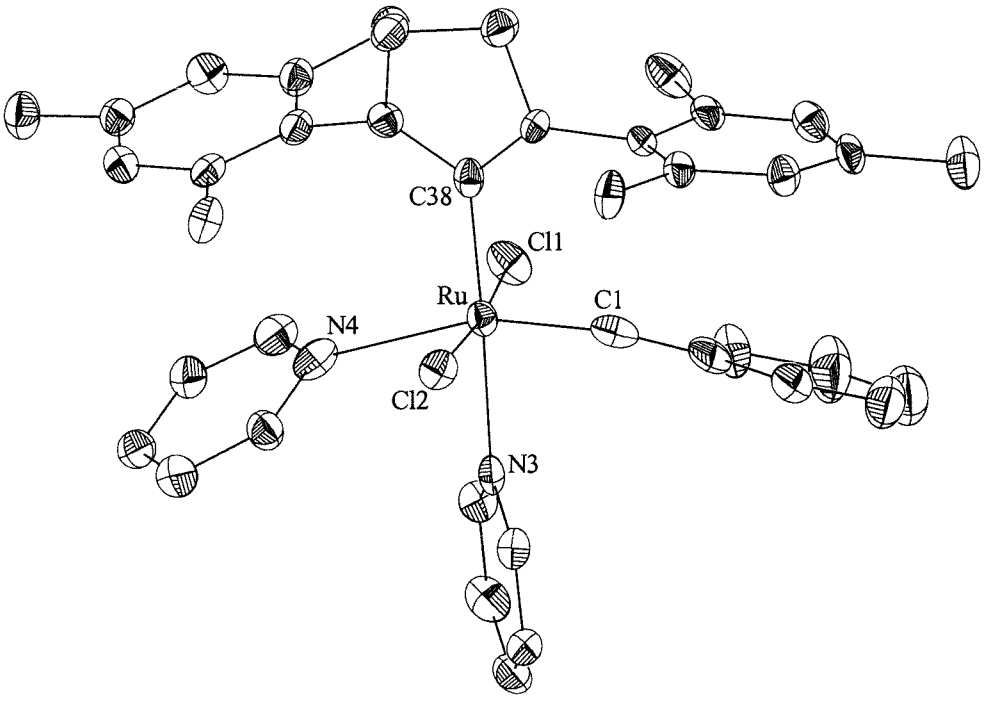

Table 2. Selected Bond Lengths [Å] and Angles [deg] for **3.7**.

	Bond Lengths (Å)		
Ru–C(1)	1.873(4)	Ru–C(38)	2.033(4)
Ru–N(3)	2.203(3)	Ru–N(4)	2.372(4)
Ru–Cl(1)	2.3995(12)	Ru–Cl(2)	2.4227(12)
	Bond Angles (deg)		
C(38)–Ru–C(1)	93.61(17)	C(1)–Ru–N(3)	87.07(15)
C(38)–Ru–N(3)	176.40(14)	C(1)–Ru–N(4)	161.18(14)
C(38)–Ru–N(4)	102.85(14)	C(1)–Ru–Cl(1)	100.57(14)
C(38)–Ru–Cl(1)	93.83(12)	C(1)–Ru–Cl(2)	84.75(14)
C(38)–Ru–Cl(2)	84.39(11)	Cl(1)–Ru–Cl(2)	174.50(4)

of 2.033(4) Å is approximately 0.05 Å shorter than that in either **3.2** and **3.3**. The shorter bond may reflect the relatively small size and moderate *trans* influence of pyridine relative to PCy_3. The 0.15 Å difference in the Ru–C(1) and Ru–C(38) bond distances highlights the covalent nature of the former and the dative nature of the latter ruthenium-carbene bond.

A particularly interesting feature of the structure of **3.7** concerns the two Ru–N bond distances [*d*(Ru–N(3)) = 2.203(3) Å and *d*(Ru–N(4)) = 2.372(4) Å], which differ by more than 0.15 Å. This data indicates that the benzylidene ligand exerts a significantly larger *trans* influence than the *N*-heterocyclic carbene,[35] which may have important mechanistic implications. In particular, a *trans/cis* isomerization of the halide ligands in the intermediate $L(X)_2Ru$ has been proposed as a critical step in ruthenium-catalyzed olefin metathesis reactions.[25,29] As depicted in Figure 7, this isomerization can produce products with two possible geometries, where the first possibility places a halide ligand *trans* to the benzylidene (complex **I**) and the second places a halide *trans* to the *N*-heterocyclic carbene ligand (complex **II**). The crystal structure of **3.7** suggests that the metal-halide bond order in the latter may be significantly greater than that of the former.

Figure 7. Possible Geometry of Four Coordinate Olefin Metathesis Intermediate.

(I) **(II)**

Kinetics of Pyridine Substitution Reaction. The kinetics of the reaction between **3.2** and pyridine (Scheme 4) were investigated in order to determine the mechanism of this ligand substitution. The reaction of **3.2** (0.88 M in toluene) with an excess of pyridine-d_5 (0.18 M to 0.69 M) is accompanied by a 150 nm red shift of the MLCT[36] visible absorbance, and this transformation can be followed by UV-vis spectroscopy. The disappearance of starting material (502 nm) was monitored at 20 °C, and, in all cases, the data fit first order kinetics over 5 half lives. A plot of k_{obs} versus $[C_5D_5N]$ is presented in Figure 8. The data show an excellent linear fit (R^2 = 0.99971)

even at high concentrations of pyridine, and the y-intercept of this line is very close to zero (intercept = 1.1 x 10^{-3}). The rate constant for phosphine dissociation (k_B) in complex **3.2** has been determined independently by ^{31}P magnetization transfer experiments, and at 20 °C, k_B is 4.1 x 10^{-5} s^{-1}.[1] The value of k_B places an upper limit on the rate of dissociative ligand exchange in **3.2**, and the observed rate constants for pyridine substitution are clearly three orders of magnitude larger than k_B. Taken together, this data indicates that the substitution of PCy_3 with pyridine in **3.2** proceeds by an associative mechanism with a second order rate constant of 5.7 x 10^{-2} M^{-1} s^{-1} at 20 °C. In marked contrast, the displacement of PCy_3 with olefinic substrates (the initiation step in olefin metathesis reactions catalyzed by complex **3.2**) has been shown to proceed by a *dissociative* mechanism.[1] These results demonstrate that both associative and dissociative ligand substitution pathways are accessible to the five-coordinate ruthenium complex **3.2**, and current efforts are aimed at the use of substituted pyridine and phosphabenzene derivatives to probe steric and electronic contributions to the mechanism of ligand substitution in this system.

Figure 8. Plot of k_{obs} versus [Pyridine] for Reaction of **3.2** with C_5H_5N.

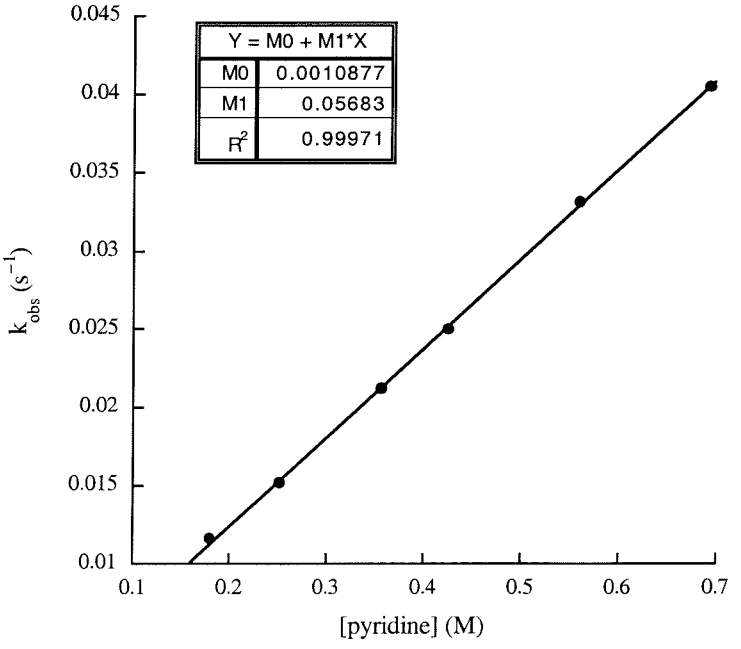

Olefin Metathesis Activity of 3.7. Complex **3.7** serves as a highly active catalyst for ring closing metathesis (RCM) reactions, and 5 mol% of **3.7** completes the ring closing of diethyl diallylmalonate within 30 minutes at 25 °C. This result compares favorably with catalysts **3.1**, **3.2**, and **3.3**, which all complete this reaction within 30 minutes at 45 °C.[5,8] However, in contrast to **3.1–3.3**, **3.7** shows significant decomposition throughout the ring closing reaction, and ^{1}H NMR spectroscopy indicates that, under typical RCM conditions, less than 5% of the original catalyst remains in solution after 30 minutes. In addition, none of the methylidene complex $(IMesH_2)(Cl)_2(C_5H_5N)_2Ru{=}CH_2$ (which is formed after one turnover of the benzylidene initiator) is observed by ^{1}H NMR spectroscopy. Taken together, these results suggest that benzylidene **3.7** is an efficient initiator for RCM,[37] but that the methylidene product is unstable under the reaction conditions.[38,39]

The activity of **3.7** for the ring opening metathesis polymerization of cyclooctadiene (COD) was also investigated. In this reaction, a ruthenium alkylidene (rather than an unstable methylidene) acts as the propagating species, and, as a result, the lifetime of the catalytically active species is significantly enhanced relative to the ring closing reaction. Upon the addition of substrate, complex **3.7** is quantitatively converted to a new alkylidene (a triplet at 19.44 ppm) within 5 minutes at 25 °C, indicating that initiation (k_{Init}) is fast in this system. In comparison, quantitative initiation of **3.2** takes 8-10 hours at room temperature.[1] However, the rate of propagation (k_P) with catalyst **3.7** is very slow, and only 50% conversion to polymeric products is observed by ^{1}H NMR spectroscopy after several hours at room temperature. The polymerization of COD with **3.7** is several orders of magnitude slower than that with **3.2**, and the depressed propagation rate may be due to catalyst inhibition by liberated pyridine. However, the relative k_{Init} and k_P values for this polymerization suggest that it will provide polycyclooctadiene with a low polydispersity index (PDI), and the molecular weights and PDI's of the products are currently under investigation.

Reactivity of 3.7. Initial reactivity studies of complex **3.7** revealed that both pyridine ligands are substitutionally labile. For example, benzylidene **3.7** reacts instantaneously with 1.1 equivalents of PCy_3 to release pyridine and regenerate complex

3.2 (Scheme 5). This equilibrium can be driven back towards the pyridine adduct by addition of an excess of C_5D_5N, but is readily reestablished by removal of the volatiles under vacuum.

Scheme 5

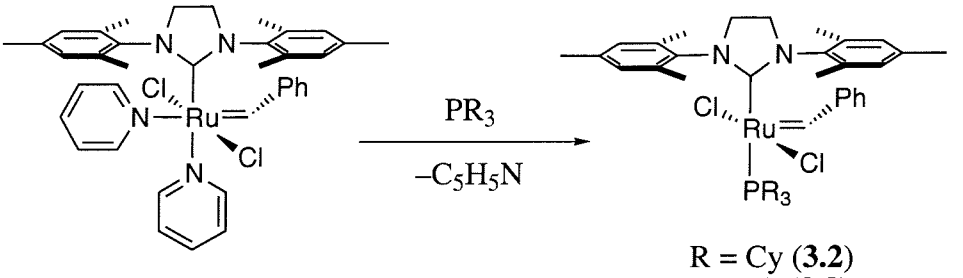

(**3.7**)

R = Cy (**3.2**)
R = Ph (**3.8**)
R = Bn (**3.9**)

The facile reaction of **3.7** with PCy_3 suggested that the pyridines might be displaced by other incoming ligands, and we have found that reaction of this bis-pyridine complex with a wide variety phosphines provides a simple and divergent route to new ruthenium benzylidenes of the general formula $(IMesH_2)(PR_3)(Cl)_2Ru{=}CHPh$. The combination of **3.7** and 1.1 equivalents of PR_3 results in a color change from green to red/brown and formation of the corresponding PR_3 adduct. Removal of the solvents under vacuum followed by several washes with pentane provides the mono-phosphine products in 80-90% yield as analytically pure solids. This ligand substitution works well for alkyl and aryl substituted phosphines including PPh_3 (to produce complex **3.8**), PBn_3 (to produce complex **3.9**), $PCyPh_2$, and P(*n*-Bu)$_3$ (Scheme 5).[40] Additionally, *para*-substituted triphenylphosphine derivatives (containing the *para* substituents CF_3, OMe, Me, Cl, and F) can be prepared using this methodology.[40] The synthetic accessibility of the P(*p*-$CF_3C_6H_4)_3$ complex is particularly remarkable, because this phosphine is extremely electron poor (χ = 20.5 cm^{-1}).[41] The triarylphosphine ruthenium complexes are valuable catalysts, because they are almost two orders of magnitude more active for olefin metathesis reactions than the parent complex **3.2**.[1]

There appear to be both steric and electronic limitations on the incoming phosphine ligand in the pyridine substitution reaction. For example, complex **3.7** does

not react with P(*o*-tolyl)$_3$ to produce a stable product, presumably due to the prohibitive size of the incoming ligand.[24,42] The cone angle of P(*o*-tolyl)$_3$ is 194°, while that of PCy_3 (the largest phosphine shown to successfully displace the pyridines of **3.7**) is 170°.[42] Additionally, the electron poor phosphine P(C_6F_6)$_3$ shows no reaction with **3.7** even under forcing conditions.[24] This ligand has a significantly lower electron donor capacity (χ = 33.6 cm^{-1})[41] than P(*p*-$CF_3C_6H_4$)$_3$ (χ = 20.5 cm^{-1}) and also has a slightly larger cone angle than PCy_3 (Θ = 184°).[42]

Scheme 6

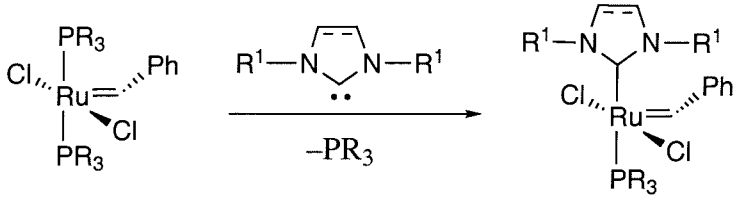

The methodology described herein represents a dramatic improvement over previous synthetic routes to the complexes (NHC)(PR_3)$(Cl)_2$Ru=CHPh. As shown in Scheme 6, earlier preparations of these compounds involved reaction of the bis-phosphine precursor $(PR_3)_2(Cl)_2$Ru=CHPh with an NHC ligand.[6e,7b] These transformations were often low yielding (particularly when the NHC was small)[7b] and required the parallel synthesis of ruthenium precursors containing each PR_3 ligand. Furthermore, bis-phosphine starting materials containing PR_3 ligands that are smaller and less electron donating than PPh_3 (cone angle = 145°; χ = 16.2 cm^{-1}; pK_a = 2.73)[41,42,43] cannot be prepared,[44,45] placing severe limitations on the complexes that are available by the methodology outlined in Scheme 6.

The chloride ligands of **3.7** are also substitutionally labile relative to those in the parent complex **3.2**. For example, complex **3.7** reacts quantitatively with KTp within 1 hour at 25 °C to afford the bright green product Tp(IMesH_2)$(Cl)_2$Ru=CHPh (**3.10**) (Scheme 7). In contrast, the reaction of **3.2** with KTp is extremely slow and proceeds to less than 50% completion even after several days at room temperature.[46] Removal of the solvents under vacuum followed by filtration and several washes with pentane and methanol provides **3.10** in 66% yield as an air and moisture stable solid. As expected, the

^{1}H and ^{13}C NMR spectra of **3.10** show nine separate resonances for the pyrazolyl protons, indicating that the ruthenium is a stereogenic center.

Scheme 7

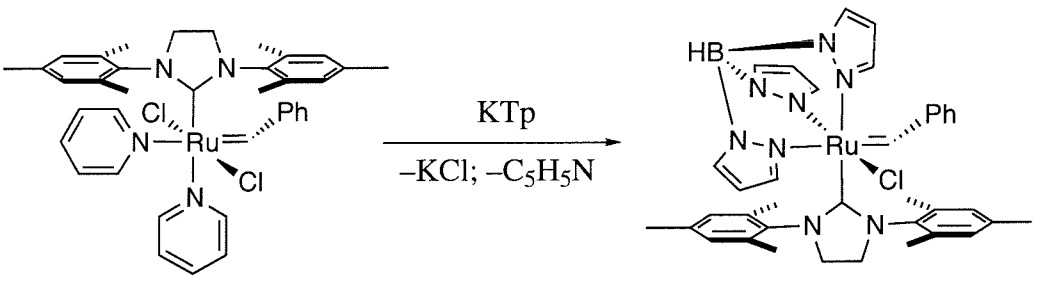

(**3.7**) (**3.10**)

In addition, ^{1}H NMR studies show that the combination of **3.7** with an excess of KO^{t}Bu produces the four-coordinate benzylidene (IMesH$_2$)(O^{t}Bu)$_2$Ru=CHPh (**3.11**) within 10 minutes at ambient temperature (Scheme 8). In contrast, the direct reaction of **3.2** with KO^{t}Bu to form **3.11** does not proceed to completion even after several days at 35 °C. The product **3.11** is an analogue of the previously reported alkoxide complex (PCy$_3$)(O^{t}Bu)$_2$Ru=CHPh,[12] and may be considered a model for the 14-electron intermediate (IMesH$_2$)(Cl)$_2$Ru=CHPh involved in olefin metathesis reactions of **3.2**.[1,47]

Scheme 8

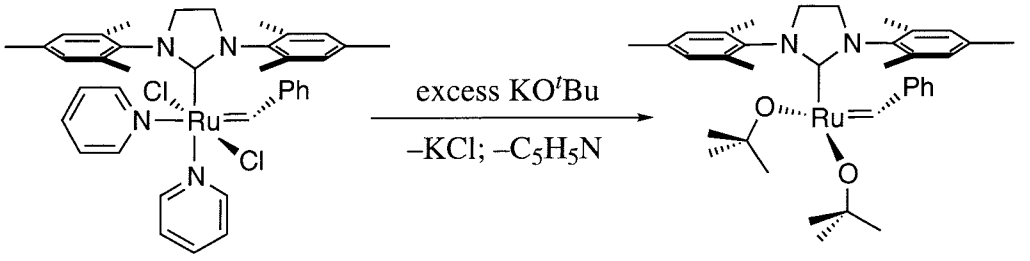

(**3.7**) (**3.11**)

Benzylidene Rotation in Ruthenium Complexes 3.1–3.9. Schrock's group has extensively investigated the barriers to rotation about the M=C$_\alpha$ bond in molybdenum and tungsten carbene complexes.[48] In the tetrahedral molybdenum olefin metathesis catalysts,

$(ArN)(OR)_2Mo{=}CHR^1$, the rate of alkylidene rotation appears to be critical to the stereochemistry of the metathesis products.[49] The values of $\Delta G^{\ddagger}$ for this rotational process vary from 16 to 22 kcal/mol at 25 °C, depending on the nature of the substituents Ar, R, and R^1. In general, more electron withdrawing alkoxide ligands increase the barrier to alkylidene rotation in these systems.[48]

Despite the potential relevance of alkylidene rotation to the mechanism[25] and selectivity of ruthenium-based olefin metathesis catalysts, this dynamic behavior has not been explored experimentally. A number of groups have addressed alkylidene rotation in [Ru]=CHR complexes with computational methods. For example, Caulton and coworkers used DFT calculations to obtain a rotational barrier of 4.6 kcal/mol for the ethylidene in $(PH_3)_2(Cl)_2Ru{=}CHCH_3$ at 25 °C.[50] Hofmann has placed an upper limit of 9 kcal/mol for the barrier to methylidene rotation in $(PH_3)_2(Cl)_2Ru{=}CH_2$, also using DFT.[51] A similar value was obtained by Benson and Cundari using Hartree-Fock calculations for a series of complexes of the general formula $(PR_3)_2(X)_2Ru{=}CH_2$.[52] These calculations represent estimates of the "inherent" electronic barrier for rotation about the [Ru]=C_α bond. However, they all involve relatively small alkylidene substituents (H, CH_3), and therefore do not take into account the steric interactions associated with this rotation.

Figure 9. Possible Rotational Modes for Ruthenium Benzylidene Catalysts.

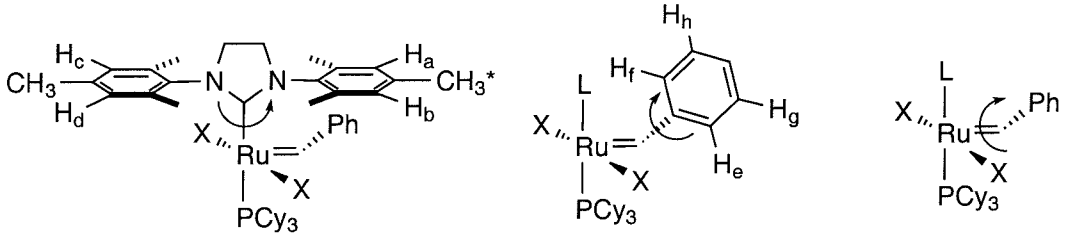

(A) **(B)** **(C)**

L = $IMesH_2$ or PCy_3

The ^1H NMR spectra of benzylidenes **3.2–3.9** show dynamic behavior that can be frozen out at –80 °C. At the low temperature limit, these complexes have no symmetry, and all of the aromatic protons of the *N*-heterocyclic carbene (H_a, H_b, H_c, and H_d) and the benzylidene (H_e, H_f, H_g, and H_h) ligands are inequivalent (Figure 2). This indicates that

the three rotational processes depicted in Figure 9 – *N*-heterocyclic carbene rotation (**A**), phenyl group rotation (**B**), and benzylidene rotation (**C**) – are all slow at –80 °C. In contrast, the ^{1}H NMR spectra of **3.2–3.9** at 100 °C show C_S symmetry. At this temperature, the mesityl aromatic protons H_a and H_b (as well as H_c and H_d) become equivalent, as do the two *ortho* (H_e and H_f) and the two *meta* (H_g and H_h) protons of the benzylidene ligand. Importantly, the two *para* methyl groups of the *N*-heterocyclic carbene (CH_3 and CH_3*) remain inequivalent at all accessible temperatures.

The data clearly indicate that *N*-heterocyclic carbene rotation (**A**) does not occur on the NMR time scale in complexes **3.2–3.9**, because fast NHC rotation would average the ^{1}H NMR signals of the *para* methyl groups, CH_3 and CH_3*. The ^{1}H NMR data also definitively show that phenyl group rotation (**B**) cannot be the only dynamic process taking place in **3.2–3.9**. Phenyl group rotation alone would result in two ^{1}H NMR signals for the equivalent sets of *ortho* and *meta* benzylidene protons, but four signals for the inequivalent $IMesH_2$ aromatic protons. Finally, benzylidene rotation (**C**) also cannot be the only dynamic process occurring in these complexes. Rotation **C** alone would produce two ^{1}H NMR signals for the equivalent sets of $IMesH_2$ protons (H_a/H_b and H_c/H_d) but four different signals for the *ortho* and *meta* benzylidene protons. Based on these arguments, we conclude that the fluxional behavior observed in **3.2–3.9** results from rotation about both the [Ru]=C_α and the C_α–C_β bonds (**B** and **C**). These two rotational events are likely coupled together in a coordinated manner, so as to minimize steric interactions between the bulky phenyl group and the L-type ligands when the L–Ru–C_α–C_β dihedral angle is 0°.[53]

Coalescence experiments were carried out to investigate the barriers to benzylidene/phenyl rotation in **3.2–3.9**, and the values of $\Delta G^\ddagger$ for this process were determined using Eq 1.[54] All of the ancillary ligands, including the *N*-heterocyclic carbene, phosphine, and halides, have a significant effect on the benzylidene/phenyl rotational barrier in these systems.[55] The largest barrier (14.1 kcal/mol) is observed in complex **3.2**, while the lowest barrier (9.8 kcal/mol) is observed in **3.9** (Table 3). In general, the experimental values of $\Delta G^\ddagger$ are significantly larger (by 5-10 kcal/mol) than those predicted by theory,[50-52] presumably because of steric contributions to the rotational barrier.

$$\Delta G^{\ddagger}([Ru]{=}C_{\alpha}) = 4.57(T_C)[9.97 - \log(T_C/\Delta\nu)] \qquad \text{(Eq 1)}$$

The data summarized in Table 3 show several trends in the magnitude of $\Delta G^{\ddagger}$ as a function of steric and electronic parameters of the ancillary ligands. For example, changing the *N*-heterocyclic carbene from $IMesH_2$ to the isosteric IMes (complexes **3.2** and **3.3**, respectively) has a minor effect on the rotational barrier ($\Delta\Delta G^{\ddagger}$ = 0.4 kcal/mol). This result suggests that the electronic contribution of the *N*-heterocyclic carbene ligand to benzylidene/phenyl rotation is relatively small. In contrast, Herrmann has reported that $(ICy)(PCy_3)(Cl)_2Ru{=}CHPh$ [ICy = 1,3-dicyclohexyl-imidazol-2-ylidene] shows fast benzylidene/phenyl rotation at room temperature,[7b] indicating that $\Delta G^{\ddagger}$ is at least 2-3 kcal/mol lower than that in **3.2** and **3.3**.[56] The ICy ligand is electronically similar to IMes,[22] and, as such, we attribute the lower rotational barrier in the ICy adduct to a steric effect. Estimates of the steric parameters associated with ICy indicate that this ligand is approximately isosteric with PCy_3 and is almost 20% smaller than IMes.[6c]

Table 3. Barriers to Benzylidene/Phenyl Rotation in **3.2–3.9**.

Complex	T (Coalescence)	$\Delta G^{\ddagger}$ (kcal/mol)	$\Delta G^{\ddagger}$ (kcal/mol) (PR_3 dissociation)
3.2	42 °C	14.1 ± 0.5	23.0 ± 0.4
3.3	32 °C	13.7 ± 0.5	24 ± 1
3.4	10 °C	12.6 ± 0.5	19.0 ± 0.5
3.8	–55 °C	9.6 ± 0.5	19.6 ± 0.3
3.1	–65 °C	9.4 ± 0.5	19.88 ± 0.06
3.9	–67 °C	9.1 ± 0.5	22.7 ± 0.3

The size of the phosphine ligand also appears to be important factor in determining the rate of benzylidene/phenyl rotation in these systems. For example, the PBn_3 (**3.9**) and PPh_3 (**3.8**) catalysts (cone angles = 165° and 145°, respectively)[42] show

rotational barriers that are almost 5 kcal/mol lower than that in the PCy_3 catalyst (**3.2**) (cone angle = 170°).[42,57] However, a larger sampling of catalysts must be investigated before definitive conclusions can be drawn about phosphine effects on the free energy of activation for this rotational event.

There has been some speculation that benzylidene/phenyl rotation is coupled to phosphine dissociation, a process that is critical for entry of **3.2–3.9** into the olefin metathesis catalytic cycle.[1] However, as summarized in Table 3, the activation energies required for phosphine dissociation in these systems (which were determined independently using magnetization transfer techniques)[1] are approximately 10 kcal/mol higher than those for benzylidene rotation. As such, these two events are clearly independent of one another.

The bis-phosphine complex **3.1** also shows dynamic behavior by ^{1}H NMR spectroscopy. At –80 °C, five signals are observed for the aromatic protons of the benzylidene, indicating that both phenyl rotation (**B**) and benzylidene rotation (**C**) are slow at this temperature. In contrast, at 25 °C, the two sets of *ortho* and *meta* protons become equivalent, and only three aromatic signals are observed for the benzylidene ligand. These observations suggest that either phenyl rotation and benzylidene rotatation (**B** and **C**) or only phenyl rotation (**B**) is fast at room temperature.[58] As outlined in Figure 10, an experiment was designed to confirm that the fluxional behavior in **3.1** involves benzylidene rotation. This experiment takes advantage of the facile anion exchange reaction between catalyst **3.1** and $(PCy_3)_2(I)_2Ru{=}CHPh$ (**3.12**) to produce the mixed halide species $(PCy_3)_2(I)(Cl)Ru{=}CHPh$ (**3.13**).[59,60] The benzylidene ligand of **3.13** can assume two distinct conformations in which H_α is rotated towards the iodide (rotamer **X**) or towards the chloride ligand (rotamer **Y**). At ambient temperature, fast benzylidene rotation is expected, and should produce a single, averaged H_α signal for the two isomeric forms of **3.13**. However, under conditions where benzylidene rotation is slow on the NMR time scale, two distinct H_α resonances for the **X** and **Y** rotamers should be observed.

Figure 10. Mixed Halide Experiment for Characterizing Benzylidene Rotation in **3.1**.

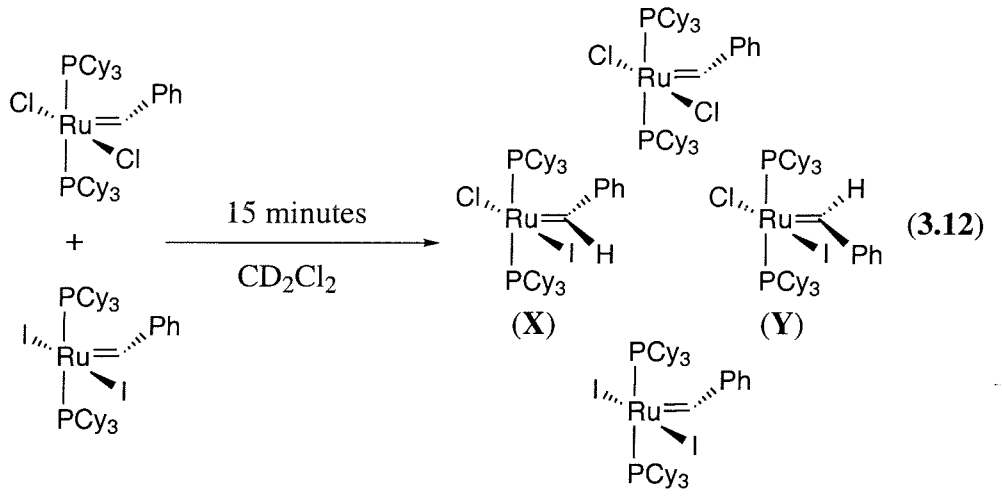

Equimolar ratios of **3.1** and **3.12** were combined in an NMR tube in CD_2Cl_2, and 1 : 2 : 1 mixture of benzylidene H_α signals (corresponding to **3.1** : **3.13** : **3.12**) was observed at room temperature. When this solution was cooled to –80 °C, ^{1}H NMR spectroscopy showed *four* distinct benzylidene resonances between 20 and 18 ppm. Furthermore, the coalescence temperature for the benzylidene signals of **3.13** was virtually identical to that observed for the exchanging *ortho* and *meta* aromatic protons in this system.[61] On the basis of the reasoning described above, we assign the fluxional behavior in **3.1** as a benzylidene/phenyl rotational process similar to that observed in complexes **3.2**–**3.9**. The value of $\Delta G^{\ddagger}$ for this rotation in **3.1** is 9.6 kcal/mol, which is almost identical to that in complexes **3.8** and **3.9**.

***N*-Heterocyclic Carbene Rotation.**[62] Rotation about the Ru–NHC bond (**A**) in **3.2**–**3.9** is slow on the NMR time scale, and coalescence is not observed up to 100 °C in toluene-d_8. As a result, ^{1}H NMR magnetization transfer (MT) was utilized to investigate *N*-heterocyclic carbene rotation in these systems. In the MT experiments, one of the mesityl *para* methyl resonances was selectively inverted using a DANTE pulse sequence,[63] and ^{1}H NMR spectra were recorded after variable mixing times (ranging between 0.00003 and 20 seconds). The time dependent magnetization data was analyzed using the computer program CIFIT,[64] and rate constants for methyl group exchange (k_E) were obtained for each catalyst. The exchange rate constant (k_E) was examined as a

function of temperature, and Eyring plots were used to calculate activation parameters for $IMesH_2$ rotation in **3.2**, **3.8**, and **3.9**. An Eyring plot for $IMesH_2$ rotation in complex **3.2** is shown in Figure 11, and the rotational barriers are summarized in Table 4.

Table 4. Barriers for *N*-Heterocyclic Carbene Rotation.

Complex	k_E (85 °C)	$\Delta H^{\ddagger}$ (kcal/mol)	$\Delta S^{\ddagger}$ (eu)	$\Delta G^{\ddagger}$ (kcal/mol)
3.2	$0.58 \pm 0.03\ s^{-1}$	23 ± 1	6 ± 4	21.8 ± 0.3
3.8	$72 \pm 5^{[a]}\ s^{-1}$	14.4 ± 0.5	-10 ± 1	17.42 ± 0.03
3.9	$23 \pm 4^{[a]}\ s^{-1}$	20 ± 1	2 ± 4	19.0 ± 0.1

[a] Value extrapolated from an Eyring plot.

Figure 11. Eyring Plot for $IMesH_2$ Rotation in Complex **3.2**.

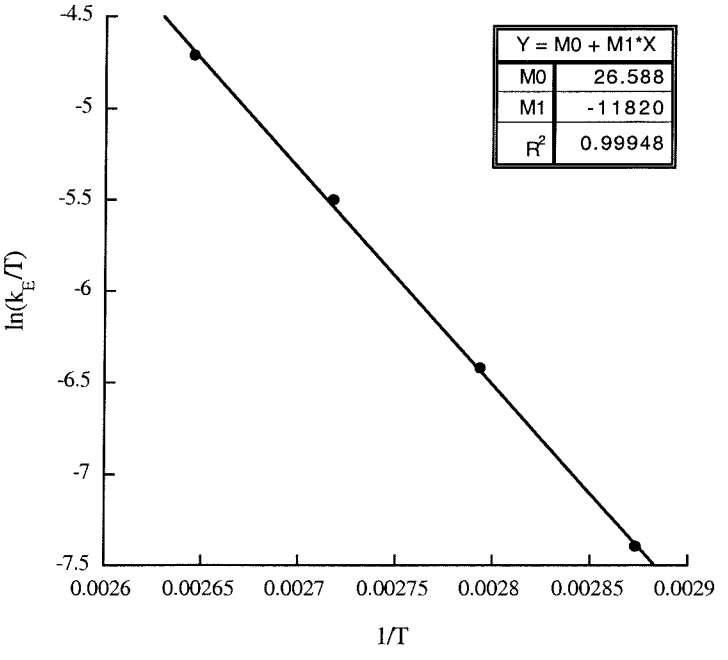

In general, the values of $\Delta G^{\ddagger}$ for NHC rotation are close to 8 kcal/mol higher than those for benzylidene/phenyl rotation. The relative magnitudes of these rotational barriers are particularly notable because the Ru-NHC interaction is typically considered a single bond while the Ru-benzylidene interaction is described as a double bond. It appears that the NHC rotational barrier may correlate with the size of the phosphine ligand, and $\Delta G^{\ddagger}$ increases upon moving from PPh_3 to PBn_3 to PCy_3 (cone angles 145°, 165° and 170°, respectively).[42]

Interestingly, the four-coordinate complex **3.11** shows fast $IMesH_2$ rotation at room temperature by ^1H NMR spectroscopy. Although the value of $\Delta G^{\ddagger}$ for this process has not yet been measured, it is estimated to be at least 8-10 kcal/mol lower than that in **3.2**, **3.8**, and **3.9**.[56] This data provides further evidence that the phosphine ligand plays a critical role in hindering NHC rotation. Additionally, this result suggests that NHC rotation is fast in the olefin metathesis intermediate $(IMesH_2)(X)_2Ru{=}CHPh$. This point may serve as a critical consideration in the design of new *N*-heterocyclic carbene ligands for stereoselective olefin metathesis reactions.

Summary and Conclusions

This chapter describes the synthesis and characterization of a series of *N*-heterocyclic carbene-containing ruthenium benzylidenes. A large amount of ligand variation is possible in only one or two steps from the commercially available starting material **3.2**. In particular, the bis-pyridine complex **3.7**, which is prepared directly from **3.2**, serves as a valuable precursor for the substitution of both the X and the L-type ligands, presumably due to the substitutional lability of the coordinated pyridines. We anticipate that this starting material will prove useful for the synthesis of new derivatives of **3.2**, and may provide access to a "combinatorial" approach for the discovery of new ruthenium olefin metathesis catalysts.

The barriers to rotation about the benzylidene and *N*-heterocyclic carbene ligands of complexes **3.2–3.9** have been investigated in detail. At this time, we have a poor understanding of the complicated electronic effects than influence these rotational

barriers, but it seems clear that steric factors play a large role in hindering rotation about both of these metal-carbon bonds. More effort will be required to definitively determine the implications of these fluxional processes for the mechanism, activity, and stereoselectivity of ruthenium olefin metathesis catalysts. In general, rigidification of these catalyst systems is important goal, because the presence of fewer conformational degrees of freedom should provide improved (and more predictive) stereoselectivity in olefin metathesis reactions.

Experimental Section

General Procedures. Manipulation of organometallic compounds was performed using standard Schlenk techniques under an atmosphere of dry argon or in a nitrogen-filled Vacuum Atmospheres drybox (O_2 < 2 ppm). NMR spectra were recorded on a Varian Inova 500 (499.85 MHz for ^{1}H; 202.34 MHz for ^{31}P; 125.69 MHz for ^{13}C), a Varian Mercury 300 (299.817 for ^{1}H; 121.39 MHz for ^{31}P; 74.45 MHz for ^{13}C), or a JEOL JNM-GX400 (399.8 MHz ^{1}H; 100.5 MHz ^{13}C; 161.9 MHz ^{31}P). ^{31}P NMR spectra were referenced using H_3PO_4 (δ = 0 ppm) as an external standard. All NMR spectra were recorded at room temperature unless otherwise indicated. UV-vis spectra were recorded on an HP 8452A Diode Array Spectrophotometer.

Materials and Methods. Pentane, methylene chloride, diethyl ether, toluene, benzene, THF, and benzene-d_6 were dried by passage through solvent purification columns.[65] Toluene-d_8 and THF-d_8 were dried by vacuum transfer from Na/benzophenone. CD_2Cl_2, pyridine, and ethyl vinyl ether were dried by vacuum transfer from CaH_2. All phosphines were obtained from commercial sources and used as received. Silica gel was obtained from TSI and KTp was obtained from Strem Chemicals. Ruthenium complex **3.1**,[3] $(PCy_3)_2(Br)_2Ru$=CHPh[25] and the $IMesH_2[BF_4]$[8] salt were prepared according to literature procedures.

$(IMesH_2)(PCy_3)(Cl)_2Ru$=CHPh (3.2). $IMesH_2[BF_4]$ (0.90 g, 2.7 mmol) and KO^{t}Bu (0.30 mg, 2.7 mmol) were combined in an oven dried Schlenk in THF (20 mL),

and the resulting yellow suspension was stirred for 1 hour. To this suspension was added a solution of **3.1** (1.1 g, 1.3 mmol) in benzene (20 mL). The reaction was heated to 80 °C for 30 minutes and then the solvents were removed under vacuum. The residue was taken up in benzene (30 mL) and filtered through a plug of Celite. The resulting solution was concentrated to approximately 2 mL and the product was precipitated with methanol (45 mL). The pink solid was washed with methanol (3 x 30 mL) and pentane (2 x 10 mL), then dried under high vacuum to afford **3.2** (0.50 g, 45% yield). ^{1}H NMR (CD_2Cl_2, 22 °C): δ 19.06 (s, 1H, Ru=C*H*Ph), 8.90 (br. s, 1H, ortho C*H*), 7.37 (t, 1H, para C*H*, J_{HH} = 7 Hz), 7.12 (t, 2H, meta C*H*, J_{HH} = 7 Hz), 7.00 (s, 2H, Mes C*H*), 6.90 (d, 1H, ortho C*H*, J_{HH} = 9 Hz), 6.74 (br. s, 1H, Mes C*H*), 5.80 (br. s, 1H, Mes C*H*), 4.00 (br. multiple peaks, 4H, CH_2CH_2), 2.31 (s, 3H, para CH_3), 1.90 (s, 3H, para CH_3), 2.70-2.10 (br. multiple peaks, 12H, ortho CH_3), 1.51-0.87 (multiple peaks, 33H, P*Cy*$_3$). ^{13}C{^{1}H} NMR (C_6D_6): δ 295.06 (m, Ru=*C*HPh), 221.82 (d, Ru-*C*(N)$_2$, J_{CP} = 78 Hz), 152.31, 139.69, 138.63, 138.11, 137.90, 137.59, 136.18, 130.59, 129.69, 52.47 (d, J_{CP} = 3 Hz), 51.49 (d, J_{CP} = 1 Hz), 32.34, 32.21, 29.99, 28.58, 28.50, 26.93, 21.55, 21.38, 20.85, 19.32.

^{1}H NMR (CD_2Cl_2, –40 °C): δ = 18.81 (s, 1H, Ru=C*H*Ph), 8.82 (d, 1H, ortho C*H*, J_{HH} = 9 Hz), 7.35 (t, 1H, para C*H*, J_{HH} = 8 Hz), 7.13 (t, 1H, meta C*H*, J_{HH} = 8 Hz), 7.05 (t, 1H, meta C*H*, J_{HH} = 7 Hz), 7.02 (s, 1H, Mes C*H*), 6.97 (s, 1H, Mes C*H*), 6.87 (d, 1H, ortho C*H*, J_{HH} = 8 Hz), 6.74 (s, 1H, Mes C*H*), 5.71 (s, 1H, Mes C*H*), 4.05-3.70 (overlapping multiplets, 4H, CH_2CH_2), 2.74 (s, 3H, Mes CH_3), 2.50 (s, 3H, Mes CH_3), 2.47 (s, 3H, Mes CH_3), 2.27 (s, 3H, Mes CH_3), 1.93 (s, 3H, Mes CH_3), 1.87 (s, 3H, Mes CH_3), 1.47-0.55 (multiple peaks, 33H, P*Cy*$_3$).

(IMesH$_2$)(PCy$_3$)(I)$_2$Ru=CHPh (3.4). Complex **3.2** (350 mg, 0.41 mmol) and NaI (1.23 g, 8.2 mmol) were combined in THF (15 mL) and stirred under argon for 8 hours. The solvent was removed under vacuum, and the green residue was taken up in benzene (10 mL). The resulting suspension was filtered through a plug of Celite, and the olive green solution was concentrated under vacuum to yield complex **3.4** as a green powder (320 mg, 75% yield). ^{31}P{^{1}H} NMR (CD_2Cl_2): δ 30.84 (s). ^{1}H NMR (CD_2Cl_2): δ 19.09 (s, 1H, Ru=C*H*Ph),[66] 7.90-6.94 (br. multiple peaks, 8H, ortho C*H*, meta C*H*, para C*H*, and Mes C*H*), 6.25 (br. s, 1H, Mes C*H*), 3.98 (br. m, 4H, CH_2CH_2), 2.71-2.34 (multiple

peaks, 15 H, P*Cy*$_3$ and Mes C*H*$_3$), 2.28 (s, 3H, Mes C*H*$_3$), 1.85 (s, 3H, Mes C*H*$_3$), 1.56-0.90 (m, 30H, P*Cy*$_3$). $^{13}C\{^1H\}$ NMR (C_7D_8): δ 302.34 (m, Ru=*C*HPh), 223.01 (d, Ru-*C*(N)$_2$, J_{CP} = 76 Hz), 152.24, 138.44, 138.04, 137.13, 136.36, 130.27, 129.57, 128.45, 127.33, 126.85, 52.67 (d, J_{CP} = 3 Hz), 51.78 (d, J_{CP} = 1 Hz), 34.84, 34.70, 30.80, 27.28, 27.28, 26.69, 23.54, 20.99, 20.87. Anal. Calcd for $C_{46}H_{65}N_2I_2PRu$: C, 53.54; H, 6.35; N, 2.71. Found: C, 53.68; H, 6.32; N, 2.40.

(IMesH$_2$)(PCy$_3$)(Br)$_2$Ru=CHPh (3.5). IMesH$_2$[BF$_4$] (115 mg, 0.29 mmol) and KO^{t}Bu (30 mg, 0.27 mmol) were combined in an oven dried Schlenk in benzene (2 mL), and the resulting yellow suspension was stirred for 1 hour. To this suspension was added a solution of (PCy$_3$)$_2$(Br)$_2$Ru=CHPh (220 mg, 0.24 mmol) in benzene (8 mL). The reaction was heated to 50 °C for 18 hours, and then the solvents were removed under vacuum. The residue was taken up in benzene and filtered through a plug of Celite. The benzene was reduced to 2 mL under vacuum, and the product was purified by column chromatography (4:1 pentane/diethyl ether) according to the procedure of Hoveyda[16] to afford **3.5** as a light pink powder (147 mg, 65% yield). $^{31}P\{^1H\}$ NMR (C_6D_6): δ 30.83 (s). ^1H NMR (C_6D_6): δ 19.87 (s, 1H, Ru=C*H*Ph), 9.75 (br. s, 1H, ortho C*H*), 7.5-7.0 (br. multiple peaks, 6H, meta C*H*, para C*H*, ortho C*H*, and Mes C*H*), 6.70 (br. s, 1H, Mes C*H*), 6.10 (br. s, 1H, Mes C*H*), 3.55 (br. m, 4H, C*H*$_2$C*H*$_2$), 2.44 (s, 3H, para C*H*$_3$), 2.06 (s, 3H, para C*H*$_3$), 3.01-1.33 (br. multiple peaks, 45 H, P*Cy*$_3$ and ortho C*H*$_3$). $^{13}C\{^1H\}$ NMR (C_6D_6): δ 296.92 (m, Ru=*C*HPh), 222.31 (d, Ru-*C*(N)$_2$, J_{CP} = 78 Hz), 152.37, 139.40, 138.57, 138.07, 137.92, 137.59, 136.34, 130.61, 129.81, 127.94, 52.72 (d, J_{CP} = 3 Hz), 51.70 (d, J_{CP} = 2 Hz), 33.07, 30.38, 28.59, 28.51, 26.95, 21.91, 21.48, 21.32, 19.91. Anal. Calcd for $C_{46}H_{65}N_2Br_2PRu$: C, 58.91; H, 6.99; N, 2.99. Found: C, 59.25; H, 7.09; N, 2.97.

(IMesH$_2$)(C$_5$H$_5$N)$_2$(Cl)$_2$Ru=CHPh (3.7).[31] Complex **3.2** (1.1 g, 1.3 mmol) was dissolved in toluene (3 mL), and pyridine (12 mL) was added. The reaction was stirred for 10 minutes during which time a color change from pink to bright green was observed. The reaction mixture was cannula transferred into 75 mL of cold (–10 °C) pentane, and a green solid precipitated. The precipitate was filtered, washed with 4 x 20 mL of pentane,

and dried under vacuum to afford **3.7** as a green powder (0.75 g, 80% yield). Samples for elemental analysis were prepared by recrystallization from C_6H_6/pentane followed by drying under vacuum. These samples analyze as the mono-pyridine adduct $(IMesH_2)(C_5H_5N)(Cl)_2Ru{=}CHPh$, probably due to loss of pyridine under vacuum. ^1H NMR (C_6D_6): δ 19.67 (s, 1H, C*H*Ph), 8.84 (br. s, 2H, pyridine), 8.39 (br. s, 2H, pyridine), 8.07 (d, 2H, ortho C*H*, J_{HH} = 8 Hz), 7.15 (t, 1H, para C*H*, J_{HH} = 7 Hz), 6.83-6.04 (br. mulitiple peaks, 9H, pyridine, Mes C*H*), 3.37 (br. d, 4H, CH_2CH_2), 2.79 (br. s, 6H, Mes CH_3), 2.45 (br. s, 6H, Mes CH_3), 2.04 (br. s, 6H, Mes CH_3). $^{13}C\{^1H\}$ NMR (C_6D_6): 314.90 (m, Ru=*C*HPh), 219.10 (s, Ru-*C*$(N)_2$), 152.94, 150.84, 139.92, 138.38, 136.87, 135.99, 134.97, 131.10, 130.11, 129.88, 128.69, 123.38, 51.98, 51.37, 21.39, 20.96, 19.32. Anal. Calcd for $C_{33}H_{37}N_3Cl_2Ru$: C, 61.20; H, 5.76; N, 6.49. Found: C, 61.25; H, 5.76; N, 6.58.

$(IMesH_2)(PPh_3)(Cl)_2Ru{=}CHPh$ (3.8). Complex **3.7** (150 mg, 0.21 mmol) and PPh_3 (76 mg, 0.28 mmol) were combined in benzene (10 mL) and stirred for 10 minutes. The solvent was removed under vacuum, and the resulting brown residue was washed with 4 x 20 mL pentane and dried *in vacuo*. Complex **3.8** was obtained as a brownish powder (125 mg, 73% yield). $^{31}P\{^1H\}$ NMR (C_6D_6): δ 37.7 (s). ^1H NMR (C_7D_8): δ 19.60 (s, 1H, Ru=C*H*Ph), 7.70 (d, 2H, ortho C*H*, J_{HH} = 8 Hz), 7.29-6.71 (multiple peaks, 20H, P*Ph*$_3$, para C*H*, meta C*H*, and Mes C*H*), 6.27 (s, 2H, Mes C*H*), 3.39 (m, 4H, CH_2CH_2), 2.74 (s, 6H, ortho CH_3), 2.34 (s, 6H, ortho CH_3), 2.23 (s, 3H, para CH_3), 1.91 (s, 3H, para CH_3). $^{13}C\{^1H\}$ NMR (C_6D_6): δ 305.34 (m, Ru=*C*HPh), 219.57 (d, Ru-*C*$(N)_2$, J_{CP} = 92 Hz), 151.69 (d, J_{CP} = 4 Hz), 139.68, 138.35, 138.10, 138.97, 137.78, 135.89, 135.21, 135.13, 131.96, 131.65, 131.36, 130.47, 129.83, 129.59 (d, J_{CP} = 2 Hz), 129.15, 128.92, 128.68, 128.00, 52.11 (d, J_{CP} = 4 Hz), 51.44 (d, J_{CP} = 2 Hz), 21.67, 21.35, 21.04, 19.21. Anal. Calcd for $C_{46}H_{47}N_2Cl_2PRu$: C, 66.50; H, 5.70; N, 3.37. Found: C, 67.18; H, 5.81; N, 3.31.

$(IMesH_2)(PBn_3)(Cl)_2Ru{=}CHPh$ (3.9). Complex **3.7** (150 mg, 0.21 mmol) and PBn_3 (88 mg, 0.29 mmol) were combined in benzene (10 mL) and stirred for 10 minutes. The solvent was removed under vacuum, and the resulting brown residue was washed

with 4 x 20 mL pentane and dried *in vacuo*. Complex **3.9** was obtained as a brown/pink powder (130 mg, 73% yield). $^{31}P\{^1H\}$ NMR (C_6D_6): δ 34.7 (s). ^1H NMR (C_6D_6): δ 19.31 (s, 1H, Ru=C*H*Ph), 8.31 (d, 2H, ortho C*H*, J_{HH} = 7 Hz,), 7.36 (7, 1H, para C*H*, J_{HH} = 7 Hz), 7.16 (br. s, 19H, $P(CH_2Ph)_3$, meta C*H*, Mes C*H*), 6.64 (s, 2H, Mes C*H*), 3.77 (m, 2H, CH_2CH_2), 3.64 (m, 2H, CH_2CH_2), 3.29 (d, 6H, benzyl CH_2, J_{HP} = 7.2 Hz), 3.18 (s, 6H, ortho CH_3), 2.78 (s, 6H, ortho CH_3), 2.18 (s, 3H, para CH_3), 2.12 (s, 3H, para CH_3). $^{13}C\{^1H\}$ NMR (C_6D_6): δ 297.50 (m, Ru=*C*HPh), 222.30 (d, Ru-*C*$(N)_2$, J_{CP} = 85 Hz), 151.52, 140.31, 139.54, 137.94, 137.77, 137.30, 135.45, 135.42, 135.39, 131.27, 131.24, 131.21, 130.21, 129.72, 129.00, 126.42, 126.40, 51.72 (d, J_{CP} = 1 Hz), 51.52 (d, J_{CP} = 4 Hz), 25.80, 25.68, 21.36, 21.20, 21.11, 19.13. Anal. Calcd for $C_{49}H_{53}N_2Cl_2PRu$: C, 67.42; H, 6.12; N, 3.21. Found: C, 67.70; H, 6.20; N, 3.26.

Tp(IMesH$_2$)(Cl)Ru=CHPh (3.10). KTp (87 mg, 0.34 mmol) and complex **3.7** (125 mg, 0.17 mmol) were combined in CH_2Cl_2 (10 mL) and stirred for 1 hour. Pentane (20 mL) was added to precipitate the salts, and the reaction was stirred for an additional 30 minutes and then cannula filtered. The resulting bright green solution was concentrated *in vacuo*, and the solid residue was washed with pentane (2 x 10 mL) and methanol (2 x 10 mL) and dried under vacuum to afford **3.10** (84 mg, 66% yield) as an analytically pure green powder. ^1H NMR (CD_2Cl_2): δ 18.73 (s, 1H, Ru=C*H*Ph), 7.87 (d, 1H, Tp, J_{HH} = 2.4 Hz), 7.41 (d, 1H, Tp, J_{HH} = 2.1 Hz), 7.35–7.30 (multiple peaks, 3H, Tp and para C*H*), 7.08 (d, 1H, Tp, J_{HH} = 1.5 Hz), 6.82 (br. s, 5H, Mes C*H*, ortho C*H* and meta C*H*), 6.24 (br. s, 3H, Mes C*H*), 6.16 (t, 1H, Tp, J_{HH} = 1.8 Hz), 5.95 (d, 1H, Tp, J_{HH} = 1.5 Hz), 5.69 (t, 1H, Tp, J_{HH} = 2.4 Hz), 5.50 (t, 1H, Tp, J_{HH} = 1.8 Hz), 3.77 (br. d, 4H, CH_2CH_2), 2.91–0.893 (br. multiple peaks, 18H, ortho CH_3, para CH_3). $^{13}C\{^1H\}$ (CD_2Cl_2): δ 324.29 (m, Ru=*C*HPh), 220.57 (s, Ru-*C*$(N)_2$), 151.50, 146.08, 145.39, 142.07, 137.94, 136.57, 134.41, 133.18, 130.60 (br), 129.55, 127.98, 106.41, 105.19, 104.51, 53.77 (br), 21.26, 20.32 (br). Anal. Calcd for $C_{37}H_{42}N_8ClBRu$: C, 59.56; H, 5.67; N, 15.02. Found: C, 59.20; H, 5.67; N, 14.72.

(IMesH$_2$)(O^{t}Bu)$_2$Ru=CHPh (3.11). Complex **3.7** (7.5 mg, 0.010 mmol) and KO^{t}Bu (3 mg, 0.027 mmol) were combined in C_6D_6 (0.6 mL) in an NMR tube. The

reaction mixture was allowed to stand for 15-20 minutes, during which time a color change from green to dark red was observed. ^{1}H NMR (C_6D_6): δ 16.56 (s, 1H, Ru=C*H*Ph), 7.63 (d, 2H, ortho C*H*, J_{HH} = 7 Hz), 7.2-7.1 (multiple peaks, 3H, meta C*H* and ortho C*H*), 6.97 (s, 4H, Mes C*H*), 3.43 (s, 4H CH_2CH_2), 2.59 (s, 12H, ortho CH_3), 2.29 (s, 6H, para CH_3), 1.18 (s, 18H, ^{t}Bu).

Kinetics of the Reaction of 3.2 with C_5D_5N. In a cuvette fitted with a rubber septum, a solution of **3.2** (0.88 mM) in toluene (1.6 mL) was prepared. The solution was allowed to thermally equilibrate in the UV-vis spectrometer at 20 °C. Neat pyridine-d_5 (25 to 100 μL) was added *via* microsyringe, and the reaction kinetics were followed by monitoring the disappearance of starting material at 502 nm. For each run, data was collected over 5 half lives, and was fitted to a first order exponential. Typical R^2 values for the exponential curve fits were greater than 0.999.

Benzylidene/Phenyl Rotation. The ruthenium benzylidene (0.012 mmol) was dissolved in CD_2Cl_2 (0.6 mL) in an NMR tube and allowed to thermally equilibrate in the NMR probe. The temperature was lowered to –80 °C (to obtain Δν at the low temperature limit) and then slowly increased until coalescence was observed. The ^{1}H NMR resonances for the two *ortho* protons of the *N*-heterocyclic carbene ligand (H_a and H_b) were typically monitored in these experiments. However, the results obtained for the coalescence of H_c and H_d as well as for H_e/H_f and H_g/H_h appear to be identical (within error) in all cases. The measurements on complexes **3.1**, **3.2**, and **3.3** were carried out on the JEOL JNM-GX400 (399.8 MHz ^{1}H) and the measurements on complexes **3.4**, **3.8**, and **3.9** were made on a Varian Mercury 300 (299.817 for ^{1}H).

***N*-Heterocyclic Carbene Rotation.** The ruthenium benzylidene (0.012 mmol) was dissolved in toluene-d_8 (600 μL) in an NMR tube, and the resulting solution was allowed to thermally equilibrate in the NMR probe. The upfield *para*-CH_3 resonance was selectively inverted using a DANTE[63] pulse sequence and, after variable mixing times (between 0.00003 and 30 s), a non-selective 90° pulse was applied and an FID recorded. Spectra were collected as 2-4 transients with relaxation delays of 30 seconds. The peak

heights of the two CH_3 signals at variable mixing times were analyzed using the computer program CIFIT[64] in order to obtain the exchange rate constant (k_E).

References and Notes

(1) Some of the experimental portion of this chapter have been previously published: (a) Sanford, M. S.; Love, J. A.; Grubbs, R. H. *J. Am. Chem. Soc.* **2001**, in press. (b) Sanford, M. S.; Ulman, M.; Grubbs, R. H. *J. Am. Chem. Soc.* **2001**, *123*, 749.

(2) Ivin, K. J.; Mol, J. C. *Olefin Metathesis and Metathesis Polymerization*, Academic Press: San Diego, CA, 1997.

(3) Schwab, P.; Grubbs, R. H.; Ziller, J. W. *J. Am. Chem. Soc.* **1996**, *118*, 100.

(4) For recent reviews on the application of catalysts **3.1** and **3.2** in organic chemistry see: (a) Furstner, A. *Angew. Chem., Int. Ed.* **2000**, *39*, 3012. (b) Grubbs, R. H.; Chang, S. *Tetrahedron* **1998**, *54*, 4413.

(5) Scholl, M.; Trnka, T. M.; Morgan, J. P.; Grubbs, R. H. *Tetrahedron Lett.* **1999**, *40*, 2247.

(6) (a) Jafarpour, L.; Stevens, E. D.; Nolan, S. P. *J. Organomet. Chem.* **2000**, *606*, 49. (b) Huang, J.; Schanz, H. J.; Stevens, E. D.; Nolan, S. P. *Organometallics* **1999**, *18*, 5375. (c) Jafarpour, L.; Schanz, H. J.; Stevens, E. D.; Nolan, S. P. *Organometallics* **1999**, *18*, 5416. (d) Schanz, H. J.; Jafarpour, L.; Stevens, E. D.; Nolan, S. P. *Organometallics* **1999**, *18*, 5187. (e) Huang, J.; Stevens, E. D.; Nolan, S. P.; Peterson, J. L. *J. Am. Chem. Soc.* **1999**, *121*, 2674.

(7) (a) Weskamp, T.; Kohl, F. J.; Hieringer, W.; Gliech, D.; Herrmann, W. A. *Angew. Chem., Int. Ed.* **1999**, *38*, 2416. (b) Weskamp, T.; Kohl, F. J.; Herrmann, W. A. *J. Organomet. Chem.* **1999**, *582*, 362.

(8) Scholl, M.; Ding, S.; Lee, C. W.; Grubbs, R. H. *Org. Lett.* **1999**, *1*, 953.

(9) (a) Choi, T.-L.; Chatterjee, A. K.; Grubbs, R. H. *Angew. Chem., Int. Ed.* **2001**, *40*, 1277. (b) Chatterjee, A. K.; Morgan, J. P.; Scholl, M.; Grubbs, R. H. *J. Am. Chem. Soc.* **2000**, *122*, 3783. (c) Bielawski, C. W.; Grubbs, R. H. *Angew. Chem. Int. Ed.* **2000**, *39*, 2903.

(10) Scholl, M., Ph.D. Thesis, California Institute of Technology, Pasdena, CA, 2000.

(11) Morgan, J. P.; Goldberg, S. D.; Grubbs, R. H. **2001**, unpublished results.

(12) (a) Sanford, M. S.; Henling, L. M.; Day, M. W.; Grubbs, R. H. *Angew. Chem., Int. Ed.* **2000**, *39*, 3451. (b) Coalter, J. N.; Bollinger, J. C.; Eisenstein, O.; Caulton, K. G. *New J. Chem.* **2000**, *24*, 925.

(13) Late transition metal hydrides are known to promote olefin isomerization reactions. Collman, J. P.; Hegedus, L. S.; Norton, J. R.; Finke, R. G. *Principles and Applications of Organotransition Metal Chemistry*, University Science Books: Mill Valley, CA, 1987.

(14) Wilhelm, T. E.; Grubbs, R. H. **2000**, unpublished results.

(15) Jafarpour, L.; Nolan, S. P. *Organometallics* **2000**, *19*, 2057.

(16) Garber, S. B.; Kingsbury, J. S.; Gray, B. L.; Hoveyda, A. H. *J. Am. Chem. Soc.* **2000**, *117*, 8168.

(17) Morgan, J. P.; Grubbs, R. H. *Org. Lett.* **2000**, *2*, 3153.

(18) Trnka, T. M.; Henling, L. M.; Day, M. W.; Grubbs, R. H. **2000**, unpublished results.

(19) (a) Nguyen, S. T.; Grubbs, R. H. *J. Am. Chem. Soc.* **1993**, *115*, 9858. (b) Nguyen, S. T.; Johnson, L. K.; Grubbs, R. H. *J. Am. Chem. Soc.* **1992**, *114*, 3974.

(20) Some correlation between the solution phase ^{1}H NMR alkylidene proton-phosphorus coupling constant and the solid state alkylidene configuration has been noted [for example, see ref. 19]. However, recent results show definitively that a direct Karplus relationship between the P–Ru–C_α–H_α) angle and J_{HP} does not apply in ruthenium alkylidene complexes. Sanford, M. S.; Matzger, A. J.; Grubbs, R. H. **1999**, unpublished results.

(21) Crystal structure collection and refinement data for **3.2** and **3.7** are reported in Appendix A1.

(22) *N*-heterocyclic carbene ligands with saturated backbones show significantly different electronic properties and reactivities relative to their unsaturated analogues. For example, see: (a) Bourissou, D.; Guerret, O.; Gabbai, F. P.; Bertrand, G. *Chem. Rev.* **2000**, *100*, 39. (b) Herrmann, W. A.; Kocher, C. *Angew. Chem., Int. Ed. Engl.* **1997**, *36*, 2162.

(23) This value represents an average of the two Ru–P bond lengths of 2.4097(6) Å and 2.4221(6) Å in complex **3.1**.

(24) Love, J. A.; Grubbs, R. H. **2000**, unpublished results.

(25) Dias, E. L.; Nguyen, S. T.; Grubbs, R. H. *J. Am. Chem. Soc.* **1997**, *119*, 3887.

(26) Bianchini, C.; Lee, H. M. *Organometallics* **2000**, *19*, 1833.

(27) Adlhart, C.; Hinderling, C.; Baumann, H.; Chen, P. *J. Am. Chem. Soc.* **2000**, *122*, 8204.

(28) Benitez, D.; Goddard, W. A.; Grubbs, R. H. **2000**, unpublished results.

(29) (a) Meier, R. J.; Aagaard, O. M.; Buda, F. *J. Mol. Cat. A* **2000**, *160*, 189. (b) Aagaard, O. M.; Meier, R. J.; Buda, F. *J. Am. Chem. Soc.* **1998**, *120*, 7174.

(30) Trnka, T. M.; Day, M. W.; Henling, L. M.; Grubbs, R. H. **2001**, submitted to *Organometallics*.

(31) An analogous procedure has been used to produce the phosphine analogue of **3.7** [$(PCy_3)(Cl)_2(C_5H_5N)_2Ru$=CHPh] from catalyst **3.1**. Dias, E. L., Ph.D. Thesis, California Institute of Technology, Pasadena, CA, 1997.

(32) Notably, the reaction of dimethylvinyl carbene complexes, particularly $(PCy_3)_2(Cl)_2Ru$=CHCH=$C(Me)_2$, with pyridine does not proceed cleanly to the bis-pyridine adduct. This is likely due to the reversible deprotonation of one of the methyl groups of the dimethylvinyl carbene ligand. Deprotonation reactions of this type are discussed in detail in Chapter 4.

(33) Molecule B has considerably less disorder (and smaller errors associated with bond distances and angles) than molecule A in the crystal structure of **3.7**.

(34) Octahedral ruthenium benzylidenes typically have Ru=C_α distances of approximately 1.87 Å. For example see: (a) Sanford, M. S.; Henling, L. M.; Grubbs, R. H. *Organometallics* **1998**, *17*, 5384. (b) Leung, W.-A.; Lau, K.-K.; Zhang, Q.-F.; Wong, W.-T.; Tang, B. *Organometallics* **2000**, *19*, 2084. (c) Esteruelas, M. A.; Lahoz, F. J.; Onate, E.; Oro, L. A.; Zeier, B. *Organometallics* **1994**, *13*, 4258.

(35) The significant *trans* influence of the Ru=CHPh moiety has been noted in the tris(pyrazolyl)borate complex, [$Tp(PCy_3)(H_2O)$Ru=CHPh]BF_4 [ref. 34a].

(36) Details behind the assignment of this visible absorbance as an MLCT band are described in ref. 1a.

(37) Initiation in **3.7** was measured independently by reacting this complex with 15 equivalents of ethyl vinyl ether. This reaction proceeded to completion within 5 minutes at room temperature, demonstrating that initiation in complex **3.7** is approximately 2-3 orders of magnitude faster than that in **3.2**.

(38) Low methylidene stability during the RCM of diethyl diallylmalonate was also observed in the phosphine analogue of **3.7**, $(PCy_3)(Cl)_2(C_5H_5N)_2Ru{=}CHPh$ [ref. 31].

(39) Attempts to prepare $(IMesH_2)(Cl)_2(C_5H_5N)_2Ru{=}CH_2$ by the direct reaction of $(IMesH_2)(PCy_3)(Cl)_2Ru{=}CH_2$ with an excess of pyridine were unsuccessful, and resulted in the disappearance of all downfield carbene resonances. Once again, this result is consistent with the instability of the bis-pyridine methylidene species. Trnka, T. M.; Grubbs, R. H. **2001**, unpublished results.

(40) The P(*n*-Bu)$_3$ phosphine complex, as well as the *para*-substituted PPh_3 derivatives, were prepared by Jennifer A. Love. Love, J. A.; Grubbs, R. H. **2001**, unpublished results.

(41) Wilson, M. R.; Woska, D. C.; Prock, A.; Giering, W. P. *Organometallics* **1993**, *12*, 1742.

(42) Tolman, C. A. *Chem. Rev.* **1977**, *77*, 113.

(43) Streuli, C. A. *Anal. Chem.* **1960**, *32*, 985.

(44) Nguyen, S. T., Ph.D. Thesis, California Institute of Technology, Pasadena, CA, 1995.

(45) Cucullu, M. E.; Li, C.; Nolan, S. P.; Nguyen, S. T.; Grubbs, R. H. *Organometallics* **1998**, *17*, 5565.

(46) Notably, the reaction of complex **3.1** with KTp proceeds quantitatively within one hour at 25 °C [ref. 34a].

(47) Complex **3.11** is discussed in more detail in Chapter 4.

(48) (a) Oskam, J .H.; Schrock, R. R. *J. Am. Chem. Soc.* **1993**, *115*, 11831. (b) Oskam, J. H.; Schrock, R. R. *J. Am. Chem. Soc.* **1992**, *114*, 7588.

(49) (a) Schrock, R. R. *Polyhedron* **1995**, *14*, 3177. (b) Schrock, R. R. *Tetrahedron* **1999**, *55*, 8141.

(50) Spivak, G. J.; Coalter, J. N.; Olivan, M.; Eisenstein, O.; Caulton, K. G. *Organometallics* **1998**, *17*, 999.

(51) Hansen, S. M.; Rominger, F.; Metz, M.; Hofmann, P. *Chem. Eur. J.* **1999**, *5*, 557.

(52) Benson, M. T.; Cundari, T. R. *Int. J. Quant. Chem.* **1997**, *65*, 987.

(53) Preliminary calculations show that this rotation occurs by a "crank shaft" type mechanism. Matzger, A. J.; Sanford, M. S.; Grubbs, R. H. **1999**, unpublished results.

(54) Gunther, H. *NMR Spectroscopy : An Introduction*, John Wiley & Sons: New York, 1980.

(55) We also wanted to study the effect of alkylidene substitution on this rotational process. Unfortunately, both the dimethylvinyl carbene complex, $(IMesH_2)(PCy_3)(Cl)_2Ru{=}CHCH{=}C(Me)_2$ and the methylidene complex, $(IMesH_2)(PCy_3)(Cl)_2Ru{=}CHD$ showed fast alkylidene rotation at all accessible temperatures, so activation barriers could not be determined in these systems. Trnka, T. M.; Sanford, M. S.; Grubbs, R. H. **2001**, unpublished results.

(56) The rotational barriers in $(ICy)(PCy_3)(Cl)_2Ru{=}CHPh$ and $(IMesH_2)(O^tBu)_2Ru{=}CHPh$ have not yet been measured directly and were estimated using "back of the envelope" calculations.

(57) The low $\Delta G^{\ddagger}$ value for **3.9** is also likely due to the large number conformational degrees freedom available to the PBn_3 ligand.

(58) An early publication erroneously assigned this dynamic behavior as purely phenyl group rotation [ref. 34a].

(59) Facile anion metathesis of $(PR_3)_2(Cl)_2Ru{=}CHR^1$ with iodide salts to form a statistical mixture of ruthenium halide species has been described in water soluble ruthenium olefin metathesis catalysts. Lynn, D. M.; Mohr, B.; Grubbs, R. H.; Henling, L. M.; Day, M. W. *J. Am. Chem. Soc.* **2000**, *122*, 6601.

(60) Direct anion metathesis between the catalysts $(PCy_3)_2(Cl)_2Ru{=}CHR$ and $(PCy_3)_2(I)_2Ru{=}CHR$ has also been observed. Wilhelm, T. E., Ph.D. Thesis, California Institute of Technology, Pasadena, CA, 1997.

(61) This "mixed halide" experiment was also carried out using the $IMesH_2$ complexes **3.2** and **3.4**, and afforded analogous results to those obtained in the bis-phosphine system.

This provides independent verification that this technique is targeting the benzylidene rotation event.

(62) Herrmann and coworkers have noted hindered NHC rotation in the related bis-NHC complexes, $(NHC)_2(Cl)_2Ru=CHPh$. However, they did not report activation barriers for these systems. Weskamp, T.; Schattenmann, W. C.; Spiegler, M.; Herrmann, W. A. *Angew. Chem., Int. Ed.* **1998**, *37*, 2490.

(63) Morris, G. A.; Freeman, R. *J. Magn. Res.* **1978**, *29*, 433.

(64) Bain, A. D.; Kramer, J. A. *J. Magn. Res.* **1996**, *118A*, 21.

(65) Pangborn, A. B.; Giardello, M. A.; Grubbs, R. H.; Rosen, R. K.; Timmers, F. J. *Organometallics* **1996**, *15*, 1518.

(66) Minor benzylidene peaks are also observed by ^1H NMR spectroscopy at 18.14 and 17.17 ppm (< 5% of total) in analytically pure samples of **3.4**.

Chapter 4: Synthesis and Reactivity of Four-Coordinate Ruthenium Benzylidenes[1]

Abstract

A series of four-coordinate ruthenium benzylidenes were prepared as analogues of the 14-electron olefin metathesis intermediate $(PCy_3)(Cl)_2Ru{=}CHPh$ (**4.3**), and their structures and reactivities were explored. The complex, $(PCy_3)(O^tBu)_2Ru{=}CHPh$ (**4.4**), was available by the reaction of $(PCy_3)_2(Cl)_2Ru{=}CHPh$ (**4.1**) with an excess of KO^tBu. Protonation of the coordinated *tert*-butoxides with mono- and bidentate ligands was then utilized to generate a variety of new ruthenium benzylidene species. For example, treatment of **4.4** with the acidic alcohols $HOC(CF_3)_2(CH_3)$ and $HOC(CF_3)_3$ resulted in the release of HO^tBu and the formation of the new alkoxide adducts $(PCy_3)[OC(CF_3)_2(CH_3)]_2Ru{=}CHPh$ (**4.8**) and $(PCy_3)[OC(CF_3)_3]_2Ru{=}CHPh$ (**4.9**), respectively. Similarly, the diol TBEC[a] reacted with **4.4** to afford the complex $(PCy_3)(TBEC)Ru{=}CHPh$ (**4.13**) that appears to be stabilized by a C-H agostic interaction. 2,6-Dichlorophenol and triphenylacetic acid reacted with **4.4** to produce the six-coordinate adducts $(PCy_3)[(\kappa^2\text{-}O,Cl)OC_6H_3Cl_2]_2Ru{=}CHPh$ (**4.10**) and $(PCy_3)(\eta^2\text{-}O_2CCPh_3)_2Ru{=}CHPh$ (**4.11**), respectively. In contrast to complex **4.1**, the dimethylvinyl carbenes $(PCy_3)_2(Cl)_2Ru{=}CHCH{=}C(Me)_2$ (**4.16**) and $(P^iPr_3)_2(Cl)(CO)Ru{=}CHCH{=}C(Me)_2$ underwent deprotonation, rather than anion metathesis, with KO^tBu to provide the ruthenium vinylvinyl species $(PCy_3)_2(Cl)Ru{-}CH{=}CHC(Me){=}CH_2$ (**4.17**) and $(P^iPr_3)_2(Cl)(CO)Ru{-}CH{=}CHC(Me){=}CH_2$ (**4.19**), respectively. Spectroscopic and X-ray crystallographic studies of the new ruthenium complexes are described in detail. In addition, the olefin metathesis activity of these ruthenium benzylidenes in the presence and absence of HCl co-catalyst is discussed.

(a) TBEC = 2',2',2'',2''–tetrakis(trifluoromethyl)–1,2–bis(2'–hydroxyethyl)cyclopentane

Introduction

The ruthenium complexes $(PCy_3)_2(Cl)_2Ru{=}CHPh$ (**4.1**)[2] and $(IMesH_2)(PCy_3)(Cl)_2Ru{=}CHPh$ [$IMesH_2$ = 1,3-dimesityl-4,5-dihydroimidazol-2-ylidene] (**4.2**)[3] (Figure 1) are highly efficient catalysts for olefin metathesis reactions in the presence of most common functional groups,[4] and have found extensive application in synthetic chemistry.[5] Detailed experimental studies have been carried out to elucidate the mechanism of activity of **4.1** and **4.2**,[6,7] and these investigations implicate the 14-electron benzylidene $(L)(Cl)_2Ru{=}CHPh$ (**4.3**) [L = PCy_3 or $IMesH_2$] as an important intermediate both on the olefin metathesis reaction coordinate[6] and in the decomposition of **4.1** and **4.2**.[8] Intermediate **4.3** is remarkable both for its unusual four-coordinate, 14-electron ruthenium center, and for its similarity to the Mo and W olefin metathesis catalysts $(ArN)(OR)_2M{=}CHR'$ developed by Schrock and coworkers (Figure 1).[9] The short lifetime of **4.3** has rendered it difficult to isolate or observe in solution, presumably due to its high reactivity with olefinic substrates,[6] free phosphine,[6] coordinating solvents,[10] or a second equivalent of **4.3**.[8]

Figure 1. Widely Used Olefin Metathesis Catalysts and Intermediates.

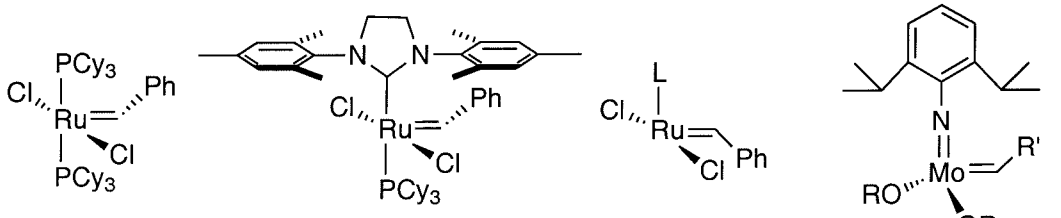

(**4.1**) (**4.2**) (**4.3**)

Prompted by considerable interest in the structure of this important intermediate, we have pursued the preparation of isolable analogues of **4.3**. Complexes of the general formula $(L)(X)_2Ru{=}CHR$ should be stabilized by more π-donating X-type ligands that would increase the electron density at the coordinatively unsaturated Ru(II) center, and by larger ligands that would prevent reassociation of phosphine and alleviate potential bimolecular decomposition pathways. We report herein that replacement of the two halide ligands of **4.1** or **4.2** with tertiary alkoxides, which possess easily modulated π-

donating and steric parameters,[11] has resulted in the synthesis of a series of four-coordinate ruthenium complexes, $(L)(RO)_2Ru{=}CHPh$. In addition to serving as models for **4.3**, these compounds are useful starting materials for the preparation of new ruthenium benzylidenes. This chapter describes detailed studies concerning the synthesis, structure, and reactivity of these complexes.

Results

Synthesis and Characterization of $(PCy_3)(O^tBu)_2Ru{=}CHPh$. The reaction of **4.1** with an excess of KO^tBu proceeds cleanly and quantitatively over 24 hours at 25 °C to produce $(PCy_3)(O^tBu)_2Ru{=}CHPh$ (**4.4**) and one equivalent of PCy_3 (Scheme 1).[12] Complex **4.4** is difficult to purify, since both **4.4** and free PCy_3 are freely soluble in pentane. Additionally, **4.4** decomposes in polar solvents, such as methanol, *iso*-propanol, and acetone, that are typically used for the purification of ruthenium alkylidenes.[2] However, **4.4** can be obtained in 90-95% purity by the addition of CuCl, which reacts with PCy_3 to generate an insoluble polymeric material.[2]

Scheme 1

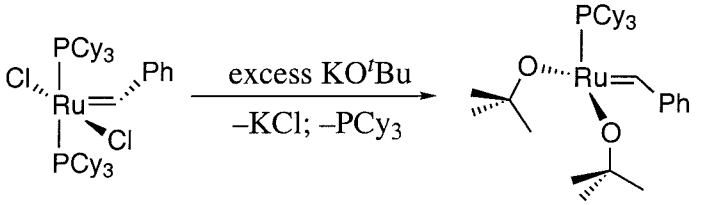

(**4.1**) (**4.4**)

Complex **4.4** can also be prepared by the reaction of KO^tBu with the 18-electron bis-pyridine complex, $(PCy_3)(Cl)_2(C_5H_5N)_2Ru{=}CHPh$ (**4.5**) (Scheme 2).[13] The combination of **4.5** and an excess of KO^tBu in benzene produces a dramatic color change from bright green to red/brown, and the reaction proceeds to completion within minutes at room temperature. The rapidity of this reaction reflects the increased lability of the pyridine ligands of **4.5** relative to the PCy_3 ligand of **4.1**.[13] Importantly, this methodology circumvents the phosphine separation step described above, and the liberated pyridine is

readily removed by exposure to vacuum. However, traces of free PCy_3 are still observed in the product obtained by this synthetic route.[14]

Scheme 2

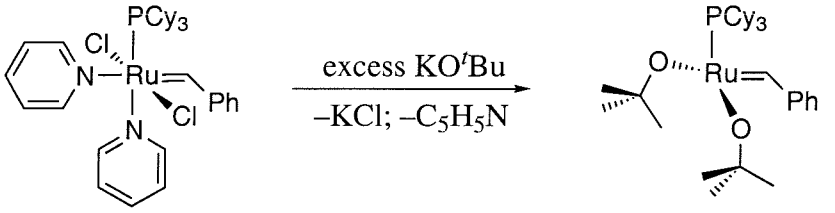

(4.5) **(4.4)**

Complex **4.4** is isolated as a brown/red powder that decomposes instantaneously upon exposure to atmospheric O_2 and moisture. However, this coordinatively unsaturated species is remarkably stable under nitrogen, and sealed solutions of **4.4** in C_6D_6 can be heated to 75 °C in a sealed tube for more than 24 hours without significant decomposition, as observed by ^1H and ^{31}P NMR spectroscopy. Complex **4.4** is diamagnetic, and NMR spectroscopy shows a single resonance for the carbene (doublet, 15.51 ppm) and alkoxide (1.29 ppm) protons as well as a single ^{31}P resonance (83.5 ppm). The 4 Hz coupling constant between H_α and coordinated PCy_3 (J_{HP}) suggests that the P–Ru–C_α–H_α dihedral angle is less than 90°.[15,16] Interestingly, both the ^1H and ^{13}C NMR resonances for the benzylidene (15.51 ppm and 230.5 ppm, respectively) are shifted significantly upfield of typical ruthenium H_α and C_α signals.[17] The chemical shifts of H_α and C_α in **4.4** and related complexes appear to reflect the basicity of the coordinated alkoxide ligands (*vide infra*).

Crystals of **4.4** suitable for X-ray crystallographic analysis were grown from a concentrated pentane solution at –30 °C. The solid state structure of this compound is shown in Figure 2, and representative bond distances and bond angles are reported in Table 1.[18] Despite the expected steric preference for the four-coordinate Ru(II) center to adopt a tetrahedral geometry (as is observed in Schrock's Mo and W systems),[9] this complex crystallizes with a slightly distorted *trigonal pyramidal* ligand array.[19] The phosphine ligand is at the vertex of the pyramid, and the angles from the phosphine to the

Figure 2. Labeled View of **4.4** with 50% Probability Ellipsoids.

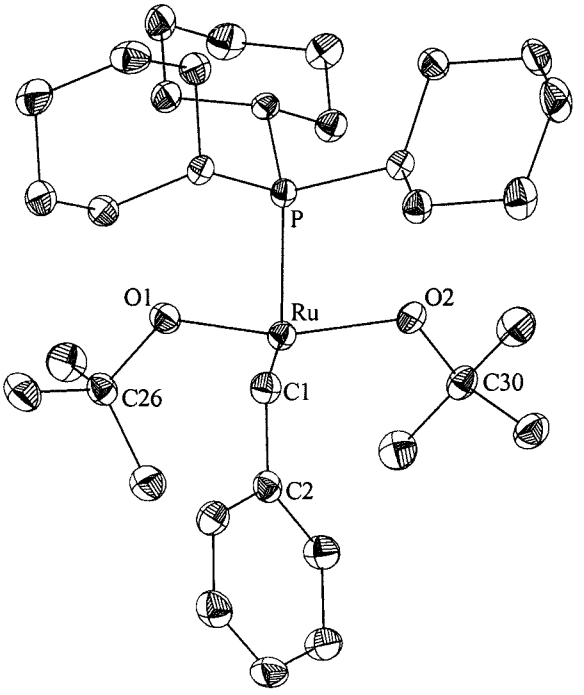

Table 1. Selected Bond Lengths [Å] and Angles [deg] for **4.4**.

	Bond Lengths (Å)		
Ru–C(1)	1.850(2)	Ru–O(2)	1.9558(15)
Ru–O(1)	1.9412(15)	Ru–P	2.2232(7)
	Bond Angles (deg)		
C(1)–Ru–O(2)	114.47(9)	C(1)–Ru–O(1)	112.17(8)
O(2)–Ru–O(1)	133.19(6)	C(1)–Ru–P	92.49(8)
O(2)–Ru–P	88.36(5)	O(1)–Ru–P	93.49(5)
Ru–O(2)–C(30)	123.27(14)	Ru–O(1)–C(26)	126.32(13)

three other ligands are close to 90°. The angles within the trigonal plane are 133.19(6)° [O(1)–Ru–O(2)], 114.47(9)° [O(2)–Ru–C(1)], and 112.17(8)° [O(1)–Ru–C(1)], suggesting that this geometry may be a sterically induced distortion from the square pyramidal structure adopted by ruthenium benzylidene **4.1**.[2] Unlike in complex **4.1**, the phenyl substituent of the carbene ligand in **4.4** is rotated away from the bulky phosphine and into the space below the trigonal plane with a P–Ru–C_α–H_α dihedral angle of 12.2(14)°.[16] As a result, this phenyl group effectively fills the coordination site that was vacated by the departed PCy_3 ligand.

Despite the numerous accessible C-H bonds in the empty coordination site below the trigonal plane of **4.4**, the ruthenium center does not appear to be stabilized by an agostic interaction. The closest "through-space" Ru-carbon distance (other than C_α) is 3.091 Å, and the closest "through-space" Ru-hydrogen distance (other than H_α) is 2.75 Å, which are both longer than typical agostic contacts.[20,21] Furthermore, an overlay of the two *tert*-butyl groups shows that they are identical, indicating that neither of these ligands is significantly distorted so as to interact with the metal center. Both IR spectroscopy and variable temperature ^{1}H NMR spectroscopy[22] suggest that **4.4** is free of agostic interactions in solution as well.[23] Only three other four-coordinate, potentially 14-electron Ru(II) complexes have been structurally characterized[21] and all of these are formally 18-electron octahedral species with two C-H agostic interactions occupying the two open coordination sites.[24] The lack of agostic stabilization in **4.4** suggests that the alkoxide ligands may engage in significant π back-bonding to stabilize the ruthenium center.

The Ru–O(1) and Ru–O(2) bond distances of 1.9412(15) and 1.9558(15) Å in **4.4** are short compared to Ru–O bond lengths in related Ru(II) alkoxide complexes;[25] for example, in the 16-electron complex $Cp^*Ru(PCy_3)(OCH_2CF_3)$, *d*(Ru–O) = 1.992(10) Å,[26] and in the 18-electron complex $Cp^*Ru(CO)(PCy_3)(OCH_2CF_3)$, *d*(Ru–O) = 2.090(3) Å.[26] The Ru–O(1)–C(26) and Ru–O(2)–C(30) angles within **4.4** are 126.32(13)° and 123.27(14)°, respectively, which both represent distortions towards sp^2 hybridization at the oxygen atoms. Taken together, this data provides further evidence that alkoxide back-donation contributes to the bonding description of **4.4**. As a result, the *tert*-

butoxides might be described as LX donor ligands (rather than simple X-type donors), which would bring the formal electron count at ruthenium to 16 or even 18 electrons.[27]

Synthesis and Characterization of $(IMesH_2)(O^tBu)_2Ru=CHPh$ (4.6). By analogy to the bis-phosphine complex **4.1**, the reaction of **4.2** with KO^tBu produces $(IMesH_2)(O^tBu)_2Ru=CHPh$ (**4.6**). However, even in the presence of a large excess of KO^tBu (up to 15 equivalents relative to **4.2**) this reaction proceeds to only approximately 50% conversion. The relatively slow rate of anion metathesis in this system is believed to be due to the low rate of phosphine dissociation in **4.2** relative to **4.1**.[28] In order to accelerate the desired transformation, we used $(IMesH_2)(C_5H_5N)_2(Cl)_2Ru=CHPh$ (**4.7**),[29] containing two relatively labile pyridine ligands, as a starting material. Complex **4.7** reacts rapidly (over several minutes at 25 °C) with an excess of KO^tBu to generate complex **4.6** in quantitative yield by ^1H NMR spectroscopy. Current efforts are aimed at structural characterization and reactivity studies of **4.6**.

Scheme 3

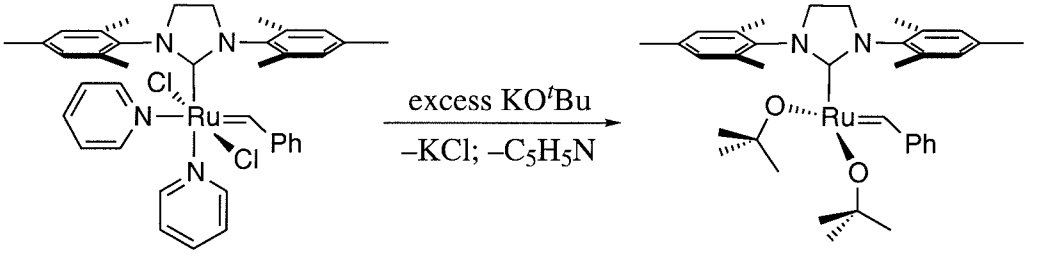

(**4.7**) (**4.6**)

Reaction of 4.4 with Alcohols. We undertook the preparation of derivatives of complex **4.4** in order to explore the effects of alkoxide substitution on the structure and reactivity of these four-coordinate ruthenium benzylidenes. The reaction of benzylidene **4.1** with $KOC(CF_3)_2CH_3$ in benzene or THF produces only traces of $(PCy_3)[OC(CF_3)_2(CH_3)]_2Ru=CHPh$ (**4.8**). NMR studies of this anion metathesis reveal that the equilibrium lies very far towards the starting materials, and even the addition of 50 equivalents of alkoxide results in low (< 30%) conversion to the desired product.[30] However, complex **4.8** and its perfluorinated analogue $(PCy_3)[OC(CF_3)_3]_2Ru=CHPh$,

(**4.9**) are readily available by the protonation of **4.4** with the free alcohols, $HOC(CH_3)(CF_3)_2$ and $HOC(CF_3)_3$, respectively (Scheme 4).[31] The fluorinated ruthenium products are significantly less soluble in hydrocarbon solvents than complex **4.4**, and recrystallization from pentane at –30 °C affords **4.8** and **4.9** as air and moisture sensitive red microcrystalline solids. The ^1H and ^{13}C benzylidene resonances of complex **4.8** appear at 17.54 and 262.6 ppm while those of **4.9** appear at 19.18 and 286.5 ppm. The downfield shift of the H_α and C_α signals with decreasing alkoxide basicity[32,33] suggests that the ruthenium center of **4.9** is the most electrophilic in the series.[34] In both complexes, the H_α signal appears as a singlet, and the lack of coupling to the PCy_3 ligand suggests that the P–Ru–C_α–H_α dihedral angle is close to 90°. However, crystallographic analysis of **4.9** (*vide infra*) shows that this dihedral angle is 0.29(5)° in the solid state. This discrepancy highlights the hazards associated with the assumption of a Karplus relationship between J_{HP} and the solid state benzylidene orientation in these and related ruthenium complexes.[16]

Scheme 4

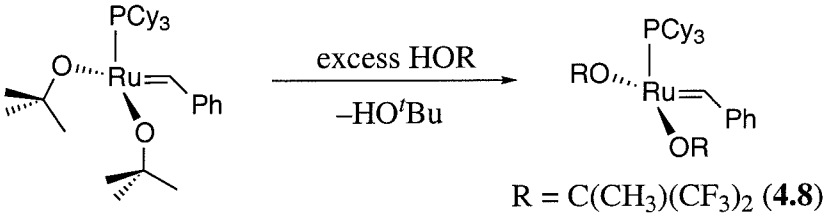

(**4.4**)

R = $C(CH_3)(CF_3)_2$ (**4.8**)

R = $C(CF_3)_3$ (**4.9**)

Dark red crystals of **4.9** were grown from a concentrated pentane solution at –30 °C, and the solid state structure of this complex was determined by X-ray crystallography. A labeled view of **4.9** is shown in Figure 3, and selected bond distances and angles are listed in Table 2.[18] Notably, a significant amount of disorder was observed in the CF_3 groups and could not be modeled effectively. Complex **4.9** adopts a distorted trigonal pyramidal geometry similar to that of **4.4**. The phosphine ligand is at the vertex of the pyramid, and the angles from the phosphine to the three other ligands are close to 90° in all cases. Complex **4.9** has a more open coordination site *trans* to the benzylidene

Figure 3. Labeled View of **4.9** with 30% Probability Ellipsoids.

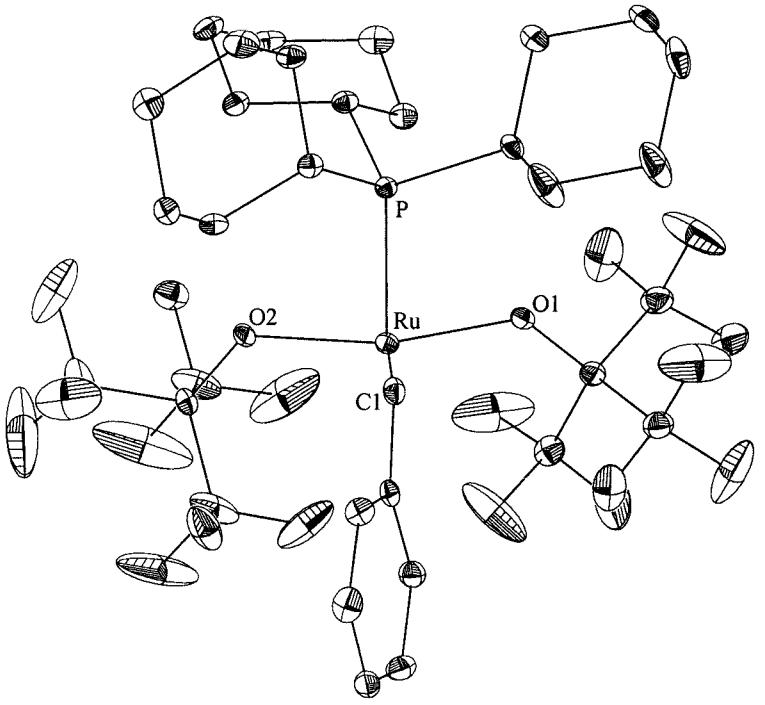

Table 2. Selected Bond Lengths [Å] and Angles [deg] for **4.9**.

	Bond Lengths (Å)		
Ru–C(1)	1.848(7)	Ru–O(2)	2.005(5)
Ru–O(1)	2.009(5)	Ru–P	2.260(2)
	Bond Angles (deg)		
C(1)–Ru–O(2)	106.6(3)	C(1)–Ru–O(1)	109.7(3)
O(2)–Ru–O(1)	143.70(19)	C(1)–Ru–P	91.7(2)
O(2)–Ru–P	90.68(14)	O(1)–Ru–P	87.97(15)
Ru–O(2)–C(12)	128.9(4)	Ru–O(1)–C(8)	135.1(4)

moiety than **4.4**, as shown by the angles within the trigonal plane. The phenyl substituent of the carbene ligand of **4.9** is rotated into the space below the trigonal plane with a P–Ru–C_α–H_α dihedral angle of 0.29(5)°. As previously described, the lack of H–P coupling in the ^{1}H NMR spectrum of **4.9** indicates that a Karplus relationship does not apply in this system.[16]

The Ru–O bond lengths of 2.005(5) Å and 2.009(5) Å in **4.9** are slightly (0.05 Å) longer than those in **4.4**, suggesting that ligand to metal back-bonding is reduced with the less basic alkoxide ligands. In contrast, the Ru–O(1)–C(8) and Ru–O(2)–C(12) angles of 135.1(4)° and 128.9(4)° are 3–10 degrees wider than those of **4.4**, which is typically indicative of an increase in alkoxide π donation to the metal center. However, several studies have shown that the M–O–C angles are poor indicators of alkoxide back-bonding, and bond lengths are generally considered to be more diagnostic.[26,35] Despite a decrease in the Ru–O bond order and a concomitant increase in electrophilicity at the ruthenium center of **4.9** relative to **4.4**, there is no evidence for close metal-CH or metal-CF contacts.[36]

Reaction with Phenols and Acids. We anticipated that the high reactivity of **4.4** with acidic functionality might be exploited for the synthesis of new ruthenium

Scheme 5

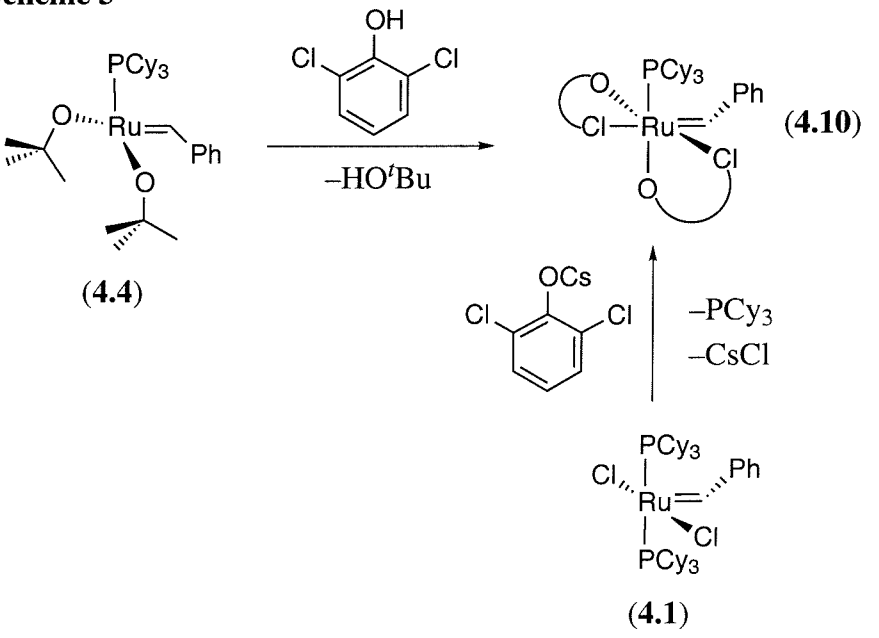

benzylidenes. As a result, the reactions of both phenols and acids with complex **4.4** were investigated by ^{1}H NMR spectroscopy. 2,6-Dichlorophenol reacts rapidly with **4.4** to protonate the coordinated alkoxide ligands and generate two equivalents of HO^{t}Bu and $(PCy_3)[(\kappa^2\text{-}O,Cl)\text{-}OC_6H_3Cl_2]_2Ru{=}CHPh$ (**4.10**) (Scheme 5).[37] The green color of this product is diagnostic of a six-coordinate, octahedral ruthenium benzylidene,[38] and we believe that the phenol binds the metal center through an O–Cl chelate. A related complex, $CpRu[(\kappa^2\text{-}O,Cl)\text{-}OC_6Cl_5](PPh_3)$, which contains a similar O–Cl bound pentachlorophenol ligand, was recently characterized by Werner and coworkers.[39] The stability of **4.10** to atmospheric O_2 and moisture (particularly in comparison to **4.4** and its analogues)[40] is also consistent with the formulation of this complex as a coordinatively saturated species.

Complex **4.10** is also available by the combination of an excess of the cesium salt of 2,6-dichlorophenol with **4.1** in C_6D_6 (Scheme 5). This reaction produces the bis-phenoxide product (**4.10**) and one equivalent of free PCy_3 in quantitative yield by ^{1}H NMR spectroscopy. However, in contrast to the protonation of **4.4** (which is instantaneous at room temperature), this anion exchange takes up to 24 hours at 25 °C to reach completion.

Scheme 6

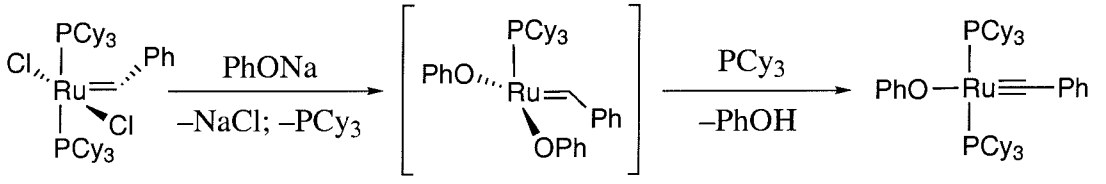

(**4.1**)

Other phenolic compounds, such as phenol, 2,3,5,6-tetrafluoro-4-(pentafluorophenyl)phenol, and *para*-nitrophenol, also undergo ligand exchange with complex **4.4**. In each case, ^{1}H NMR indicates that **4.4** is completely consumed, but the products do not contain any of the downfield signals diagnostic of ruthenium alkylidenes. Caulton and coworkers have shown that ruthenium phenoxide benzylidenes undergo α-hydrogen elimination followed by reductive elimination of phenol to generate four-

coordinate ruthenium carbynes (Scheme 6).[12] In our systems, the analogous transformation would produce unstable three-coordinate, 14-electron ruthenium adducts that presumably decompose to a mixture of products.

Scheme 7

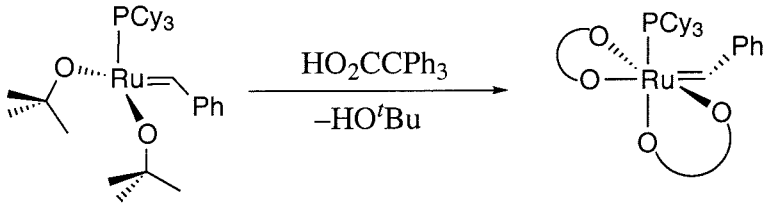

(4.4) **(4.11)**

Complex **4.4** also reacts readily with carboxylic acids. For example, the combination of **4.4** with HO_2CCPh_3 in C_6D_6/THF-d_8 results in a color change from red/brown to bright green, and formation of the bis-carboxylate adduct $(PCy_3)(\eta^2\text{-}O_2CCPh_3)_2Ru{=}CHPh$ (**4.11**) (Scheme 7). Its bright green color[38] and relative stability to air and moisture[40] are both consistent with an 18-electron configuration at the ruthenium center in complex **4.11**.[41] Bis-η^2-ruthenium carboxylates have been widely reported, and, for example, [(*S*)-BINAP]Ru[η^2-$O_2C(^tBu)$]$_2$ is a catalyst for asymmetric hydrogenation.[42]

Scheme 8

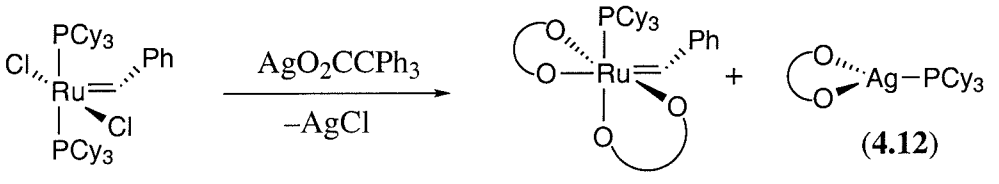

(4.1) **(4.11)** **(4.12)**

Complex **4.11** may also be prepared by the combination of 3 equivalents of AgO_2CCPh_3 with benzylidene **4.1** in CD_2Cl_2 (Scheme 8). An extra equivalent of AgO_2CCPh_3 is required because the silver salt reacts with the liberated phosphine to produce the three coordinate silver complex $(PCy_3)Ag(\eta^2\text{-}O_2CCPh_3)$ (**4.12**). Complex

4.12 can be identified by its characteristic ^{31}P NMR resonance (doublet, 42.17 ppm, $J_{P\text{-}Ag}$ = 44 Hz).[43] Unfortunately, complexes **4.11** and **4.12** have extremely similar solubility and are difficult to separate, even by fractional crystallization. A wide variety of other silver carboxylates, including those derived from benzoic acid, phenylacetic acid, 2-phenylbutyric acid, α-methoxy-α-(trifluoromethyl)phenylacetic acid, and 6-methoxy-α-methyl-2-napthaleneacetic acid also react with **4.1** to produce products of the general formula, $(PCy_3)(\eta^2\text{-}O_2CR)_2Ru{=}CHPh$ and $(PCy_3)Ag(\eta^2\text{-}O_2CR)$. For an unknown reason, an aromatic group attached either directly to the carboxylate-carbon or to the α-carbon is required for the clean formation of a single ruthenium product in these transformations.

Reaction with Chelating Phenols and Alcohols. Complex **4.4** reacts readily with the chelating diol BINOL (2,2'-dihydroxyl-1,1'-dinapthyl) to produce a mixture of alkylidenes that rapidly decompose in solution. In contrast, **4.4** does not undergo any reaction with BIPHEN (5,5',6,6'-tetramethyl-3,3'-di-*tert*-butyl-1,1'-biphenyl-2,2'-diol),[44] even under forcing conditions. The apparent inability of either of these ligands to form stable four-coordinate ruthenium adducts may be due to their relatively small bite angles. Schrock and coworkers have prepared both BINOL and BIPHEN-substituted tetrahedral molydenum alkylidenes, and these complexes show an average O–Mo–O angle of approximately 109.5°.[44,45] In contrast, a trigonal pyramidal geometry requires an O–Mo–O angle of approximately 120°, which may be incompatible with these ligands. Additionally, the BINOL reaction product may undergo decomposition by α-H elimination as outlined in Scheme 6.[12]

We reasoned that a more flexible chelating ligand containing aliphatic rather than aromatic alcohols, might produce a stable ruthenium chelate complex. As a result, the reactivity of the TBEC[46] ligand, which is well-known to form nine-membered chelates with transition metals,[47] was explored. As shown in Scheme 9, the TBEC ligand reacts with **4.4** to produce a light brown product that we formulate as a four-coordinate ruthenium complex with a stabilizing C-H agostic interaction. The product, (PCy_3)(TBEC)Ru=CHPh (**4.13**), can be isolated as a brown microcrystalline solid by recrystallization from pentane, and this species is *air stable* for several days in the solid state. Even as a solution in C_6D_6, **4.13** decomposes relatively slowly (over approximately two hours as monitored by ^1H NMR spectroscopy) when exposed to atmospheric O_2 and

moisture. In comparison, the four-coordinate complexes **4.4**, **4.8**, and **4.9** are extremely air and moisture sensitive, both in the solid state and in solution.

Scheme 9

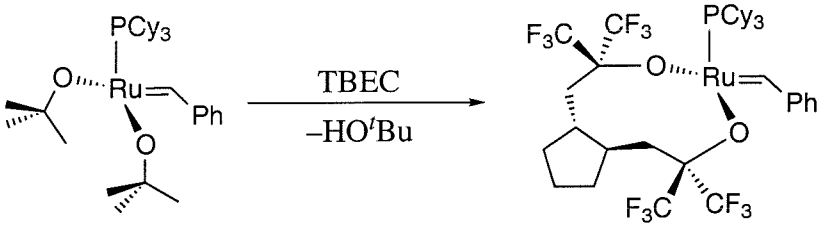

(4.4) **(4.13)**

Preliminary studies suggest the presence of a stabilizing C-H agostic interaction in complex **4.13**. ^{1}H and ^{13}C NMR spectroscopy of **4.13** show H_α as a doublet at 17.73 ppm and C_α as a multiplet at 266.9 ppm. The chemical shifts of these resonances are very close to those of the hexafluoro-*tert*-butoxide complex **4.8**, providing further support for a correlation between benzylidene chemical shift and alkoxide basicity in these systems.[34] The ^{1}H NMR spectrum of **4.13** also shows an unusual upfield resonance as a broad singlet (line width at half height = 15 Hz) at –3.48 ppm, and this peak integrates as one proton relative to the benzylidene H_α. This signal does not change significantly over a wide range of temperatures (+70 °C to –70 °C) by ^{1}H NMR spectroscopy, and shows no coupling to phosphine or to other protons.[48] Importantly, resonances in this range are

Figure 4. Possible Agostic Interaction in Complex **4.13**.

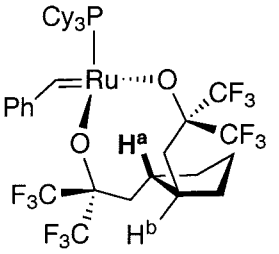

(4.13)

diagnostic of protons involved in Ru–CH agostic interactions.[20,49,50] A preliminary X-ray crystal structure of **4.13** was obtained, but the connectivity could not be assigned definitively.[51] However, this tenative structure (as well as ball-and-stick renditions of **4.13**) suggests that the agostic interaction may involve one of the two hydrogens at the stereocenters of the ligand (H_a or H_b in Figure 4).

Since the structure of **4.13** could not be accurately determined by X-ray crystallography, we must consider several alternative formulations of this complex. In particular, the ^{1}H NMR resonance at –3.48 ppm could be explained by the presence of a hydride or a hydroxide ligand, for both typically show ^{1}H NMR signals upfield of TMS. For example, the hydroxide proton of $(PMe_3)_4(Ph)Ru(OH)$ appears as a multiplet at –4.47 ppm while the hydride proton of $(PMe_3)_4(Ph)Ru(H)$ appears as a doublet of doublet of triplets at –9.50 ppm.[52] However, as the ^{1}H NMR spectrum of the $(PMe_3)_4(Ph)Ru(X)$ fragment indicates, ruthenium hydrides and hydroxides usually exhibit coupling to coordinated ^{31}P nuclei. In contrast, the –3.38 ppm signal in **4.13** shows no coupling to the PCy_3 ligand between +70 and –70 °C. In addition, the presence of a third X-type ligand would change the oxidation state at ruthenium from Ru(II) to Ru(III), and the paramagnetic nature of the metal center should to be reflected in its NMR spectrum. Finally, the reactivity of complex **4.13** speaks against the presence of coordinated OH^- or H^-. Complex **4.13** reacts readily with 2 equivalents of HO_2CCPh_3 in C_6D_6/THF-d_8 to produce the green bis-carboxylate complex, **4.11**, in quantitative yield. Neither H_2 nor free H_2O (the expected products of hydride or hydroxide protonation) are observed in this reaction mixture by ^{1}H NMR spectroscopy.

Reaction of $(PCy_3)(OR)_2Ru$=CHPh with L-Type Ligands. We next explored the reactions of benzylidenes **4.4**, **4.8**, and **4.9** with L-type donor ligands. We thought that the binding of these ligands might be related to the olefin binding event during a metathesis reaction, and could provide valuable information about the nature and structure of intermediates along the metathesis reaction coordinate. Related studies of L-type ligand binding to Schrock's molybdenum and tungsten alkylidenes have afforded mechanistic insights concerning the ancillary ligand orientation in olefin metathesis intermediates.[9]

The ruthenium alkoxides **4.4**, **4.8**, and **4.9** do not react directly with olefins or alkynes, including cyclohexene, diphenylacetylene, and acenaphthylene. In addition, these complexes do not react with ethereal solvents, and their NMR spectra in THF-d_8 are essentially identical to those in non-coordinating solvents such as C_6D_6, toluene-d_8, or CD_2Cl_2. Neither PPh_3 nor PCy_3 react with isolated samples of **4.4**, **4.8**, and **4.9**, but treatment of all three of these complexes with PMe_3 produces intractable mixtures of products that include free PCy_3. Interestingly, PMe_3 also reacts with the parent complex **4.1** to produce PCy_3 and a mixture of ruthenium species. In both cases, the complexity of the reaction mixtures *may* be due to competition between phosphine substitution at the metal center and nucleophilic attack by PMe_3 on the electrophilic carbene carbon.[53]

Treatment of **4.4**, **4.8**, or **4.9** with H_2 results in "hydrogenation" of the coordinated alkoxide ligands to release the corresponding free alcohols. The organometallic products of this reaction appear to be a mixture of ruthenium hydrides, as indicated by their characteristic ^1H NMR resonances upfield of TMS. However, a single ruthenium product could not be isolated in pure form. Olivan and Caulton have demonstrated that complex **4.1** also reacts with H_2 to produce the ruthenium hydrides $(PCy_3)_2(Cl)Ru(H_2)(H)$ and $(PCy_3)_2(Cl)_2Ru(H)_2$.[54]

Scheme 10

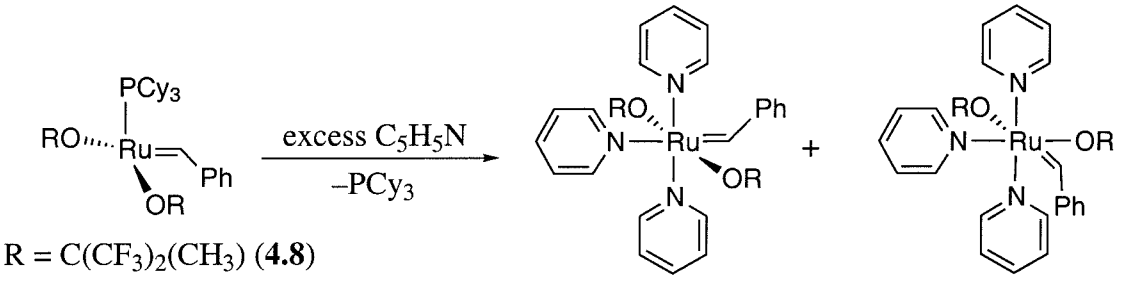

R = $C(CF_3)_2(CH_3)$ (**4.8**)

(**4.14a**) (**4.14b**)

The reaction of **4.8** with an excess of pyridine results in an instantaneous color change from red to green accompanied by the release of PCy_3 (Scheme 10). Recrystallization of the reaction products from a mixture of toluene, pyridine and pentane affords emerald green crystals that can be identified by X-ray crystallography as the octahedral complex $(C_5D_5N)_3[OC(CF_3)_2(CH_3)]_2Ru{=}CHPh$ (**4.14a**). However, the ^1H

NMR spectrum of this green crystalline material in C_6D_6 indicates the presence of two different ruthenium benzylidenes in an approximately 3 : 1 ratio. The minor species shows two separate peaks for the methyl groups of the hexafluoro-*tert*-butoxides, indicating that these ligands are inequivalent. As such, we suggest that the minor compound is the *cis*-alkoxide adduct (**4.14b**), and the major product, containing equivalent CH_3 groups, is assigned as the *trans*-alkoxide complex **4.14a**. A closely related isomerization of X-type ligands from a *trans* to a *cis* geometry has been observed in the diimino-pyridine complex $(Cl)_2$[2,6-py$(NCy)_2$]Ru=$CHCO_2Et$[55] (Figure 5).[56] However, other isomers of **4.14**, including other tris-pyridine diastereomers as well as bis- or mono-pyridine complexes, cannot be disregarded based on the evidence presented herein.

Figure 5. *Cis* and *Trans* Isomers of $(Cl)_2$[2,6-py$(NCy)_2$]Ru=$CHCO_2Et$.

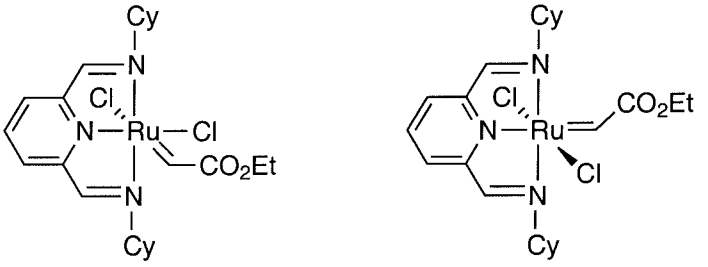

Bright green crystals of **4.14a** were grown from a mixture of toluene, pyridine, and pentane at –30 °C. A labeled view is shown in Figure 6 and a list of selected bond lengths and bond angles is shown in Table 3.[18] Complex **4.14a** adopts a distorted octahedral geometry in the solid state, and the largest deviation from an idealized octahedron involves the O(1)–Ru–O(2) angle of 159.61(6)°. The Ru–N(2) bond length (to the pyridine *trans* to the benzylidene moiety) is more than 0.25 Å longer than the Ru–N(1) and Ru–N(3) bond distances. This observation points to the large *trans* influence of the benzylidene relative to pyridine.[57] The Ru–O bond lengths of 2.0505(14) Å and 2.0653(14) Å in **4.14a** are 0.1 Å longer than those in **4.4** and 0.05 Å longer than those in **4.9**, indicating a decrease in alkoxide to metal back-bonding in this 18-electron complex.[58]

Figure 6. Labeled View of **4.14** with 50% Probability Ellipsoids.

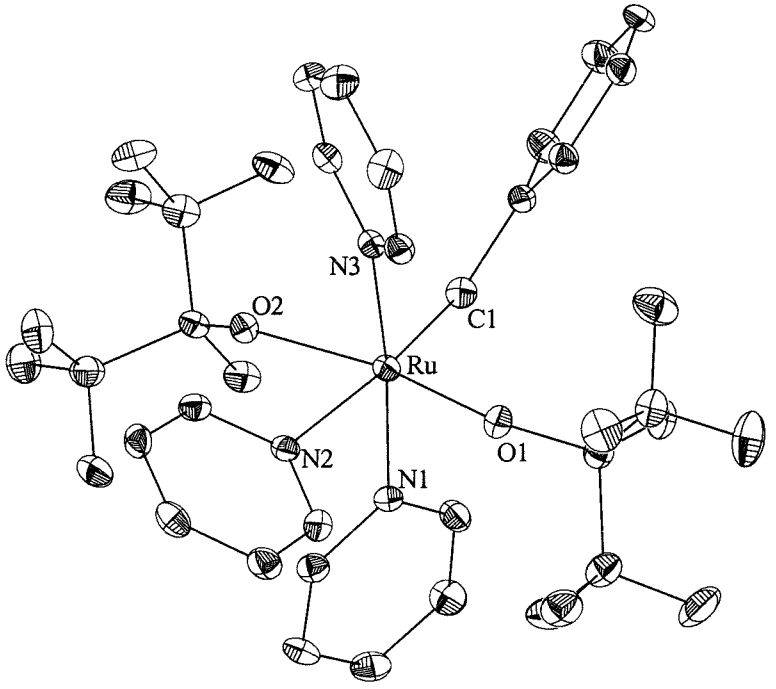

Table 3. Selected Bond Lengths [Å] and Angles [deg] for **4.14**.

	Bond Lengths (Å)		
Ru–C(1)	1.867(2)	Ru–O(1)	2.0505(14)
Ru–O(2)	2.0653(14)	Ru–N(1)	2.1048(17)
Ru–N(2)	2.3547(18)	Ru–N(3)	2.0888(17)
	Bond Angles (deg)		
C(1)–Ru–O(1)	102.76(8)	C(1)–Ru–O(2)	96.55(8)
O(1)–Ru–O(2)	159.61(6)	C(1)–Ru–N(3)	92.72(9)
C(1)–Ru–N(1)	92.19(8)	C(1)–Ru–N(2)	174.27(8)
Ru–O(1)–C(23)	138.99(13)	Ru–O(2)–C(27)	137.12(13)

^{1}H NMR spectroscopic studies show that complex **4.4** also reacts with C_5D_5N to liberate PCy_3 and produce a single new carbene resonance at 19.32 ppm. The product is believed to be a ruthenium pyridine adduct, $(C_5D_5N)_n(O^tBu)_2Ru{=}CHPh$ (**4.15**), with an undetermined number (n) of bound pyridine molecules. Unfortunately, **4.15** could not be isolated and rigorously characterized because decomposition of this complex competes with its generation. In contrast to the formation of **4.14**, which is essentially instantaneous at room temperature, the reaction of **4.4** in neat pyridine proceeds to only approximately 35% completion after three hours at 25 °C. The relative rates of these two ligand exchange reactions (which are presumably associative substitutions) are consistent with an increase in electrophilicity at the ruthenium center coordinated with fluorinated alkoxide ligands.

Reaction of Dimethylvinyl Alkylidenes with KO^{t}Bu. The dimethylvinyl ruthenium alkylidene $(PCy_3)_2(Cl)_2Ru{=}CHCH{=}C(Me)_2$ (**4.16**) is inexpensive and easy to prepare in comparison to complex **4.1**.[59] As a result, we hoped to use **4.16** as a starting material to access four-coordinate ruthenium complexes analogous to **4.4**. Although **4.16** reacts rapidly with KO^{t}Bu in C_6D_6 or THF-d_8, ^{1}H NMR analysis indicates that a ruthenium vinylcarbene product is not formed. Instead, as shown in Scheme 11, **4.16** undergoes deprotonation by KO^{t}Bu to produce the 14-electron vinylvinyl species, $(PCy_3)_2(Cl)Ru{-}CH{=}CHC(Me){=}CH_2$ (**4.17**) and KCl.[60] The product **4.17** could not be isolated, but could be identified by ^{1}H NMR spectroscopy, which shows two characteristic doublets at 8.93 and 6.27 ppm for the two vinylic protons. These signals are similar to those of the related cyclohexyl vinylvinyl complex (**4.18**) (Figure 7) in

Scheme 11

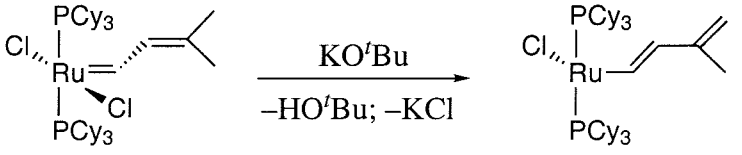

(4.16) **(4.17)**

which the vinylic protons appear as doublets at 7.59 and 5.58 ppm.[61] The identity of **4.17** can be further confirmed by the reaction of **4.16** with a series of different bases, including NaH, NaOH, and LDA. In all cases, the product **4.17** is observed, although these reactions are not as clean as that with KO^{t}Bu. Interestingly, this reaction is fully reversible, and the addition of 1 equivalent of HCl to solutions of **4.17** results in the quantitative regeneration of the ruthenium starting material (**4.16**).

Figure 7. The Related Vinylvinyl Complex **4.18**.

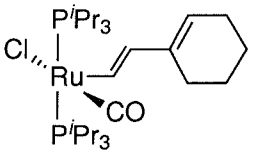

(4.18)

Although the coordinatively unsaturated complex **4.17** could not be isolated, we reasoned that an 18-electron dimethylvinyl alkylidene starting material should undergo a similar deprotonation to produce a stable 16-electron product. As anticipated, the reaction of $(P^iPr_3)_2(Cl)_2(CO)Ru{=}CHCH{=}C(Me)_2$[61] with KO^{t}Bu affords an isolable ruthenium vinylvinyl species, $(P^iPr_3)_2(Cl)(CO)Ru{-}CH{=}CHC(Me){=}CH_2$ (**4.19**), in 78% yield (Scheme 12). Other bases, including NaH, NaOH and LDA, can also be used to carry out this transformation, but the best yields are achieved with KO^{t}Bu. The product is isolated as a light pink solid that is soluble in C_6H_6 and CH_2Cl_2 and is insoluble in pentane. This complex is moderately air and moisture stable, but reacts with acidic

Scheme 12

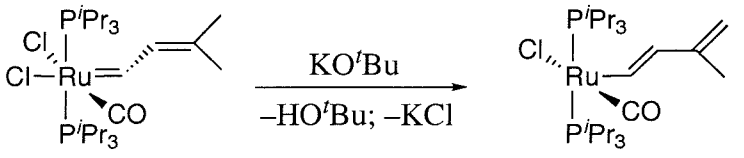

(4.19)

Figure 8. Labeled View of **4.19** with 50% Probability Ellipsoids.

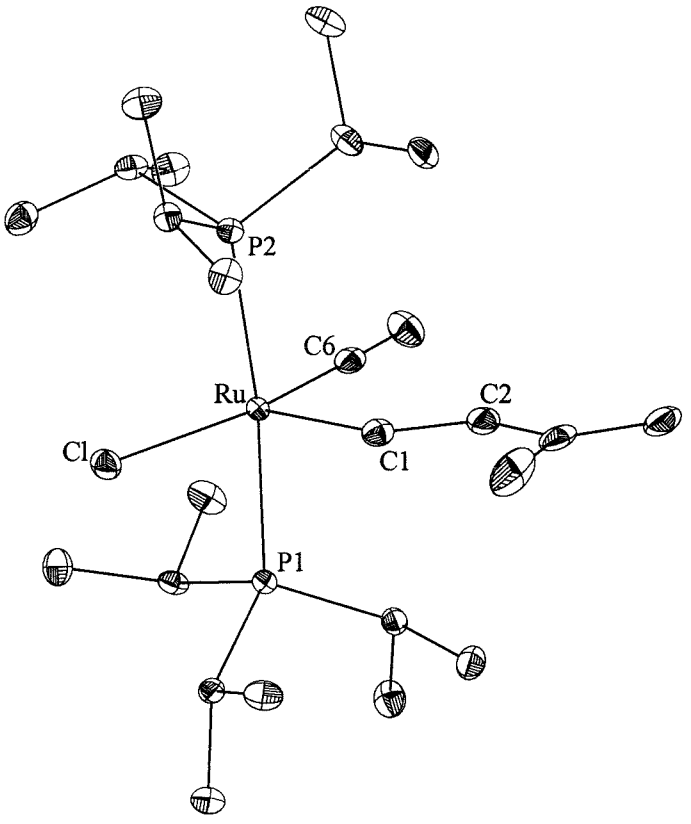

Table 4. Selected Bond Lengths [Å] and Angles [deg] for **4.19**.

	Bond Lengths (Å)		
Ru–C(6)	1.818(2)	Ru–P(2)	2.4016(9)
Ru–C(1)	1.9913(18)	Ru–Cl	2.4191(8)
Ru–P(1)	2.4012(9)	C(1)–C(2)	1.331(3)
	Bond Angles (deg)		
C(6)–Ru–C(1)	89.85(8)	C(6)–Ru–P(l)	89.50(6)
C(1)–Ru–P(1)	95.40(6)	C(6)–Ru–P(2)	90.02(6)
C(1)–Ru–P(2)	93.29(6)	P(1)–Ru–P(2)	171.288(16)
C(6)–Ru–Cl	167.81(6)	C(1)–Ru–Cl	102.33(6)
P(1)–Ru–Cl	89.86(3)	P(2)–Ru–Cl	88.77(3)

functionality including perfluoro-*tert*-butanol and HO_2CCPh_3 to produce mixtures of ruthenium dimethylvinyl carbene complexes. Complex **4.19** also reacts quantitatively (by ^1H NMR spectroscopy) with an excess of HCl to regenerate the starting material, $(P^iPr_3)_2(Cl)_2(CO)Ru{=}CHCH{=}C(Me)_2$. ^1H NMR spectroscopy of **4.19** shows the vinylic protons as two doublets at 7.96 and 5.80 ppm, with a coupling constant (16 Hz) that is strongly indicative of a *trans* olefinic geometry.[62] The neat film IR spectrum of this species shows a ν(C=C) band at 1549 cm^{-1} and a ν(C–O) band at 1910 cm^{-1}. These values are virtually identical to those observed for complex **4.18** (ν(C=C) = 1555 cm^{-1} and ν(C–O) = 1902 cm^{-1}).[61]

Crystals suitable for X-ray crystallographic analysis were grown by vapor diffusion of pentane into a toluene solution of **4.19**. A labeled view of the molecule is shown in Figure 8 and selected bond distances and bond angles are shown in Table 4. In the solid state, **4.19** assumes a square pyramidal structure that is similar to that of complexes **4.1**[63] and **4.2**.[64] The bond distances within the alkyl ligand clearly indicate that it is a vinylvinyl rather than a vinylcarbene moiety. For example, the Ru–C_α distance of 1.9913(18) Å is significantly longer than that of the ruthenium vinylcarbene complexes $[(P^iPr_3)_2(Cl)(CO)Ru{=}C(OMe)CH{=}CPh_2]BF_4$ [*d*(Ru–C) = 1.874(3) Å][61] and $(PPh_3)_2(Cl)_2Ru{=}CHCH{=}CPh_2$ [*d*(Ru=C) = 1.887(7) Å].[15b] As anticipated from the ^1H NMR spectroscopic data, the vinylvinyl ligand assumes a *trans* configuration about the internal double bond.

Olefin Metathesis Activity. The activity of the new ruthenium benzylidenes for the ring closing metathesis (RCM) of diethyl diallylmalonate was examined, and the results are summarized in Table 5. As shown in entries 1–4 of Table 5, all of the alkoxide adducts are essentially inactive for RCM at room temperature. Additionally, the coordinatively saturated bis-carboxylate complex **4.11** (entry 5) does not catalyze this ring closing metathesis reaction at room temperature or at 60 °C over several days.

In contrast, the four-coordinate complexes **4.8**, **4.9**, and **4.13** exhibit moderate catalytic ring closing activity at 60 °C (entries 6–8). In general, the reactivity of these species (particularly **4.9**) with diethyl diallylmalonate is limited by their low thermal stability in the presence of the substrate, and all of these catalysts decompose significantly during the RCM reaction. Catalyst **4.13** shows the highest activity and

longevity in the series, but this complex is still only capable of approximately 0.4 turnovers per hour at 60 °C. Interestingly, methylidene intermediates are *not* observed in any of these reactions (by ^{1}H or ^{31}P NMR spectroscopy) suggesting that very little catalyst (<2%) is initiating and/or that the corresponding methylidenes are extremely unstable in these systems.

Table 5. Ring Closing Metathesis of Diethyl Diallylmalonate.[a]

Entry	Catalyst	Additive	T [°C]	Time [hrs]	Yield [%]
1	**4.4**	——	25 or 60	96	< 5
2	**4.8**	——	25	96	< 5
3	**4.9**	——	25	96	< 5
4	**4.13**	——	25	96	< 10
5	**4.10**	——	25 or 60	96	< 5
6	**4.8**	——	60	96	70
7	**4.9**	——	60	96	40
8	**4.13**	——	60	12	> 96[b]
9	**4.9**	HCl	25	0.65	> 96
10	**4.11**	HCl	25	0.65	> 96
11	**4.14**	none or HCl	25	24	< 5
12	**4.1**	——	25	1.5	> 96[b]

[a] Reactions in C_6D_6; [catalyst] = 0.0089 M; [substrate] = 0.045 M; unless indicated, catalyst decomposition terminated the reaction. [b] Catalyst remained at the completion of the reaction.

The RCM results involving **4.4**, **4.8**, and **4.9** are qualitatively similar to earlier studies with analogues of complex **4.1**, in which it was found that more electron withdrawing X-type ligands afford more active olefin metathesis catalysts.[6c] These results are also consistent with Schrock's molybdenum and tungsten catalyst systems in which catalytic activity decreases with increasing basicity of the alkoxide ancillary ligands.[9] The low reactivities of these four-coordinate complexes for the RCM reaction

are likely due to the same factors which render these species stable to isolation: the steric bulk of the alkoxides effectively shields the metal from coordination of the incoming substrate, while π donation by these ligands discourages olefin binding by decreasing the electrophilicity of the metal.[11]

Complexes **4.4**, **4.8**, and **4.9** become excellent catalysts for ring closing metathesis when activated with HCl, and the representative example of **4.8**/HCl is shown in Table 5, entry 9. The addition of two equivalents of HCl to a C_6D_6 solution of complex **4.8** results in an instantaneous color change from red to brown. Although no new carbene resonances are observed by ^{1}H NMR spectroscopy, a small amount of a highly metathesis active species is generated. Under identical conditions, the RCM of diethyl diallylmalonate proceeds *at least twice as fast* with **4.9**/HCl than it does with catalyst **4.1** alone (entry 12), despite the fact that undetectably small amounts of active catalyst are present in the former reaction mixture. By analogy to the ligand exchange reaction of **4.4** with acidic alcohols, we believe that HCl serves to protonate off the alkoxide ligands of **4.8**, generating free $HOC(CF_3)_2CH_3$ (which is the sole species observed by ^{19}F NMR) and the four-coordinate species $(PCy_3)(Cl)_2Ru{=}CHR$ (**4.3**) (Scheme 13). Some evidence for

Scheme 13

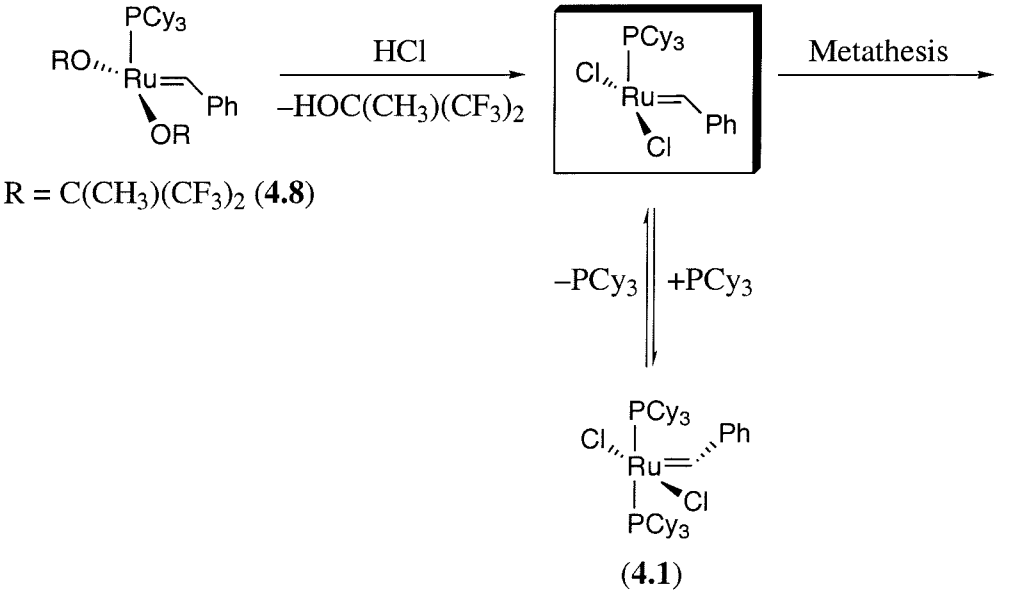

this claim is provided by the reaction of **4.8** with HCl in the presence of one equivalent of PCy_3, which results in the regeneration of catalyst **4.1**. Notably, the bis-carboxylate complex **4.11** is also activated by 2 equivalents of HCl (entry 10), and the co-catalyst is believed to act in a similar fashion to produce 2 equivalents of HO_2CCPh_3 and **4.3**.

The 18-electron tris-pyridine complex **4.14** is completely inactive for the ring closing metathesis of diethyl diallylmalonate, both in the absence and in the presence of HCl co-catalyst (Table 5, entry 11). ^1H and ^{19}F NMR experiments indicate that 2 equivalents of HCl react quantitatively with **4.14** to protonate off the alkoxide ligands, generating $HOC(CF_3)_2(CH_3)$ and the stable ruthenium adduct $(C_5H_5N)_3(Cl)_2Ru=CHPh$. The low metathesis activity of both of these 18-electron, nitrogen-ligated ruthenium benzylidenes is not unexpected based on the literature.[65] A variety of complexes containing related nitrogen-based ligand systems (*e.g.*, $(Cl)_2$[2,6-$py(NCy)_2$]$Ru=CHCO_2Et$)[56] have been reported and shown to be inefficient olefin metathesis catalysts.[65]

Discussion

Mechanistic studies have implicated the 14-electron complex $L(Cl)_2Ru=CHPh$ (**4.3**) as a critical intermediate in olefin metathesis reactions catalyzed by benzylidenes **4.1** and **4.2** (Figure 9).[6,7] However, the preparation of **4.4** and its analogues has provided the first direct spectroscopic and structural evidence for the viability of four-coordinate ruthenium complexes of this type. Clearly, it is not certain that the bis-alkoxide complexes adopt the same geometry as their di-chloride analogues. In fact, it may be argued that the isolation of **4.4** speaks against its relevance to a true catalytic intermediate.[66] Nonetheless, these new complexes provide a working model for beginning to understand the chemistry of intermediate **4.3**.

The stability of **4.4** and **4.6** is consistent with our current mechanistic understanding of the ruthenium olefin metathesis catalysts $(L)(PR_3)(X)_2Ru=CHR^1$. Detailed mechanistic studies of these species have shown that large and electron donating X ligands promote phosphine dissociation.[6a] For example, when X is changed from chloride to iodide, phosphine dissociation increases by two orders of magnitude.[6a]

Complexes **4.4** and **4.6**, which contain both bulky and highly electron donating alkoxide ligands, represent the logical extreme in a series of X-type ligands. In **4.4** and **4.6**, phosphine dissociation is quantitative and irreversible, and the phosphine can be completely removed from the system, producing four-coordinate analogues of **4.3**.

Figure 9. Proposed Mechanism of Olefin Metathesis Reactions Catalyzed by **4.1** and **4.2**.

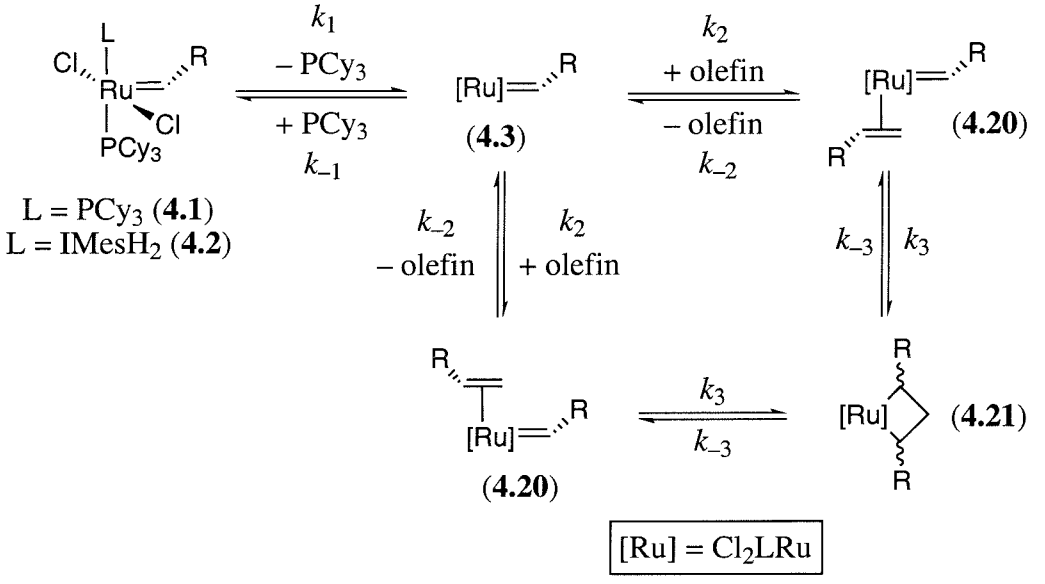

An important topic of debate in the olefin metathesis literature involves the structure of the olefin metathesis intermediate, **4.20** (Figure 10).[6c,7,67] The geometry of this olefin adduct may provide insight into the origins of *cis/trans* selectivity and enantioselectivity in olefin metathesis reactions catalyzed by ruthenium benzylidenes. Unfortunately, metathesis "inert" olefins and alkynes (including cyclohexene, diphenylacetylene, and acenaphthylene) did not react appreciably with complex **4.4** to produce analogues of **4.20**. Furthermore, no olefin-bound ruthenium intermediates are observed in the ring closing metathesis of diethyl diallylmalonate catalyzed by **4.8** or **4.9**. We originally anticipated that the pyridine adducts of **4.4**, **4.8**, and **4.9** might serve as models for olefin coordination in these systems. However, the reaction of pyridine with the four-coordinate alkoxide complexes resulted in loss of PCy_3 and the formation of stable, octahedral tris-pyridine adducts (*e.g.*, **4.14**). As a result, these products are not

believed to be relevant to the catalytic intermediates formed in olefin metathesis reactions.[68]

Figure 10. Possible Geometries of Intermediate **4.20**.

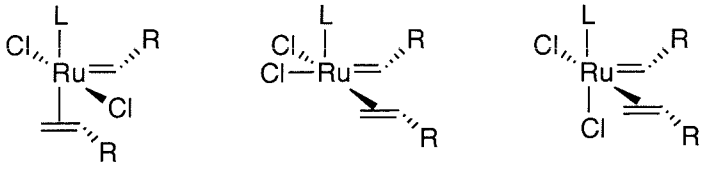

(4.20a) **(4.20b)** **(4.20c)**

We anticipate that complex **4.4** and its analogues may serve as useful starting materials for the preparation of derivatives of **4.20**. As described above, we have considerable evidence that the protonation of **4.4** with 2 equivalents of HCl produces the 14-electron olefin metathesis intermediate **4.3** (L = PCy_3). This intermediate is unstable on its own, but it is readily trapped by PCy_3 to regenerate **4.1**. An analogous trapping experiment, using an appropriately chosen metathesis "inert" olefin or alkyne should provide direct access to intermediate **4.20**. Preliminary (^{1}H NMR) experiments have shown that protonation of **4.8** with HCl in the presence of diphenylacetylene or acenaphthylene results in the formation of several new carbene-containing products that we tenatively assign as **4.20**. However, these promising reactions have yet to be pursued in further detail.[69]

Conclusions and Future Perspectives

In summary, a series of four-coordinate ruthenium complexes of the general formula $(L)(OR)_2Ru{=}CHPh$ have been prepared and characterized. These complexes serve as models for the 14-electron olefin metathesis intermediate $L(Cl)_2Ru{=}CHPh$, and can be used as starting materials for the preparation of a diverse array of new ruthenium benzylidenes. Future studies will involve investigation of the *N*-heterocyclic carbene complex, $IMesH_2(O^tBu)_2Ru{=}CHPh$ (**4.6**), which was briefly discussed in this chapter. We anticipate that detailed comparison of the structure and reactivity of the PCy_3 (**4.4**) and $IMesH_2$ (**4.6**) adducts may provide further insight into the dramatically different

activities of the parent catalysts **4.1** and **4.2** in olefin metathesis reactions.[3,6] Additionally, the isolation and characterization of ruthenium benzylidene-olefin adducts is expected to elucidate the geometry of metathesis intermediate **4.20**.

Experimental Section

General Procedures: Manipulation of organometallic compounds was performed using standard Schlenk techniques under an atmosphere of dry argon or in a nitrogen-filled Vacuum Atmospheres drybox ($O_2 < 2$ ppm). NMR spectra were recorded on a Varian Inova (499.85 MHz for ^1H; 202.34 MHz for ^{31}P; 125.69 MHz for ^{13}C), a Varian Mercury 300 (299.82 for ^1H; 282.16 for ^{19}F; 121.39 MHz for ^{31}P; 74.45 MHz for ^{13}C), or a JEOL JNM-GX400 (399.8 MHz ^1H; 100.5 MHz ^{13}C; 161.9 MHz ^{31}P). ^{31}P NMR spectra were referenced using H_3PO_4 (δ = 0 ppm) as an external standard, and ^{19}F NMR spectra were referenced using CHF_3 (δ = 0 ppm) as an external standard. All NMR spectra were recorded at room temperature unless otherwise indicated. IR spectra were recorded on a Perkin Elmer Paragon 1000 IR Spectrometer. Elemental analyses were obtained at Midwest Microlabs (Indianapolis, IN). In general, elemental analyses for many of these complexes were difficult to obtain due to their air and moisture sensitivities.

Materials and Methods. Pentane, methylene chloride, diethyl ether, toluene, benzene, THF, and benzene-d_6 were dried by passage through solvent purification columns and degassed under a purge of argon.[70] Toluene-d_8 and THF-d_8 were dried by vacuum transfer from Na/benzophenone. CD_2Cl_2 and pyridine were dried by vacuum transfer from CaH_2. Hexafluoro-*tert*-butanol and perfluoro-*tert*-butanol were dried by vacuum transfer from P_2O_5. Diethyl diallylmalonate was dried by vacuum transfer from CaH_2 and then passed through a plug of basic alumina in the drybox. KO^{t}Bu, CuCl, HO_2CCPh_3, and 2,6-dichlorophenol were obtained from commercial sources and used as received. AgO_2CCPh_3 was prepared from $AgNO_3$ and NaO_2CCPh_3. The ruthenium complexes **4.1**,[2] **4.5**,[13] **4.7**,[29] **4.16**,[59] and $(P^iPr_3)_2(Cl)_2(CO)Ru{=}CHCH{=}C(Me)_2$[61] as well as the TBEC ligand[47c] were prepared as described in the literature.

$(PCy_3)(O^tBu)_2Ru=CHPh$ (4.4). (a) Complex **4.1** (750 mg, 0.91 mmol) and KO^tBu (400 mg, 3.2 mmol) were combined in C_6H_6 (30 mL), and the reaction mixture was stirred for 24 hours during which time it changed color from purple to brownish-red. The solvent was frozen and removed by sublimation under vacuum. The resulting solids were redissolved in a mixture of C_6H_6 (0.5 mL) and pentane (50 mL). CuCl (900 mg, 9.1 mmol) was added, and the suspension was stirred for 20 minutes, and then cooled at –30 °C for 24 hours. The resulting solution was decanted away from the precipitated solids, and the solvent was removed under vacuum, leaving **4.4** as a dark brown foamy solid (290 mg, 52% yield). This solid is typically about 95% pure (by ^{31}P NMR), but contains traces of the $CuCl(PCy_3)$ polymer.

(b) Ruthenium complex **4.5** (300 mg, 0.43 mmol) and KO^tBu (154 mg, 1.4 mmol) were combined in toluene (5 mL) under N_2. The reaction mixture was stirred for 15 minutes during which time a color change from bright green to red/brown was observed. The solvent was removed under vacuum. The resulting solids were suspended in pentane (50 mL) and cooled to –30 °C for 12 hours. The resulting solution was decanted away from the precipitated solids, and the solvent was removed under vacuum providing complex **4.4** as a dark brown solid (180 mg, 68% yield). ^{31}P NMR spectroscopy indicated that the product contained traces (< 3%) of PCy_3. ^1H NMR (C_6D_6): δ 15.51 (d, 1H, Ru=C*H*Ph, J_{HP} = 4 Hz), 7.88 (d, 2H, ortho C*H*, J_{HH} = 7 Hz), 7.27 (t, 1H, meta C*H*, J_{HH} = 7 Hz), 7.17 (2H, para C*H*), 2.4-1.1 (multiple peaks, 33H, P*Cy*$_3$), 1.29 (s, 18H, ^{t}Bu). $^{31}P\{^1H\}$ NMR (C_6D_6): δ 83.5 (s). $^{13}C\{^1H\}$ NMR (C_6D_6): δ 230.5 (d, Ru=*C*HPh, J_{CP} = 15 Hz), 152.1, 129.9, 125.3, 124.6, 74.50, 36.69, 34.57, 34.48, 34.14, 33.68, 33.44, 31.52, 29.61, 28.84, 28.70, 28.51, 28.37, 27.48, 27.24. Anal. Calcd for $C_{33}H_{57}O_2PRu$: C, 64.15; H, 9.30; Found: C, 62.02; H, 9.10.

$(IMesH_2)(O^tBu)_2Ru=CHPh$ (4.6). Complex **4.2** (7.5 mg, 0.010 mmol) and KO^tBu (3 mg, 0.027 mmol) were combined in C_6D_6 (0.6 mL) in an NMR tube. The reaction mixture was allowed to stand for 15-20 minutes, during which time a color change from green to dark red was observed. ^1H NMR (C_6D_6): δ 16.56 (s, 1H, Ru=C*H*Ph), 7.63 (d, 2H, ortho C*H*, J_{HH} = 7 Hz), 7.2-7.1 (multiple peaks, 3H, meta C*H*

and ortho C*H*), 6.97 (s, 4H, Mes C*H*), 3.43 (s, 4H CH_2CH_2), 2.59 (s, 12H, ortho CH_3), 2.29 (s, 6H, para CH_3), 1.18 (s, 18H, ^{t}Bu).

$(PCy_3)[(CF_3)_2(CH_3)CO]_2Ru=CHPh$ (4.8). Complex **4.4** (250 mg, 0.41 mmol) was dissolved in pentane (25 mL) and 0.5 mL of hexafluoro-*tert*-butanol was added. The reaction was stirred for 30 minutes then cooled to –30 °C for 24 hours. The resulting solution was decanted away from the precipitated solids (residual Cu salts present in the starting material, **4.4**), and the solvent was removed under vacuum to provide an oily dark brown solid. The product was recrystallized from a minimum volume of pentane to afford red crystals of **4.8** (135 mg, 40% yield). Multiple recrystallizations were often required in order to obtain pure material. ^{1}H NMR (C_6D_6): δ 17.54 (s, 1H, Ru=C*H*Ph), 7.88 (d, 2H, ortho C*H*, J_{HH} = 6 Hz), 7.14 (3H, meta C*H* and para C*H*), 2.4-1.1 (multiple peaks, 39H, PCy_3 and CH_3). ^{31}P{^{1}H} NMR (C_6D_6): δ 80.1 (s). ^{19}F NMR (C_6D_6): δ = –77.93 (s), –79.27 (s). ^{13}C{^{1}H} NMR (C_6D_6): δ 262.6 (d, Ru=*C*HPh, J_{CP} = 18 Hz), 150.6, 131.0, 130.4, 126.1 (q, J_{CF} = 288 Hz), 125.4 (q, J_{CF} = 288 Hz), 124.5, 34.33, 34.00, 29.49, 28.40, 28.26, 27.02, 20.46. Anal. Calcd for $C_{33}H_{45}F_{12}O_2PRu$: C, 47.54; H, 5.44; Found: C, 47.19; H, 5.41.

$(PCy_3)[(CF_3)_3CO]_2Ru=CHPh$ (4.9). Complex **4.4** (150 mg, 0.24 mmol) was dissolved in pentane (25 mL) and 0.5 mL of perfluoro-*tert*-butanol was added. The reaction was stirred for 30 minutes then cooled to –30 °C for 24 hours. The resulting solution was decanted away from the precipitated solids (residual Cu salts present in the starting material, **4.4**) and the solvents were removed under vacuum to provide an oily dark brown solid. The product was recrystallized from a minimum volume of pentane to afford red crystals of **4.9** (85 mg, 37% yield). Multiple recrystallizations were often required in order to obtain pure material. ^{1}H NMR (C_6D_6): δ 19.18 (s, 1H, Ru=C*H*Ph), 7.72 (d, 2H, ortho C*H*, J_{HH} = 7 Hz), 7.14 (3H, meta C*H* and para C*H*), 2.1-0.8 (multiple peaks, 33H, PCy_3). ^{31}P{^{1}H} NMR (C_6D_6): δ 75.1 (s). ^{19}F NMR (C_6D_6): δ –73.55 (s). ^{13}C{^{1}H} NMR (C_6D_6): δ 286.5 (d, Ru=*C*HPh, J_{PC} = 15 Hz), 151.4, 130.0, 129.6, 125.6, 123.0 (q, J_{CF} = 292 Hz), 35.20, 34.90, 32.23, 31.91, 31.66, 31.63, 29.91, 28.34, 28.21,

27.95, 27.80, 26.94, 26.75. Anal. Calcd for $C_{33}H_{39}F_{18}O_2PRu$: C, 42.09; H, 4.17; Found: C, 41.60; H, 4.18.

$(PCy_3)(\kappa^2$-*O,Cl*)-$OC_6H_3Cl_2)_2Ru$=CHPh (4.10). (a) Complex **4.4** (8 mg, 0.013 mmol) and 2,6-dichlorophenol (5 mg, 0.029 mmol) were combined in an NMR tube in 600 μL of C_6D_6. The reaction mixture underwent a color change from dark red to green within two minutes at room temperature. ^1H and ^{31}P NMR spectra were recorded after 45 minutes. This reaction proceeded to produce complex **4.10** in quantitative yield by ^1H NMR spectroscopy.

(b) $CsOC_6H_3Cl_2$ (11 mg, 0.032 mmol) and complex **4.1** (15 mg, 0.018 mmol) were combined in an NMR tube in 600 μL of CD_2Cl_2 and THF-d_8 (60 μL) was added to solubilize the cesium salt. The reaction mixture changed color from purple to green after several hours at room temperature, and the reaction proceeded in quantitative yield by ^1H NMR spectroscopy over 24 hours to produce complex **4.10** and 1 equivalent of PCy_3. ^1H NMR (C_6D_6): δ 18.75 (d, 1H, Ru=C*H*Ph, J_{HP} = 11 Hz), 8.06 (d, 2H, ortho C*H*, J_{HH} = 7 Hz), 7.24-7.14 (multiple peaks, 3H, meta C*H* and para C*H*),), 6.87 (d, 4H, phenoxide ortho C*H*, J_{HH} = 8 Hz),), 6.00 (t, 2H, phenoxide para C*H*, J_{HH} = 8 Hz), 2.4-1.2 (multiple peaks, 33H, P*Cy*$_3$). $^{31}P\{^1H\}$ NMR (C_6D_6): δ 55.0 (s).

$(PCy_3)(\eta^2$-$O_2CCPh_3)_2Ru$=CHPh (4.11). (a) Complex **4.4** (8 mg, 0.013 mmol) and HO_2CCPh_3 (8 mg, 0.029 mmol) were combined in an NMR tube and dissolved in 600 μL of C_6D_6. THF-d_8 (50 μL) was added to solubilize the free acid. A color change from red/brown to green was observed after 15 minutes at room temperature, and ^1H and ^{31}P NMR spectra were recorded after 30 minutes. This reaction produced **4.11** in quantitative yield by ^1H NMR spectroscopy.

(b) Complex **4.1** (15 mg, 0.018 mmol) and AgO_2CCPh_3 (21 mg, 0.054 mmol) were combined in 600 μL of CD_2Cl_2 in an NMR tube. A color change from purple to bright green was observed after several minutes at room temperature, and ^1H and ^{31}P NMR spectra were recorded after 20 minutes. This reaction proceeded to produce 1 equivalent of **4.11** and 1 equivalent of **4.12** in quantitative yield by ^1H NMR spectroscopy. ^1H NMR (C_6D_6): δ 19.80 (d, 1H, Ru=C*H*Ph, J_{HP} = 11 Hz), 8.21 (d, 2H

ortho C*H*, J_{HH} = 8 Hz), 7.56-7.08 (multiple peaks, 33H, meta C*H*, para C*H*, C*Ph*$_3$), 2.3-1.1 (multiple peaks, 33H, P*Cy*$_3$). $^{31}P\{^1H\}$ NMR (C_6D_6): δ 64.6 (s).

(PCy_3)Ag(η^2-O_2CCPh_3) (4.12). AgO_2CCPh_3 (8 mg, 0.020 mmol) and PCy_3 (6 mg, 0.021 mmol) were combined in 600 μL C_6D_6 in an NMR tube. ^1H and ^{31}P NMR spectra were recorded after 3 hours at room temperature. Complex **4.12** was also generated in the reaction of **4.1** with AgO_2CCPh_3. ^1H NMR (C_6D_6): δ 7.93 (d, 6H, J_{HH} = 7 Hz, ortho C*H*), 7.17 (t, 6H, J_{HH} = 8 Hz, meta C*H*), 7.05 (t, 3H, J_{HH} = 7 Hz, para C*H*), 1.5-0.96 (br. multiple peaks, 33H, P*Cy*$_3$). $^{31}P\{^1H\}$ NMR (C_6D_6): δ 42.17 (br. d, $J_{P\text{-}Ag}$ = 44 Hz).

(PCy_3)(TBEC)Ru=CHPh (4.13). Complex **4.4** (100 mg, 0.16 mmol) and TBEC (77 mg, 0.18 mmol) were combined in pentane (10 mL). The reaction mixture was stirred for 30 minutes then cooled to –30 °C for 24 hours. The resulting solution was decanted away from the precipitated solids (residual Cu salts present in the starting material, **4.4**) and the solvents were removed under vacuum to give an oily dark brown solid. The product was recrystallized from a minimum volume of pentane to afford brown crystals of **4.13** (51 mg, 35% yield). ^1H NMR (C_6D_6): δ 17.73 (d, 1H, Ru=C*H*Ph, J_{HP} = 7 Hz), 7.56 (d, 2H, ortho C*H*, J_{HH} = 7 Hz), 7.2-6.9 (3H, meta C*H* and para C*H*), 2.5-0.8 (multiple peaks, 45H, P*Cy*$_3$), –3.59 (s, 1H, C*H* agostic). $^{31}P\{^1H\}$ NMR (C_6D_6): δ 67.0 (s). ^{19}F NMR (C_6D_6): δ –73.89 (q, J_{FF} = 9 Hz), –74.23 (q, J_{FF} = 9 Hz), –76.62 (q, J_{FF} = 9 Hz), –76.91 (q, J_{FF} = 12 Hz). $^{13}C\{^1H\}$ NMR (C_6D_6): δ 266.9 (m, Ru=*C*HPh). Anal. Calcd for $C_{38}H_{51}F_{12}O_{22}Ru$: C, 50.72; H, 5.71; Found: C, 49.17; H, 5.41.

(C_5D_5N)$_3$[(CF_3)$_2$$CH_3CO$]$_2$Ru=CHPh (4.14). Complex **4.8** (100 mg, 0.12 mmol) was dissolved in 0.5 mL of toluene, and pyridine-d_5 (0.5 mL) was added. The reaction mixture was stirred for two minutes, and a color change from dark red to green was observed. Pentane (5 mL) was added, and the resulting solution was cooled to –30 °C for 2 hours, during which time an oily brown precipitate formed. The reaction mixture was decanted away from the brown solids and cooled at –30 °C for five days which afforded green crystals of the **4.14** (12 mg, 13% yield). The ^1H NMR spectrum of **4.14** shows a

mixture of two compounds in an approximately 3 to 1 ratio. Notably, the pyridine peaks are not reported because pyridine-d_5 was used in this reaction. ^{1}H NMR (C_6D_6): (major) δ 21.33 (s, 1H, Ru=C*H*Ph), 7.71 (d, 2H, ortho C*H*, J_{HH} = 8 Hz), 7.34 (t, 1H, para C*H*, J_{HH} = 8 Hz), 7.00 (t, 2H, meta C*H*, J_{HH} = 8 Hz), 0.803 (s, 6H, CH_3). ^{1}H NMR (C_6D_6): (minor) δ 21.34 (s, 1H, Ru=C*H*Ph), 7.59 (d, 2H, ortho C*H*, J_{HH} = 7 Hz), 7.29 (t, 1H, para C*H*, J_{HH} = 7 Hz), 6.88 (t, 2H, meta C*H*, J_{HH} = 8 Hz), 1.75 (s, 3H, CH_3), 0.486 (s, 3H, CH_3).

($C_5D_5N)_n(O^tBu)_2Ru=CHPh$ (4.15). Complex **4.4** was dissolved in pyridine-d_5 (600 μL) in an NMR tube. ^{1}H and ^{31}P NMR spectra were recorded after 3.5 hours at 25 °C, at which time the reaction was approximately 33% complete. Significant decomposition of the benzylidene product was also observed at this time. ^{1}H NMR (C_5D_5N): δ 19.32 (s, 1H, Ru=C*H*Ph). ^{31}P{^{1}H} NMR (C_5D_5N): δ 10.71 (s, PCy_3).

$(PCy_3)_2(Cl)RuCH=CHC(Me)=CH_2$ (4.17). Complex **4.16** (10 mg, 0.012 mmol) and KO^{t}Bu (1.4 mg, 0.012 mmol) were combined in 600 μL of C_6D_6 in an NMR tube. An immediate color change from purple to deep red was observed. ^{1}H and ^{31}P NMR spectra were recorded after 15 minutes at room temperature. ^{1}H NMR (C_6D_6): δ 8.93 (d, 1H, Ru–C*H*, J_{HH} = 13 Hz), 6.27 (d, 1H, Ru–CH=C*H*, J_{HH} = 13 Hz), 4.75 (s, 1H, C(Me)=C*H*), 4.58 (s, 1H, C(Me)=C*H*), 2.58–1.17 (multiple peaks, 69H, C(*Me*)=CH, P*Cy*$_3$). ^{31}P{^{1}H} NMR (C_6D_6): δ 23.55 (s). Small amounts of a ruthenium hydride were also observed in the reaction mixture. ^{1}H NMR (C_6D_6): δ –27.57 (t, 1H, Ru–*H*, J_{HP} = 15 Hz). ^{31}P{^{1}H} NMR (C_6D_6): δ = 48.78 (s).

$(P^iPr_3)_2(Cl)(CO)RuCH=CHC(Me)=CH_2$ (4.19). KO^{t}Bu (0.057 g, 0.51 mmol) and $(P^iPr_3)_2(Cl)_2(CO)Ru=CHCH=C(Me)_2$ (0.15 g, 0.26 mmol) were combined in C_6H_6 (15 mL). The reaction was stirred for 30 minutes during which time it changed color from orange to pink. The resulting pink suspension was cannula filtered, and the solvent was removed by sublimation under vacuum to afford a light pink powder (0.11 g, 78% yield). ^{1}H NMR (CD_2Cl_2): δ 7.96 (d, 1H, Ru–C*H*, J_{HH} = 16 Hz), 5.80 (d, 1H, Ru–CH=C*H*, J_{HH} = 16 Hz), 4.30 (s, 1H, C(Me)=C*H*), 4.16 (s, 1H, C(Me)=C*H*), 2.71 (m, 6H, PC*H*(CH_3)$_2$), 1.70 (s, 3H, C(*Me*)=CH), 1.28 (m, 18H, PC(*C*H_3)$_2$). ^{31}P{^{1}H} NMR

(C_6D_6): δ 38.45 (s). $^{13}C\{^1H\}$ NMR (CD_2Cl_2): δ 199.84 (t, Ru–*C*, J_{CP} = 14 Hz), 146.78 (t, Ru-*C*O, J_{CP} = 9 Hz), 138.64, 134.92, 125.08, 101.02, 21.20 (t), 16.21 (m). IR (CH_2Cl_2) 1910 cm^{-1} (C–O). Anal. Calcd for $C_{24}H_{49}ClOP_2Ru$: C, 52.21; H, 8.95; Found: C, 52.17; H, 8.88.

Ring Closing of Diethyl Diallylmalonate. The ruthenium benzylidene complex (0.0053 mmol) was dissolved in C_6D_6 (600 μL) in an NMR tube. Diethyl diallylmalonate (6.4 μL, 0.027 mmol) was added, and the reaction was heated to the appropriate temperature and monitored every 12 hours by ^1H NMR spectroscopy. The percent ring closure was calculated based on the ratios of the 4 β hydrogens in the product (H_P) and the starting material (H_S) (% ring closure = $H_P/(H_P + H_S)$). This calculation assumes that ring closing is the only transformation that takes place, which is a reasonable approximation in these systems.

Ring Closing of Diethyl Diallylmalonate with HCl Co-catalyst. The ruthenium benzylidene complex (0.0053 mmol) and diethyl diallylmalonate (6.4 μL, 0.027 mmol) were dissolved in C_6D_6 (600 μL) in an NMR tube. HCl (0.030 mmol) was added as a 2 M solution in diethyl ether, and the reaction was monitored by ^1H NMR spectroscopy at 22 °C. Once again, the percent ring closure was calculated based on the ratios of the 4 β hydrogens in the product (H_P) and the starting material (H_S) [% ring closure = $H_P/(H_P + H_S)$].

References and Notes

(1) Portions of this chapter have been previously published in: Sanford, M. S.; Henling, L. M.; Day, M. W.; Grubbs, R. H. *Angew. Chem., Int. Ed.* **2000**, *39*, 3451.

(2) Schwab, P.; Grubbs, R. H.; Ziller, J. W. *J. Am. Chem. Soc.* **1996**, *118*, 100.

(3) Scholl, M.; Ding, S.; Lee, C. W.; Grubbs, R. H. *Org. Lett.* **1999**, *1*, 953.

(4) Trnka, T. M.; Grubbs, R. H. *Acc. Chem. Res.* **2001**, *34*, 18.

(5) (a) Ivin, K. J.; Mol, J. C. *Olefin Metathesis and Metathesis Polymerization*, Academic Press: San Diego, CA, 1997. (b) Furstner, A. *Angew. Chem., Int. Ed.* **2000**, *39*, 3012. (c) Grubbs, R. H.; Chang, S. *Tetrahedron* **1998**, *54*, 4413.

(6) (a) Sanford, M. S.; Love, J. A.; Grubbs, R. H. *J. Am. Chem. Soc.* **2001**, in press. (b) Sanford, M. S.; Ulman, M.; Grubbs, R. H. *J. Am. Chem. Soc.* **2001**, *123*, 749. (c) Dias, E. L.; Nguyen, S. T.; Grubbs, R. H. *J. Am. Chem. Soc.* **1997**, *119*, 3887.

(7) (a) Adlhart, C.; Hinderling, C.; Baumann, H.; Chen, P. *J. Am. Chem. Soc.* **2000**, *122*, 8204. (b) Hinderling, C.; Adlhart, C.; Chen, P. *Angew. Chem., Int. Ed.* **1998**, *37*, 2685.

(8) Ulman, M.; Grubbs, R. H. *J. Org. Chem.* **1999**, *64*, 7202.

(9) Schrock, R. R. *Tetrahedron* **1999**, *55*, 8141.

(10) (a) Lynn, D. M.; Mohr, B.; Grubbs, R. H.; Henling, L. M.; Day, M. W. *J. Am. Chem. Soc.* **2000**, *122*, 6601. (b) Lynn, D. M.; Mohr, B.; Grubbs, R. H. *J. Am. Chem. Soc.* **1998**, *120*, 1627.

(11) For a comprehensive review see: Caulton, K. G. *New J. Chem.* **1994**, *18*, 25-41.

(12) The synthesis of complex **4.4** was described independently in the literature several months after our initial report. Coalter, J. N.; Bollinger, J. C.; Eisenstein, O.; Caulton, K. G. *New J. Chem.* **2000**, *24*, 925.

(13) Dias, E. L., Ph.D. Thesis, California Institute of Technology, Pasadena, CA, 1997.

(14) The origin of this free PCy_3 is unknown, but its generation is likely accompanied by the formation of unidentified ruthenium decomposition products.

(15) (a) Nguyen, S. T.; Grubbs, R. H. *J. Am. Chem. Soc.* **1993**, *115*, 9858. (b) Nguyen, S. T.; Johnson, L. K.; Grubbs, R. H. *J. Am. Chem. Soc.* **1992**, *114*, 3974.

(16) Detailed analysis has shown that a Karplus relationship does not apply over a wide range of structurally diverse ruthenium alkylidenes. Sanford, M. S.; Matzger, A. J.; Grubbs, R. H. **1999**, unpublished results.

(17) In fact, the observed ^{1}H and ^{13}C chemical shifts in **4.4** are more typical of electron rich Fischer-type ruthenium carbene complexes than ruthenium benzylidenes. (a) Katayama, H.; Urushima, H.; Nishioka, T.; Wada, C.; Nagao, M.; Ozawa, F. *Angew. Chem., Int. Ed.* **2000**, *39*, 4513. (b) van der Schaaf, P. A.; Kolly, R.; Kirner, H. J.; Rime, F.; Muhlebach, A.; Hafner, A. *J. Organomet. Chem.* **2000**, *606*, 65. (c) Katayama, H.;

Urushima, H.; Ozawa, F. *J. Organomet. Chem.* **2000**, *611*, 332. (d) Wu, Z.; Nguyen, S. T.; Grubbs, R. H.; Ziller, J. W. *J. Am. Chem. Soc.* **1995**, *117*, 5503.

(18) Crystal structure collection and refinement data for complexes **4.4**, **4.9**, **4.14**, and **4.19** are summarized in Appendix A2.

(19) This geometry has also been described as distorted "saw horse" [see ref. 12].

(20) Representative examples of Ru–CH agostic interactions include: (a) Takahashi, S.; Hikichi, S.; Akita, M.; Moro-oka, Y. *Organometallics* **1999**, *18*, 2571. (b) Bennett, M. A.; Pelling, S.; Robertson, G. B.; Wickramaginghe, W. A. *Organometallics* **1991**, *10*, 2166.

(21) (a) Huang, D.; Bollinger, J. C.; Streib, W. E.; Folting, K.; Young, V.; Eisenstein, O.; Caulton, K. G. *Organometallics* **2000**, *19*, 2281. (b) Huang, D. J.; Folting, K.; Caulton, K. G. *J. Am. Chem. Soc.* **1999**, *121*, 10318. (c) Huang, D. J.; Streib, W. E.; Bollinger, J. C.; Caulton, K. G.; Winter, R. F.; Scheiring, T. *J. Am. Chem. Soc.* **1999**, *121*, 8087. (d) Baratta, W.; Herdtweck, E.; Rigo, P. *Angew. Chem., Int. Ed.* **1999**, *38*, 1629.

(22) ^{1}H NMR spectroscopy shows that the *tert*-butyl peaks of **4.4** are equivalent to –120 °C in C_5D_{12}.

(23) Additionally, benzylidene rotation cannot be frozen out down to –120 °C.

(24) The square planar complex $(P^iPr_3)_2RuHCl$ was also recently structurally characterized. van der Schaaf, P. A.; Kolly, R.; Hafner, A. *Chem. Commun.* **2000**, 1045. However, the structure of this molecule is believed to include an additional dihydrogen ligand which was not identified in the original crystallographic analysis. Coalter, J. N.; Eisenstein, O. **2000**, personal communication.

(25) Several Ru(III) alkoxides with Ru–O bond lengths similar to those of **4.4** have been described. For example, *d*(Ru–O) = 1.943(1) Å in TpRu(OMe)(PCy_3)(Cl) [ref. 25a] and *d*(Ru–O) =1.937(2) Å in $[Ru(Cl)(OMe)(C_5H_5N)_4]^+$ [ref. 25b]. (a) Gemel, C.; Kickelbick, G.; Schmid, R.; Kirchner, K. *J. Chem. Soc., Dalton Trans.* **1997**, 2113. (b) Nagao, H.; Aoyagi, K.; Yukawa, Y.; Howell, F. S.; Mukaida, M.; Kakihana, H. *Bull. Chem. Soc. Jpn.* **1987**, *60*, 3247.

(26) Johnson, T. J.; Folting, K.; Streib, W. E.; Martin, J. D.; Huffman, J. C.; Jackson, S. A.; Eisenstein, O.; Caulton, K. G. *Inorg. Chem.* **1995**, *34*, 488.

(27) Alkoxide ligands can be counted as X or XL type donors depending on the circumstance. Crabtree, R. H. *The Organometallic Chemistry of the Transition Metals*, John Wiley and Sons: New York, 1994.

(28) Phosphine dissociation in **4.2** is two orders of magnitude slower than in **4.1** [ref. 6a and 6b].

(29) The synthesis of complex **4.7** is described in Chapter 3.

(30) The low reactivity of hexafluoro-*tert*-butoxide with catalyst **4.1** makes it a superior base for use in the synthesis of **4.2** (which involves reacting catalyst **4.1** with $IMesH_2[HCl]$, and base [ref. 3]). Ward, D. W.; Grubbs, R. H. **2000**, unpublished results.

(31) The use of MeOH and other 1° alcohols in this reaction results in the formation of a complex mixture of ruthenium hydrides, presumably *via* β-hydrogen elimination from the coordinated alkoxide.

(32) The pK_a's of HO^{t}Bu, $HOC(CF_3)_2(CH_3)$ and $HOC(CF_3)_3$ in water are 19.2, 9.6, and 5.4, respectively. Schrock, R. R. *Polyhedron* **1995**, *14*, 3177.

(33) A similar trend of more downfield H_α chemical shifts with less basic alkoxide ligands is observed in Schrock's Mo-based alkylidenes. Oskam, J. H.; Schrock, R. R. *J. Am. Chem. Soc.* **1993**, *115*, 11831.

(34) A similar trend of more downfield H_α chemical shifts with more electron withdrawing X-type ligands was also noted in a series of bimetallic ruthenium complexes. However, generalizations about the chemical environment of ruthenium alkylidenes based on the observed ^1H and ^{13}C chemical shifts of H_α and C_α should be made with caution, because many related complexes do not follow a discernible trend. Dias, E. L.; Grubbs, R. H. *Organometallics* **1998**, *17*, 2758.

(35) Coffindaffer, T. W.; Steffy, B. D.; Rothwell, I. P.; Folting, K.; Huffman, J. C.; Streib, W. E. *J. Am. Chem. Soc.* **1989**, *111*, 4742.

(36) For example, the closest "through-space" Ru–F distance in **4.9** is 2.961 Å.

(37) While **4.10** is depicted as a single diastereomer in Scheme 5, this complex can clearly assume multiple isomeric structures. However, a single set of aromatic resonances is observed for the two phenol ligands at room temperature, suggesting that these isomers are interconverting fast on the NMR time scale.

(38) Octahedral ruthenium benzylidenes such as $Tp(PCy_3)(Cl)Ru=CHPh$ [ref. 38a], $(PCy_3)(C_5H_5N)_2(Cl)_2Ru=CHPh$ [ref. 13], $(PCy_3)(acac)Ru=CHPh$ [ref. 13], $(PCy_3)[P(OEt)_2S_2]_2Ru=CHPh$ [ref. 38b], and $[([9]aneS_3)(PCy_3)(Cl)Ru=CHPh]Cl$ [ref. 38b] are typically green in color. (a) Sanford, M. S.; Henling, L. M.; Grubbs, R. H. *Organometallics* **1998**, *17*, 5384. (b) Leung, W.-H.; Lau, K.-K.; Zhang, Q.-F.; Wong, W.-T.; Tang, B. *Organometallics* **2000**, *19*, 2084.

(39) Werner, H.; Braun, T.; Daniel, T.; Gevert, O.; Schulz, M. *J. Organomet. Chem.* **1997**, *541*, 127.

(40) Both **4.10** and **4.11** are air stable in the solid state, and decompose over 20 minutes to 1 hour in solution (C_6D_6) when exposed to atmospheric O_2 and moisture.

(41) In addition, complex **4.11** is completely inactive for olefin metathesis in the absence of a co-catalyst while the related bis-η^1-ruthenium carboxylate complexes, $(\eta^1\text{-}O_2CCF_3)_2(PPh_3)_2Ru=CHCH=CPh_2$, are known to be excellent metathesis catalysts. Nguyen, S. T., Ph.D. Thesis, California Institute of Technology, Pasadena, CA, 1995.

(42) Ohta, T.; Takaya, H.; Noyori, R. *Inorg. Chem.* **1988**, *27*, 566.

(43) Related three coordinate silver-phosphine complexes (*e.g.*, $(PMe_3)Ag(hfac)$ [hfac = hexafluoroacetylacetonanto]) have been reported. Lin, W.; Warren, T. H.; Nuzzo, R. G.; Girolami, G. S. *J. Am. Chem. Soc.* **1993**, *115*, 11644.

(44) Alexander, J. B.; La, D. S.; Cefalo, D. R.; Hoveyda, A. H.; Schrock, R. R. *J. Am. Chem. Soc.* **1998**, *120*, 4041.

(45) Tetrahedral molybdenum alkylidene complexes containing substituted BINOL ligands have recently been described. Zhu, S.; Cefalo, D. R.; La, D. S.; Jamieson, J. Y.; Davis, W. M.; Hoveyda, A. H.; Schrock, R. R. *J. Am. Chem. Soc.* **1999**, *121*, 8251.

(46) TBEC = 2',2',2",2"-tetrakis(trifluoromethyl)-1,2-bis(2'-hydroxyethyl)cyclopentane.

(47) (a) Fujimura, O.; Grubbs, R. H. *J. Org. Chem.* **1998**, *63*, 824. (b) Fujimura, O.; Grubbs, R. H. *J. Am. Chem. Soc.* **1996**, *118*, 2499. (c) Fujimura, O.; de la Mata, F. J.; Grubbs, R. H. *Organometallics* **1996**, *15*, 1865.

(48) The absence of coupling to other TBEC ligand protons cannot be explained at this time, but broad ^1H NMR signals for agostic interactions are not unusual [ref. 49b].

Notably, it was not possible to characterize **4.13** using two-dimensional ^{1}H NMR spectroscopy because the phosphine resonances obscure the TBEC ligand protons.

(49) (a) Kuhlman, R.; Folting, K.; Caulton, K. G. *Organometallics* **1995**, *14*, 3188. (b) Ogasawara, M.; Aoyagi, K.; Saburi, M. *Organometallics* **1993**, *12*, 3393.

(50) IR spectroscopy of **4.13** was inconclusive with regards to the presence of an agostic interaction.

(51) Sanford, M. S.; Henling, L. M.; Day, M. W. **2000**, unpublished results.

(52) Hartwig, J. F. ; Bergman, R. G.; Anderson, R. A. *J. Am. Chem. Soc.* **1991**, *113*, 3404.

(53) There is some precedent for nucleophilic attack by phosphines on C_α in complex **4.1**. Hansen, S. M.; Rominger, F.; Metz, M.; Hofmann, P. *Chem. Eur. J.* **1999**, *2*, 557.

(54) Olivan, M.; Caulton, K. G. *Inorg. Chem.* **1999**, *38*, 566.

(55) 2,6-py(NCy)$_2$ = 2,6-bis{1-cyclohexylimine)ethyl}pyridine.

(56) Bianchini, C.; Lee, H. M. *Organometallics* **2000**, *19*, 1833.

(57) A similarly large *trans* influence of the benzylidene moiety was noted in Tp(PCy$_3$)(Cl)Ru=CHPh [ref. 38a].

(58) Notably, the Ru=C_α distance changes by less than 0.02 Å between **4.14** and complexes **4.4** and **4.9**.

(59) Wilhelm, T. E.; Belderrain, T. R.; Brown, S. N.; Grubbs, R. H. *Organometallics*, **1997**, *16*, 3867.

(60) This deprotonation reaction accounts for the low yields obtained when the one pot synthesis of (IMesH$_2$)(PCy$_3$)(Cl)$_2$Ru=CHCH=C(Me)$_2$ is attempted using KO^{t}Bu, IMesH$_2$[HCl], and **4.16**. Wilhelm, T. E.; Grubbs, R. H. **2000**, unpublished results. Hexafluoro-*tert*-butoxide is a preferable choice of base for this reaction.

(61) Esteruelas, M. A.; Lahoz, F. J.; Onate, E.; Oro, L. A.; Zeier, B. *Organometallics* **1994**, *13*, 4258.

(62) Silverstein, R. M.; Bassler, G. C.; Morrill, T. C. *Spectroscopic Identification of Organic Compounds*, John Wiley and Sons: New York, 1991.

(63) Trnka, T. M.; Henling, L. M.; Day, M. W.; Grubbs, R. H. **2000**, unpublished results.

(64) The crystal structure of complex **4.2** is reported in Chapter 3.

(65) Ruthenium(II) alkylidenes possessing an N_3Cl_2 coordination environment have been described in the literature. In all cases, these complexes show minimal olefin metathesis activity. For a review on this topic see: Noels, A. F.; Demonceau, A. *J. Phys. Org. Chem.* **1998**, *11*, 602.

(66) Halpern, J. *Science* **1982**, *217*, 401.

(67) Tallarico, J. A.; Bonitatebus, P. J.; Snapper, M. L. *J. Am. Chem. Soc.* **1997**, *119*, 7157.

(68) It will be interesting to attempt the analogous pyridine reaction with complex **4.6**, which does not contain a labile PCy_3 ligand. We anticipate that the products of this transformation will be more relevant to the olefin metathesis intermediate **4.20**.

(69) It will be interesting to attempt these HCl/olefin reactions with **4.6**. Complex **4.3** (L = $IMesH_2$) is believed to have a significantly higher affinity for binding olefins than **4.3** (L = PCy_3) [ref. 6a and 6b].

(70) Pangborn, A. B.; Giardello, M. A.; Grubbs, R. H.; Rosen, R. K.; Timmers, F. J. *Organometallics* **1996**, *15*, 1518.

Chapter 5: Synthesis and Reactivity of Neutral and Cationic Ruthenium Tris(pyrazolyl)borate Benzylidenes[1]

Abstract

A series of neutral and cationic ruthenium (II) benzylidenes containing the hydrotris(pyrazolyl)borate (Tp) ligand have been prepared. The complex $Tp(PCy_3)(Cl)Ru=CHPh$ (**5.2**) was obtained by the reaction of $(PCy_3)_2(Cl)_2Ru=CHPh$ (**5.1**) and KTp. Treatment of **5.2** with $AgBF_4$ or $AgSbF_6$ in the presence of a variety of coordinating solvents afforded $[Tp(PCy_3)(L)Ru=CHPh]^+$ [L = H_2O (**5.3**), CH_3CN (**5.4**), pyridine (**5.5**)] in high yield. The dynamic NMR behavior of these new complexes is discussed, and the X-ray crystal structure of $[Tp(PCy_3)(H_2O)Ru=CHPh]BF_4$ (**5.3**) is reported. Benzylidenes **5.2–5.5** alone do not catalyze olefin metathesis reactions. However, complex **5.2** is activated for ring closing metathesis by the addition of HCl, CuCl and $AlCl_3$.

Introduction

Transition metal catalyzed olefin metathesis is an important method for the formation of carbon-carbon bonds and has received intensive study over the past four decades.[2] The diverse applications of olefin metathesis include the synthesis of polymers by ring opening metathesis polymerization (ROMP),[3] the formation of carbocycles and heterocycles by ring closing metathesis (RCM),[4,5] and the preparation of new substituted acyclic olefins by cross metathesis.[6] Ruthenium benzylidene **5.1** and its derivatives (Figure 1) were the first examples of well-defined ruthenium catalysts for the olefin metathesis reaction,[7] and these complexes (particularly **5.1**) have proven useful as initiators for the ROMP of substituted monomers[8] and for the RCM of functionalized dienes to form 5, 6, and 7-membered rings and in some cases larger macrocycles.[4d] Most importantly, unlike common early transition metal metathesis catalysts,[9] **5.1** and its derivatives are tolerant of most functional groups and water,[10] making them useful for a variety of applications in organic and polymer chemistry.

Figure 1. Ruthenium-Based Olefin Metathesis Catalysts.

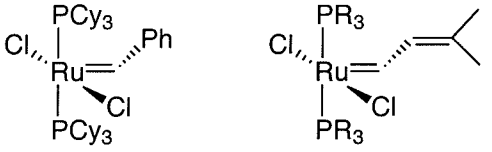

(5.1)

Although **5.1** has proven a versatile olefin metathesis catalyst, it still has several important limitations. Most notably, this complex is less active than Mo and W based catalyst systems and cannot ring close highly substituted dienes.[4] Catalyst **5.1** does not tolerate some important functional groups, including unhindered amines and nitriles, and is moderately O_2 and temperature sensitive in solution. In addition, this catalyst exhibits low *cis/trans* selectivity in the ring closing of large macrocycles.[4,5]

In an effort to improve the stability, activity, and selectivity of **5.1**, recent work in our laboratory has focused on modification of the ligand sphere of this catalyst.[11,12] As part of this ongoing investigation, we became interested in examining the synthesis and reactivity of ruthenium benzylidene complexes containing the tris(pyrazolyl)borate (Tp)

ligand. The Tp ligand has been shown to stabilize early transition metal carbenes. For example, Boncella and coworkers have prepared a series of neutral and cationic Tp alkylidenes of Mo[13] and W[14] which exhibit unprecedented tolerance of air and moisture. Recent reports have shown that both neutral[15,16] and cationic[17] Tp complexes of Ru(II) are readily available and are generally air stable and thermally robust. In addition, many of these compounds show activity for catalytic reactions including hydrogenation[17d,18] and the dimerization of terminal alkynes.[19]

This chapter describes the preparation of $Tp(PCy_3)(Cl)Ru{=}CHPh$ (**5.2**) by a transmetallation reaction between KTp and benzylidene **5.2**. The chloride ligand of **5.2** is abstracted by $AgBF_4$ or $AgSbF_6$ in the presence of coordinating solvents to generate a series of cationic solvent-bound benzylidene complexes. Some structural aspects and dynamic NMR behavior of the new compounds are described herein. The metathesis activity of these neutral and cationic Tp Ru(II) benzylidenes has also been explored.

Results and Discussion

Synthesis of $Tp(PCy_3)(Cl)Ru{=}CHPh$ (5.2). The addition of 1.1 equivalents of KTp to Ru benzylidene **5.1** results in the clean displacement of one chloride and one PCy_3 ligand to afford $Tp(PCy_3)(Cl)Ru{=}CHPh$ (**5.2**) in 84% yield (Scheme 1).[20] This reaction can be followed by a dramatic color change from purple to bright green and is complete within one hour. The product is isolated as an air stable green powder that is insoluble in pentane, slightly soluble in diethyl ether, and soluble in chlorinated solvents, THF and benzene. Complex **5.2** is air stable indefinitely in the solid state and shows no

Scheme 1

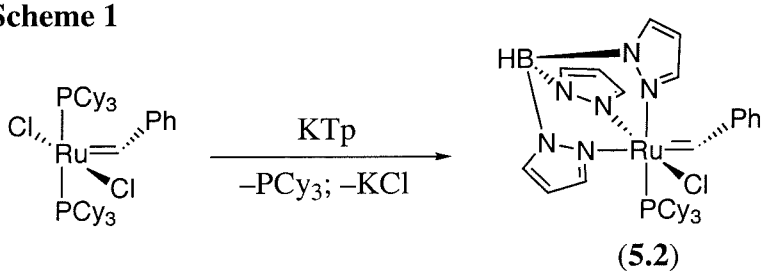

(**5.2**)

decomposition (by ^{1}H NMR) after a week in reagent grade CD_2Cl_2 under air. Notably, efforts to prepare the analogous complex, Tp*(PCy_3)(Cl)Ru=CHPh (Tp* = 3,5-dimethyl-tris(pyrazolyl)borate) were unsuccessful and resulted in the decomposition of **5.1** to a complex mixture of products. This is likely due to the significant steric bulk of both the Tp*[21] and the PCy_3[22] ligands which prohibits formation of a stable six-coordinate benzylidene product.

Benzylidene **5.2** was characterized by ^{31}P, ^{1}H, and ^{13}C NMR spectroscopy and elemental analysis. The proton decoupled ^{31}P NMR spectrum of **5.2** shows a sharp singlet at 33.61 ppm. The ^{1}H NMR spectrum shows the α-proton of the benzylidene as a doublet at 20.01 ppm (J_{HP} = 10 Hz). The observed coupling between H_α and the bound ^{31}P nucleus suggests that the dihedral angle between the phosphine and the benzylidene ($\angle$P–Ru–C_α–H_α) is less than 90°.[7,23] Nine separate resonances are observed for the protons and carbons on the pyrazole rings, indicating that the ruthenium is a stereogenic center.

Synthesis of Cationic Analogs of 5.2. The reaction of **5.2** with $AgBF_4$ or $AgSbF_6$ in CD_2Cl_2 results in instantaneous precipitation of AgCl accompanied by a color change from green to brown. In each case, ^{1}H NMR analysis shows complete consumption of the starting material and the formation of at least five new carbene resonances which remain stable in solution over 24 hours at room temperature. However, the isolation and/or identification of these species has proven impossible due to the complexity of the reaction mixture.

Scheme 2

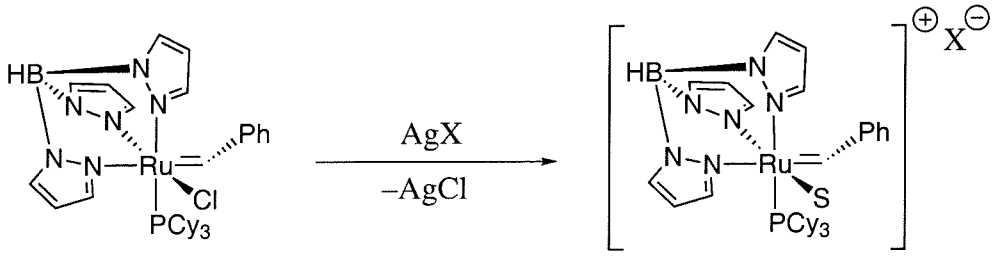

S = H_2O; X = BF_4 (**5.3**)
S = C_5H_5N; X = SbF_6 (**5.4**)
S = $NCCH_3$; X = SbF_6 (**5.5**)

When the same reaction is carried out in the presence of an excess of water, pyridine, or acetonitrile, the cationic Ru benzylidenes **5.3–5.5** form rapidly and cleanly (Scheme 2).[24,25] After filtration to remove AgCl, these compounds can be isolated in 60–77% yield as green microcrystalline solids. The new complexes are soluble in chlorinated solvents and THF, slightly soluble in benzene (depending on the counteranion), and insoluble in pentane. Benzylidenes **5.3–5.5** are moderately air sensitive in solution and are best stored under inert atmosphere.

Complexes **5.3–5.5** have been characterized by ^{1}H, ^{13}C and ^{31}P NMR and IR spectroscopy and elemental analysis. Like benzylidene **5.2**, these complexes exhibit large proton-phosphorus coupling constants (J_{HP} = 8 to 11 Hz) for the H_α proton, suggesting that the dihedral angle between the carbene and the phosphine ($\angle$P–Ru–C_α–H_α) is less than 90°.[7,23] The proton and carbon NMR spectra of **5.3–5.5** show nine separate resonances for the pyrazole protons and carbons indicating that the Ru is an asymmetric center. IR spectroscopy of complex **5.3** shows broad υ_{OH} absorptions at 3406 and 3126 cm^{-1}, similar to those of the related compounds [TpRu(COD)(H_2O)][CF_3SO_3][17e] and [TpRu(H_2O)($L)_2$][CF_3SO_3].[17a] Complex **5.5** exhibits a characteristic υ_{CN} absorption at 2287 cm^{-1}, suggesting that minimal backbonding is involved in the metal–acetonitrile interaction.[17e]

X-ray Diffraction Study of 5.3. Crystals suitable for X-ray structure determination were obtained by slow diffusion of diethyl ether into an acetone solution of **5.3** at –30 °C.[26] A labeled view of the cation is shown in Figure 2 and selected bond distances and bond angles in Table 1. Complex **5.3** co-crystallizes with one equivalent of acetone and one equivalent of diethyl ether. The acetone molecule and the BF_4 anion are each hydrogen-bound to the H_2O ligand as reflected by the O(1)–F(2) and O(1)–O(2) distances of 2.738(4) Å and 2.697(5) Å, respectively. The Ru–O(1) distance of 2.143(3) Å is similar to that in [TpRu(COD)(H_2O)][CF_3SO_3] (d(Ru–O) = 2.161(4) Å)[17e] and [TpRu(THF)($H_2O)_2$][CF_3SO_3] (d(Ru–O(1)) = 2.155(5) Å and d(Ru–O(2)) = 2.151(5) Å).[17a] The Ru–C(1) (carbene carbon) distance of 1.878(4) Å is slightly longer than that of the five coordinate benzylidenes: ($PCy_3)_2(Cl)_2$Ru=CHC_6H_4Cl (1.838(3) Å),[7a] ($IMesH_2$)(PCy_3)($Cl)_2$Ru=CHPh[27] (1.841(11) Å),[28] and (IMes)(PCy_3)($Cl)_2$Ru=CHPh[29]

Figure 2. Labeled View of **5.3** with 50% Probability Ellipsoids.

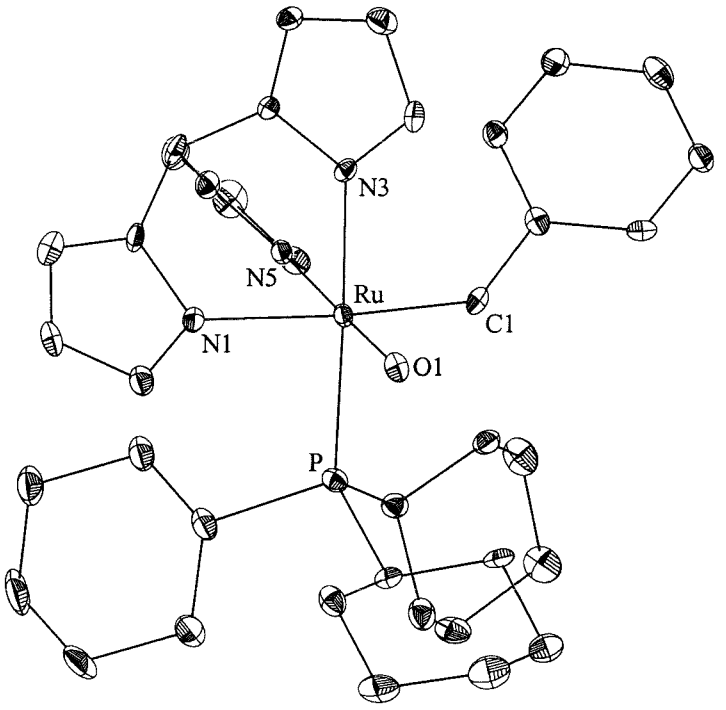

Table 1. Selected Bond Lengths [Å] and Angles [deg] for **5.3**.

	Bond Lengths (Å)		
Ru–C(1)	1.878(4)	Ru–O(1)	2.143(3)
Ru–N(1)	2.200(4)	Ru–P	2.3822(13)
Ru–N(3)	2.129(3)	C(1)–C(2)	1.460(6)
Ru–N(5)	2.056(4)	C(1)–H(1)	0.93(4)
	Bond Angles (deg)		
C(1)–Ru–N(5)	97.65(16)	N(3)–Ru–N(1)	82.91(13)
C(1)–Ru–N(3)	90.04(16)	O(1)–Ru–N(1)	87.34(13)
N(5)–Ru–N(3)	86.73(13)	C(1)–Ru–P	92.40(14)
C(1)–Ru–O(1)	86.65(16)	N(5)–Ru–P	94.45(10)
N(5)–Ru–O(1)	172.48(13)	N(3)–Ru–P	177.12(10)
N(3)–Ru–O(1)	87.09(13)	O(1)–Ru–P	91.53(9)
C(1)–Ru–N(1)	170.95(16)	N(1)–Ru–P	94.51(10)
N(5)–Ru–N(1)	87.64(13)	C(2)–C(1)–H(1)	108(2)

(1.841(11) Å).[30] The elongated Ru=C_α bond in this octahedral complex is believed to be due to the presence of a *trans* pyrazolyl ligand.[31] The three Ru–N bond distances vary from 2.056(4) Å to 2.200(4) Å and are consistent with the increasing *trans* influence of the ligands (benzylidene > PCy_3 > H_2O). The torsion angle about P–Ru–C(1)–C(2) is 138.3(4)°. As described earlier, this angle is consistent with the large value of J_{HP} (8.78 Hz) in this complex.[23]

Dynamic NMR Behavior of Complexes 5.2–5.5. In addition to sharp pyrazole and H_{para} resonances, the aromatic region in the room temperature ^{1}H NMR spectra of benzylidenes **5.2–5.5** shows a broad peak at about 7 ppm. This peak integrates to four hydrogens and is assigned as the overlapping *ortho* and *meta* protons of the carbene phenyl group in the intermediate exchange regime. Upon warming, this resonance resolves into a virtual doublet and a virtual triplet which are assigned as the two *ortho* protons (H_a and H_b in Figure 3) and two *meta* protons (H_c and H_d) of the carbene phenyl group, respectively. Upon cooling, the broad peak decoalesces into a pair of virtual doublets and a pair of virtual triplets which correspond to each of the rotationally frozen *ortho* and *meta* protons. Importantly, the tris(pyrazolyl)borate protons show no exchange within the accessible temperature range (–78 to +100 °C). Furthermore, a single carbene conformer is observed throughout the experiment.

Figure 3. Exchanging Phenyl Group Protons.

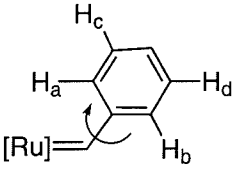

As shown in Figure 3, we believe that this dynamic behavior is the result of rotation about the C_α–phenyl bond.[32] The activation barrier for this rotation was calculated for each complex using a modification of the Eyring equation,[33] and the results are summarized in Table 2. Most notably, complexes **5.3–5.5** show rotational barriers about 1 kcal/mol higher than that of their neutral analogue **5.2**. The cationic benzylidenes **5.3–5.5** are expected to have slightly shorter Ru–N bond lengths than **5.2** (due to the

electrophilicity of the cationic Ru center),[34] and the increased steric crowding at the metal center would account for the observed increase in $\Delta G^{\ddagger}$ for this rotation.

Table 2. Phenyl Group Rotational Barriers for Complexes **5.2**–**5.5**.

Complex	T(coalescence)	$\Delta G^{\ddagger}$ (kcal/mol)
5.2	–15 °C	11.75 ± 0.29
5.3	–2.5 °C	12.32 ± 0.43
5.4	12 °C	12.97 ± 0.18
5.5	2.5 °C	12.60 ± 0.80

Olefin Metathesis Activity of Complex 5.2. Compound **5.2** alone shows no activity for olefin metathesis and does not react with common substrates, such asnorbornene or diethyl diallylmalonate, even after several days at 70 °C. (Interestingly, a recent report has shown that a similar compound – $Tp(Cl)(PPh_3)Ru{=}C{=}CHPh$ – *is* active for the polymerization of norbornene under similar conditions.)[15f] This lack of reactivity can be attributed to the ability of the Tp ligand to enforce an octahedral coordination geometry and to render the ligands non-labile. Since benzylidene **5.2** is coordinatively saturated, ligand dissociation is necessary before olefin coordination and metathesis can take place.[35]

As summarized in Table 3, we have found that a variety of co-catalysts activate benzylidene **5.2** for the ring closing metathesis of diethyl diallylmalonate. These co-catalysts, which include Bronstead acids, "phosphine sponges" and Lewis acids, were chosen for their ability to assist in the dissociation of a ligand of complex **5.2** to generate a 16-electron, coordinatively unsaturated species. HCl has proven the most effective co-catalyst for this reaction, and a 20 mol% solution of **5.2**/HCl (1 eq) ring closed the substrate within 4 hours at room temperature. No propagating species or free phosphine were observed during this reaction by ^{31}P or ^{1}H NMR, and the initiator appeared intact at its completion. The lack of an observable propagating species is most likely due to the

fact that an undetectable (by ^{1}H NMR) amount of catalyst initiates and efficiently catalyzes the reaction.[36]

HCl has been shown to activate a variety of Ru benzylidenes for olefin metathesis by protonation of Ru-bound ligands.[37] In the case of complex **5.2**, it is possible that activation occurs by protonation of a pyrazole arm of the Tp ligand to generate a transient κ^2-coordinated ligand. The protonation of an undetectable amount of phosphine would also explain the observed activity. However, the stability of complex **5.2** in the presence of HCl (no decomposition is observed by ^{1}H or ^{31}P NMR after one week in the presence of 10 equivalents of HCl under inert atmosphere) has hampered studies concerning the mechanism of HCl activation.

Table 3. RCM of Diethyl Diallylmalonate with **5.2** and Co-catalysts.[a]

Co-catalyst	Eq (relative to **5.2**)	% Closed	Time
HCl	1 eq	100	4 hr
CuCl	10 eq	100	18 hr
$AlCl_3$	1 eq	82	24 hr

[a] Reactions in CD_2Cl_2; [Ru] = 0.035 M; [Substrate] = 0.175 M.

The addition of CuCl also induced modest RCM activity in complex **5.2**. A 20 mol% solution of **5.2**/CuCl (10 eq) ring closed diethyl diallylmalonate within 18 hours at room temperature. Only the parent carbene resonance was observed throughout the reaction, and the catalyst appeared intact at the completion of the ring closure. (Notably, benzylidene **5.2** did decompose after about a week in the presence of excess CuCl.) The role of CuCl in this system has not been established definitively, but this reagent is known to react with phosphines to form ill-defined, marginally soluble complexes.[11c,38] As a result, we suggest that CuCl causes an undetectable amount of phosphine dissociation to generate the highly reactive 16-electron species "Tp(Cl)Ru=CHPh". Interestingly, other phosphine sponges including $[(p\text{-cymene})RuCl_2]_2$ and $Rh(C_2H_4)_2(acac)$ induced little metathesis activity in complex **5.2**, while no metathesis activity was observed in the presence of $Ni(COD)_2$. This trend is consistent with earlier

observations concerning the relationship between electronic and steric properties of phosphine sponges and their ability to activate Ru olefin metathesis catalysts.[11b]

$AlCl_3$ was also an effective co-catalyst for the ring closing of diethyl diallylmalonate. The addition of 1 equivalent of $AlCl_3$ to **5.2** in the presence of the diene substrate resulted in instantaneous conversion to a new carbene species with an H_α signal at 19.8 ppm in the ^1H NMR spectrum. Within 24 hours the substrate was 82% ring closed and all carbene resonances had disappeared.[39] Other Lewis acids, including $GaBr_3$ and $B(C_6F_5)_3$ induced less than 10% ring closing before complete decomposition of the benzylidene was observed. The reaction of **5.2** with weaker Lewis acids like $MgCl_2$ did not lead to the formation of any detectable new species or cause any RCM activity.

Lewis acids have been used to induce olefin metathesis activity in a number of transition metal alkylidenes, and their role has never been definitively established.[13a,15f,40] Osborn has suggested that activation can occur by halide abstraction to generate a cationic active species.[27] However, this seems unlikely in the case of complex **5.2** since its cationic analogues **5.3–5.5** show no activity for olefin metathesis (*vide infra*). Boncella has proposed that the $AlCl_3$ activation of Tp[N(2,6-$^iPr_2C_6H_3$)](CH$_3$)MoCH(C(CH$_3$)$_2$Ph) occurs by cleavage of a pyrazole ring from the Tp ligand to generate a coordinatively unsaturated species.[13a] This mechanism also appears unlikely since no free pyrazole is observed (by ^1H NMR) in the reaction of **5.2** with excess $AlCl_3$. We propose that the $AlCl_3$ may function as a phosphine scavenger in this reaction. The association of the strongly basic phosphine with the strongly Lewis acidic $AlCl_3$ is expected to irreversibly open a coordination site at the metal center and enable olefin coordination and metathesis to occur. It is also possible that the $AlCl_3$ associates with a pyrazole arm to generate an active species with a κ^2-coordinated Tp ligand. However, these possibilities could not be distinguished due to the complexity of the reaction mixture.

Metathesis Activity of Cationic Benzylidenes 5.3–5.5. Disappointingly, complexes **5.3–5.5** show no activity for the RCM of diethyl diallylmalonate. Neither heat (50 °C for two days) nor UV light (broad band irradiation for several hours) induce any metathesis activity in these compounds, and benzylidenes **5.3–5.5** merely decompose after several days in the presence of the diene substrate. This result is particularly

surprising in the case of complex **5.3**, as studies show that the water ligand is relatively labile. When excess pyridine or acetonitrile are added to a CD_2Cl_2 solution of **5.3**, liberation of free H_2O and conversion to the appropriate new benzylidene species are observed within seconds at room temperature.[41] In contrast, the bound pyridine in complex **5.4** does not exchange with free CH_3CN, and the bound CH_3CN of complex **5.5** does not exchange with an excess of pyridine under ambient conditions.

In conclusion, a series of neutral and cationic Ru benzylidenes containing the tris(pyrazolyl)borate ligand have been prepared. These complexes are completely unreactive towards olefinic substrates, but the neutral complex **5.2** can be activated for olefin metathesis by the addition of HCl, CuCl or $AlCl_3$.

Experimental Section

General Considerations. All manipulations were carried out using standard Schlenk techniques under an atmosphere of dry argon. Solid organometallic compounds were transferred in a nitrogen filled Vacuum Atmospheres dry box. All NMR spectra were recorded on a JEOL JNM-GX400 (399.8 MHz ^1H; 100.5 MHz ^{13}C; 161.9 MHz ^{31}P). When resolved, the coupling constants of all tris(pyrazolyl)borate protons were about 2 Hz. IR spectra were recorded on a Perkin Elmer Paragon 1000 IR Spectrometer. Elemental analysis was performed at the Caltech Analytical Facility.

Materials. Pentane, methylene chloride, tetrahydrofuran, and diethyl ether were dried by passage through solvent purification columns.[42] Pyridine and acetonitrile were distilled from CaH_2, and acetone was vacuum transferred from $CaSO_4$. All solvents were deoxygenated with a purge of argon. Deuterated solvents were vacuum transferred from the appropriate drying agents, degassed by three continuous freeze-pump-thaw cycles, and stored in the drybox. Diethyl diallylmalonate (Aldrich) was passed through a plug of activated alumina and degassed by three freeze-pump-thaw cycles. CuCl, $AlCl_3$, $AgSbF_6$, and $AgBF_4$ were obtained from Aldrich and used as received. KTp was obtained from Strem and used as received. $(PCy_3)_2(Cl)_2Ru{=}CHPh$ was prepared according to literature procedures.[7a]

$Tp(PCy_3)(Cl)Ru=CHPh$ (5.2). A 200 mL Schlenk flask was charged with KTp (0.505 g, 20.0 mmol) and $(PCy_3)_2(Cl)_2Ru=CHPh$ (1.5 g, 18.0 mmol). CH_2Cl_2 (20 mL) was added, and the solution was stirred for one hour during which time a color change from purple to bright green was observed. The solvent was reduced to 15 mL, and pentane (30 mL) was added to precipitate KCl. The reaction mixture was filtered through a plug of Celite and concentrated *in vacuo* to about 5 mL. Pentane (60 mL) was added with vigorous stirring to precipitate the product. The green solid was collected on a glass frit, washed with 4 x 20 mL of pentane, and dried *in vacuo*, to afford 1.1 g (84%) of a light green powder. Analytically pure samples were obtained by recrystallization from CH_2Cl_2/diethyl ether. $^{31}P\{^1H\}$ NMR (CD_2Cl_2): δ 33.64 (s). ^1H NMR (CD_2Cl_2): δ 20.01 (d, 1H, Ru=C*H*Ph, J_{HP} = 10 Hz), 8.51 (s, 1H, Tp), 7.86 (s, 2H, Tp), 7.61 (s, 1H, Tp), 7.49(t, 1H, para C*H*, J_{HH} = 7 Hz), 7.05 (br. s, 4H, ortho C*H* and meta C*H*), 6.42 (s, 1H, Tp), 6.29 (s, 1H, Tp), 6.24 (s, 1H, Tp), 6.04 (s, 1H, Tp), 5.81 (s, 1H, Tp), 1.97-0.85 (m, 33H, P*Cy*$_3$). $^{13}C\{^1H\}$ NMR (CD_2Cl_2): δ 333.68 (d, Ru=*C*HPh, J_{CP} = 19 Hz), 150.91, 145.79, 144.79, 143.24, 136.82, 135.49, 134.01, 131.46, 130.73, 128.54, 106.17, 105.99, 104.98, 34.43 (d, *J* = 16.5 Hz), 29.01, 28.81, 28.01 (d, *J* = 8 Hz), 27.71 (d, *J* = 11 Hz), 26.34. IR (NaCl): 2470 cm^{-1} (B–H). Anal. Calcd for $C_{34}H_{49}N_6BClPRu$: C, 56.71; H, 6.86; N, 11.67. Found: C, 56.46; H, 7.00; N, 11.65.

Ring Closing of Diethyl Diallylmalonate with 5.2. Benzylidene **5.2** (15 mg, 0.021 mmol) and the appropriate co-catalyst were combined in an NMR tube. CD_2Cl_2 (0.60 mL) was added and the reaction mixture was shaken for two minutes. Diethyl diallylmalonate (23.9 μL, 0.10 mmol) was added and the reaction was removed from the drybox and monitored by ^1H NMR. The catalyst loading of 20 mol% was chosen because it resulted in reaction times on the order of 24 hours. The percent ring closure was calculated based on the ratios of the 4 β hydrogens in the product (H_P) and the starting material (H_S) (% ring closure = $H_P/(H_P + H_S)$). This calculation assumes that ring closing is the only transformation taking place, which is a reasonable approximation in this system.

[Tp(PCy$_3$)(H$_2$O)Ru=CHPh][BF$_4$] (5.3). A 50 mL Schlenk flask was charged with **2** (250 mg, 0.35 mmol) and $AgBF_4$ (68 mg, 0.35 mmol). Water (5 mL) was added followed by 10 mL of THF, and the reaction mixture was stirred for 5 hours. The solvents were removed *in vacuo*, and the resulting dark green solid was dissolved in CH_2Cl_2 and filtered through a plug of Celite. The solvent was then reduced to 5 mL and pentane (40 mL) was added to precipitate the product. The solids were collected on a glass frit, washed with copious pentane, and dried under vacuum to afford 160 mg (77%) of a green microcrystalline product. Analytically pure samples were obtained by recrystallization from acetone/diethyl ether, and contained 1 equivalent of each recrystallization solvent. Elemental analysis was slightly low in C and H due to partial loss of diethyl ether. $^{31}P\{^1H\}$ NMR (CD_2Cl_2): δ 38.11 (s). ^1H NMR (CD_2Cl_2): δ 19.80 (d, 1H, Ru=C*H*Ph, J_{HP} = 9 Hz), 8.31 (s, 1H, Tp), 8.02 (d, 1H, Tp), 7.92 (d, 1H, Tp), 7.73 (s, 1H, Tp), 7.60 (t, 1H, para C*H*, J_{HH} = 7 Hz), 7.15 (br. s, 4H, ortho C*H* and meta C*H*), 6.57 (t, 1H, Tp), 6.37 (s, 1H, Tp), 6.18 (s, 1H, Tp), 6.09 (t, 1H, Tp), 5.93 (s, 1H, Tp), 2.46 (s, 2H, H_2O, 2.06-1.21 (m, 33H, P*Cy*$_3$). $^{13}C\{^1H\}$ NMR (CD_2Cl_2): δ 337.43 (d, Ru=*C*HPh, J_{CP} = 12 Hz), 151.70, 146.27, 144.76, 143.57, 138.30, 137.01, 135.37, 132.89, 132.12, 128.84, 107.21, 107.07, 106.50, 33.93 (d, *J* = 19 Hz), 29.30, 29.16, 27.85 (d, *J* = 8 Hz), 27.59 (d, *J* = 11 Hz), 26.13. IR (NaCl): 3406 cm^{-1} (O–H); 3126 cm^{-1} (O–H); 2482 cm^{-1} (B–H). Anal. Calcd for $C_{41}H_{67}N_6B_2F_4O_3PRu$: C, 53.43; H, 7.33; N, 9.12. Found: C, 52.96; H, 7.22; N, 9.24.

[Tp(PCy$_3$)(C$_5$H$_5$N)Ru=CHPh][SbF$_6$] (5.4). A 100 mL Schlenk flask was charged with **2** (200 mg, 0.28 mmol) and $AgSbF_6$ (95.4 mg, 0.28 mmol). Pyridine (20 mL) was added, and the reaction was stirred for 90 minutes. The solvent was removed *in vacuo*, and the resulting green solid was redissolved in CH_2Cl_2 (15 mL) and filtered through a plug of Celite. The blue/green solution was concentrated to about 5 mL, and the product was precipitated with pentane. The solids were transferred to a frit, washed with copious pentane, and dried *in vacuo* to give 190 mg (68%) of a green microcrystalline product. Analytically pure samples were obtained by recrystallization from CH_2Cl_2/diethyl ether. $^{31}P\{^1H\}$ NMR (CD_2Cl_2): δ 22.77 (s). ^1H NMR (CD_2Cl_2) : δ 19.96 (d, 1H, Ru=C*H*Ph, J_{HP} = 11 Hz), 9.81 (br. s, 1H, ortho C*H*), 8.13 (d, 1H, Tp), 8.01

(s, 1H, Tp), 7.95 (d, 1H, Tp), 7.84 (s, 1H, Tp), 7.76 (t, 1H, para C*H*, J_{HH} = 7 Hz), 7.62 (t, 1H, para C*H*, J_{HH} = 7 Hz), 7.15 (br. s, 7H, ortho C*H* and meta C*H*), 6.63 (t, 1H, Tp), 6.52 (s, 1H, Tp), 6.10 (t, 1H, Tp), 5.87 (s, 1H, Tp), 5.32 (s, 1H, Tp), 1.67-1.21 (m, 23H, P*Cy*$_3$). $^{13}C\{^1H\}$ NMR (CD_2Cl_2): δ 339.30 (m, Ru=*C*HPh, J_{CP} = 14 Hz), 154.29, 152.01, 147.71, 145.32, 143.25, 138.47, 137.70, 136.05, 133.83, 132.41, 129.06, 128.25, 125.10, 108.10, 106.76, 34.90 (d, *J* = 18 Hz), 29.77, 29.18, 27.77 (d, *J* = 15 Hz), 27.49 (d, *J* = 8 Hz), 26.13. IR (NaCl): 2484 cm^{-1} (B–H). Anal. Calcd for $C_{39}H_{54}N_7BF_6PRuSb$: C, 46.87; H, 5.45; N, 9.81. Found: C, 46.91; H, 5.49; N, 9.56.

[Tp(PCy$_3$)(CH$_3$CN)Ru=CHPh][SbF$_6$] (5.5). (a) A 50 mL Schlenk flask was charged with **2** (200 mg, 0.28 mmol) and $AgSbF_6$ (95.4 mg, 0.28 mmol). CH_3CN (5 mL) was added, followed by 5 mL of CH_2Cl_2. The reaction was stirred for 90 minutes, and the solvent was removed *in vacuo*. The resulting olive green solid was redissolved in CH_2Cl_2 (15 mL), and filtered through a plug of Celite. The solution was concentrated to 10 mL, and the product was precipitated with 50 mL of pentane. The resulting solids were transferred to a frit, washed with pentane, and dried under vacuum. Yield = 160 mg (60%).

(b) A 25 mL Schlenk flask was charged with **3** (50 mg, 0.060 mmol). CH_2Cl_2 (5 mL) was added followed by CH_3CN (5 mL). The reaction mixture was stirred for 30 minutes and then dried in vacuo leaving the product as a dark green solid. Yield = 49 mg (100%). $^{31}P\{^1H\}$ NMR (CD_2Cl_2): δ 39.09 (s). ^1H NMR (CD_2Cl_2): δ 18.90 (d, 1H, Ru=C*H*Ph, J_{HP} = 8 Hz), 8.27 (s, 1H, Tp), 7.94 (t, 2H, Tp), 7.73 (s, 1H, Tp), 7.59 (t, 1H, para C*H*, J_{HH} = 7 Hz), 7.16 (br. s, 4H, para C*H* and meta C*H*), 6.53 (s, 1H, Tp), 6.34 (s, 1H, Tp), 6.27 (s, 1H, Tp), 6.14 (s, 1H, Tp), 5.98 (s, 1H, Tp), 2.45 (s, 3H, C*H*$_3$CN), 2.06-1.12 (m, 33H, P*Cy*$_3$). ^{13}C $\{^1H\}$ (CD_2Cl_2) δ 338.11 (d, Ru=*C*HPh, J_{CP} = 12 Hz), 151.01, 145.05, 144.96, 142.79, 137.73, 136.70, 135.30, 133.93, 132.48, 128.91, 126.84, 107.16, 106.96, 106.39, 34.20 (d, *J* = 29 Hz), 29.44, 27.59 (d, *J* = 14), 27.27 (d, *J* = 12), 26.29, 4.26. IR (NaCl): 2484 cm^{-1} (B–H); 2287 cm^{-1} (CH_3CN). Anal. Calcd for $C_{36}H_{52}N_7BF_6PRuSb$: C, 44.97; H, 5.45; N, 10.20. Found: C, 44.44; H, 5.44; N, 9.95.

X-ray structure determination of 5.3. Crystals suitable for X-ray structure determination were grown by slow diffusion of diethyl ether into an acetone solution of **5.3** at –30 °C. An emerald green flake was mounted in Paratone-N oil (Exxon) on a glass fiber and centered in a cold stream (Crystal Logic) on a Nonius CAD-4 diffractometer. Unit cell parameters were determined from 25 reflections with $12 < \Theta < 14°$. The crystallographic data is summarized in Appendix A3. Two equivalent sets of data were collected with 1.15° ω-scans and merged in point group 2/m using CRYM programs. Individual backgrounds were replaced by a function of Θ based on weak data with $I < 8(\sigma)(I)$. Lorentz and polarization factors were applied; no decay (monitored by 3 reflections measured every 75 minutes) or absorption corrections (based on 6 Ψ-scans) were needed. Weights *w* were calculated as $1/\sigma^2(F_o^2)$; variances $(\sigma^2(F_o)^2)$ were derived from counting statistics plus an additional term $(0.0014I)^2$; variances on the observed data were obtained by propagation of error plus another additional term $(0.0014 < I)^2$. The structure was solved by direct methods (SHELXS)[43] and refined by full matrix least squares on F^2 (SHELXL).[44] The diethyl ether solvent is slightly disordered and partially present [refined population of 0.872(5)]. The hydrogen atoms on the ether were placed at calculated positions; the coordinates of all other hydrogen atoms were refined. The U_{iso} of every hydrogen atom was fixed at 120% of the U_{eq} of the attached atom. All non-hydrogen atoms were refined anisotropically.

References and Notes

(1) The majority of this chapter has been previously published: Sanford, M. S.; Henling, L. M.; Grubbs, R. H. *Organometallics* **1998**, *17*, 5384.

(2) Ivin, K. J.; Mol, J. C. *Olefin Metathesis and Metathesis Polymerization*, Academic Press: London, 1997.

(3) (a) Stelzer, F. *Pure Appl. Chem.* **1996**, *A33(7)*, 941. (b) Grubbs, R. H. *J. Macromol. Sci. Chem.* **1994**, *A31*(11), 1829.

(4) (a) Grubbs, R. H.; Chang, S. *Tetrahedron* **1998**, *54*, 4413. (b) Schuster, M.; Blechert, S. *Angew. Chem., Int. Ed. Engl.* **1997**, *36*, 2036. (c) Grubbs, R. H.; Miller, S. J.;

Fu, G. C. *Acc. Chem. Res.* **1995**, *28*, 446. (d) Kirkland, T. A.; Grubbs, R. H. *J. Org. Chem.* **1997**, *62*, 7310.

(5) Furstner, A. *Angew. Chem., Int. Ed.* **2000**, *39*, 3012.

(6) (a) Choi, T.-L.; Chatterjee, A. K.; Grubbs, R. H. *Angew. Chem., Int. Ed.* **2001**, *40*, 1277. (b) Chatterjee, A. K.; Morgan, J. P.; Scholl, M.; Grubbs, R. H. *J. Am. Chem. Soc.* **2000**, *122*, 3783. (c) Blackwell, H. E.; O'Leary, D. J.; Chatterjee, A. K.; Washenfelder, R. A.; Bussmann, D. A.; Grubbs, R. H. *J. Am. Chem. Soc.* **2000**, *122*, 58, and references therein.

(7) (a) Schwab, P.; Grubbs, R. H.; Ziller, J. W. *J. Am. Chem. Soc.* **1996**, *118*, 100. (b) Schwab, P.; France, M. B.; Ziller, J. W.; Grubbs, R. H. *Angew. Chem., Int. Ed. Engl.* **1995**, *34*, 2039. (c) Nguyen, S. T.; Grubbs, R. H.; Ziller, J. W. *J. Am. Chem. Soc.* **1993**, *115*, 9858.

(8) For recent examples see: (a) Maynard, H. D.; Okada, S. Y.; Grubbs, R. H. *Macromolecules* **2000**, *33*, 6239. (b) Morita, T.; Maughon, B. R.; Bielawski, C. W.; Grubbs, R. H. *Macromolecules* **2000**, *33*, 6621.

(9) (a) Schrock, R. R. *Acc. Chem. Res.* **1990**, *23*, 158. (b) Feldman, J.; Schrock, R. R. *Prog. Inorg. Chem.* **1991**, *39*, 1.

(10) Trnka, T. M.; Grubbs, R. H. *Acc. Chem. Res.* **2001**, *34*, 18.

(11) (a) Chang, S.; Jones, L.; Wang, C.; Henling, L. M.; Grubbs, R. H. *Organometallics* **1998**, *17*, 3460. (b) Dias, E. L.; Grubbs, R. H. *Organometallics* **1998**, *17*, 2758. (c) Dias, E. L.; Nguyen, S. T.; Grubbs, R. H. *J. Am. Chem. Soc.* **1997**, *119*, 3887.

(12) (a) Scholl, M.; Ding, S.; Lee, C. W.; Grubbs, R. H. *Org. Lett.* **1999**, *1*, 953. (b) Scholl, M.; Trnka, T. M.; Morgan, J. P.; Grubbs, R. H. *Tetrahedron Lett.* **1999**, *40*, 2247.

(13) (a) Vaughan, W. M.; Abboud, K. A.; Boncella, J. M. *Organometallics* **1995**, *14*, 1567. (b) Vaughan, W. M.; Abboud, K. A.; Boncella, J. M. *J. Organomet. Chem.* **1995**, *485*, 37.

(14) (a) Gamble, A. S.; Boncella, J. M.; *Organometallics* **1993**, *12*, 2814. (b) Blosch, L. L.; Gamble, A. S.; Abboud, K.; Boncella, J. M.; *Organometallics* **1992**, *11*, 2342. (c) Blosch, L. L.; Abboud, K.; Boncella, J. M.; *J. Am. Chem. Soc.* **1991**, *113*, 7066.

(15) (a) Burns, I. D.; Hill, A. F.; White, J. P. A.; Williams, D. J.; Wilton-Ely, J. D. E. T. *Organometallics* **1998**, *17*, 1552. (b) Slugovc, C.; Mereiter, K.; Schmid, R.; Kirchner, K. *Organometallics* **1998**, *17*, 827. (c) Slugovc, C.; Sapunov, V. N.; Wiede, P.; Mereiter, K.; Schmid, R.; Kirchner, K. *J. Chem. Soc., Dalton Trans.* **1997**, 4209. (d) Gemel, C.; Kickelbick; Schmid, R.; Kirchner, K. *J. Chem. Soc., Dalton Trans.* **1997**, 2113. (e) Moreno, B.; Sabo-Etienne, S.; Chaudret, B.; Rodrigez, A.; Jalon, F.; Trofimenko, S. *J. Am. Chem. Soc.* **1995**, *117*, 7441. (f) Katayama, H.; Yoshida, T.; Ozawa, F. *J. Organomet. Chem.* **1998**, *562*, 203.

(16) For a recent review see: Slugovc, C.; Schmid, R.; Kirchner, K. *Coord. Chem. Rev.* **1999**, *186*, 109.

(17) (a) Takahashi, Y.; Akita, M.; Hikichi, S.; Moro-oka, Y. *Inorg. Chem.* **1998**, *37*, 3186. (b) Trimmel, G.; Slugovc, C.; Wiede, P.; Mereiter, K.; Sapunov, V. N.; Schmid, R.; Kirchner, K. *Inorg. Chem.* **1997**, *36*, 1076. (c) Bohanna, C.; Esteruelas, M. A.; Gomez, A. V.; Lopez, A. M.; Martinez, M.–P. *Organometallics* **1997**, *16*, 4464. (d) Chan, W.-C.; Lau, C.-P.; Chen, Y.-Z.; Fang, Y.-Q.; Ng, S.-M.; Jia, G. *Organometallics* **1997**, *16*, 34. (e) Gemel, C.; Trimmel, G.; Slugovc, C.; Kremel, S.; Meretier, K.; Schmid, R.; Kirchner, K. *Organometallics* **1996**, *15*, 3998.

(18) Vincente C.; Shul'pin, G. B.; Moreno, B.; Sabo-Etienne, S.; Chaudret, B. *J. Mol. Cat. A* **1995**, L5.

(19) Slugovc, C.; Mereiter, K.; Zobetz, E.; Schmid, R.; Kirchner, K. *Organometallics* **1996**, *15*, 5275.

(20) This same reaction was described by Wilton-Ely and coworkers several months after our initial report. Harlow, K. J.; Hill, A. F.; Wilton–Ely, J. D. E. T. *J. Chem. Soc., Dalton Trans.* **1999**, 285.

(21) Trofimenko, S. *Chem. Rev.* **1993**, *93*, 943.

(22) Tolman, C. A. *Chem. Rev.* **1977**, *77*, 313.

(23) Some correlation between the solid state alkylidene configuration and the solution phase ^{1}H NMR alkylidene proton-phosphorus coupling constant has been noted [ref. 7]. However, recent results show definitively that a direct Karplus relationship between the

P–Ru–C_α–H_α angle and J_{HP} does not apply in ruthenium alkylidene complexes. Sanford, M. S.; Matzger, A. J.; Grubbs, R. H. **1999**, unpublished results.

(24) When $AgBF_4$ is added to $(PCy_3)_2Cl_2Ru$=CHPh (**5.1**) in the presence of pyridine, acetone or acetonitrile, the precipitation of AgCl is observed (indicating that chloride abstraction is successful), but complete decomposition of all carbene species occurs within minutes at room temperature.

(25) Preparation of analogous cationic benzylidenes containing THF, 2-picoline, 2,6-lutidine, triflate, or PPh_3 was attempted, but these complexes did not form cleanly under a variety of conditions.

(26) The collection and refinement parameters for the crystallographic analysis of **5.3** are summarized in Appendix A3.

(27) $IMesH_2$ = 1,3-dimesityl-4,5-dihydroimidazol-2-ylidene.

(28) The crystal structures of $(IMesH_2)(PCy_3)(Cl)_2Ru$=CHPh and $(IMesH_2)(Cl)_2(C_5H_5N)_2Ru$=CHPh are described in Chapter 3.

(29) IMes = 1,3-dimesitylimidazol-ylidene.

(30) Huang, J.; Stevens, E. D.; Nolan, S. P.; Peterson, J. L. *J. Am. Chem. Soc.* **1999**, *121*, 2674.

(31) Octahedral ruthenium benzylidenes typically have Ru=C_α distances of approximately 1.87 Å. For example see: (a) Leung, W.-A.; Lau, K.-K.; Zhang, Q.-F.; Wong, W.-T.; Tang, B. *Organometallics* **2000**, *19*, 2084. (b) Esteruelas, M. A.; Lahoz, F. J.; Onate, E.; Oro, L. A.; Zeier, B. *Organometallics* **1994**, *13*, 4258.

(32) The dynamic behavior in **5.2–5.5** could also be the result of rotation about both the Ru=C_α bond (benzylidene rotation) and the C_α–C_β bond (phenyl rotation) as described in Chapter 3. At the low temperature limit, this hindered rotation is expected to result in two distinct chemical environments for H_α due to asymmetry at the ruthenium center. As described in the text, a single benzylidene resonance is observed by ^{1}H NMR spectroscopy. However, the possibility that these two peaks are overlapping cannot be ruled out.

(33) Gunther, H. *NMR Spectroscopy : An Introduction*, John Wiley & Sons: New York, 1980.

(34) For example see ref. 17b and the X-ray structures of TpRu(COD)Br versus TpRu(COD)(H_2O)]CF_3SO_3.

(35) Olefin metathesis catalyzed by **5.1** is also dissociative in PCy_3. Sanford, M. S.; Ulman, M.; Grubbs, R. H. *J. Am. Chem. Soc.* **2001**, *123*, 749.

(36) A similar phenomenon is exhibited by recently reported Ru benzylidene complexes containing Schiff base ligands [ref. 11a]. These compounds are active as single component metathesis catalysts; however, no propagating species is observed by NMR at any time during the metathesis reactions. Unfortunately, with the Schiff base complexes and with complex **5.2**/HCl, the use of lower catalyst loadings decreases the efficiency of the ring closing reactions. Chang S.; Grubbs, R. H. **1998**, unpublished results.

(37) (a) Morgan, J. P.; Grubbs, R. H. *Org. Lett.* **2000**, *2*, 3153. (b) Lynn, D. M.; Mohr, B.; Grubbs, R. H.; Henling, L. M.; Day, M. W. *J. Am. Chem. Soc.* **2000**, *122*, 6601. (c) Dias, E. L., Ph.D. Thesis; California Institute of Technology, 1998.

(38) Wilkinson, G. *Comprehensive Coordination Chemistry*, Pergamon: New York, 1987, Vol. 5.

(39) Related studies have shown that $AlCl_3$ also increases the activity of complex **5.1**.

(40) (a) Youinou, M. T.; Kress, J.; Fisher, J.; Aguero, A.; Osborn, J. A. *J. Am. Chem. Soc.* **1988**, *110*, 1488. (b) Kress, J.; Aguero, A.; Osborn, J. A. *J. Mol. Cat.* **1986**, *36*, 1. (c) Kress, J.; Osborn, J. A. *J. Am. Chem. Soc.* **1983**, *105*, 6346.

(41) Boncella has reported cationic W alkylidenes which have similarly labile solvent ligands but are not active for olefin metathesis [ref. 13 and 14].

(42) Pangborn, A. B.; Giardello, M. A.; Grubbs, R. H.; Rosen, R. K.; Timmers, F. J. *Organometallics* **1996**, *15*, 1518.

(43) Sheldrick, G. M. *Acta Crystallogr.* **1990** *A46*, 467.

(44) Sheldrick, G. M. SHELX-97 University of Gottingen, Germany.

Chapter 6: Reaction of $Tp(PPh_3)Ru(\eta^2-O_2CCHPh_2)$ with Carbene and Vinylidene Precursors

Abstract

$Tp(PPh_3)Ru(\eta^2-O_2CCHPh_2)$ **6.1**, has been prepared by the reaction of $TpRu(Cl)(PPh_3)_2$ with 1.2 equivalents of NaO_2CCHPh_2. Complex **6.1** reacts with diphenylcyclopropene to generate the metallacycle $Tp(PPh_3)Ru[\kappa^2-(C,O)-C(=CHCHPh_2)OC(CHPh_2)=O]$, **6.2**. A trace of the carbene, $Tp(PPh_3)(\eta^1-O_2CCHPh_2)Ru=CHCH=C(Ph)_2$, **6.3**, is also observed in the crude reaction mixture. Compound **6.1** reacts with phenyldiazomethane to form the benzylidene $Tp(PPh_3)(\eta^1-O_2CCHPh_2)Ru=CHPh$, **6.4**. A similar species is also available by the reaction of AgO_2CCHPh_2 with $Tp(PCy_3)(Cl)Ru=CHCH=C(CH_3)_2$, **6.5**, which affords $Tp(PCy_3)(\eta^1-O_2CCHPh_2)Ru=CHCH=C(CH_3)_2$, **6.6**. With the addition of an excess of HCl, complexes **6.4** and **6.6** release free HO_2CCHPh_2 and are converted to, $Tp(PPh_3)(Cl)Ru=CHPh$, **6.7**, and **6.5**, respectively. The reaction of **6.1** with phenylacetylene yields the five-membered chelate $Tp(PPh_3)Ru[\kappa^2-(C,O)-C(=CHPh)OC(CHPh_2)=O]$, **6.8**. Complex **6.8** is also formed in the reaction of $Tp(PPh_3)(Cl)Ru=C=CHPh$ with 1.2 equivalents of AgO_2CCHPh_2. Compounds **6.1**, **6.2**, **6.7**, and **6.8** have been characterized by X-ray crystallography. Complexes **6.2**, **6.5**, **6.6**, **6.7** and **6.8** do not catalyze olefin metathesis reactions while **6.4** has been found to be an active initiator for the ring opening metathesis polymerization of norbornene.

Introduction

Tris(pyrazolyl)borate ruthenium complexes have been well studied over the past five years.[1] A wide variety of Tp[Ru] species containing Ru-C bonds including vinylidene,[2,3,4] allenylidene,[2,5] alkylidene[5,6] and alkyl[7] ligands have been prepared, and these compounds have proven useful for carbon-carbon bond forming reactions including alkyne-alkyne[3a,8] and alkyne-olefin[9] couplings and olefin metathesis.[6,10] Due to our ongoing research program involving the preparation of new ruthenium carbene complexes for applications in olefin metathesis,[11] we became interested in the reactions of carbene precursors with the Tp[Ru] compounds. Our group and others have reported that cyclopropene derivatives,[12] diazo compounds[13,14] and terminal alkynes[2,3,15] can react with transition metals to generate alkylidene and vinylidene complexes. The use of alkynes for the preparation of Tp[Ru] vinylidenes has been well explored by a number of groups.[2-4] However, the reaction of Tp[Ru] complexes with cyclopropenes or diazo compounds has not been described in the literature.

We report here the first example of an isolable Tp[Ru] η^2–carboxylate complex, $Tp(PPh_3)Ru(\eta^2\text{–}O_2CCHPh_2)$, **6.1** (Scheme 1). This compound reacts cleanly with several carbene precursors to form new ruthenium-carbon bonds where the carboxylate shifts from η^2 to η^1 coordination and, in some cases, couples to the incoming ligand. For example, the reaction of **6.1** with diphenylcyclopropene results in the generation of the five-membered chelate $Tp(PPh_3)Ru[\kappa^2\text{-}(C,O)\text{-}C(=CHCHPh_2)OC(CHPh_2)=O]$, **6.2** (Scheme 2). Complex **6.1** reacts with phenylacetylene to produce the related metallacycle $Tp(PPh_3)Ru[\kappa^2\text{-}(C,O)\text{-}C(=CHPh)OC(CHPh_2)=O]$, **6.8** (Scheme 4). The η^2-carboxylate complex also undergoes reaction with phenyldiazomethane, yielding the new ruthenium benzylidene $Tp(PPh_3)(\eta^1\text{-}O_2CCHPh_2)Ru=CHPh$, **6.4** (Scheme 3). This chapter describes the synthesis and characterization of these new compounds as well as several related species. Complexes **6.1**, **6.2**, **6.7**, and **6.8** have been structurally characterized and all new compounds have been NMR and IR spectroscopy as well as elemental analysis. The olefin metathesis activities of these Tp[Ru] complexes have also been preliminarily explored.

Results and Discussion

Synthesis of Tp(PPh$_3$)Ru(η^2-O$_2$CCHPh$_2$) (6.1). The reaction of NaO$_2$CCHPh$_2$ with TpRu(Cl)(PPh$_3$)$_2$ for 24 hours in refluxing THF results in clean displacement of one chloride and one PPh$_3$ ligand to afford Tp(PPh$_3$)Ru(η^2-O$_2$CCHPh$_2$) (**6.1**) in 82% isolated yield (Scheme 1). In contrast to Tp(PPh$_3$)Ru(η^2-O$_2$CH), which was recently reported by Hill and coworkers,[2b] complex **6.1** is thermally stable and is readily purified by recrystallization from CH$_2$Cl$_2$/pentane.

Scheme 1

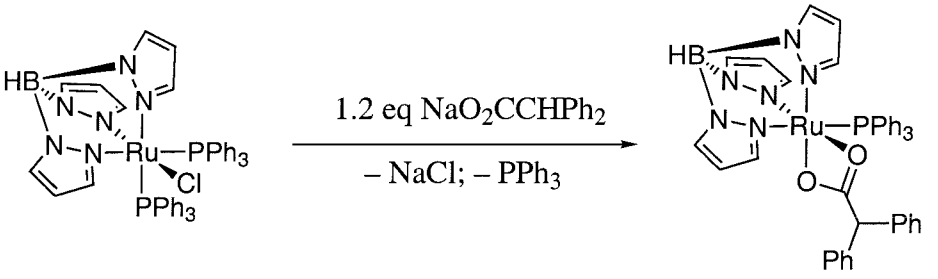

(6.1)

The product is isolated as an air-stable light yellow solid that is insoluble in pentane, slightly soluble in benzene, and soluble in chlorinated solvents and THF. ^{1}H NMR spectroscopy of complex **6.1** shows six resonances (in a 2:1 ratio) for the pyrazolyl protons, indicating that the carboxylate is bound to the metal center in a symmetrical η^2 fashion. The η^2 binding mode is confirmed by IR spectroscopy which shows the OCO asymmetric stretch at 1526 cm^{-1}, which is slightly higher frequency than that of Cp(PPh$_3$)Ru[η^2-O$_2$C(*t*-Bu)] (1495 cm^{-1})[16] and Cp(PPh$_3$)Ru(η^2-O$_2$CCH$_3$) (1490 cm^{-1}).[16] The difference in IR stretching frequencies in these otherwise similar complexes may be due to the increased electron donating ability of the Tp ligand relative to the Cp ligand.[17]

The solid state structure of complex **6.1** was determined by X-ray crystallography. Large orange-yellow crystals were grown by vapor diffusion of pentane into a concentrated CH$_2$Cl$_2$ solution of **6.1** at room temperature. A labeled view of the complex is shown in Figure 1, and selected bond distances and bond angles are reported in Table 1.[18] Complex **6.1** co-crystallizes with one equivalent of pentane and one equivalent of

Figure 1. Labeled View of **6.1** with 50% Probability Ellipsoids.

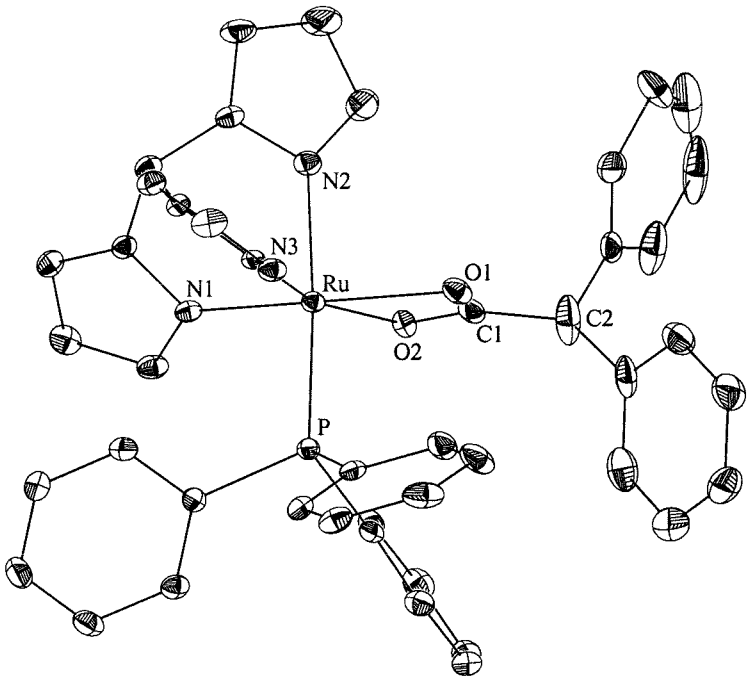

Table 1. Selected Bond Lengths [Å] and Angles [deg] for **6.1**.

	Bond Lengths (Å)		
Ru–N(1)	2.0359(18)	Ru–O(1)	2.1481(14)
Ru–N(2)	2.0584(17)	Ru–O(2)	2.1631(16)
Ru–N(3)	2.1361(16)	O(1)–C(1)	1.271(2)
Ru–P	2.2795(7)	O(2)–C(2)	1.263(2)
	Bond Angles (deg)		
N(1)–Ru–O(2)	103.44(6)	O(2)–Ru–P	95.66(4)
N(3)–Ru–O(2)	164.64(6)	O(1)–Ru–P	92.55(4)
N(2)–Ru–O(2)	87.98(6)	O(2)–Ru–O(1)	60.95(5)
N(1)–Ru–O(1)	164.02(6)	C(1)–O(1)–Ru	89.44(12)
N(3)–Ru–O(1)	105.26(6)	C(1)–O(2)–Ru	90.32(12)
N(2)–Ru–O(1)	90.96(6)	O(2)–C(1)–O(1)	119.26(19)

CH_2Cl_2. The Ru–O bond lengths are 2.1481(14) and 2.1631(16) Å. These distances are in the range of other crystallographically characterized ruthenium η^2-carboxylates, such as $Cp(PPh_3)Ru[\eta^2\text{-}O_2C(t\text{-}Bu)]$ (d(Ru–O) = 2.200(3) and 2.202(4) Å),[16] [(*S*)-BINAP]Ru[η^2-$O_2C(t$-Bu)]$_2$ (d (Ru–O) = 2.216(8) Å and 2.137(6) Å),[19] and $(PPh_3)_2(CO)(Cl)Ru(\eta^2\text{-}O_2CMe)$ (d(Ru–O) = 2.152(6) and 2.144(6) Å).[20] In general, the structure of **6.1** exhibits no unusual features compared to these and other related ruthenium adducts.

Reaction of 6.1 with 3,3-Diphenylcyclopropene. Complex **6.1** serves as a versatile starting material for ruthenium-carbon bond forming reactions, since the carboxylate ligand undergoes facile η^2 to η^1 interconversion to open up a coordination site at the metal center. For example, complex **6.1** reacts slowly with diphenylcyclopropene in toluene over 24 hours to form the metallacyclic species $Tp(PPh_3)Ru[\kappa^2\text{-}(C,O)\text{-}C(=CHCHPh_2)OC(CHPh_2)=O]$ (**6.2**) in 48% isolated yield (Scheme 2). A small amount of the analogous carbene $Tp(PPh_3)(\eta^1\text{-}O_2CCHPh_2)Ru{=}CHCH{=}C(Ph)_2$ (**6.3**) (< 3%) is also observed by ^{1}H NMR spectroscopy. Complex **6.2** is isolated as an orange powder, and forms light yellow crystals upon recrystallization from toluene/pentane. This compound is air-stable indefinitely in the solid state, but decomposes in air when in solution to form an intractable dark red mixture.

Scheme 2

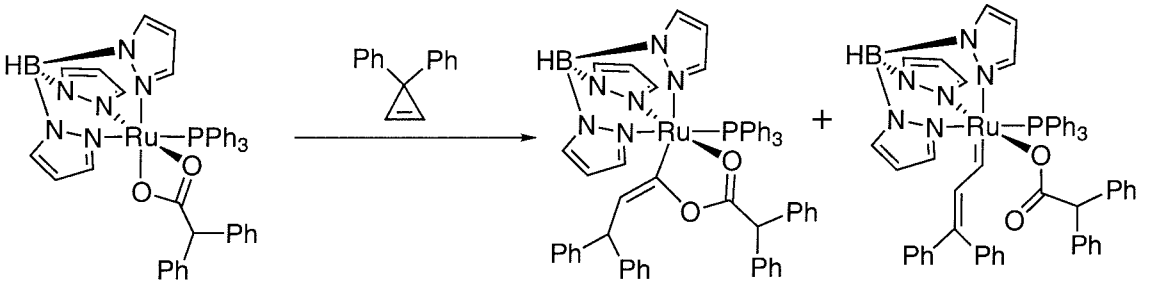

(**6.1**) (**6.2**) (**6.3**)

The ^{1}H NMR spectrum of **6.2** shows nine separate resonances for the pyrazolyl protons, indicating that the metal is a stereogenic center. The protons attached to the β and γ carbons appear as doublets (J_{HH} = 9 Hz) at 5.42 ppm and 4.81 ppm, respectively,

and show no coupling to the remote ^{31}P nucleus. ^{13}C NMR spectroscopy of complex **6.2** shows C_{α} as a doublet (J_{CP} = 17 Hz) at 203.97 ppm and C_{β} as a singlet at 118.97 ppm. The downfield shift of C_{α}, as well as the observed carbon-phosphorus coupling, indicate that this carbon is sp^2 hybridized and is bound to the metal center. However, this peak is significantly upfield of a typical Ru vinylidene or alkylidene carbon resonance.[21]

A trace of carbene **6.3** can be identified in solution if this reaction is monitored by ^{1}H NMR spectroscopy. The α-proton of the alkylidene appears as an overlapping doublet of doublets (apparent triplet) at 18.56 ppm.[22] Unfortunately, this product could not be characterized by any other spectroscopic methods due to its low concentration in solution. Attempts to improve the yield of complex **6.3** by changing the reaction conditions (solvent, temperature, time) were unsuccessful, and **6.2** does not convert to **6.3** (or *vice versa*) upon exposure to heat or UV irradiation.[23] In general, these data suggest that complexes **6.2** and **6.3** are formed independently, and that **6.3** is not an intermediate in the generation of **6.2**. Complex **6.3** is the product of a well-precedented ring opening of diphenylcyclopropene at a Ru(II) center.[12] In contrast, the mechanism of formation of **6.2** (which requires a formal 1,3-hydrogen shift within the alkyl fragment) is not well understood at this time.[24]

The structure of complex **6.2** was confirmed by X-ray crystallography. Suitable crystals were grown by vapor diffusion of pentane into a concentrated toluene solution at room temperature. A labeled view is shown in Figure 2 and selected bond distances and bond angles are in Table 2.[18] Complex **6.2** crystallizes with three independent molecules (which are very similar in structure) in the asymmetric unit, and the bond distances and bond angles for molecule A are reported in Table 2. The Ru–C(1) distance of 2.005(3) Å

Figure 3. Tautomeric Forms of Complex **6.2**.

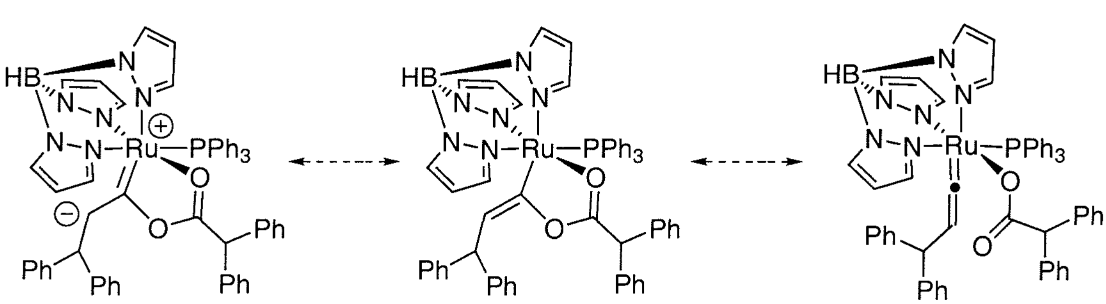

(**6.2b**) (**6.2**) (**6.2a**)

Figure 2. Labeled View of **6.2** with 50% Probability Ellipsoids. (Phenyl Groups on Phosphine Ligand Omitted for Clarity.)

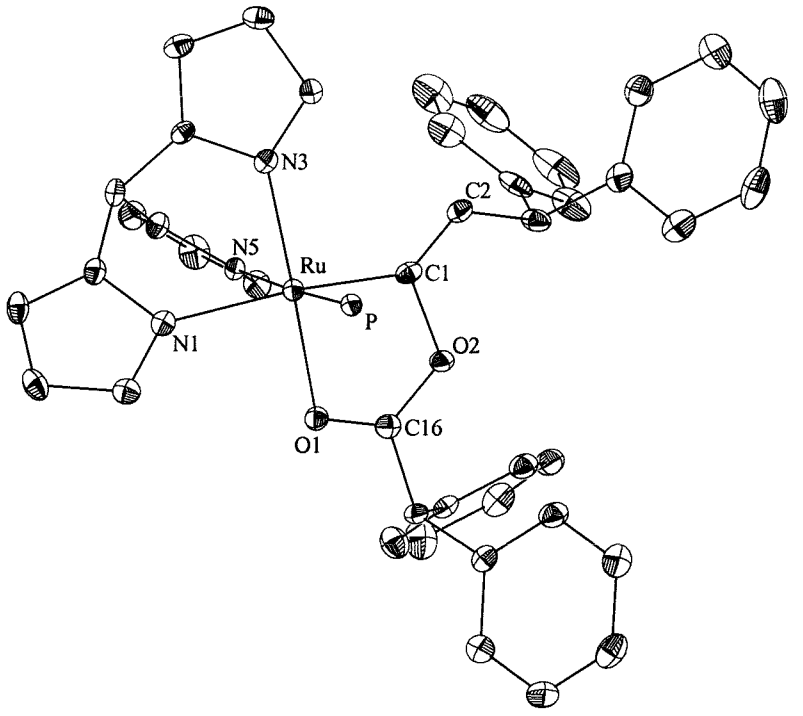

Table 2. Selected Bond Lengths [Å] and Angles [deg] for **6.2**.

	Bond Lengths (Å)		
Ru–C(1)	2.005(3)	Ru–P	2.2820(12)
Ru–N(1)	2.152(3)	O(1)–C(16)	1.242(4)
Ru–N(3)	2.052(3)	O(2)–C(16)	1.302(4)
Ru–N(5)	2.129(3)	O(2)–C(1)	1.526(3)
Ru–O(1)	2.098(2)	C(1)–C(2)	1.327(4)
	Bond Angles (deg)		
N(1)–Ru–O(1)	91.67(9)	O(1)–Ru–P	96.28(6)
N(3)–Ru–O(1)	171.63(9)	Ru–O(1)–C(16)	112.49(19)
N(5)–Ru–O(1)	87.32(9)	Ru–C(1)–O(2)	108.64(18)
N(1)–Ru–C(1)	169.05(10)	Ru–C(1)–C(2)	141.7(2)
N(3)–Ru–C(1)	97.51(11)	N(5)–Ru–C(1)	87.06(11)
O(1)–C(16)–O(2)	123.1(3)	O(2)–C(1)–C(2)	108.8(3)

is intermediate between that in the Ru(II) benzylidene $[Tp(PCy_3)(H_2O)Ru{=}CHPh]BF_4$ (d(Ru–C) = 1.878(4) Å)[6] and that in the Ru(II) vinyl species $Cp(CO)(PPh_3)Ru{-}C(O^iPr){=}CHPh$ (d(Ru–C) = 2.130(6) Å).[25] In related structures, Werner and coworkers have suggested that this type of intermediate bond distance indicates significant contribution of the zwitterionic alkylidene complex **6.2b** (Figure 3) to the bonding of the metallacycle.[26] The C(1)–O(2) distance of 1.526(3)Å in complex **6.2** is much longer than a typical C–O single bond. (For example, the C_α–O bond length in $Cp(CO)(PPh_3)Ru{-}C(O^iPr){=}CHPh$ is 1.381(7) Å).[25] Additionally, the Ru–C(1)–C(2) angle is 141.7(2)° while the O(2)–C(1)–C(2) angle is 108.8(3)°, which are both significant distortions from ideal sp^2 angles of 120°. Taken together, these data reflect a contribution of the tautomeric structure, vinylidene **6.2a** (Figure 3), to the bonding in complex **6.2**.

Reaction of 6.1 with Phenyldiazomethane. Complex **6.1** reacts with an excess of phenyldiazomethane to generate $Tp(PPh_3)(\eta^1\text{-}O_2CCHPh_2)Ru{=}CHPh$ (**6.4**) in 78% yield (Scheme 3). The reaction can be followed by observing a dramatic color change from light yellow to dark green and is complete within 3 hours. ^1H and ^{13}C NMR spectroscopy clearly confirm the identity of complex **6.4** as a transition metal carbene and *not* its metallacyclic tautomer **6.4a** (Scheme 3). The α-proton of the carbene appears as a doublet (J_{HP} = 15 Hz) at 19.06 ppm, while the α-carbon appears as a doublet (J_{HP} = 11 Hz) at 339.63 ppm. Interestingly, a number of similar compounds of the general formula $Cp(PPh_3)(\eta^1\text{-}O_2CR^1)Ru(CR_2)$ [R = Ar; $R^1 = CH_3$, ^{t}Bu] have been reported,[16] and their ^{13}C NMR spectra show *no* downfield resonance for C_α. As such, the authors have suggested that these complexes are better described as the tautomeric metallacycles $Cp(PPh_3)Ru[\kappa^2\text{-}(C,O)\text{-}C(R)_2OC(CR^1){=}O]$.[16] This is yet another example underlying the inherent reactivity differences between Cp[Ru] compounds and the analogous Tp[Ru] species.[27]

A complex similar to **6.4** can also be prepared by the reaction of 1.2 equivalents of AgO_2CCHPh_2 with $Tp(PCy_3)(Cl)Ru{=}CHCH{=}C(CH_3)_2$ (**6.5**) (Scheme 3). This reaction proceeds instantaneously to afford $Tp(PCy_3)(\eta^1\text{-}O_2CCHPh_2)Ru{=}CHCH{=}C(CH_3)_2$ (**6.6**) in 61% isolated yield. Again, ^1H and ^{13}C NMR spectroscopy verify the identity of this species as a transition metal alkylidene and not a metallacyclic species. The α-proton

appears as an apparent triplet ($J_{HP} = J_{HH} = 13$ Hz) at 19.26 ppm by ^{1}H NMR, while the α-carbon appears as a doublet ($J_{CP} = 14$ Hz) at 324.65 ppm by ^{13}C NMR spectroscopy.

Scheme 3

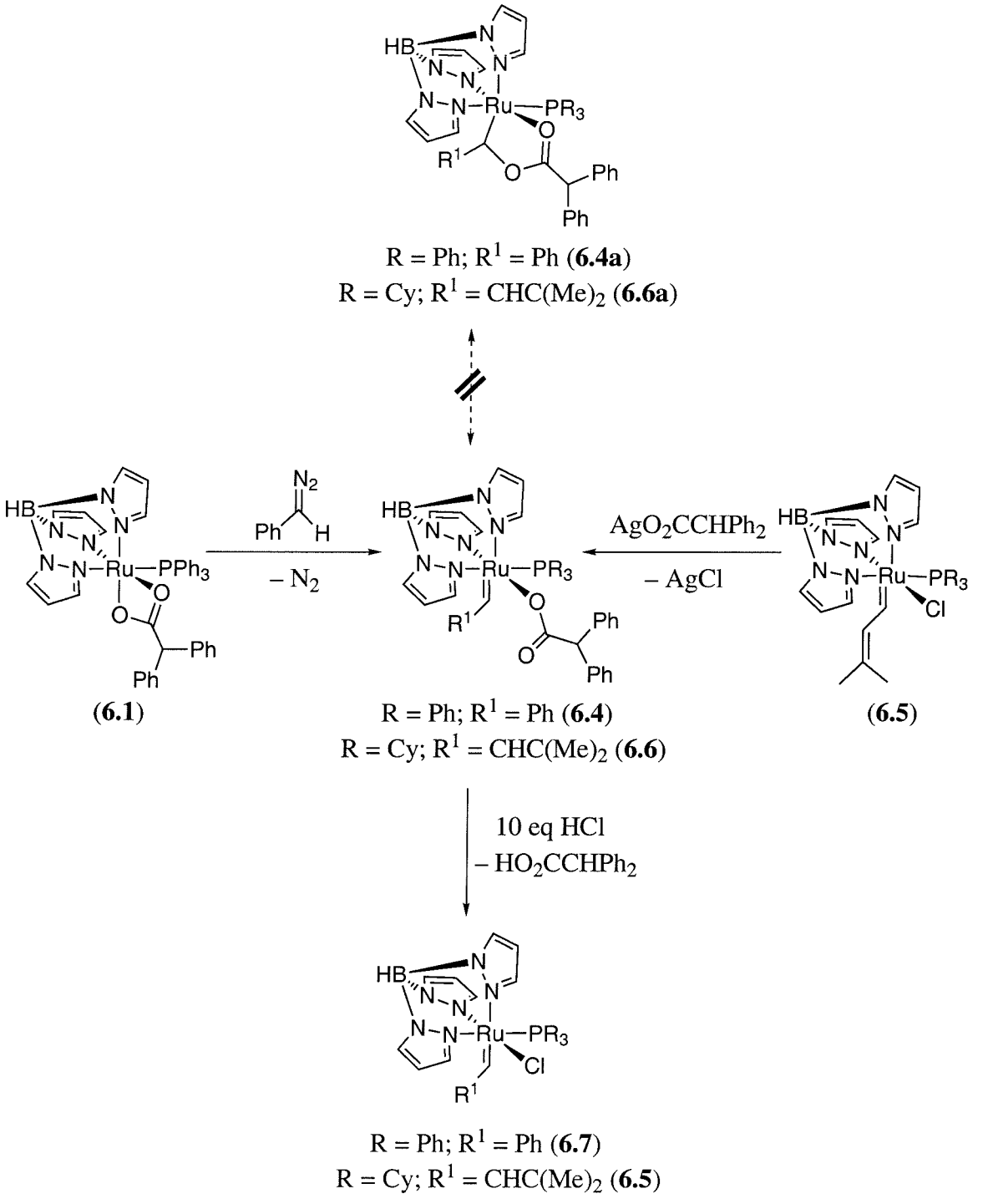

Figure 4. Labeled View of **6.7** with 30% Probability Ellipsoids.

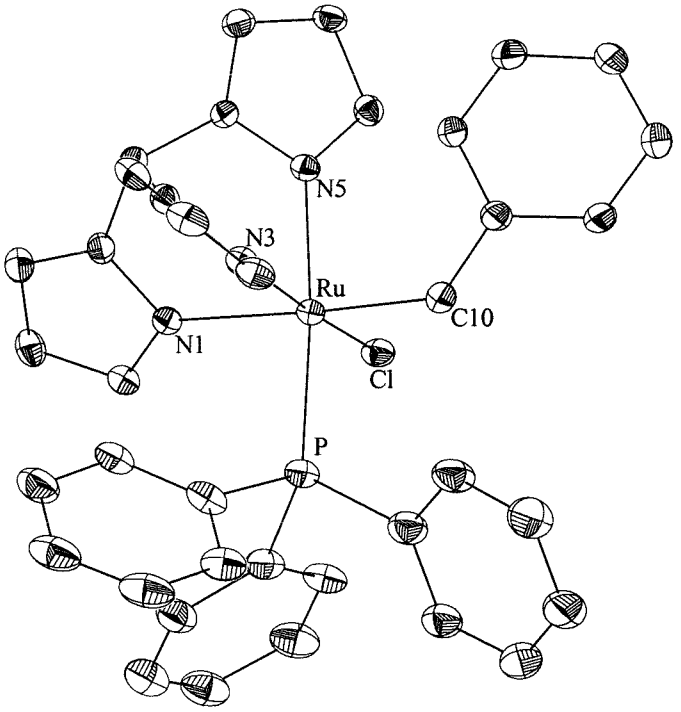

Table 3. Selected Bond Lengths [Å] and Angles [deg] for **6.7**.

	Bond Lengths (Å)		
Ru–C(10)	1.90(2)	Ru–Cl	2.410(5)
Ru–N(1)	2.186(16)	Ru–P	2.335(6)
Ru–N(3)	2.077(17)	Ru–N(5)	2.105(16)
	Bond Angles (deg)		
C(10)–Ru–N(1)	172.9(8)	N(1)–Ru–Cl	87.4(4)
C(10)–Ru–N(3)	97.5(8)	N(3)–Ru–Cl	171.7(5)
C(10)–Ru–N(5)	92.7(8)	N(5)–Ru–Cl	86.6(4)
C(10)–Ru–P	92.5(7)	C(10)–Ru–Cl	87.0(7)

Both complexes **6.4** and **6.6** react rapidly and quantitatively with an excess of HCl to generate the appropriate complex $Tp(PR_3)(Cl)Ru{=}CHR^1$ [R = Cy; R^1 = CH=C$(CH_3)_2$ (**6.5**) or R = Ph; R^1 = Ph (**6.7**)] and the free acid HO_2CCHPh_2 (Scheme 3). Complex **6.7** is analogous to the previously reported species $Tp(PCy_3)(Cl)Ru{=}CHPh$; however, it was not available by the same synthetic methodology.[6] This compound is a light green solid which can be separated from the free acid by several washes with toluene at –10 °C. NMR spectroscopy shows the α-proton of the carbene as a doublet (J_{HP} = 12 Hz) at 19.40 ppm, while the α-carbon appears as a doublet (J_{CP} = 19 Hz) at 340.57 ppm. Notably, Werner has reported that the metallacycles $Cp(PPh_3)Ru[\kappa^2\text{-}(C,O)\text{-}C(Ar)_2OC(CMe){=}O]$ react in a similar fashion with the chloride sources like Et_3NHCl and Al_2O_3/Cl^- (although HCl was not reported) to generate the corresponding alkylidenes $Cp(PPh_3)(Cl)Ru{=}CAr_2$.[16]

The molecular structure of complex **6.7** was confirmed by X-ray crystallography. Dark green crystals were grown by vapor diffusion of pentane into a concentrated CH_2Cl_2 solution of at room temperature. A labeled view is shown in Figure 4 and selected bond distances and bond angles in Table 3.[18] Complex **6.7** co-crystallizes with a highly disordered solvent region that was modeled with toluene and CH_2Cl_2. The Ru–C(10) (carbene carbon) distance of 1.90(2) Å is comparable to that of related Ru(II) alkylidenes – $(PCy_3)_2(Cl)_2Ru{=}CHCH{=}CPh_2$ (*d*(Ru–C) = 1.851(21) Å),[12a] $(PCy_3)_2(Cl)_2Ru{=}CHC_6H_4Cl$ (*d*(Ru–C) = 1.838(3) Å),[13a] and $[Tp(PCy_3)(H_2O)Ru{=}CHPh]BF_4$ (*d*(Ru–C) = 1.878(4) Å).[6] The three Ru-N bond distances vary from 2.077(17) Å to 2.186(16) Å and are consistent with the increasing trans influence of the ligands (benzylidene > PPh_3 > Cl).

Reaction of 6.1 with Phenylacetylene. Complex **6.1** reacts rapidly with an excess of phenylacetylene to produce the metallacycle $Tp(PPh_3)Ru[\kappa^2\text{-}(C,O)\text{-}C(=CHPh)OC(CHPh_2){=}O]$, **6.8**, in 53% isolated yield (Scheme 4). The identity of complex **6.8** as the five-membered chelate as opposed to the tautomeric vinylidene structure (**6.8a**) can be confirmed by NMR spectroscopy. ^{1}H NMR shows 9 separate resonances for the pyrazolyl protons, and the proton attached to the β carbon appears as a singlet at 5.16 ppm. ^{13}C NMR shows the α carbon as a doublet at 210.44 ppm (J_{HP} = 13 Hz), significantly upfield of a typical vinylidene ^{13}C chemical shift.[21] Complex **6.8** is spectroscopically similar to **6.2**, as well as to the previously reported metallacycles $Cp(PPh_3)Ru[\kappa^2\text{-}(C,O)\text{-}C(=CHCO_2Me)OC(Me){=}O]$[26] ($C_\alpha$ = 227.9 ppm) and $(CO)[\eta^1\text{-}$

$O=C(Me_2)](P^iPr_3)_2Ru[\kappa^2$-(C,O)-C(=CHPh)OC(Me)=O]$BF_4$[28] ($C_\alpha$ = 204.7 ppm) which are the products of attack of coordinated carboxylates on vinylidene or alkynyl ligands.

Scheme 4

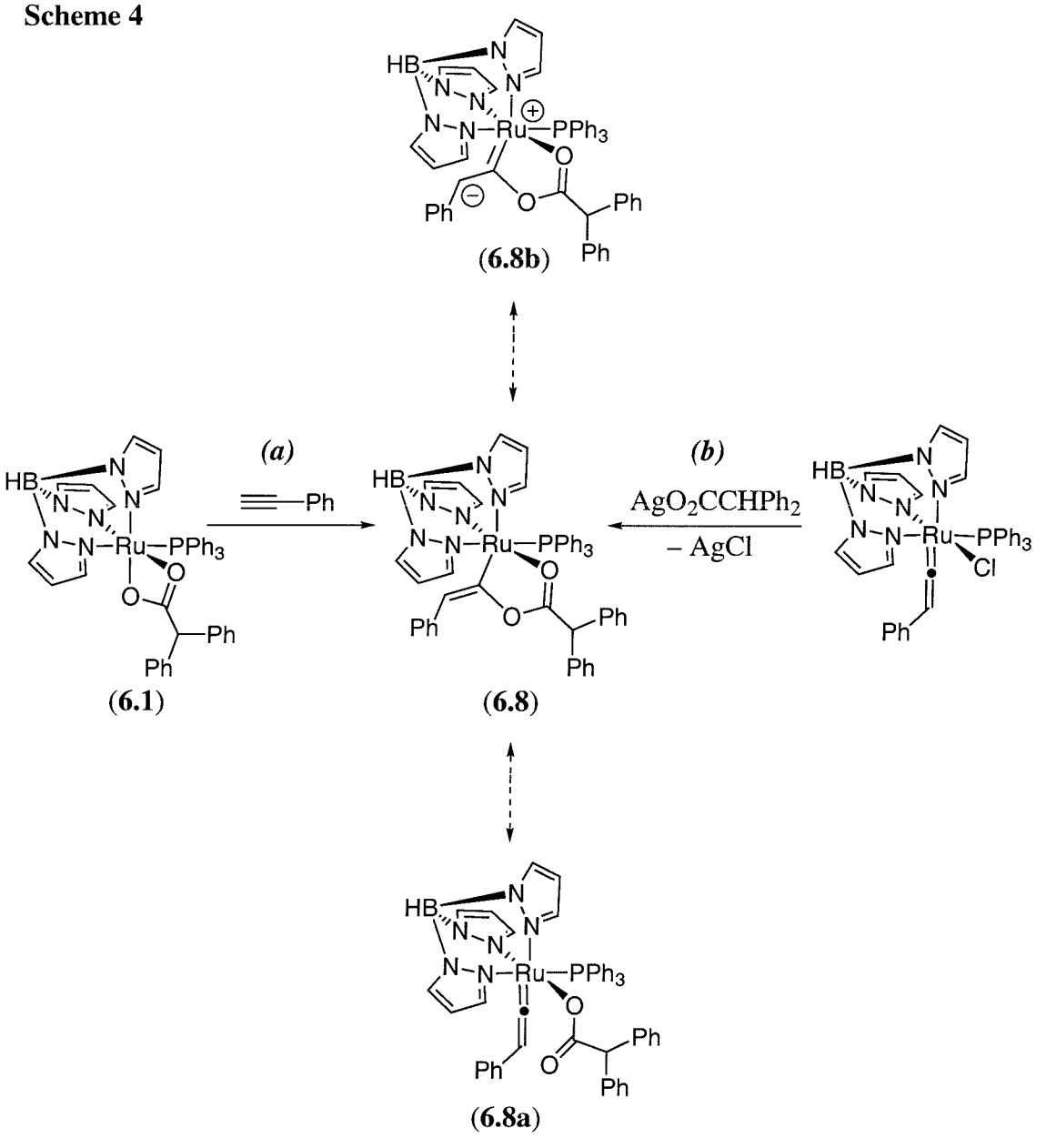

In an attempt to generate the η^1-carboxylate, vinylidene complex $Tp(PPh_3)(\eta^1$-$O_2CCHPh_2)Ru=C=CHPh$, **6.8a**, $Tp(PPh_3)(Cl)Ru=C=CHPh$[8d] was reacted with 1.2 equivalents of AgO_2CCHPh_2 (Scheme 4). The reaction mixture instantaneously changed color from light red to yellow with the precipitation of AgCl. However ^1H, ^{31}P, and ^{13}C

NMR analysis indicated the quantitative formation of chelate **6.8**, rather than vinylidene **6.8a**. Notably, Hill and coworkers have reported a similar reaction between $Tp(PPh_3)(Cl)Ru=C=CHAr$ and $[Et_2NH_2][S_2C(NMe_2)]$, resulting in coupling of the dithiocarbamate to the vinylidene moiety to generate the metallacycle $Tp(PPh_3)Ru[\kappa^2$-(C,S)-$C(=CHAr)SC(NEt_2)=S]$.[2] The α-carbon of this complex appears at a comparable chemical shift (201.2 ppm) by ^{13}C NMR spectroscopy.

Based on the above evidence, we believe that the formation of **6.8** by paths (***a***) and (***b***) (Scheme 4) proceeds through the unstable vinylidene complex, **6.8a**. This proposed intermediate cannot be observed by NMR or IR spectroscopy but undergoes rapid nucleophilic attack to produce the metallacycle, **6.8**. The propensity of vinylidenes to undergo attack by intramolecular nucleophiles has been well documented in the literature. A variety of groups have recently observed similar metallacycle formation with ligand nucleophiles including alcohols,[4b] amides,[4c] and pyrazole[7a] in Tp[Ru] vinylidene systems. Intramolecular nucleophilic attack on a vinylidene by an adjacent carboxylate oxygen has also been reported in a Cp[Ru] system.[26] However, it is interesting to note that the recently reported O–O chelate complex $Tp(acac)Ru=C=CHPh$[4a] is completely stable to this type of intramolecular attack. This is presumably because reaction of an acac oxygen with the vinylidene ligand would result in an unstable, coordinatively unsaturated species.

As further confirmation of its connectivity, the solid state structure of complex **6.8** was obtained. Suitable crystals were grown by vapor diffusion of pentane into a concentrated CH_2Cl_2 solution of **6.8** at room temperature. A labeled view is shown in Figure 5, and selected bond distances and bond angles are in Table 4.[18] The Ru–C(1) distance of 1.979(2) Å is comparable to that of complex **6.2** (*d*(Ru–C) = 1.997(3) Å) as well as to that of the related metallacycles $Cp(PPh_3)Ru[\kappa^2$-(C,O)-$C(=CHCO_2Me)OC(Me)=O]$[26] (*d*(Ru–C) = 2.002(2) Å) and $(CO)(\eta_1$-$OC(Me_2)(P^iPr_3)_2Ru[\kappa^2$-$(C,O)$-$C(=CHPh)OC(Me)=O]BF_4$[28] (*d*(Ru–C) = 1.967(8) Å). As described earlier for complex **6.2**, this short Ru–C distance points to a contribution from the zwitterionic resonance form **6.8b**. Additionally, the relatively long C–O distance of 1.505(3) Å and the distorted Ru–C(1)–C(2) and C(1)–C(2)–O(2) angles of 137.0(2)° and 112.2(2)°, respectively suggest that the η^1-carboxylate, vinylidene tautomer **6.8a** may also play a role in the bonding of this molecule.

Figure 5. Labeled View of **6.8** with 30% Probability Ellipsoids. (Phenyl Groups on Phosphine Ligand Omitted for Clarity.)

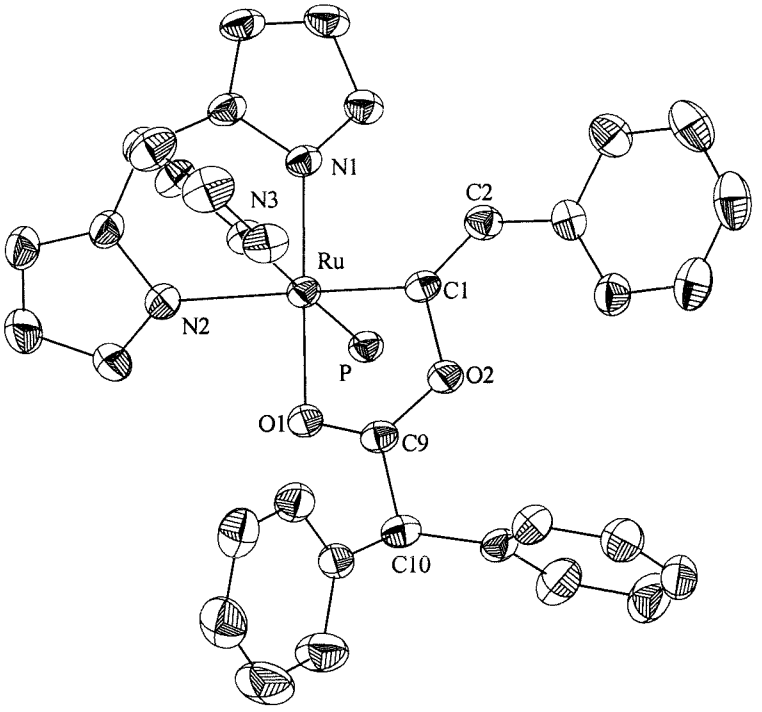

Table 4. Selected Bond Lengths [Å] and Angles [deg] for **6.8**.

	Bond Lengths (Å)		
Ru–C(1)	1.979(2)	Ru–P	2.2967(7)
Ru–N(1)	2.046(2)	O(1)–C(9)	1.232(3)
Ru–N(2)	2.192(2)	O(2)–C(9)	1.309(3)
Ru–N(3)	2.124(2)	O(2)–C(1)	1.505(3)
Ru–O(1)	2.1064(16)	C(1)–C(2)	1.330(3)
	Bond Angles (deg)		
N(1)–Ru–O(1)	173.37(7)	N(3)–Ru–O(1)	89.22(8)
N(2)–Ru–O(1)	96.03(7)	Ru–O(1)–C(9)	111.85(15)
Ru–C(1)–O(2)	110.52(15)	O(2)–C(9)–C(10)	115.5(2)
O(2)–C(1)–C(2)	112.2(2)	O(1)–C(9)–C(10)	120.9(2)
O(1)–C(9)–O(2)	123.5(2)	Ru–C(1)–C(2)	137.0(2)

Investigation of the Olefin Metathesis Activities of Complexes 6.2–6.8. The activities of complexes **6.2–6.8** for both ring opening metathesis polymerization (ROMP) and ring closing metathesis (RCM) reactions were investigated. Compounds **6.2–6.8** do not to react with diethyl diallylmalonate or other common RCM substrates even after several days at elevated temperatures.[29] Complexes **6.2** and **6.8** also fail to react with norbornene, and merely decompose in the presence of this substrate after 2 days at 45 °C. This lack of olefin metathesis activity is consistent with the formulation of **6.2** and **6.8** as metallacycles rather than the tautomeric vinylidene species. After a week at 45 °C, **6.5**, **6.6**, and **6.7** also fail to polymerize norbornene. Notably, the recently reported Tp[Ru] benzylidenes $Tp(PCy_3)(X)Ru{=}CHPh$ [X = Cl, pyridine, CH_3CN, H_2O] are similarly unreactive towards norbornene and strained cyclic olefins.[6]

In contrast, complex **6.4** exhibits low activity as a single component catalyst for the ROMP of norbornene. After 24 hours at 45 °C, ^1H NMR shows approximately 5–15% of ROMP product relative to the norbornene starting material. No propagating species can be observed during this polymerization (presumably due to poor initiation), and the catalyst decomposes completely after 24 hours of reaction. Attempts to precipitate the resulting poly(norbornene)s into methanol were unsuccessful, suggesting that the products are low molecular weight and oligimeric in nature.

It is interesting to note that complexes **6.4** and **6.7** exhibit significantly lower activity for the ROMP of norbornene than the previously reported vinylidene adduct, $Tp(PPh_3)(Cl)Ru{=}C{=}CHPh$.[8d,10] The dramatic differences in reactivity between these apparently similar compounds are currently under investigation in our laboratory.

Summary

A new complex, $Tp(PPh_3)Ru(\eta^2\text{-}O_2CCHPh_2)$ (**6.1**) has been prepared and has proven a versatile precursor for the preparation of new Tp[Ru] organometallics. Complex **6.1** reacts with 3,3-diphenylcyclopropene and phenylacetylene to generate the metallacyclic species $Tp(PPh_3)Ru[\kappa^2\text{-}(C,O)\text{-}C(=CHCHPh_2)OC(CHPh_2)=O]$ (**6.2**) and $Tp(PPh_3)Ru[\kappa^2\text{-}(C,O)\text{-}C(=CHPh)OC(CHPh_2)=O]$ (**6.8**), respectively. Complex **6.1** also reacts cleanly with phenyldiazomethane to form the new transition metal benzylidene, $Tp(PPh_3)(\eta^1\text{-}O_2CCHPh_2)Ru{=}CHPh$ (**6.4**). Preliminary results show that the carbene complex **6.4** is active as a single component catalyst for the ring open metathesis polymerization of norbornene. The product polymer is obtained in low yield and is of

low molecular weight suggesting that the active catalyst has a relatively short lifetime under the polymerization conditions.

Experimental Section

General Considerations. All manipulations were carried out using standard Schlenk techniques under an atmosphere of dry argon. Solid organometallic compounds were transferred in a nitrogen filled Vacuum Atmospheres dry box. All NMR spectra were recorded on a JEOL JNM-GX400 (399.8 MHz ^{1}H; 100.5 MHz ^{13}C; 161.9 MHz ^{31}P). When resolved, the coupling constants of the tris(pyrazolyl)borate protons were about 2 Hz. Elemental analyses were performed at the Caltech Analytical Facility or at Midwest Microlabs (Indianapolis, IN). High resolution mass spectral data was obtained from UCLA.

Materials. Toluene, benzene, pentane, and methylene chloride were dried by passage through solvent purification columns.[30] Deuterated solvents were vacuum transferred from the appropriate drying agents, degassed by three consecutive freeze-pump-thaw cycles, and stored in the dry box. Diethyl diallylmalonate (Aldrich) and phenylacetylene (Aldrich) were passed through a plug of activated alumina and degassed by three consecutive freeze-pump-thaw cycles. Norbornene was sublimed prior to use and was stored in the dry box freezer. $CHPh_2COOH$ and KTp were obtained from commercial sources and used as received. NaO_2CCHPh_2 was prepared by the reaction of the free acid with NaOH, and AgO_2CCHPh_2 was prepared by the reaction of the sodium salt with $AgNO_3$ in H_2O. $(PCy_3)_2(Cl)_2Ru{=}CHCHC(CH_3)_2$,[15b] $TpRuCl(PPh_3)_2$,[31] $Tp(PPh_3)(Cl)Ru{=}C{=}CHPh$,[8d] diphenylcyclopropene[32] and phenyldiazomethane[33] were prepared according to literature procedures.

$Tp(PPh_3)Ru(\eta^2\text{-}O_2CCHPh_2)$ (6.1). $TpRu(PPh_3)_2Cl$ (2.4 g, 2.7 mmol) and NaO_2CCHPh_2 (0.77 g, 3.3 mmol) were combined in THF (50 mL), and the resulting suspension was refluxed for 24 hours. The THF was removed under vacuum and the solids were washed with pentane (4 x 25 mL). The resulting yellow product was dissolved in a 3:1 mixture of CH_2Cl_2 to pentane, filtered through a plug of Celite, and concentrated to dryness to give 1.75 g (82% yield) of a yellow powder. Analytically pure samples were obtained by recrystallization from CH_2Cl_2/pentane. $^{31}P\{^{1}H\}$ NMR (CD_2Cl_2): δ 63.7 (s). ^{1}H NMR (CD_2Cl_2): δ 7.83 (s, 1H, Tp), 7.65 (s, 2H, Tp), 7.35-7.11

(multiple peaks, 26H, P*Ph*$_3$, CH*Ph*$_2$, Tp), 6.84 (s, 2H, Tp), 6.19 (s, 1H, Tp), 5.75 (s, 2H, Tp), 4.56 (s, 1H, C*H*Ph$_2$). ^{13}C{^{1}H} NMR (CD_2Cl_2): δ 186.97, 147.90, 139.56, 139.03, 136.34, 135.11, 128.93, 128.36, 126.72, 105.82, 105.22, 60.62. IR (C_6H_6): 2468 cm^{-1} (B–H), 1526 cm^{-1} (OCO). Anal. Calcd for $C_{41}H_{36}N_6BO_2PRu$: C, 62.52; H, 4.61; N, 10.67. Found: C, 62.79; H, 4.70; N, 11.00.

Tp(PPh$_3$)Ru[κ^2-(C,O)-C(=CHCHPh$_2$)OC(CHPh$_2$)=O] (6.2). Complex **6.1** (300 mg, 0.38 mmol) and diphenylcyclopropene (300 mg, 1.56 mmol) were dissolved in toluene (20 mL). The resulting solution was stirred for 18 hours during which time it changed color from yellow to light orange. The reaction mixture was evaporated to dryness and the solids were washed with cold (–10 °C) pentane (3 x 15 mL). The resulting yellow-orange solid was dried in vacuo to give 180 mg (48%) of product. Analytically pure samples were obtained by recrystallization from toluene/pentane. ^{31}P{^{1}H} NMR (CD_2Cl_2): δ 61.3 (s). ^{1}H NMR (CD_2Cl_2): δ 7.71 (s, 1H, Tp), 7.67 (s, 1H, Tp), 7.56 (s, 1H, Tp), 7.3-6.75 (multiple peaks, 36 H, C*Ph*$_2$, P*Ph*$_3$, CH*Ph*$_2$, Tp), 6.45 (s, 1H, Tp), 6.41 (s, 1H, Tp), 5.90 (s, 1H, Tp), 5.84 (s, 1H, Tp), 5.78 (s, 1H, Tp), 5.42 (d, 1H, J_{HH} = 9 Hz, Ru–C=C*H*CH(Ph)$_2$), 4.86 (s, 1H, C*H*Ph$_2$), 4.81 (d, 1H, J_{HH} = 9 Hz, CHC*H*(Ph)$_2$). ^{13}C{^{1}H} NMR (CD_2Cl_2): δ 203.97 (d, Ru–*C*, J_{CP} = 17 Hz), 180.43, 147.15, 146.57, 146.12, 144.05, 140.73, 138.09, 137.89, 135.74, 135.01, 134.65, 134.55, 134.01, 133.91, 129.55-127.76 (multiple peaks), 127.03, 125.47, 125.30, 118.97, 105.45, 104.93, 104.42, 56.47, 47.76. IR (CD_2Cl_2): 2477 cm^{-1} (B–H), 1618 cm^{-1} (OCO). Anal. Calcd for $C_{56}H_{48}N_6BO_2PRu$: C, 68.64; H, 4.94; N, 8.58. Found: C, 68.43; H, 4.58; N, 8.84.

Observation of Tp(PPh$_3$)(η^1-O$_2$CCHPh$_2$)Ru=CHCH=C(Ph)$_2$ (6.3). Complex **6.1** (30 mg, 0.038 mmol) and diphenylcyclopropene (30 mg, 0.16 mmol) were combined in an NMR tube in the dry box. CD_2Cl_2 (0.75 mL) was added and the reaction was shaken for 24 hours at room temperature. ^{1}H NMR after 24 hours showed a trace of the alkylidene product as an apparent triplet at 18.56 ppm.

Tp(PPh$_3$)(η^1-O$_2$CCHPh$_2$)Ru=CHPh (6.4). To a solution of **6.1** (500 mg, 0.635 mmol) in CH_2Cl_2 (25 mL) was added phenyldiazomethane (150 mg, 1.27 mmol). The resulting solution was stirred for 3 hours at room temperature during which time it changed color from yellow to red to brown-green, and finally to dark green. The

volatiles were removed in vacuo and the solids were washed with 3 x 20 mL of pentane and dried under vacuum to leave 435 mg (78%) of a dark green powder. $^{31}P\{^1H\}$ NMR (CD_2Cl_2): δ 44.8 (s). ^1H NMR (CD_2Cl_2): δ 19.01 (d, 1H, J_{HP} = 15 Hz, Ru=C*H*Ph), 7.92 (s, 1H, Tp), 7.78 (s, 1H, Tp), 7.67 (s, 1H, Tp), 7.62–7.03 (multiple peaks, 31H, P*Ph*$_3$, CH*Ph*$_2$, CH*Ph*, and Tp), 6.61 (s, 1H, Tp), 6.11 (s, 1H, Tp), 5.73 (s, 1H, Tp), 5.61 (s, 1H,Tp), 5.58 (s, 1H, Tp), 4.80 (s, 1H, C*H*Ph$_2$). $^{13}C\{^1H\}$ NMR (CD_2Cl_2): δ 339.63 (d, Ru=*C*HPh, J_{CP} = 11 Hz), 177.22, 149.48, 145.87, 145,16, 144.40, 142.76, 142.52, 136.27, 135.55, 134.21, 134.02, 133.93, 132.50, 132.41, 132.09, 131.14, 129.70, 129.11, 128.84, 128.34, 127.99, 127.90, 127.62, 125.89, 125.53, 105.68, 105.62, 104.96, 60.90. IR (CD_2Cl_2): 2480 cm^{-1} (B–H), 1614 cm^{-1} (OCO). Anal. Calcd for $C_{48}H_{42}N_6BO_2PRu$: C, 65.68; H, 4.82; N, 9.57. Found: C, 65.87; H, 4.80; N, 9.54.

Tp(PCy$_3$)(Cl)Ru=CHCH=C(CH$_3$)$_2$ (6.5). (PCy$_3$)$_2$Cl$_2$Ru=CHCH=C(CH$_3$)$_2$ (1.0 g, 0.13 mmol) and KTp (0.32 g. 0.13 mmol) were dissolved in CH_2Cl_2 (20 mL), and the reaction was stirred for 5 hours over which time a color change from purple to light green was observed. Pentane (50 mL) was added and the reaction was filtered through a plug of Celite. The resulting solution was concentrated to 5 mL, and pentane (70 mL) was added to precipitate the bright green product. The solids were collected on a frit, washed with pentane (4 x 20 mL) and dried under vacuum to provide 0.63 g (72%) of product. $^{31}P\{^1H\}$ NMR (CD_2Cl_2): δ 35.02 (s). ^1H NMR (CD_2Cl_2): δ 19.53 (d of d's, 1H, J_{HP} = 9 Hz, J_{HH} = 13 Hz, Ru=C*H*CH), 8.42 (s, 1H, Tp), 7.84 (s, 1H, Tp), 7.77 (s, 1H, Tp), 7.53 (s, 1H, Tp), 7.24 (d, 1H, J_{HH} = 13 Hz, Ru=CHC*H*), 6.74 (s, 1H, Tp), 6.71 (s, 1H, Tp), 6.39 (s, 1H, Tp), 6.12 (s, 1H, Tp), 5.95 (s, 1H, Tp), 1.88-0.96 (multiple peaks, 33H, P*Cy*$_3$), 1.64 (s, 3H, C*Me*), 1.21 (s, 3H, C*Me*). $^{13}C\{^1H\}$ NMR (CD_2Cl_2): δ 332.62 (d, Ru=*C*HPh, J_{CP} = 14 Hz), 147.86, 145.68, 144.79, 142.57, 139.59, 136.57, 135.40, 133.68, 105.96, 105.78, 104.71, 34.56, 34.38, 29.16, 28.51, 28.10, 28.01, 27.99, 28.92, 27.57, 26.46, 21.00. IR (CD_2Cl_2): 2478 cm^{-1} (B–H). Anal. Calcd for $C_{32}H_{51}N_6BClPRu$: C, 55.06; H, 7.36; N, 12.04. Found: C, 54.91; H, 7.22; N, 12.08.

Tp(PCy$_3$)(η^1-O$_2$CCHPh$_2$)Ru=CHCH=C(CH$_3$)$_2$ (6.6). Complex **6.5** (200 mg, 0.29 mmol)) and AgO$_2$CCHPh$_2$ (110 mg, 0.32 mmol) were combined in CH_2Cl_2 (15 mL). The reaction was stirred for 3 hours and then filtered through a plug of Celite. The solvent was removed under vacuum to afford 150 mg (61%) of a dark green product.

$^{31}P\{^1H\}$ NMR (CD_2Cl_2): δ 39.19 (s). ^1H NMR (CD_2Cl_2): δ 19.26 (t, 1H, $J_{HP}=J_{HH}$ = 13 Hz, Ru=C*H*CH), 7.97 (s, 1H, Tp), 7.87 (s, 1H, Tp), 7.77 (s, 1H, Tp), 7.55 (s, 1H, Tp), 7.37-7.25 (multiple peaks, 3H, P*Ph*$_3$, Tp), 7.04-6.72 (multiple peaks, 14H, P*Ph*$_3$, Ru=CHC*H*), 6.52 (s, 1H, Tp), 6.29 (s, 1H, Tp), 6.05 (s, 1H, Tp), 5.84 (s, 1H, Tp), 4.74 (s, 1H, C*H*Ph$_2$), 1.84-0.82 (multiple peaks, 33H, P*Cy*$_3$), 1.75 (s, 3H, C*Me*), 1.30 (s, 3H, C*Me*). $^{13}C\{^1H\}$ NMR (CD_2Cl_2): δ 324.65 (d, Ru=*C*HPh, J_{CP} = 14 Hz), 177.21, 145.82, 145.19, 144.85, 144.77, 143.62, 143.02, 140.09, 136.65, 134.65, 133.28, 129.00, 128.96, 127.69, 127.51, 125.44, 125.13, 105.78, 105.29, 104.24, 61.62, 34.12, 33.94, 28.76, 27.97, 27.87, 27.75, 26.48, 20.69. IR (CD_2Cl_2): 2475 cm^{-1} (B–H), 1617 cm^{-1} (OCO). Anal. Calcd for $C_{46}H_{62}N_6BO_2PRu$: C, 63.22; H, 7.15; N, 9.62. Found: C, 63.33; H, 7.00; N, 9.29.

Tp(PPh$_3$)(Cl)Ru=CHPh (6.7). To a solution of **6.6** (190 mg, 0.22 mmol) in CH_2Cl_2 (20 mL) was added HCl (1 mL of a 1.0 M solution in diethyl ether, 1.0 mmol). An immediate color change from dark to light green was observed, and the reaction was stirred for 30 minutes. The solvents were removed under vacuum and the resulting green residue was washed with –10 °C toluene (3 x 10 mL) and then with a 3:1 mixture of pentane:toluene (2 x 15 mL). The solids were redissolved in CH_2Cl_2 (15 mL), filtered through a plug of Celite, and concentrated under vacuum to afford 49 mg (33%) of the light green product. Satisfactory elemental analyses could not be obtained, however the structure of this complex was confirmed by X-ray crystallography and by mass spectrometry. $^{31}P\{^1H\}$ NMR (CD_2Cl_2): δ 39.74 (s). ^1H NMR (CD_2Cl_2): δ 19.40 (d, 1H, J_{HP} = 12 Hz, Ru=C*H*Ph), 7.93 (s, 1H, Tp), 7.78 (s, 1H, Tp), 7.73 (s, 1H, Tp), 7.56 (s, 1H, Tp), 7.40–6.95 (multiple peaks, 19H, P*Ph*$_3$, Ru=CH*Ph*), 6.50 (s, 1H, Tp), 6.13 (s, 1H, Tp), 5.92 (s, 1H, Tp), 5.56 (s, 2H, Tp). $^{13}C\{^1H\}$ NMR (CD_2Cl_2): δ 340.57 (d, Ru=*C*HPh, J_{CP} = 19 Hz), 135.95, 134.67, 134.28, 134.11, 132.37, 132.16, 131.95, 131.79, 129.84, 128.73, 127.88, 127.72, 106.06, 105.60, 105.35. IR (CD_2Cl_2): 2480 cm^{-1} (B–H). Anal. Calcd for $C_{34}H_{31}N_6BClPRu$: C, 58.17; H, 4.45; N, 11.97. Found: C, 59.46; H, 4.69; N, 11.18. FAB-HRMS: m/z calcd for M^+ 702.1173; m/z found 702.1184.

Tp(PPh$_3$)Ru[κ^2-(C,O)-C(=CHPh)OC(CHPh$_2$)=O] (6.8). (a) To a solution of **6.1** (150 mg, 0.19 mmol) in CH_2Cl_2 (10 mL) was added phenylacetylene (84 μL, 0.76 mmol). The reaction was stirred for 30 minutes during which time a color change from orange to light yellow was observed, and the volatiles were removed under vacuum. The

resulting solids were washed with 3 x 15 mL of pentane, then dissolved in 10 mL of C_6H_6 and filtered through a plug of Celite. The light yellow solution was concentrated in vacuo to give 90 mg (53%) of product. Analytically pure samples were obtained by recrystallization from CH_2Cl_2/pentane.

(b) TpRu=C=CHPh(PPh_3)(Cl) (15 mg, 0.021 mmol) and AgO_2CCHPh_2 (8 mg, 0.025 mmol) were combined in an NMR tube. CD_2Cl_2 was added and the reaction was shaken for 5 minutes. $^{31}P\{^1H\}$ NMR (CD_2Cl_2): δ 62.12 (s). ^1H NMR (CD_2Cl_2): δ 7.76 (s, 1H, Tp), 7.71 (s, 1H, Tp), 7.61 (s, 1H, Tp), 7.31–6.76 (multiple peaks, 32H, CH*Ph*, P*Ph*$_3$, CH*Ph*$_2$, Tp), 6.49 (s, 1H, Tp), 5.99 (s, 1H, Tp), 5.95 (s, 1H, Tp), 5.85 (s, 1H, Tp), 5.16 (s, 1H, Ru–C=C*H*Ph), 4.93 (s, 1H, C*H*Ph_2). $^{13}C\{^1H\}$ NMR (CD_2Cl_2): δ 210.44 (d, Ru–*C*=CHPh, J_{CP} = 13 Hz), 181.40, 145.93, 144.27, 140.26, 137.74, 137.54, 137.47, 136.03, 134.76, 134.39, 134.21, 134.12, 133.91, 129.35, 129.11, 128.87, 127.75, 127.70, 127.60, 127.26, 123.15, 117.03, 105.60, 105.12. IR (CD_2Cl_2): 2479 cm^{-1} (B–H), 1612 cm^{-1} (OCO). Anal. Calcd for $C_{49}H_{42}N_6BO_2PRu$: C, 66.14; H, 4.76; N, 9.45. Found: C, 66.21; H, 4.18; N, 9.18.

Polymerization of norbornene with complex 6.4. Complex **6.4** (5.0 mg, 0.0057 mmol) and norbornene (30 mg, 0.31 mmol, 53 eq) were combined in an NMR tube. CD_2Cl_2 (1 mL) was added and the reaction mixture was shaken for one minute. The reaction was allowed to stand at room temperature for 2 hours and was then heated to 45 °C and monitored every 12 hours by ^1H NMR spectroscopy. After 24 hours, the carbene resonance had completely disappeared, and traces (approximately 5–10%) of polynorbornene (approximately 1:1 cis/trans) were observed by ^1H NMR. The reaction mixture was poured into methanol, however no polymer precipitated suggesting that a very low molecular weight product is formed.

References and Notes

(1) For a recent review see: Slugovc, C.; Schmid, R.; Kirchner, K. *Coord. Chem. Rev.* **1999**, *186*, 109.

(2) (a) Buriez, B.; Cook, D. J.; Harlow, K. J.; Hill, A. F.; Welton, T.; White, A. J. P.; Williams, D. J.; Wilton-Ely, J. D. E. T. *J. Organomet. Chem.* **1999**, *578*, 264. (b) Buriez,

B.; Burns, I. D.; Hill, A. F.; White, A. J. P.; Williams, D. J.; Wilton-Ely, J. D. E. T. *Organometallics*, **1999**, *18*, 1504.

(3) (a) Tenorio, M. A. J.; Tenorio, M. J.; Puerta, M. C.; Valerga, P. *Organometallics* **2000**, *19*, 1333. (b) Tenorio, M. A. J.; Tenorio, M. J.; Puerta, M. C.; Valerga, P. *Organometallics*, **1997**, *16*, 5528.

(4) (a) Slugovc, C.; Gemel, C.; Shen, J. Y.; Doberer, D.; Schmid, R.; Kirchner, K.; Mereiter, K. *Monat. fur Chem.* **1999**, *130*, 363. (b) Ruba, E.; Gemel, C.; Slugovc, C.; Mereiter, K.; Schmid, R.; Kirchner, K. *Organometallics* **1999**, *18*, 2275. (c) Slugovc, C.; Mereiter, K.; Schmid, R.; Kirchner, K. *Organometallics* **1998**, *17*, 827. (d) Slugovc, C.; Sapunov, V. N.; Wiede, P.; Mereiter, K.; Schmid, R.; Kirchner, K. *J. Chem. Soc., Dalton Trans.* **1997**, 4209. (e) Gemel, C.; Kickelbick, G.; Schmid, R.; Kirchner, K. *J. Chem. Soc., Dalton Trans.* **1997**, 2113. (f) Trimmel, G.; Slugovc, C.; Wiede, P.; Mereiter, K.; Sapunov, V. N.; Schmid, R.; Kirchner, K. *Inorg. Chem.* **1997**, *36*, 1076. (g) Gemel, C.; Wiede, P.; Mereiter, K.; Sapunov, V. N.; Schmid, R.; Kirchner, K. *J. Chem. Soc., Dalton Trans.* **1996**, 4071.

(5) (a) Harlow, K. J.; Hill, A. F.; Wilton-Ely, J. D. E. T. *J. Chem. Soc., Dalton Trans.* **1999**, 285.

(6) Sanford, M. S.; Henling, L. M.; Grubbs, R. H. *Organometallics* **1998**, *17*, 5385.

(7) (a) Lo, Y. H.; Lin, Y. C.; Lee, G. H.; Wang, Y. *Organometallics* **1999**, *18*, 982. (b) Chen, Y. Z.; Chan, W. C.; Lau, C. P.; Chu, H. S.; Lee, H. L. *Organometallics* **1997**, *16*, 1241. (c) Maruyama, Y.; Ikeda, S.; Ozawa, F. *Bull. Chem. Soc. Jpn.* **1997**, *70*, 689. (d) Corrochano, A. E.; Jaoln, F. A.; Otero, A.; Kubicki, M. M.; Richard, P. *Organometallics* **1997**, *16*, 145.

(8) (a) Pavlik, S.; Gemel, C.; Slugovc, C.; Mereiter, K.; Schmid, R.; Kirchner, K. *J. Organomet. Chem.* **2001**, *617*, 301. (b) Slugovc, C.; Mauthner, K.; Kacetl; Mereiter, K.; Schmid, R.; Kirchner, K. *Chem. Eur. J.* **1998**, *4*, 2043. (c) Slugovc, C.; Doberer, D.; Gemel, C.; Schmid, R.; Kirchner, K.; Winkler, B.; Stelzer, F. *Monat. fur Chem.* **1998**, *129*, 221. (d) Slugovc, C.; Mereiter, K.; Zobetz, E.; Schmid, R.; Kirchner, K. *Organometallics* **1996**, *15*, 5275.

(9) (a) Slugovc, C.; Mereiter, K.; Schmid, R., Kirchner, K. *Eur. J. Inorg. Chem.* **1999**, 1141. (b) Slugovc, C.; Mereiter, K.; Schmid, R., Kirchner, K. *J. Am. Chem. Soc.* **1998**, *120*, 6175.

(10) Katayama, H.; Yoshida, T.; Ozawa, F. *J. Organomet. Chem.* **1998**, *562*, 203.

(11) (a) Scholl, M.; Ding, S.; Lee, C. W.; Grubbs, R. H. *Org. Lett.* **1999**, *1*, 953. (b) Scholl, M.; Trnka, T. M.; Morgan, J. P.; Grubbs, R. H. *Tetrahedron Lett.* **1999**, *40*, 2247.

(c) Chang, S.; Jones, L.; Wang, C. M.; Henling, L. M.; Grubbs, R. H. *Organometallics* **1998**, *17*, 3460. (d) Dias, E. L.; Grubbs, R. H. *Organometallics* **1998**, *17*, 2758.

(12) Some examples of the ring opening of cyclopropenes at transition metal centers include: (a) Nguyen, S. T.; Grubbs, R. H.; Ziller, J. W. *J. Am. Chem. Soc.* **1993**, *115*, 9858. (b) Johnson, L. K.; Grubbs, R. H.; Ziller, J. W. *J. Am. Chem. Soc.* **1993**, *115*, 8130. (c) Nguyen, S. T.; Johnson, L. K.; Grubbs, R. H. *J. Am. Chem. Soc.* **1992**, *114*, 3974. (d) Binger, P.; Muller, P.; Benn, R.; Mynott, R. *Angew. Chem., Int. Ed. Engl.* **1989**, *28*, 610.

(13) (a) Schwab, P.; Grubbs, R. H.; Ziller, J. W. *J. Am. Chem Soc.* **1996**, *118*, 100. (b) Schwab, P.; France, M. B.; Grubbs, R. H.; Ziller, J. W. *Angew. Chem., Int. Ed. Engl.* **1995**, *34*, 2039.

(14) Some recent examples of the preparation of metal alkylidenes from diazo compounds from other groups include: (a) Lee, H. M.; Bianchini, C.; Jia, G. C.; Barbaro, P. *Organometallics* **1999**, *18*, 1961. (b) Ortmann, D. A.; Weberndorfer, B.; Schoneboom, J.; Werner, H. *Organometallics* **1999**, *18*, 952. (c) Galardon, E.; Le Maux, P.; Toupet, L.; Simonneaux, G. *Organometallics* **1998**, *17*, 565. (d) Werner, H.; Schwab, P.; Bleuel, E.; Mahr, N.; Steinert, P.; Wolf, J. *Chem. Eur. J.* **1997**, *3*, 1375.

(15) Recent examples of the synthesis of metathesis-active ruthenium olefin metathesis catalysts from alkynes include: (a) Wolf, J.; Stuer, W.; Grunwald, C.; Werner, H.; Schwab, P.; Schulz, M. *Angew. Chem., Int. Ed.* **1998**, *37*, 1124. (b) Wilhelm, T. E.; Brown, S. N.; Belderrain, T. R.; Grubbs, R. H. *Organometallics* **1997**, *16*, 3867. (c) Grunwald, C.; Gevert, O.; Wolf, J.; Gonzalez-Herrero, P.; Werner, H. *Organometallics* **1996**, *15*, 1960.

(16) Werner, H; Braun, T.; Daniel, T.; Gevert, O.; Schulz, M. *J. Organomet. Chem.* **1997**, *541*, 127.

(17) Sharp, P. R.; Bard, A. J.; *Inorg. Chem.* **1983**, *22*, 2689.

(18) Crystal structure collection and refinement data for **6.1**, **6.2**, **6.7**, and **6.8** are reported in Appendix A4.

(19) Ohta, T.; Takaya, H.; Noyori, R. *Inorg. Chem.* **1988**, *27*, 566.

(20) Sanchez-Delgado, R. A.; Thewalt, U.; Valencia, N.; Andriollo, A.; Marquez-Silva, R.-L.; Puga, J.; Schollhorn, H.; Klein, H.-P.; Fontal, B. *Inorg. Chem.* **1986**, *25*, 1097.

(21) Carbon-13 NMR shifts between 350 and 300 ppm are typical of ruthenium vinylidenes (for examples see ref. 2 and ref. 3) and alkylidenes (for example see ref. 5).

(22) Proton NMR shifts between 18 and 21 ppm are typical of ruthenium alkylidene. For examples see ref. 5.

(23) After 2 days at 45 °C both species decompose entirely. The identity of the multiple decomposition products is unknown at this time.

(24) At this time the pathway of formation of complex **6.2** is unknown. NMR studies of the reaction between **6.1** and diphenylcyclopropene show no intermediates, and, with the exception of traces of carbene **6.3**, only starting material and product can be observed as the reaction progresses. We have also found that the rate of this reaction is not affected by the addition of up to 10 equivalents of phosphine or by the dielectric constant of the solvent [C_6D_6 (ε = 2.3) versus CD_2Cl_2 (ε = 8.9)].

(25) Bruce, M. I.; Duffy, D. N; Humphrey, M. G.; Swincer, A. G. *J. Organomet. Chem.* **1985**, *282*, 383.

(26) Daniel, T.; Mahr, N.; Braun, T.; Werner, H. *Organometallics* **1993**, *12*, 1475.

(27) For a review of the unique chemistry of the Tp ligand see: Trofimenko, S. *Chem. Rev.* **1993**, *93*, 943.

(28) Esteruelas, M. A.; Lahoz, F. J.; Lopez, A. M.; Onate, E.; Oro, L. A. *Organometallics* **1994**, *13*, 1669.

(29) RCM is generally a more challenging reaction than ROMP for olefin metathesis catalysts. For example $(PPh_3)_2Cl_2Ru$=CHPh is an active catalyst for the ROMP of norbornene and cyclobutene, but is completely unreactive towards RCM substrates such as diethyl diallylmalonate. Dias, E. L.; Nguyen, S. T.; Grubbs, R. H. **1996**, unpublished results.

(30) Pangborn, A. B.; Giardello, M. A.; Grubbs, R. H.; Rosen, R. K.; Timmers, F. J. *Organometallics* **1996**, *15*, 1518.

(31) Alcock, N. W.; Burns, I. D.; Claire, K. S.; Hill A. F. *Inorg. Chem.* **1992**, *31*, 2906.

(32) Nguyen, S. T., Ph.D. Thesis, California Institute of Technology, **1995**.

(33) (a) Closs, G. L.; Moss, R. A. *J. Am. Chem. Soc.* **1964**, *86*, 4042. (b) Yates, P.; Shapiro, B. L. *J. Org. Chem.* **1958**, *23*, 759.

Appendices

Appendix A1. X-ray Crystallographic Data for Chapter 3.

Complex	**3.2**	**3.7**
Empirical formula	$C_{46}H_{65}Cl_2N_2PRu \cdot C_6H_6 \cdot 0.5C_5H_{12}$	$C_{76}H_{84}Cl_4N_8Ru_2$
Formula weight	963.17	1453.46
Crystal Habit	Block	Rod
Crystal size	0.21 x 0.26 x 0.30 mm^3	0.41 x 0.11 x 0.07 mm^3
Crystal color	Burgundy	Emerald Green
Diffractometer	CCD Area Detector	CCD Area Detector
Wavelength	0.71073 MoKα	0.71073 MoKα
Temperature	98 K	98 K
Unit cell dimensions	a = 12.2949(7) Å	a = 12.3873(16) Å
	b = 14.9666(8) Å	b = 15.529(2) Å
	c = 27.1432(15) Å	c = 18.562(2) Å
	α = 90°	α = 78.475(2)°
	β = 97.601(1)°	β = 81.564(2)°
	γ =90°	γ = 76.745(2)°
Volume	4950.8(5) $Å^3$	3386.2(8) $Å^3$
Z	4	4
Crystal system	Monoclinic	Triclinic
Space group	$P2_1/n$	$P1$
Density (calculated)	1.292 g/cm^3	2.758 Mg/m^3
Theta range	1.5 to 28.5°	1.61 to 28.51°
h min, max	–16, 16	–16, 16
k min, max	–19, 19	–20, 20
l min, max	–34, 34	–24, 24
Reflections collected	87057	76469
Independent reflections	11892	15655
R_{int}	0.0465	0.0867
GOF on F^2	2.658	1.438
Final R indices [I>2σ(I)]	0.0374	0.0609
Final weighted R [F_o^2]	0.0764	0.0855

Appendix A2. X-ray Crystallographic Data for Chapter 4.

Complex	**4.4**	**4.9**	**4.14**	**4.19**
Empirical formula	$C_{33}H_{57}O_2PRu$	$C_{33}H_{39}F_{18}O_2PRu$	$C_{30}H_{27}F_{12}N_3O_2Ru \cdot C_6H_6$	$C_{24}H_{49}ClOP_2Ru$
Formula weight	617.83	941.68	868.72	552.09
Crystal Habit	Blade	Blade	Fragment	Block
Crystal size	0.21 x 0.16 x 0.03 mm^3	0.34 x 0.22 x 0.08 mm^3	0.31 x 0.26 x 0.17 mm^3	0.21 x 0.29 x 0.30 mm^3
Crystal color	Dark Red	Red	Green	Ruby Red
Diffractometer	CCD Area Detector	CCD Area Detector	CCD Area Detector	CAD-4
Wavelength	0.71073 MoKα	0.71073 MoKα	0.71073 MoKα	0.71073 MoKα
Temperature	93 K	98(2) K	98(2) K	84 K
Unit cell dimensions	a = 10.0120(7) Å	a = 10.427(6) Å	a = 11.7011(6) Å	a = 8.725(2) Å
	b = 20.5338(14) Å	b = 10.716(6) Å	b = 24.1916(12) Å	b = 12.130(4) Å
	c = 15.7802(11) Å	c = 18.417(10) Å	c = 12.4624(6) Å	c = 13.442(4) Å
		α = 85.454(13)°		α = 90.37(3)°
	β = 92.1300(10)°	β = 89.699(16)°	β = 96.2370(10)°	β = 99.60(2)°
		γ = 65.599(14)°		γ = 95.32(2)°
Volume	3241.9(4) $Å^3$	1840.0(18) $Å^3$	3506.8(3) $Å^3$	1396.3(7) $Å^3$
Z	4	2	4	2
Crystal system	Monoclinic	Triclinic	Monoclinic	Triclinic
Space group	$P2_1/n$	$P\bar{1}$	$P2_1/n$	$P\bar{1}$
Density (calculated)	1.266 Mg/m^3	1.700 Mg/m^3	1.645 Mg/m^3	1.313 Mg/m^3
Theta range	1.63 to 28.74°	2.09 to 28.35°	1.68 to 25.58°	1.54 to 25°
h min, max	–12, 12	–13, 13	–15, 15	–10, 10

Appendix A2. X-ray Crystallographic Data for Chapter 4 (continued).

Complex	**4.4**	**4.9**	**4.14**	**4.19**
k min, max	–26, 26	–14, 14	–32, 32	–14, 14
l min, max	–20, 20	–24, 24	–16, 16	–15, 15
Reflections collected	29820	32991	62085	10522
Independent reflections	7759	8428	8374	4908
R_{int}	0.0683	0.0352	0.0625	0.0157
GOF on F^2	1.048	4.824	1.657	1.652
Final R indices [$I>2\sigma(I)$]	0.0328	0.0913	0.0354	0.0195
Final weighted R [F_o^2]	0.0527	0.1627	0.0588	0.0476

Appendix A3. X-ray Crystallographic Data for Chapter 5.

Complex	**4.3**
Empirical formula	$C_{40.5}H_{65.75}B_2F_4N_6O_{2.88}PRu$
Formula weight	912.40
Crystal Habit	Flake
Crystal size	0.30 x 0.26 x 0.04 mm^3
Crystal color	Emerald Green
Diffractometer	CAD4
Wavelength	0.71073 MoKα
Temperature	85 K
Unit cell dimensions	a = 20.195(5) Å
	b = 10.629(3) Å
	c = 21.205(7) Å
	β = 91.14(2)°
Volume	4551(2) $Å^3$
Z	4
Crystal system	Monoclinic
Space group	$P2_1/c$
Density (calculated)	1.332 Mg/m^3
Theta range	1.5 to 22.5°
h min, max	–21, 21
k min, max	–11, 10
l min, max	0, 22
Reflections collected	13603
Independent reflections	5952
GOF on F^2	1.322
Final R indices [I>2σ(I)]	0.0446
Final weighted R [F_o^2]	0.0780

Appendix A4. X-ray Crystallographic Data for Chapter 6.

Complex	**6.1**	**6.2**	**6.7**	**6.8**
Empirical formula	$C_{43}H_{40}BCl_2N_6O_2PRu$	$C_{58.83}H_{53.33}BN_6O_2PRu$	$C_{34}H_{30}BCl_3N_6PRu(CH_2Cl_2, C_7H_8)$	$C_{56}H_{49}BN_6O_2PRu$
Formula weight	872.53	1019.298	817.89	980.86
Crystal Habit	Plate	Wedge	Feathered Blocks	Lozenge
Crystal size	0.35 x 0.28 x 0.07 mm^3	0.44 x 0.33 x 0.11 mm^3	0.33 x 0.26 x 0.19 mm^3	0.15 x 0.296 x 0.37 mm^3
Crystal color	Yellow	Canary Yellow	Emerald Green	Yellow/Orange
Diffractometer	CAD4	CAD4	CCD Area Detector	CCD Area Detector
Wavelength	0.71073 MoKα	0.71073 MoKα	0.71073 MoKα	0.71073 MoKα
Temperature	85 K	84 K	98 K	293 K
Unit cell dimensions	a = 15.112(3) Å	a = 14.146(5) Å	a = 10.0980(6) Å	a = 13.7367(7) Å
	b = 14.287(3) Å	b = 21.309(8) Å	b = 30.0953 (17) Å	b = 19.5683(10) Å
	c = 19.039(4) Å	c = 25.345(8) Å	c = 11.9758(7) Å	c = 18.5679(10) Å
		α = 84.57(3)°		
	β = 105.32(3)°	β = 79.86(3)°	β = 90.2250(10)°	β = 102.091(1)°
		γ = 87.45(3)°		
Volume	3964.6(14) $Å^3$	7484(5) $Å^3$	3639.4(4) $Å^3$	4880.4(4) $Å^3$
Z	4	6	4	4
Crystal system	Monoclinic	Triclinic	Monoclinic	Monoclinic
Space group	$P2_1/c$	$P\bar{1}$	$P2_1/n$	$P2_1/n$
Density (calculated)	1.462 Mg/m^3	1.357 Mg/m^3	1.493 Mg/m^3	1.3335 Mg/m^3
Theta range	1.18 to 24.98°	1.5 to 25°	1.83 to 23.27°	1.53 to 28.53°
h min, max	0, 17	–16, 16	–11, 11	–17, 17

Appendix A4. X-ray Crystallographic Data for Chapter 6 (continued).

Complex	**6.1**	**6.2**	**6.7**	**6.8**
k min, max	–16, 16	–25, 25	–33, 33	–26, 26
l min, max	–22, 22	–29, 30	–13, 13	–24, 24
Reflections collected	15540	53947	25421	47152
Independent reflections	6953	26257	5225	11439
R_{int}	0.016	0.0306	0.0504	0.0418
GOF on F^2	1.782	1.567	1.027	2.642
Final R indices [$I>2\sigma(I)$]	0.0261	0.0415	0.0670	0.0420
Final weighted R [F_o^2]	0.0582	0.0778	0.1784	0.0853

Appendix A5. UV-vis Spectral Data for Selected Ruthenium Alkylidenes.

MLCT band for Selected Ruthenium Alkylidenes.[a]

Complex	Color	MLCT λ_{max} (nm)	ε (dm^3 mol^{-1} cm)
A5.1	Purple	526	880
A5.2	Red/purple	542	180
A5.3	Green	582	500
A5.4	Red/Purple	498	750
A5.5	Purple	514	1050
A5.6	Red/purple	510	1320
A5.7	Purple	518	1580
A5.8	Red/purple	526	1100
A5.9	Green	698	280
A5.10	Red	502	590
A5.11	Red	504	860

[a] Measurements made in toluene solution at 20 °C. [Ru] = 8.15 x 10^{-4} mol/dm^3

Ruthenium Catalysts **A5.1–A5.11**.

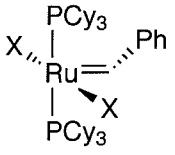

X = Cl (**A5.1**)
X = Br (**A5.2**)
X = I (**A5.3**)

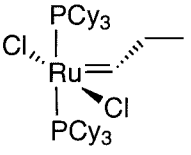

(**A5.4**)

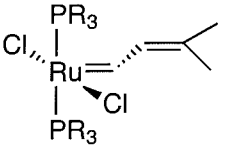

R = Cy (**A5.5**)
R = Cp (**A5.6**)
R = ^{i}Pr (**A5.7**)

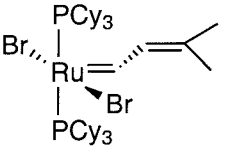

(**A5.8**)

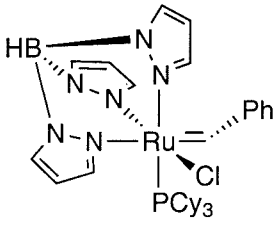

(**A5.9**)

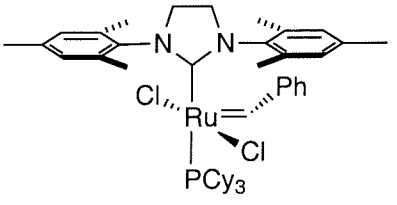

(**A5.10**)

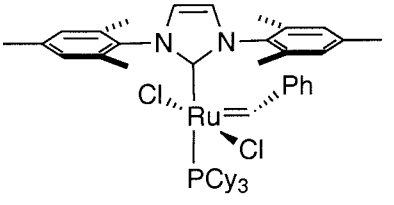

(**A5.11**)